THE JOURNAL
OF
CHEMICAL PHYSICS

VOLUME 17, NUMBER 2 FEBRUARY, 1949

# Hindered Rotation in Ethyl Alcohol

J. O. HALFORD
*Chemistry Department, University of Michigan, Ann Arbor, Michigan*
(Received July 15, 1948)

Previous evaluations of the barriers hindering the internal rotations in ethyl alcohol are shown to be unsatisfactory because they fail to produce agreement between molecular and calorimetric entropies over a wide enough temperature range. The principal source of difficulty is found in an inconsistency between the modified Berthelot equation of state and the calorimetric data and vapor pressures used in calculating the third law entropies. Corrections for gas imperfection should be much higher at the temperatures at which the barrier evaluations have been made, but these corrections cannot be determined accurately with the available data. The larger entropies permit the assignment of lower and more reasonable potential barriers.

For the hydroxyl group rotation, to keep the heat capacity, and therefore the change of entropy with the temperature, within the indicated limits, the simple expression $V=V_0(1-\cos 3\theta)/2$ is more suitable than more detailed potential energy functions. With a reasonable assignment of the vibrational frequencies, the sum of the barriers restricting the hydroxyl and methyl group rotations is approximately 6000 cal.

THIS study was originally undertaken to provide an illustration of the approximate method recently proposed by the author[1] for the calculation of the thermodynamic properties of an unsymmetrical internal rotation. The intention was to recalculate the entropy by this new method from the molecular properties assigned by Aston,[2] Isserow, Szasz, and Kennedy to see if the result was appreciably different and if further light might be thrown on the validity of their empirical potential energy function. Unfortunately, their result does not adequately justify their molecular properties, because the entropy calculated by their method from these properties increases too rapidly between the two temperatures which they have chosen for comparison with the calorimetric values. As a consequence, if a third comparison is made at room temperature, a serious disagreement appears. The situation is not improved by the use of the new entropy evaluation for the hydroxyl group rotation.

The empirical potential energy function gives too much heat capacity to the internal rotations and raises the question as to how to change the barrier assignment in order to lose heat capacity without producing much change in the entropy. This can be done by going to a symmetrical barrier system of the form $V=V_0(1-\cos 3\theta)/2$ to eliminate the change of "composition" with the temperature, and by raising one barrier and lowering the other.

This conclusion suggests a further examination of the properties assigned by Schumann[3] and Aston, who used the symmetrical cosine function in conjunction with barriers of 3000 and 10,000 cal. for the methyl and hydroxyl group rotations.

[1] J. O. Halford, J. Chem. Phys. **15**, 645 (1947); **16**, 410 (1948); **16**, 560 (1948).
[2] J. G. Aston, S. Isserow, G. J. Szasz, and R. M. Kennedy, J. Chem. Phys. **12**, 336 (1944).
[3] S. C. Schumann and J. G. Aston, J. Chem. Phys. **6**, 480 (1938).

Their tabulation shows a perfect fit between molecular and calorimetric entropies at 351.5°K and 403.2°K. Recalculation, however, reveals an error of 0.4 unit in the vibrational entropy at 351.5°, with the result that the use of their properties at 298.2° again produces a serious disagreement with the calorimetric value. If they had based their barrier assignment upon the third law value at 298.2°K, rather than 403.2°K, they would have obtained a barrier of 3400 cal. for the hydroxyl group rotation, with no more serious disagreements at other temperatures than those produced by their 10,000-cal. barrier. In a later paper, Aston[4] used the barriers assigned by himself and Schumann to calculate the ethyl alcohol entropy at a series of temperatures, but failed to recognize that his value at 350°K was far enough below the calorimetric one at 351.5°K to bring the barrier assignment into question.

The problem contains three unknowns: the two potential barriers and the mean value of the six rocking ($\delta$) frequencies. In the interpretations by Aston and his collaborators, two of these were assumed or assigned in advance, and the third one was obtained by difference at one or two temperatures. It is possible to reproduce the calorimetric values at two well spaced temperatures with molecular constants, of which one has been assigned and the other two have been evaluated from the data. The extension to an independent evaluation of the three constants by means of comparisons at three temperatures does not appear to be practical. In the present attempts to find a solution for the unknowns the methyl group barrier is assigned, and a combination of a hydroxyl group barrier with a mean $\delta$-frequency is sought which will produce a numerical fit at 351.5°K and 403.2°K. The result is then tested at 298.2°. In general, for each assumed methyl barrier up to about 5000 cal., one numerically satisfactory combination of the other unknowns is found, but at least one of the two always has an unreasonable value. If the reasonable assumption is made that the frequency must lie below 1100 $cm^{-1}$, the resulting barriers are extreme. Thus, the properties $V(CH_3)=500$, $V(OH)=15{,}000$, and $\nu(\delta)=1065$ will come close to fitting the calorimetric data over the entire temperature range. Lower $\delta$-frequencies require practically free rotation for the methyl group and a high frequency vibration for the hydroxyl group.

The third law values which lead to these extreme results are calculated from excellent data in the usual manner, but they do not provide a rapid enough increase in entropy with the temperature to permit the assignment of reasonable molecular properties. The assumption of a residual entropy at the absolute zero would not take care of the situation, which is concerned almost entirely with the thermal data above room temperature. Neither does the vibrational entropy appear to be at fault. The frequency assignment of Schumann and Aston, except for the missing rocking motions, is a very reasonable one which probably introduces no serious errors. It appears, then, that the source of the difficulty must be in the third law values themselves.

The several terms entering into these values are summarized in Eq. (1),

$$S_T^0 = \underset{298.2}{S(1)} + \int_{298.2}^{T} C\,d\ln T + L/T + (27/32)RpT_c^3/(p_cT^3) + R\ln p, \quad (1)$$

in which $S_T^0$ is the hypothetical perfect gas entropy at one atmosphere, $\underset{298.2}{S(1)}$ is the entropy of the liquid obtained by Kelley,[5] $C$ is the heat capacity of the liquid at saturation pressure by Fiock, Ginnings, and Holton,[6] $L$ is the heat of vaporization by the same authors, and $p_c$ and $T_c$ are the critical constants, which appear in a term derived from the modified Berthelot equation of state for the correction for gas imperfection.

The quantities introduced into Eq. (1) are interdependent, through the Clapeyron equation, and should be checked for consistency before the results are accepted. It is found that the gas imperfections indicated by the thermal data and vapor pressures are consistently larger than those of the Berthelot equation, and that the gas imperfection correction required at the highest temperature may be as much as five times as high as the one given by the Berthelot equation.

[4] J. G. Aston, Ind. Eng. Chem. **34**, 514 (1942).

[5] K. K. Kelley, J. Am. Chem. Soc. **51**, 779 (1929).

[6] E. F. Fiock, D. C. Ginnings, and W. B. Holton, J. Research Nat. Bur. Stand. **6**, 881 (1931).

TABLE I. The entropy of ethyl alcohol from molecular constants by the method of Aston, Isserow, Szasz, and Kennedy.

| | 298.2°K | | 351.5°K | | 403.2°K | |
|---|---|---|---|---|---|---|
| | Straight | Bent | Straight | Bent | Straight | Bent |
| $S(T+R)$ | 59.82 | 61.20* | 61.13 | 62.51* | 62.22 | 63.60* |
| $S$(vib.) | 1.76 | | 2.78 | | 3.94 | |
| $S(CH_3)$ | 2.79 | 2.18 | 3.09 | 2.53 | 3.34 | 2.83 |
| $S$(OH) | 1.41 | 0.79 | 1.71 | 1.05 | 1.95 | 1.30 |
| $S$ | 65.78 | 65.93 | 68.71 | 68.87 | 71.45 | 71.67 |
| % present | 91 | 9 | 87 | 13 | 84 | 16 |
| Mixing | 0.60 | | 0.77 | | 0.87 | |
| $S^0(T)$ | 66.39 | | 69.50 | | 72.36 | |
| $S^0$(3rd law)** | 67.29 | | 69.71 | | 72.09 | |

* $S(T+R)$ includes the entropy of mixing of the optical isomers.
** Gas imperfection increment by the modified Berthelot equation.

As the temperature increases, and the vapor pressure rises rapidly, the perfect gas entropy becomes increasingly uncertain. Consequently, conclusions about the molecular properties will be most reliable if they are based upon calculations at the lowest temperatures and pressures. If a mean rocking frequency is assumed, a series of combinations of methyl and hydroxyl group barriers becomes arithmetically possible at each temperature, and, in principle, an acceptable solution is a combination which is valid for two well spaced low temperatures. When the entropy at 298.2° is used in conjunction with the less accurate value at 351.5°, approximate agreement is found only for the highest estimates of the gas imperfection at the higher temperature. The sum of the two barriers is approximately 6000 cal., and the fit is about equally good for methyl barriers between 2500 and 4000 cal. The introduction of the constant probable error of ±0.30 in Kelley's value for the liquid at 298.2° into the calculation serves to make the sum uncertain by about ±1000 cal.

It is to be hoped that the situation uncovered here is peculiar to ethyl alcohol and related associated substances, and does not mean that similar reconsiderations for other cases in which the Berthelot equation of state has been used are necessary.

## I. METHOD OF ASTON, ISSEROW, SZASZ, AND KENNEDY

In this method the potential energies of the internal rotations are obtained from an empirical function based upon the repulsion between hydrogen atoms. The potential energy is taken to be proportional to the inverse $n$th power of the distance, and the proportionality constant and the exponent $n$ are evaluated from the potential barriers assigned to ethane and neopentane. The barrier for the methyl group is of the form $V=V_0(1-\cos 3\theta)/2$, but $V_0$ is a function of the angular position of the hydroxyl group. For the hydroxyl group, the potential energy has approximately the form $V=V_1(1-\cos\theta)/2+V_2(1-\cos 3\theta)/2$, and contains three minima and three maxima.

The system is regarded as a mixture of isomers for which the entropy of each one can be taken from the tables of Pitzer[7] and Gwinn for the symmetrical rotator. The "composition" is estimated from the free energies of the individuals, and the difference between the minima and the appropriate mixing terms are included to give the required entropy total. Reduced moments of inertia are taken directly from the paper by Aston, Isserow, Szasz, and Kennedy. The barriers and moments are summarized below:

| | $V(CH_3)$ | $V$(OH) |
|---|---|---|
| "Straight" form | 1800 cal. | 2375 cal. |
| "Bent" form | 3000 cal. | 4410 cal. |

$I(CH_3)=4.83\cdot10^{-40}$ g cm²,
$I(OH)=1.40\cdot10^{-40}$ g cm².

The frequency assignment is the same as that of Aston, Isserow, Szasz, and Kennedy, and is taken from Schumann and Aston, except that the average effective value of the six doubtful rocking frequencies is set at 985 cm$^{-1}$.

Table I contains the recalculated values required for the comparison of molecular and third law entropies at 351.5°K and 403.2°K—the

[7] K. S. Pitzer and W. D. Gwinn, J. Chem. Phys. 10, 428 (1942).

TABLE II. Thermodynamic properties of the hydroxyl group rotation in ethyl alcohol calculated by means of mean energy levels from the potential energy function of Aston, Isserow, Szasz, and Kennedy.

| $T$(°K) | 298.2 | 351.5 | 403.2 |
|---|---|---|---|
| $-F/T$ | 0.83±0.03 | 1.12±0.03 | 1.39±0.03 |
| $H/T$ | 1.60±0.02 | 1.84±0.01 | 2.05±0.01 |
| $S$ | 2.43±0.05 | 2.96±0.04 | 3.44±0.04 |
| $C$ | 3.12±0.07 | 2.96±0.08 | 2.67±0.07 |

temperatures chosen by Aston, Isserow, Szasz, and Kennedy. A further comparison at 298.2°K has been added. The table contains several small differences from the original summation by Aston and his collaborators, but the fit obtained at 351.5°K and 403.2°K is not changed in any significant way by the recalculation. The expected large discrepancy at 298.2°K is 0.90 unit, which clearly shows that the molecular properties are not satisfactory. This is also evident from the entropy change between 351.5° and 403.2°K, which is 2.86 units from the molecular properties against 2.38 from the third law values. This corresponds to a difference of nearly 4 units, or approximately 20 percent, in the mean heat capacity for this temperature range.

The method of evaluating the contribution of the rotating hydroxyl group is an unproved approximation which might lead to a serious error. As a check on this possibility, the comparison is repeated with the evaluation for the hydroxyl group carried out with the aid of mean energy levels found by the method recently proposed by the present author. This approximation is also unproved, but it should be more accurate than the earlier one in spite of the fact that its application to ethyl alcohol is a rather severe test because of the low reduced moment of inertia and the presence of shallow valleys in the potential energy curve.

## II. MOLECULAR CONSTANTS FROM ASTON, ISSEROW, SZASZ, AND KENNEDY; HYDROXYL GROUP CONTRIBUTION FROM MEAN ENERGY LEVELS

The potential energy curve for the hydroxyl group rotation is replaced by a series of linked sections of cosine function, and a set of mean energy levels is found for each region of the energy—rotational coordinate surface, thus permitting a direct evaluation of the partition function and its derivatives. To find the mean energy levels, a quantum number index is set up in terms of $E/V_1$, where $V_1$ is one of the potential barriers, according to the equation,

$$\mathfrak{R}=\sum(\rho_i/a_i)(V_i/V_1)^{\frac{1}{2}}/2. \qquad (2)$$

The index $\rho$ is obtained from Table II of reference 1b, and the quantities $V_i$ and $a_i$ are taken from the text and the published potential energy curve of Aston, Isserow, Szasz, and Kennedy as follows:

| | 1 | 2 | 3 |
|---|---|---|---|
| $V$ | 2375 | 815 | 4410 |
| $1/a$ | 0.3518 | 0.2259 | 0.4222 |

The potential barriers, and the quantity $a_3$, as well as the sum $1/a_1+1/a_2$, can be taken from values given in their paper, but the individual quantities $a_1$ and $a_2$ depend upon the rotational coordinates of the lower maxima, which are not given in the text. It is accurate enough for the present purpose to estimate these coordinates from the printed potential energy curve. The reduced moment of inertia is the same as in Section I.

When values of the index $\mathfrak{R}$ for the mean energy levels are assigned as described in earlier papers, the following ratios $E/V_1$ are obtained: 0.212, 0.597, and 0.909 within the lower valley and belonging to the "straight" form; 0.864 or 0.801, two states at the same level, one for each valley corresponding to a "bent" form, with the alternatives given because the low barrier $V_2$ leaves the accurate position in doubt; 1.030, 1.247 (2), 1.552 (2), 1.860, 1.887, 2.180, 2.232, 2.484, 2.548, 2.787, 2.904, 3.158, 3.338, 3.586, 3.830, 4.065, 4.371, 4.595, 4.962, 5.168, vibrational and rotational states at energies above the lower potential maxima. It is interesting that for each "bent" form only one uniquely characteristic level appears.

From these mean energy ratios the thermodynamic properties of the hydroxyl group rotation are calculated at three temperatures as shown in Table II. The indicated uncertainty is solely that due to the alternative positions of the states in the shallow valleys for the "bent" forms. There is no basis for estimating other uncertainties inherent in the approximation.

Each entropy is higher by about 0.4 unit than the corresponding one obtained by the method of Aston and his collaborators. The heat capacity is in agreement at 403.2°K and is higher by 0.4 unit at 298.2°K. In Table II the entropy is higher than in Table I because here the mixing terms are automatically included, while in Table I they were listed separately.

In Table III, the entropy summations obtained with this new treatment of the hydroxyl group rotation are compared with the calorimetric values. With two potential barriers for the methyl group, according to the angular position of the hydroxyl group, there is no clear way to evaluate the contribution of the methyl group rotation. It is evident, however, from Table I, that this quantity is not sensitive to the calculated "composition." Consequently, no significant error will be made if the contribution is taken from Table I and used in the new summation.

With all three temperatures considered, the new approximation does not materially change the character of the fit shown in Table I. The situation is improved in the lower part of the temperature range but is worse at higher temperatures because of the general upward revision of the entropies from molecular constants. The heat capacity is still much too high for the rate of change of the entropy with the temperature.

A comparison of Tables I and II shows that the mean heat capacity obtained by two distinctly different approximations is very nearly the same, and is therefore probably near to the correct value for the chosen potential energy function. To obtain a better agreement with the calculated third law values it will be necessary to adopt a potential energy function which leads to lower heat capacities. The symmetrical function of the form $V=V_0(1-\cos 3\theta)/2$, which, according to the tables of Pitzer and Gwinn, has maximum heat capacities of about 2.35, fulfills this requirement.

These considerations suggest that a description of the type originally proposed by Schumann and Aston should be more successful. Because their tabulations show agreement at 351.5°K and 403.2°K, it appears possible that their potential barriers will be satisfactory at 298.2°K.

TABLE III. The entropy of ethyl alcohol from molecular data, evaluated from the constants of Aston, Isserow, Szasz, and Kennedy with the aid of mean energy levels for the hydroxyl group rotation.

| $T$(°K) | 298.2 | 351.5 | 403.2 |
|---|---|---|---|
| $S(T+R)$ | 59.82 | 61.13 | 62.22 |
| $S$(vib.) | 1.76 | 2.78 | 3.94 |
| $S(CH_3)$ | 2.74 | 3.02 | 3.26 |
| $S$(OH) | 2.43 | 2.96 | 3.44 |
| $S^0(T)$ | 66.75 | 69.89 | 72.86 |
| $S^*$(3rd law) | 67.26 | 69.71 | 72.09 |

* Gas imperfection increment by the modified Berthelot equation.

## III. POTENTIAL BARRIERS ACCORDING TO SCHUMANN AND ASTON

Schumann and Aston assigned individual frequencies to the rocking motions equivalent, in effect, to a mean value of about 905 $cm^{-1}$. They assumed 3000 cal. for the barrier to the methyl group rotation and obtained 10,000 cal. by difference, at 403.2°K, for the hydroxyl group rotation. In Table IV the entropy calculated with their molecular constants is compared with the third law values calculated with the aid of the modified Berthelot equation.

The difference between Table IV and the original summation by Schumann and Aston is in the vibrational entropy at 351.5°K. Although the fit is somewhat better than that of Tables I and III, it is still unsatisfactory for similar reasons. The totals from molecular constants are in good agreement with the calculations of Aston.[4]

## IV

A closer numerical interpretation is now sought with the type of potential energy function used by Schumann and Aston. The entire region of possible values of the three unknowns can be scanned in the manner described in the introductory section. For the first combination found in which the numerical fit is close and the mean

TABLE IV. The entropy of ethyl alcohol from the molecular constants assigned by Schumann and Aston.

| $T$(°K) | 298.2 | 351.5 | 403.2 |
|---|---|---|---|
| $S(T+R)$ | 59.82 | 61.13 | 62.22 |
| $S$(vib.) | 2.03 | 3.13 | 4.32 |
| $S(CH_3)$ | 2.18 | 2.53 | 2.83 |
| $S$(OH) | 2.45 | 2.60 | 2.75 |
| $S^0(T)$ | 66.48 | 69.39 | 72.11 |
| $S^0$(3rd law)** | 67.26 | 69.71 | 72.09 |

** Gas imperfection increment by the modified Berthelot equation.

TABLE V. Molal volumes of ethyl alcohol vapor at saturation pressures (liters).

| $T$(°K) | $V^0=RT/p$ | $V$(Berthelot) | $V$(thermal) | $V$(direct) |
|---|---|---|---|---|
| 298.2 | 317.42 | 316.63 | 316.69 | |
| 313.2 | 146.37 | 145.66 | 144.22 | |
| 333.2 | 59.34 | 58.72 | 57.42 | |
| 353.2 | 27.14 | 26.59 | 25.79 | |
| 373.2 | 13.75 | 13.27 | 12.78 | 13.30 |
| 403.2 | 5.82 | 5.41 | 5.17 | 5.21 |

rocking frequency falls below 1100 $cm^{-1}$, the constants are $V_{CH_3}=500$, $V_{OH}=15{,}000$, and $\nu(\delta)=1065$.

It can be concluded with confidence, if not with certainty, that the only acceptable numerical interpretations will involve properties close to those just listed. As a result, it is evident not only that the interpretation of Aston, Isserow, Szasz, and Kennedy is inadequate, but also that the hydroxyl group barrier consistent with an acceptable frequency assignment is even more extreme than the one proposed by Schumann and Aston. This barrier is now so far out of line with other barrier evaluations as to be almost certainly wrong, but the indications are that such a barrier is necessary to produce an acceptable numerical agreement with the third law values over the entire temperature range.

## V. REVISION OF THE THIRD LAW ENTROPY

It is this situation which has led to an inquiry into the validity of the modified Berthelot equation of state for ethyl alcohol vapor. For this purpose, as shown in Table V, molal volumes of the vapor, calculated in several ways, are compared. The first column shows the absolute temperature, the second the perfect gas volume, the third the Berthelot volume, the fourth the volume calculated from the specific volumes obtained by Fiock, Ginnings, and Holton from the vapor pressure, the heat of vaporization, and the density of the liquid, and the fifth column gives two estimates obtained by interpolation from vapor density data found in the International Critical Tables.

The volume from the thermal data and the vapor pressures is consistent with the modified Berthelot equation only at the lowest temperature. At all other temperatures the consistent gas imperfections are appreciably larger than those given by the Berthelot equation. No conclusion can be drawn from the last column, for which one entry checks the Berthelot equation and the other is consistent with the thermal data.

TABLE VI. Estimated entropy increments for gas imperfection in ethyl alcohol at saturation pressures.

| $T$°K Increments | 298.2 | 351.5 | 403.2 |
|---|---|---|---|
| Source of $a$ and $b$: | | | |
| Critical constants | 0.01 | 0.08 | 0.32 |
| Volume at 298 and 353 | 0.03 | 0.22 | 0.82 |
| Volume at 353 and 403 | 0.05 | 0.42 | 1.61 |
| Minimum entropy | 67.26 | 69.71 | 72.09 |
| Maximum entropy | 67.30 | 70.05 | 73.38 |

To obtain reliable gas imperfection corrections would require accurate knowledge of the volumes or vapor densities as a function of the pressure from high attenuation to the saturation pressure at each temperature. Such data are not available, and, consequently, it is not possible to calculate accurate third law entropies, corrected for gas imperfection, at the higher temperatures and pressures. It is possible, however, if the form of the equation of state is assumed, to evaluate the constants in the assumed equation and use them to make rough estimates of the corrections for gas imperfection. For this purpose, it is convenient to use the form of the modified Berthelot equation:

$$pV/RT=1+(p/T)(a-b/T^2). \qquad (3)$$

For this equation the gas imperfection increment is

$$S^0-S=2bRp/T^3. \qquad (4)$$

When the constants are evaluated from the volumes from thermal data at 353.2°K and 403.2°K, $b$ is $4.61\times10^6$, and, when the temperatures used are 298.2 and 353.2°K, $b$ is $2.35\times10^6$. In the ordinary form of the modified Berthelot equation $b$ is $0.90\times10^6$. The corresponding estimates of the correction for gas imperfection are shown in Table VI. In addition to the above estimates a three constant equation with a term in $(p/T)(1/T)$ was fitted and tried, but it did not reproduce the volumes as well as the two constant equation based upon the volumes at 353 and 403°. The correction calculated from the three constant equation was higher at 351.5° and lower at 403.2°K.

The selection of molecular properties should be based upon the entropy at 298.2°, which is essentially independent of the gas imperfection problem. In making a barrier assignment, the minimum entropy at 298.2°K in conjunction with the maximum value at 351.5°K has been chosen. This arbitrary choice is made principally because it leads to a nearly consistent result. It is justified by the calculated volumes in Table V. The highest temperature (403.2°K) is left out of consideration.

## VI. NEW APPROXIMATION TO THE MOLECULAR CONSTANTS

Except for the OH ($\delta$) frequency, the vibrational assignment of Schumann and Aston has been adopted. If for this quantity (700 $cm^{-1}$) the more probable value[8] of 1100 $cm^{-1}$ is substituted, the mean frequency is close to that of Aston, Isserow, Szasz, and Kennedy at 985 $cm^{-1}$. Vibrational entropy contributions are therefore taken from Tables I and III. For the simple cosine potential function, with equal stability for the straight and bent forms, the barriers at 298.2°K and 351.5°K may be found as summarized in Table VII, which shows for each temperature the selected total entropy and a series of consistent barrier combinations.

The combinations shown in Table VII are not in exact agreement at the two temperatures. To produce a closer agreement would require a set of properties in the direction of those listed in Section IV, but a more detailed treatment along these lines would not be justified because of the uncertainty in the gas imperfection correction at the higher temperature. It can be concluded that a fit at 298.2°K is not inconsistent with the data at 351.5°K, and that for an assumed mean $\delta$-frequency of 985 $cm^{-1}$ the sum of the methyl and hydroxyl group barriers is about 6000 cal.

TABLE VII. Potential barriers in ethyl alcohol.

| $T$(°K) | 298.2 | | 351.5 | |
|---|---|---|---|---|
| $S^0$(total) | 67.26 | | 70.05 | |
| $\nu(\delta)$ | 985 $cm^{-1}$ | | 985 $cm^{-1}$ | |
| Barriers | $V(CH_3)$ | $V$(OH) | $V(CH_3)$ | $V$(OH) |
| | 2000 | 4200 | 2000 | 4800 |
| | 2500 | 3200 | 2500 | 3800 |
| | 3000 | 2700 | 3000 | 3100 |
| | 3500 | 2200 | 3500 | 2600 |
| | 4000 | 1800 | 4000 | 2200 |

The uncertainty of ±0.3 in Kelley's calorimetric entropy of the liquid at 298.2°K must be applied to all the entropies in exactly the same manner, and has no effect upon the difference between the entropies at two temperatures. Its application to the values in Table VII will make the barrier sum for the two rotations uncertain by about ±1000 cal., and will have little effect upon the relative value of this sum at the two temperatures.

A further interesting result of the new approximations to the third law entropy is that the empirical potential energy function of Aston, Isserow, Szasz, and Kennedy is not eliminated from consideration. It is still possible that a mean $\delta$-frequency and new methyl group barriers could be found which would lead to satisfactory agreement with the new entropy estimates.

The barrier combinations presented in Table VII are proposed only as a set of tentative solutions to the problem. They should be regarded as subject to revision whenever more extensive and accurate vapor densities are made available to permit better evaluations of the hypothetical perfect gas entropy. If, at the same time, the results can be made consistent with accurate vapor heat capacities over an extended temperature range, it will become possible to assign reliable molecular constants.

[8] J. O. Halford, L. C. Anderson, and G. H. Kissin, J. Chem. Phys. 5, 927 (1937).

THE JOURNAL OF CHEMICAL PHYSICS VOLUME 17, NUMBER 2 FEBRUARY, 1949

# The Superficial Density of Matter at a Liquid-Vapor Boundary

RICHARD C. TOLMAN
*California Institute of Technology, Pasadena, California*
(Received July 19, 1948)

The distribution of matter within the transition layer between the two phases of a fluid system is considered. Approximate values are obtained for the superficial density of matter $\Gamma$, calculated with reference to the Gibbs surface of tension as the dividing surface between the phases.

## I. INTRODUCTION

IN accordance with the Gibbs theory of capillarity as applied to the surface between a one-component liquid and its vapor, it is found that the surface tension $\sigma$ at the boundary and the Gibbs potential $\mu$ for the fluid should be connected at constant temperature by the equation[1]

$$d\sigma = -\Gamma d\mu, \tag{I.1}$$

where $\Gamma$ is the so-called superficial density of matter at the boundary. This quantity $\Gamma$ may be defined as the difference—per unit area of boundary surface—between the actual amount of fluid in the two-phase system and the amount which it would contain if the liquid and vapor phases retained uniform densities to the Gibbs surface of tension as the dividing surface between the phases.

In order to make actual applications of this important equation, it is necessary to have a value for the superficial density $\Gamma$ at the liquid-vapor boundary in question. It is the purpose of the present article to calculate the values that can be expected for $\Gamma$ in the case of typical fluid systems such as are commonly investigated in experiments on surface tension.

The calculations will involve certain assumptions and approximations which cannot be regarded as strictly correct. Nevertheless, it is believed that the treatment will be sufficiently sound to provide reliable results for the sign and order of magnitude of $\Gamma$. This is important for understanding the consequences of the Gibbs theory, since previously it has not even been clear whether the superficial density would have a positive or negative sign when referred to the surface of tension. Application of the results obtained will be made in a subsequent article.

We may now proceed to the derivation of the desired relations. Since this proves to be a somewhat lengthy and involved task, we may begin by giving a brief outline of the sequence of treatment.

In the immediately following Section II, we shall use van der Waals' equation to investigate the values of fluid pressure and density to be expected in the transition layer between phases. We shall thereby be led to quantitative results needed in the subsequent development, as well as to the important qualitative conclusion that the density of the fluid $\gamma$ can be expected, on passage through the layer from vapor to liquid, first to rise continuously from its value $\gamma''$ in the bulk of the vapor to a maximum value $\gamma_{max}$ possible for vapor, then to rise abruptly to a minimum value $\gamma_{min}$ possible for liquid, and then finally to rise again continuously to the value $\gamma'$ which it has in the bulk of the liquid.

In Section III, we shall consider the condition of the fluid as a function of position within the transition layer, and shall introduce approximate expressions giving fluid pressure—first as a function of position as we pass through the vapor phase from the region of homogeneous vapor to the point of abrupt change in density and pressure—and then as a function of position as we pass from this point through the liquid phase to the region of homogeneous liquid.

In Section IV, we shall then substitute our expressions for fluid pressure as a function of position into two previously derived relations,[2] which give surface tension $\sigma$ in terms of pressure distribution, and give a condition on the location of the surface of tension also in terms of pressure

[1] J. W. Gibbs, *Collected Works*, (Longmans Green and Company, New York, 1928), Vol. I, Eq. (508), p. 230.

[2] R. C. Tolman, J. Chem. Phys. **16**, 758 (1948).

distribution. The first of these substitutions will provide information as to the magnitudes of the parameters that appear in our selected expressions for pressure as a function of position, and the second substitution will allow us to fix the location of the surface of tension in the transition layer.

In Section V, we shall now have all that is necessary to calculate values of the superficial density $\Gamma$ by evaluating the appropriate integrals for density differences as a function of position on the two sides of the surface of tension. The values found for $\Gamma$ will, of course, depend on the nature and temperature of the fluid, but will, in general, be positive in typical cases.

Finally, in Section VI, we shall make some concluding remarks as to the extent of validity that can be expected for our results.

## II. APPLICATION OF VAN DER WAALS' EQUATION

### a. Introduction of the Equation

In order to investigate the distribution of fluid within the transition layer between a liquid and its vapor, we shall need to have a relation connecting the pressure of the fluid at the temperature of interest with the succession of fluid densities that would be encountered on passing through the transition layer from one phase to the other. To meet this need we shall make use of the familiar equation of van der Waals,

$$[p+(a/v^2)](v-b)=RT. \tag{II.1}$$

It is appreciated that this equation does not give an exact representation of $p$, $v$, $T$ relations for any actual fluid. Nevertheless, it appears to be the obvious equation to adopt for our purposes as a first approximation, and we shall comment briefly later in Section VI on the validity of its application.

For our use, it will be desirable to re-express Eq. (II.1) by considering its application to unit mass of fluid. Replacing the volume $v$ by the reciprocal of the density of the fluid $\gamma$, and solving for pressure $p$, we can then evidently write

$$p=(\gamma rT/1-\gamma/\gamma_\infty)-a\gamma^2, \tag{II.2}$$

where $r$ is the gas constant per unit mass of the fluid, and $a$ and $1/\gamma_\infty=b$ are the previous van der Waals' constants taken for unit mass.

TABLE I. Choice of parameters.

| $a\gamma'/rT$ | 5 | 7 | 8 | 9 | 10 | 11 | 13 | Chosen |
|---|---|---|---|---|---|---|---|---|
| $\gamma'/\gamma_\infty$ | 0.8 | 0.8571 | 0.875 | 0.8889 | 0.9 | 0.9091 | 0.9231 | See Eq. (II.10) |
| $\gamma'/\gamma''$ | 80.69 | 425.9 | 1013 | 2447 | 5988 | 14800 | 92530 | See Eq. (II.11) |

### b. Conditions on Parameters

In applying van der Waals' Eq. (II.2) to our problem we shall want to select values, or a range of values, for the parameters in the equation that will correspond to the conditions that are encountered in usual surface tension measurements.

For the parameter $r$, which is the gas constant per unit mass of the fluid, we can, of course, immediately take

$$r=R/M, \tag{II.3}$$

where $R$ is the gas constant per mole and $M$ the molecular weight of the fluid.

To obtain a first condition on the other two parameters $a$ and $\gamma_\infty$ we can make use of the circumstance that we are going to be concerned, at least for the present, with plane surfaces of separation between liquids and vapors at temperatures well below the boiling point. We can then take the pressures $p'$ and $p''$ in the interior of the homogeneous parts of the liquid and vapor phases as equal and small,

$$p'=p''=p_0\approx 0, \tag{II.4}$$

where $p_0$ is the ordinary vapor pressure of the liquid for a plane surface, and by the order zero we mean small compared with the large values that will be assumed by the quantities on the right-hand side of (II.2) on substitution of the large value $\gamma'$ for the density of the liquid. As a consequence we see that we can then take

$$1/(1-\gamma'/\gamma_\infty)=(a\gamma'/rT) \tag{II.5}$$

as giving a closely approximate condition on the values of the parameters $\gamma_\infty$ and $a$.

To obtain a second condition on the values of these parameters, we can write in accordance with a well-known thermodynamic consequence of van der Waals' equation, the relation

$$\int_{\gamma''}^{\gamma'}\left(\frac{\gamma rT}{1-\gamma/\gamma_\infty}-a\gamma^2\right)\frac{d\gamma}{\gamma^2}=\int_{\gamma''}^{\gamma'}p_0\frac{d\gamma}{\gamma^2}, \tag{II.6}$$

TABLE II. Limiting values of pressure and density.

| $a\gamma'/rT$ | 5 | 7 | 8 | 9 | 10 | 11 | 13 | Chosen |
|---|---|---|---|---|---|---|---|---|
| $\gamma_{max}/\gamma'$ | 0.123 | 0.083 | 0.071 | 0.062 | 0.055 | 0.050 | 0.042 | See Eq. (II.13) |
| $\gamma_{min}/\gamma'$ | 0.811 | 0.823 | 0.829 | 0.835 | 0.840 | 0.845 | 0.853 | See Eq. (II.13) |
| $p_{max}/\gamma' rT$ | 0.061 | 0.041 | 0.035 | 0.031 | 0.028 | 0.025 | 0.021 | See Eq. (II.14) |
| $-p_{min}/\gamma' rT$ | 0.980 | 1.947 | 2.479 | 3.036 | 3.614 | 4.208 | 5.446 | See Eq. (II.14) |
| $p_0/\gamma' rT$ | $1.24\ 10^{-2}$ | $2.35\ 10^{-3}$ | $9.87\ 10^{-4}$ | $4.09\ 10^{-4}$ | $1.67\ 10^{-4}$ | $6.76\ 10^{-5}$ | $1.08\ 10^{-5}$ | $\gamma''/\gamma'$ from Table I |

which equates two different expressions for the reversible isothermal work that would accompany the transformation of unit mass of vapor into liquid, in one case by passing through all the intermediate metastable and unstable equilibrium states, predicted by van der Waals' equation as having densities between that of the vapor $\gamma''$ and that of the liquid $\gamma'$, and in the other case by carrying out a direct condensation at the vapor pressure $p'=p''=p_0$. Performing the indicated integrations, we can then write

$$rT\log\frac{\gamma'(1-\gamma''/\gamma_\infty)}{\gamma''(1-\gamma'/\gamma_\infty)}-a(\gamma'-\gamma'')=\frac{p_0}{\gamma''}-\frac{p_0}{\gamma'}, \quad \text{(II.7)}$$

or, since we shall be interested in applying this result at temperatures where the vapor is sufficiently dilute, so that we can take

$$\gamma''\ll\gamma'<\gamma_\infty, \quad \text{and} \quad p_0=p''=\gamma''rT, \quad \text{(II.8)}$$

we can rewrite this in the approximate form

$$\log\frac{\gamma'}{\gamma''}=\log\left(1-\frac{\gamma'}{\gamma_\infty}\right)+\frac{a\gamma'}{rT}+1, \quad \text{(II.9)}$$

which gives us a second condition connecting the parameters $\gamma_\infty$ and $a$.

Finally, by solving Eq. (II.5), and by substitution in Eq. (II.9), we can write

$$\gamma'/\gamma_\infty=1-(rT/a\gamma'), \quad \text{(II.10)}$$

and

$$\log(\gamma'/\gamma'')=1+(a\gamma'/rT)-\log(a\gamma'/rT), \quad \text{(II.11)}$$

as the equations which we shall wish to use in determining appropriate values for the parameters.

### c. Choice of Parameters

The foregoing equations will now permit us to relate the dimensionless quantity $a\gamma'/rT$, containing the parameter $a$, both to the dimensionless quantity $\gamma'/\gamma_\infty$, containing the parameter $\gamma_\infty$, and to the observed ratio $\gamma'/\gamma''$ between the densities of the fluid in liquid and vapor form. Taking a range of values for $a\gamma'/rT$ that will cover the desired range of applications, we have used Eqs. (II.10) and (II.11) to calculate the values of $\gamma'/\gamma_\infty$ and $\gamma'/\gamma''$ given in Table I.

It will be noted from Table I that we have chosen a range of values for $a\gamma'/rT$ that corresponds to a wide range of possible values for the observed ratio $\gamma'/\gamma''$, between the densities, in liquid and vapor form, of fluids that we may wish to consider. As will be seen later in Section V, this will be sufficient to permit a wide variation in the substances and temperatures to which our results can be applied.

### d. Limiting Values of Pressure and Density

We are now ready to use van der Waals' Eq. (II.2) to provide information as to the values of density and pressure that the fluid can be expected to assume as we pass through the transition layer from the homogeneous part of the vapor phase at density $\gamma''$ and pressure $p''=p_0$ to the homogeneous part of the liquid phase at density $\gamma'$ and, in the case of plane dividing surfaces, again at the pressure $p'=p''=p_0$. For this purpose we may first consider the maximum and minimum values of pressure which are known to be predicted by van der Waals' equation for temperatures below critical.

Differentiating (II.2) with respect to $\gamma$, we have

$$\frac{dp}{d\gamma}=\frac{rT}{(1-\gamma/\gamma_\infty)^2}-2a\gamma \quad \text{(II.12)}$$

for the rate of change of pressure with density. Setting this expression equal to zero, and rearranging so as to express the result in conveni-

ent form, we then obtain

$$\left(1-\frac{\gamma'}{\gamma_\infty}\frac{\gamma}{\gamma'}\right)^2\frac{\gamma}{\gamma'}=\frac{1}{2}\frac{rT}{a\gamma'} \qquad \text{(II.13)}$$

as an equation which determines the values of density $\gamma$ at which the pressure $p$ passes through a maximum or minimum.

In accordance with its cubic form, this equation has three solutions for the value of $\gamma$ at which $p$ is an extremum. At temperatures below critical, the smallest of these values occurs at a point which we may label $(\gamma_{max}, p_{max})$ where the pressure passes through a maximum, the next value occurs at a point $(\gamma_{min}, p_{min})$ where the pressure passes through a minimum, and the third solution is not of physical interest since it occurs at a value of $\gamma$ greater than $\gamma_\infty$.

Substituting the numerical values of $a\gamma'/rT$ and $\gamma'/\gamma_\infty$ given in Table I as covering the range of interest, we can obtain numerical solutions of (II.13) for the values of $\gamma/\gamma'$ at which the maximum and minimum of pressure occur. And rewriting van der Waals' Eq. (II.2) in a form which is more convenient for our present purposes,

$$p=\gamma' rT\left\{\frac{\gamma/\gamma'}{1-\frac{\gamma'}{\gamma_\infty}\frac{\gamma}{\gamma'}}-\frac{a\gamma'}{rT}\left(\frac{\gamma}{\gamma'}\right)^2\right\}, \qquad \text{(II.14)}$$

we can also calculate the values of $p/\gamma' rT$ at these points of maximum and minimum pressure. The results of the calculations are given in Table II, where we also include a final line giving values of $p_0/\gamma' rT$ where $p_0=p'=p''$ is the vapor pressure.

It will be seen from Table II, for the range of values of $a\gamma'/rT$ considered, that the densities $\gamma_{max}$ at the pressure maximum are small compared with the densities $\gamma_{min}$ at the pressure minimum. It will also be seen that the vapor pressures $p_0$ are small compared with the maximum pressures $p_{max}$, and that these in turn are small compared with the negative pressures $-p_{min}$ at the pressure minimum. It will further be noted that the values of the ratios $\gamma_{max}/\gamma_{min}$, $p_0/p_{max}$ and $p_{max}/-p_{min}$ decrease as we go to larger values of $a\gamma'/rT$. These findings will play a role in our later introduction of approximations. It may be remarked in this connection that the value of $a\gamma'/rT$ will be greater than 7 in all but one of the applications which we shall make.

The determination of the points $(\gamma_{max}, p_{max})$ and $(\gamma_{min}, p_{min})$ is of importance in setting the upper limit for the stable and metastable states of vapor that can exist at densities less than $\gamma_{max}$, and the lower limit for the stable and metastable states of liquid that can exist at densities greater than $\gamma_{min}$. States of the fluid at densities between $\gamma_{max}$ and $\gamma_{min}$ would be highly unstable since increase in density would be accompanied by decrease in pressure. In this connection it is illuminating to think of $p_{max}$ as the maximum pressure which the vapor can withstand without collapse, and $-p_{min}$ as the maximum tension which the liquid can withstand without rupture. Extended regions containing fluid at densities between $\gamma_{max}$ and $\gamma_{min}$ are not to be expected.

### e. Sequence of Values of Density and Pressure in the Transition Layer

We can now use the results of the foregoing discussion to predict the sequence of values of fluid density that we might expect to encounter on passage through the transition layer from vapor to liquid. Because of the short range of molecular forces, the density of the vapor can be expected to remain substantially constant at the value $\gamma=\gamma''$ which it has in the bulk of the vapor, until we come very close to the liquid. Under the action of attraction from the "liquid face," it can then be expected to rise at a rapidly increasing rate until it reaches the value $\gamma=\gamma_{max}$ at the upper limit of metastable vapor states. At this point we have $d\gamma/dp=\infty$, and the density can be expected to rise abruptly—through the range of densities corresponding to unstable states—to the value $\gamma=\gamma_{min}$ at the lower limit of metastable liquid states. Beyond this point, the density can then again be expected to increase at a slowly diminishing rate until it reaches the substantially constant value $\gamma=\gamma'$ in the bulk of the liquid.

The foregoing picture for the sequence of density changes also implies a corresponding picture for the sequence of pressure changes, which will prove useful in the next section. In accordance with the relation between pressure and density given by van der Waals' equation,

we are led to conclude, on considering passage through the transition layer from vapor to liquid, that the fluid pressure will first rise at a continuously increasing rate from its value $p=p''=p_0$ in the interior of the vapor to the maximum value $p=p_{max}$ possible for vapor, will then fall abruptly to the minimum value $p=p_{min}$ possible for liquid, and then finally will again rise at a continuously decreasing rate to its value $p=p'=p_0$ in the interior of the liquid. We note the contrast to the unreversed rise in fluid density on passage from vapor to liquid.

## III. CONDITION OF FLUID AS A FUNCTION OF POSITION IN THE TRANSITION LAYER

The preceding section has provided qualitative information as to the sequence of fluid conditions to be expected on passage through the transition layer but has not provided any quantitative expressions for the condition of the fluid as a definite function of position in the layer. To meet this need, in the absence of a complete theory of fluid distribution in the layer, we shall now introduce approximate expressions, having a rational form compatible with available knowledge, and containing adjustable parameters with values to be determined later.

In formulating the desired expressions for fluid condition as a function of position, it is expedient to specify the condition of the fluid at any point by its pressure $p$, rather than by its density $\gamma$, since the rate of change of density with position becomes very large compared with the rate of change of pressure with position in regions where $d\gamma/dp$ approaches infinity. Hence, let us now consider the pressure of the fluid $p$ as a function of a variable $y$, which we introduce to designate distances along an axis normal to the dividing surface between phases, and which we take as increasing in the direction from vapor to liquid, with the value $y=0$ at the point of abrupt change in density and pressure.

As appropriate expressions for pressure as a function of position, we shall than take

$$p-p''=(p_{max}-p'')e^{+y/\lambda_v}, \qquad \text{(III.1)}$$

as holding over the range of vapor states from $y=-\infty$ to the point $y=0$ where the abrupt change in density and pressure occurs, and shall take

$$p-p'=(p_{min}-p')e^{-y/\lambda_l}, \qquad \text{(III.2)}$$

as holding over the range of liquid states from $y=0$ to $y=\infty$. The quantities $\lambda_v$ and $\lambda_l$ in these expressions are parameters whose values will be later considered.

These expressions are consonant with the information that we do have as to the distribution of fluid in the transition layer, and appear to be the most reasonable three parameter approximations that we can introduce at this stage. In accordance with (III.1), as we pass from $y=-\infty$ to $y=0$, the pressure $p$ will rise from its value $p''$ in the bulk of the vapor phase to its maximum possible value $p_{max}$, asymptotically as we leave the interior of the vapor, and at a continuously increasing rate as we approach the "liquid face" exerting its strong, short range, attractive forces. And in accordance with (III.2), as we pass from $y=0$ to $y=+\infty$, the pressure $p$ will rise from the minimum value $p_{min}$ possible for liquid states to the value $p'$ in the bulk of the liquid phase, at a continuously decreasing rate which gives asymptotic approach to the final conditions in the interior of the liquid. In accordance with van der Waals' equation, these changes in pressure will be accompanied by corresponding changes in density, where it will be noted that $d\gamma/dy$ becomes positive infinite at $y=0$, in agreement with our original picture of the abrupt increase in density at that point.

## IV. APPLICATION OF PREVIOUSLY DERIVED EXPRESSIONS FOR SURFACE TENSION AND FOR THE LOCATION OF THE SURFACE OF TENSION

We may now consider the application to our present problem of two already existing expressions, for the magnitude of surface tension and for the location of the surface of tension, which have been previously derived for a one-component, two-phase system by treating the fluid within the transition layer by usual thermodynamic methods. These expressions, which are specialized for the case of spherical surfaces of separation, are of the form[3]

$$\sigma=\int_{-a}^{0}(p'-p)(1+cx)^2dx + \int_{0}^{b}(p''-p)(1-cx)^2dx, \qquad \text{(IV.1)}$$

[3] See reference 2, Eqs. (12.6) and (12.7).

TABLE III. Factors for computation of Γ.

| $a\gamma'/rT$ | 5 | 7 | 8 | 9 | 10 | 11 | 13 | Chosen |
|---|---|---|---|---|---|---|---|---|
| $A$ | 0.908 | 0.910 | 0.922 | 0.929 | 0.931 | 0.934 | 0.940 | See Eq. (V.8) |
| $B\times10^{8}$ | 1.114 | 0.5619 | 0.4772 | 0.3680 | 0.3097 | 0.2669 | 0.2075 | See Eq. (V.9) |
| $C\times10^{-8}$ | 0.8977 | 1.780 | 2.236 | 2.717 | 3.229 | 3.747 | 4.819 | See Eq. (V.10) |
| $\log_{10}\gamma'/\gamma''$ | 1.9068 | 2.6293 | 3.0056 | 3.3888 | 3.7773 | 4.1702 | 4.9663 | See Table I |

and

$$0=\int_{-a}^{0}(p'-p)(1+cx)xdx+\int_{0}^{b}(p''-p)(1+cx)xdx, \quad \text{(IV.2)}$$

where $p$, $p'$, and $p''$ have the same significance as in the foregoing, $c$ is the curvature of the surface of tension, and the integrations are taken with respect to a variable $x$ which designates distances normal to the surface of tension and which increases in the direction from liquid to vapor with the value $x=0$ at the surface of tension and the values $x=-a$ and $x=b$ at points where the fluid reaches conditions in substantial agreement with those for the contiguous homogeneous phase.

To make use of Eqs. (IV.1) and (IV.2) in the present connection, we shall wish to substitute the expressions for $(p-p'')$ and $(p-p')$ given by (III.1) and (III.2) in the preceding section. In doing so, we note that the variable $x$ in (IV.1) and (IV.2) and the variable $y$, which we found convenient for setting up the expressions (III.1) and (III.2), are connected by the relation

$$x=y_t-y, \quad \text{(IV.3)}$$

where $y_t$ gives the position of the surface of tension as measured from the point of abrupt rise in density in the direction from vapor to liquid. We further note that we can also take

$$c=0, \quad \text{and} \quad p''\equiv p'=p_0, \quad \text{(IV.4)}$$

since we are now concerned with plane dividing surfaces, where we have zero curvature $c$ and have internal pressures in the two phases equal to the ordinary vapor pressure $p_0$.

Making the suggested substitutions, and expressing the results in terms of integrals taken with respect to the variable $y$, it will be seen that we can now obtain the expressions

$$\sigma=\int_{-\infty}^{0}(p_0-p_{\max})e^{y/\lambda_v}dy+\int_{0}^{\infty}(p_0-p_{\min})e^{-y/\lambda_l}dy, \quad \text{(IV.5)}$$

and

$$0=\int_{-\infty}^{0}(p_0-p_{\max})e^{y/\lambda_v}(y_t-y)dy+\int_{0}^{\infty}(p_0-p_{\min})e^{-y/\lambda_l}(y_t-y)dy. \quad \text{(IV.6)}$$

Performing the indicated integrations, we then find, as expressions for surface tension and for the location of the surface of tension,

$$\sigma=(p_0-p_{\max})\lambda_v+(p_0-p_{\min})\lambda_l, \quad \text{(IV.7)}$$

and

$$y_t=\frac{-(p_0-p_{\max})\lambda_v^2+(p_0-p_{\min})\lambda_l^2}{(p_0-p_{\max})\lambda_v+(p_0-p_{\min})\lambda_l}. \quad \text{(IV.8)}$$

In order to make use of these equations, we may now introduce some approximations. In accordance with our discussion of the figures given in Table II, we can take

$$p_0\ll p_{\max}, \quad p_0\ll|p_{\min}|, \quad p_{\max}\ll|p_{\min}|. \quad \text{(IV.9)}$$

Furthermore, in accordance with the form of our expressions (III.1) and (III.2) and in accordance with the short range of molecular forces, it would seem reasonable to take

$$\lambda_v\approx \text{ or } <\lambda_l, \quad \text{(IV.10)}$$

since we can expect the rise in the pressure of the vapor from $p''$ to $p_{\max}$ to be sharply concentrated as we approach the "liquid face," and the rise in pressure of the liquid from $p_{\min}$ to $p'$ to take place as the result of increasing liquid density. Accepting these relations, we then see that Eqs. (IV.7) and (IV.8) would reduce to the

simplified approximate forms

$$\sigma = -p_{\min}\lambda_t \quad \text{and} \quad y_t = \lambda_t. \qquad \text{(IV.11)}$$

Dropping the subscript of $\lambda_t$, and noting the approximations that can be introduced in (III.2), we may now write, as the expressions which we shall need in the next section,

$$\lambda = \frac{-\sigma}{p_{\min}}, \quad y_t = \lambda, \quad \text{and}$$

$$p = p_{\min} e^{-y/\lambda} \quad (0 < y < \infty), \qquad \text{(IV.12)}$$

where the first of these relations will permit us to determine $\lambda$ from experimental values of $\sigma$ and calculated values of $p_{\min}$, the second relation will then give us the location of the surface of tension as measured from the point of abrupt rise in density at $y=0$, and the third relation will give us the fluid pressure for the range of liquid states beyond that point.

## V. CALCULATION OF SUPERFICIAL DENSITY

### a. Deduction of Relations

We now have all that is needed to undertake the determination of superficial density $\Gamma$. In accordance with the definition of that quantity, it is evident that we can write

$$\Gamma = \int_{-\infty}^{y_t} (\gamma - \gamma'')dy + \int_{y_t}^{\infty} (\gamma - \gamma')dy, \qquad \text{(V.1)}$$

where we integrate the excess density above that for homogeneous vapor up to the surface of tension, and integrate the excess density above that for homogeneous liquid from that point on—the first of the integrals being actually positive in value and the second negative. In view of the small value of $\gamma''$ and of the small values of $\gamma$ until we reach the point $y=0$ (see Tables I and II), we shall now approximate this expression by

$$\Gamma = \int_0^{\lambda} \gamma dy + \int_{\lambda}^{\infty} (\gamma - \gamma')dy$$

$$= \lambda\gamma' + \int_0^{\infty} (\gamma - \gamma')dy$$

$$= \lambda\gamma' - \gamma' \int_0^{\infty} \left(1 - \frac{\gamma}{\gamma'}\right) dy, \qquad \text{(V.2)}$$

where we have substituted $y_t = \lambda$ in accordance with (IV.12).

In order to re-express the integral in this equation in a form which can be evaluated, we note by equating the expressions for pressure given by (II.15) and (IV.2) that we can write

$$p_{\min} e^{-y/\lambda} = \gamma' rT \left\{ \frac{\gamma/\gamma'}{1 - (\gamma'/\gamma_\infty)(\gamma/\gamma')} - \frac{a\gamma'}{rT}\left(\frac{\gamma}{\gamma'}\right)^2 \right\}, \qquad \text{(V.3)}$$

as a valid relation over the range of values of $y$ from zero to infinity and over the corresponding range of values of $\gamma/\gamma'$ from $\gamma_{\min}/\gamma'$ to unity. Introducing into (V.3) the convenient abbreviations

$$\frac{\gamma}{\gamma'} = z, \quad \frac{\gamma'}{\gamma_\infty} = g \quad \text{and} \quad \frac{a\gamma'}{rT} = \frac{1}{1-g} \text{ (cf. II.5)} \qquad \text{(V.4)}$$

and then differentiating with respect to $y$ and $z$, we can now obtain

$$dy = -\lambda \left\{ \frac{1}{z} + \frac{g}{1-gz} - \frac{1-2gz}{(1-z)(1-g-gz)} \right\} dz, \qquad \text{(V.5)}$$

as an expression for $dy$ in terms of $z$ and $dz$. Substituting in (V.2), we may then write our expression for $\Gamma$ in a form

$$\Gamma = \lambda\gamma' \left\{ 1 + \int_{z=\gamma_{\min}/\gamma'}^{z=1} \left[ \frac{1}{z} - 1 + \frac{g}{1-gz} - \frac{gz}{1-gz} - \frac{1}{1-g-gz} + \frac{2gz}{1-g-gz} \right] dz \right\}, \qquad \text{(V.6)}$$

where the integral can be readily evaluated.

TABLE IV. Values of superficial density $\Gamma$ at 20°C.

| Substance | $M$ g | $\sigma$ dyne/cm | $\gamma'$ g/cm³ | $\gamma''$ $10^{-6}$g/cm³ | $\Gamma$ $10^{-8}$g/cm² | $\Gamma/(\gamma'-\gamma'')$ $10^{-8}$ cm | $(M/N_0\gamma')^{\frac{1}{3}}$ $10^{-8}$ cm |
|---|---|---|---|---|---|---|---|
| Water | 18.016 | 72.75 | 0.9982 | 1.73 | 0.98 | 0.99 | 3.11 |
| Methyl alcohol | 32.04 | 22.61 | 0.7915 | 16.95 | 0.80 | 1.01 | 4.07 |
| Ethyl alcohol | 46.07 | 22.27 | 0.7894 | 11.1 | 1.05 | 1.33 | 4.59 |
| Acetic acid | 60.05 | 27.63 | 1.0491 | 7.64 | 1.53 | 1.46 | 4.56 |
| Ethyl ether | 74.12 | 16.96 | 0.7135 | 187.0 | 2.49 | 3.50 | 5.57 |

Performing the integration indicated in (V.6) and substituting the limits given, we then obtain

$$\Gamma=\lambda\gamma'\left\{2\frac{\gamma_{\min}}{\gamma'}-1+\log\frac{\gamma'}{\gamma_{\min}}\right.$$

$$-\left(\frac{\gamma_\infty}{\gamma'}-1\right)\log\left(\frac{\gamma_\infty}{\gamma'}-\frac{\gamma_{\min}}{\gamma'}\Big/\frac{\gamma_\infty}{\gamma'}-1\right)$$

$$\left.+\left(2-\frac{\gamma_\infty}{\gamma'}\right)\log\frac{2-\dfrac{\gamma_\infty}{\gamma'}}{1+\dfrac{\gamma_{\min}}{\gamma'}-\dfrac{\gamma_\infty}{\gamma'}}\right\}, \quad \text{(V.7)}$$

as our desired expression for superficial density $\Gamma$ referred to the Gibbs surface of tension. This expression permits us to compute specific values for $\Gamma$ in terms of quantities that can be either directly measured or computed from appropriate values of van der Waals' constants. For the purpose of such computations the expression can be put into somewhat more usable forms.

Designating the sum of terms within the parentheses in (V.7) by the letter $A$, we can write

$$\Gamma=A\lambda\gamma', \quad \text{(V.8)}$$

where $A$ is a numerical factor that can be computed from appropriate values for $\gamma_{\min}/\gamma'$ and $\gamma'/\gamma_\infty$. Using the values of these quantities that are given in Tables I and II as corresponding to our selected range of values for $a\gamma'/rT$, we calculate for $A$ the values given in the second line of Table III, where the nearly constant value for the factor $A$ over a wide range of fluid conditions will be noted.

Furthermore, substituting into (V.8) the value of $\lambda$ in terms of surface tension $\sigma$ and of minimum pressure $p_{\min}$ as given by (IV.12), we can also write our expression for superficial density in the form

$$\Gamma=\frac{A\sigma\gamma'}{|p_{\min}|}=\frac{A\sigma M}{RT|p_{\min}|/\gamma' rT}=B\frac{\sigma M}{T}, \quad \text{(V.9)}$$

where $T$ and $M$ are the temperature and molecular weight of the fluid considered, and $B$ is a factor which can be computed from the value of the gas constant per mole $R$, and from the values of $A$ and of the ratio $|p_{\min}|/\gamma' rT$ as already given in Tables II and III. The calculated values of $B$ corresponding to different values of $a\gamma'/rT$ are given in the third line of Table III.

Table V. Superficial density of water 10°–50°C.

| Temperature °C | $\sigma$ dyne/cm | $\gamma'$ g/cm³ | $\gamma''$ $10^{-5}$g/cm³ | $\Gamma$ $10^{-5}$g/cm³ | $\Gamma/(\gamma'-\gamma'')$ $10^{-8}$ cm | $(M/N_0\gamma')^{\frac{1}{3}}$ $10^{-8}$ cm |
|---|---|---|---|---|---|---|
| 10 | 74.22 | 0.9997 | 0.941 | 0.96 | 0.96 | 3.11 |
| 20 | 72.75 | 0.9982 | 1.73 | 0.98 | 0.99 | 3.11 |
| 30 | 71.18 | 0.9957 | 3.035 | 1.00 | 1.01 | 3.11 |
| 40 | 69.56 | 0.9922 | 5.11 | 1.02 | 1.03 | 3.11 |
| 50 | 67.91 | 0.9881 | 8.32 | 1.05 | 1.06 | 3.12 |

Finally, we shall also find it useful to introduce the reciprocal of $B$ and rewrite our expression for superficial density in the form

$$\Gamma=(1/C')(\sigma M/T), \quad \text{(V.10)}$$

where $C=1/B$. This is a convenient form for application to observational data, since the computed values of $C$ are found to increase nearly linearly with computed values for $\log\gamma'/\gamma''$, where the densities $\gamma'$ and $\gamma''$ of the fluid in liquid and vapor form are quantities subject to direct experimental determination. The calculated values for $C$ and for $\log_{10}\gamma'/\gamma''$, which correspond to our selected range of values for $a\gamma'/rT$, are given in the last two lines of Table III, where interpolation is facilitated by the approximately linear relation between the two sets of quantities.

### b. Application to Observational Data

With the help of Eq. (V.10) and the values for $C$ and $\log_{10}\gamma'/\gamma''$ given in the last two lines of Table III, we may now compute numerical values for superficial density $\Gamma$ for two-phase fluid systems from given values of the surface tension $\sigma$ at the boundary, of the molecular weight $M$ and temperature $T$ of the fluid, and of the densities of the fluid $\gamma'$ and $\gamma''$ in the liquid and in the vapor phase. We have made such computations for several different fluids at the same temperature (20°), and for a single fluid (water) at different temperatures.

The data and results for five different fluids at 20°C are given in Table IV. The substances

considered are given in the first column in the order of increasing molecular weights, and the molecular weights $M$ are given in the second column. Values of the surface tension $\sigma$ at 20°C are given in the third column.[4] The values for the densities $\gamma'$ of the liquid and $\gamma''$ of the vapor at 20°C are given in the fourth and fifth columns.[5] And the desired values for the superficial density $\Gamma$ at the Gibbs surface of tension are then given in the sixth column, as calculated from Eq. (V.10) with the help of the last two lines in Table III.

In addition to $\Gamma$, two other quantities which are given in the two final columns of the table will be of interest. The first of these quantities, $\Gamma/(\gamma'-\gamma'')$, will be seen from the definition of $\Gamma$ as provided by Eq. (V.1) to give the distance, measured in the direction vapor to liquid, from a dividing surface located so as to make the superficial density vanish to the surface of tension with respect to which the superficial density has the value $\Gamma$. The second of the quantities, $(M/N_0\gamma')^{\frac{1}{3}}$, where $N_0$ is Avogadro's number, will be seen to give a measure of the distance between molecules of the liquid, treating them as points located in a cubical array.

The data and results for water at a series of temperatures from 10° to 50°C will be found in Table V. The sources of the data are the same as those already mentioned for the case of water in connection with the preceding table.

From Table IV, it would be concluded, for the liquid-vapor systems considered at 20°C, that the superficial density of matter $\Gamma$ referred to the surface of tension is a positive quantity of the order of 0.8 to $2.5\times10^{-8}$ g/cm², and that the distance $\Gamma/(\gamma'-\gamma'')$ from a dividing surface located so as to make the superficial density vanish to the surface of tension is of the order of 0.25 to 0.6 of intermolecular distances $(M/N_0\gamma')^{\frac{1}{3}}$ in the liquid.

From Table V, it would be concluded that the superficial density $\Gamma$ and the ratio of the distances $\Gamma/(\gamma'-\gamma'')$ to $(M/N_0\gamma')^{\frac{1}{3}}$ would be subject to a slight increase with temperature for a given liquid. This finding, together with the internal evidence in Table IV, would indicate that more concordant results would be found for different liquids if we could compare them at corresponding temperatures.

In connection with the foregoing results, it may be remarked that we could also have calculated values for the parameter $\lambda$, which determines the rate of exponential rise in the pressure of the liquid as we proceed from the value $p_{\min}$ at the point of abrupt change to the value $p_0$ in the interior of the liquid phase. Rewriting Eq. (V.8) in the form

$$\lambda=\Gamma/A\gamma', \qquad (V.11)$$

we see, in accordance with the values of $A$ in Table III and with the relation $\gamma''\ll\gamma'$, that the values of $\lambda$ would be 6 to 10 percent greater than the values given in the next to the last columns of Tables IV and V. Hence the distance $\lambda=y_t$ from the point of abrupt rise in density to the surface of tension will be of the order of magnitude of intermolecular distances in the liquid.

## VI. CONCLUDING REMARKS

In forming a judgment as to the degree of reliance to be placed on the foregoing results, we must begin by criticizing the general character of a method of investigation which treats microscopic distributions of matter by considerations primarily justified by their successful application to macroscopic distributions. In studying the behavior of matter in the transition layer between phases, we have treated it as a fluid which obeys a macroscopic equation of state (van der Waals' equation), and we have applied equations to its distribution (IV.1 and IV.2) which were themselves previously derived by the use of familiar macroscopic thermodynamic principles. It is evident from the outcome of the

[4] The values for surface tension $\sigma$ are taken from the *International Critical Tables*, (McGraw-Hill Book Company, Inc., New York, 1948), Vol. IV, pp. 447, 448, 449, and 451. Although our treatment is concerned with liquids in contact solely with vapor, we have actually taken values of $\sigma$ for liquids in contact with air as well as vapor. We have done this to obtain a consistent set of values including cases where measurements in the absence of air are not available. The small decreases in $\sigma$ resulting from the presence of air cannot be expected to have an important effect on our final figures.

[5] The values for the densities $\gamma'$ and $\gamma''$ for water are taken from the *Handbook of Chemistry and Physics* (Chemical Rubber Publishing Company, Cleveland, Ohio, 1946), thirtieth edition. See p. 1695 and p. 1876 ff. The values of $\gamma'$ and $\gamma''$ for the other liquids are from the results of Young as given in the tables of Landolt and Börnstein (Verlag Julius Springer, Berlin, 1923), fifth edition, Vol. I, Tables 79, 79d, 79g.

work itself, however, that the distribution of matter within the layer must change markedly within distances of the order of those between molecules. Hence the extent of the validity of our macroscopic modes of procedure is not clear. In justification for such a procedure, in agreement with our previous more extended discussion of the problem,[6] we can express the expectation, or at least the hope, that a more rigorous statistical mechanical treatment would lead to approximately similar results. And in extenuation for our procedure, we may emphasize the importance of doing the best we can at the present time to obtain information as to the sign and order of magnitude of the important quantity $\Gamma$.

Coming to more specific questions, we may next inquire into the validity of our use of van der Waals' equation as the equation of state for our fluid. In this connection it is to be emphasized that our method of selecting parameters for the equation is such as to secure values of $\gamma'$ and $\gamma''$ which agree with the empirical densities of liquid and vapor at each actual temperature of interest. This avoids the serious errors that might otherwise arise from the known strong dependence of van der Waals' constant $a$ on temperature. It may also be emphasized that we only need reliable results from the equation over a limited range of states. Nevertheless, it is not clear that van der Waals' equation with the adopted choice of parameters will give us a very accurate representation of the metastable liquid states that lie in the important range between $(\gamma_{\min}, p_{\min})$ and $(\gamma', p')$. We can perhaps be justified, however, in assuming that the equation does provide a correct qualitative picture of the succession of fluid states in the transition layer, and provides quantitative results of the correct order of magnitude.

We may next inquire into the validity of assuming exponential expressions of the form (III.1) and (III.2) to represent pressure as a function of position in the layer. In this connection we may again emphasize the rational character of these expressions, which was discussed in more detail in Section III, and may also emphasize the circumstance that the quantities $\lambda_v$ and $\lambda_l$ are treated as adjustable parameters with values left open for later determination in Section IV. It will also be appreciated that our final results will be primarily dependent on the values found for $\gamma_{\min}$ and $p_{\min}$ and will not be very sensitive to the exact way in which density and pressure rise from these values to their final values $\gamma'$ and $p'$ in the interior of the liquid. Indeed, if we make the extreme assumption that $\gamma$ and $p$ both rise linearly in a distance $l$ from their initial to their final values, we calculate values for $\Gamma$ of the same order of magnitude as those to which we have actually been led.

To complete this inquiry into validity, we must also consider the various simplifications which have been introduced in the course of the deductions. These, however, all appear to be based on approximations which are justified by the relative magnitudes of the quantities involved.

In the light of the foregoing discussion, we are led to the tentative conclusion that our method of treatment has provided a qualitatively correct picture of the transition layer between a liquid and its vapor, has demonstrated that the superficial density of matter $\Gamma$ referred to the surface of tension in our layer would be a positive quantity in cases of common interest, and has provided values for $\Gamma$ which are of the correct order of magnitude. This conclusion is reinforced by the general internal consistency of our picture as made evident in the course of the treatment. It is also reinforced by the reasonable character of our specific finding (see V.11) that the distances $\lambda$—from the surface where the abrupt rise in density takes place to the surface of tension where changes in curvature alone do not require work—would be of the order of magnitude of those between molecules. Our findings will be employed in a proposed later application.

[6] See reference 2—discussion in Section 16.

THE JOURNAL OF CHEMICAL PHYSICS VOLUME 17, NUMBER 2 FEBRUARY, 1949

# The Infra-Red and Raman Spectra of Dimethyl Mercury and Dimethyl Zinc*

H. S. GUTOWSKY**
*Mallinckrodt Chemical Laboratory, Harvard University, Cambridge, Massachusetts*
(Received July 19, 1948)

The infra-red spectra of dimethyl mercury and dimethyl zinc and the Raman spectrum of dimethyl mercury have been observed. A frequency assignment has been proposed for dimethyl mercury, and that of dimethyl zinc has been modified. The results support a linear C−M−C structure, in agreement with quantum-mechanical predictions, and also $D_{3h}'$ symmetry with essentially free rotation of the methyl groups. A normal coordinate analysis has been made of the fundamental frequencies and valence-type force constants deduced therefrom. The values of the force constants pertaining only to the methyl groups agree very well with values obtained in other molecules; others indicate the relatively easy deformability of the C−M−C figure axis. Differences between the dimethyl mercury and dimethyl zinc force constants indicate greater ionic character in the C−Zn bond. Values of 2.45 and $2.39\times10^5$ dynes/cm are obtained for the C−Hg and C−Zn stretching force constants. The relation of these values to current suggestions concerning the dependence of bond strengths on atomic parameters is briefly discussed.

## INTRODUCTION

DIMETHYL zinc[1] and several of the Group *IV* tetramethyl derivatives[2] appear to be the only metal alkyls whose infra-red and Raman spectra have been investigated in detail and reasonably complete frequency assignments proposed. However, many of the various M−C force constants have not been calculated from these assignments, and in general there is a lack of quantitative physical data for the metallo-organic compounds. Difficulty of preparation and handling are probably the main deterrents to their study, but these may be overcome by the exercise of reasonable care.

Further data on the metal alkyls are of interest for several reasons. The co-relation of bond force constants with atomic parameters requires a wide range of data, and reliable results for various M−C bonds are useful in this connection.[3] Quantum theory predicts certain bond hybridization in various cases, and structural determination from spectral data affords a check on the theory in favorable instances. Also, the nature and distance dependence of the repulsive forces restricting rotation of groups of atoms about a chemical bond is a problem of fundamental importance. Available data on ethane and dimethyl acetylene might profitably be extended to intermediate linear compounds $CH_3-M-CH_3$. Accordingly, a detailed investigation of the infra-red and Raman spectra of dimethyl mercury and dimethyl zinc was undertaken.

Several investigations of the spectra of these compounds have been reported. Fehér, Kolb, and Leverenz[4] give the results of two independent studies of the Raman spectra, including polarization measurements. They also discuss critically the earlier Raman data published by Pai[5] and Venkateswaran.[6] The infra-red spectrum of dimethyl zinc has been observed by Thompson, Linnett, and Wagstaffe,[1] who proposed a frequency assignment using the then available Raman data. They considered their results as most consistent with a linear C−Zn−C structure.

## EXPERIMENTAL

### 1. Dimethyl Mercury

a. Preparation of sample. The dimethyl mercury used in these experiments was prepared by

* Based on a thesis submitted in partial fulfillment of the requirements for the Ph.D. degree at Harvard University. The research reported herein was facilitated by support extended Harvard University by the Navy Department, Office of Naval Research, under ONR Contract N5ori76.
** Present address: Department of Chemistry, University of Illinois, Urbana, Illinois.
[1] H. W. Thompson, J. W. Linnett, and F. J. Wagstaffe, Trans. Faraday Soc. **36**, 797 (1940).
[2] C. W. Young, J. S. Koehler, and D. S. McKinney, J. Am. Chem. Soc. **69**, 1410 (1947).
[3] W. Gordy, J. Chem. Phys. **14**, 305 (1946).
[4] F. Fehér, W. Kolb, and L. Leverenz, Zeits. f. Naturforsch. **2a**, 454 (1947).
[5] N. G. Pai, Proc. Roy. Soc. (London) **A149**, 29 (1935).
[6] S. Venkateswaran, Ind. J. Phys. **5**, 145 (1930).

the reaction between $CH_3MgBr$ and $HgCl_2$ in ether solution.[7] It was purified by redistillation over freshly precipitated $Ag_2O$. The product used had a boiling point range of 92.3 to 92.5°C at 772 mm.

b. Infra-red spectrum. Measurements were made on the gas in a 30-cm cell with KBr windows using the automatic prism spectrometer described by Gershinowitz and Wilson,[8] subsequently modified.[9] All spectral data were obtained at room temperature. Pressures of 4.7, 2.6, and 0.5 cm of the gas were used. Since the vapor pressure of dimethyl mercury is only 6.5 cm at room temperature, the absorption of the liquid was also measured, primarily to determine whether any bands were missing in the gas at the low pressures used. The liquid was run in a 0.13-mm NaCl cell on a Baird Associates infra-red spectrophotometer.[10] The absorption curves for gas and liquid are given in Figs. 1 and 2, respectively, and the band frequencies are summarized in Table I. The band at 1125 $cm^{-1}$ in the liquid spectrum, 1135 $cm^{-1}$ in the gas, appeared only in samples which had been exposed to light for long periods of time and is attributed to an impurity formed by photo-chemical decomposition, perhaps $CH_3-Hg-Hg-CH_3$.[11] The calibration of the Harvard spectrometer was checked during the period of operation, and the data from it are probably accurate to $\pm 2$ $cm^{-1}$ at wave-lengths below 2000 $cm^{-1}$ and $\pm 5$ $cm^{-1}$ above. For the Baird instrument, the calibration is well within the manufacturer's maximum tolerances of $\pm 0.02$ micron, or $\pm 1.0$ $cm^{-1}$ at 625 $cm^{-1}$ and $\pm 15$ $cm^{-1}$ at 3000 $cm^{-1}$.

c. The Raman spectrum. Since Pai's observations[5] of the Raman spectrum do not include polarization data, and the author was unaware of Fehér's[4] work at the time, it seemed advisable to re-examine the Raman spectrum and make polarization determinations. The spectrograph used[12] will be described in detail elsewhere at a later date. The dispersion is approximately 48.3A/mm in the region of the Hg 4358.3A line which was used as the exciting line in these experiments; shorter wave-lengths were eliminated with a Wratten 2A filter.

Polarization data were obtained by the use of

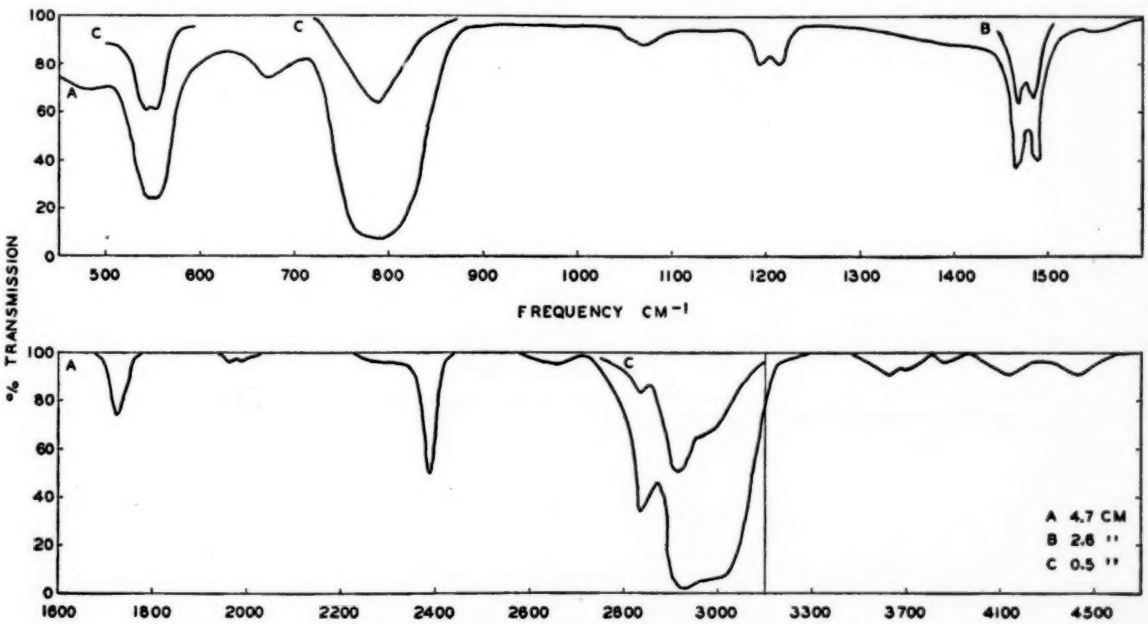


FIG. 1. Infra-red absorption spectrum of $Hg(CH_3)_2$ gas.

[7] H. Gilman and R. E. Brown, J. Am. Chem. Soc. 52, 3314 (1930).
[8] H. Gershinowitz and E. B. Wilson, Jr., J. Chem. Phys. 6, 197 (1938).
[9] W. L. Hyde, 1948 Ph.D. thesis, Harvard University.
[10] W. S. Baird, H. M. O'Bryan, G. Ogden, and D. Lee, J. Opt. Soc. Am. 37, 754 (1947).
[11] F. O. Rice and B. L. Evering, J. Am. Chem. Soc. 56, 2105 (1934).
[12] W. E. Brown, 1948 Ph.D. thesis, Harvard University.

TABLE I. The infra-red spectrum of $Hg(CH_3)_2$, gas and liquid.*

| Gas ν cm⁻¹ | | Liquid ν cm⁻¹ | |
|---|---|---|---|
| 550 | (8) | | |
| 675 | (1) | | |
| 788 | (9) | 778 | (10) |
| 1070 | (2a) | 1050 | (2) |
| | | 1125 | (1) impurity |
| 1205 | (2a) | 1190 | (5) |
| 1475 | (6a) | 1445 | (8a) |
| 1735 | (3) | 1720 | (4) |
| 1980 | (0a) | 1950 | (1a) |
| 2390 | (5) | | |
| 2660 | (0) | | |
| 2835 | (6) Only | 2885 | (10) unresolved |
| 2970 | (10a) partially resolved | | |
| 3660 | (1a) | 3630 | (2a) |
| 3855 | (0) | 3840 | (0) |
| 4150 | (1) | 4140 | (2) |
| 4435 | (1) | 4400 | (3) |

* a, bimodal band; the $cm^{-1}$ value is for the band center. The numbers after the band frequency are relative apparent intensities.

Polaroid, separate exposures being made with the plane of polarization parallel to and perpendicular to the axis of the Raman tube as suggested by Edsall and Wilson.[13] Semiquantitative estimates of the degree of polarization were made by comparing microphotometer tracings of the $\parallel$ and $\perp$ exposures analogous to the method described by Crawford and Horwitz.[14] The various results are included in Table II.

### 2. Dimethyl Zinc

a. Preparation of sample. Two samples of $Zn(CH_3)_2$ were used. The first of these was prepared by heating $Hg(CH_3)_2$ with an excess of granular zinc in a sealed Pyrex tube at about 185°C for five days. The other sample was furnished through the kindness of Professor E. G. Rochow. It had been prepared by the reaction between zinc and methyl iodide.

b. Infra-red spectrum. The observed infra-red spectrum of the gas is given in Fig. 3, and the data are summarized in Table III, along with the results of Thompson, Linnett, and Wagstaffe.[1] The parts of the spectrum marked B were observed with the Harvard instrument at a gas pressure of 5 cm of mercury in a 30-cm cell with KBr windows. The region from 450 to 650 $cm^{-1}$ was run with a KRS-5 prism in conjunction with a LiF mirror to reduce the amount of stray radiation. The region from 2700 to 3100 $cm^{-1}$ was run with the $CaF_2$ prism on the Harvard instrument to obtain some resolution of the C—H stretching frequencies. The balance of the

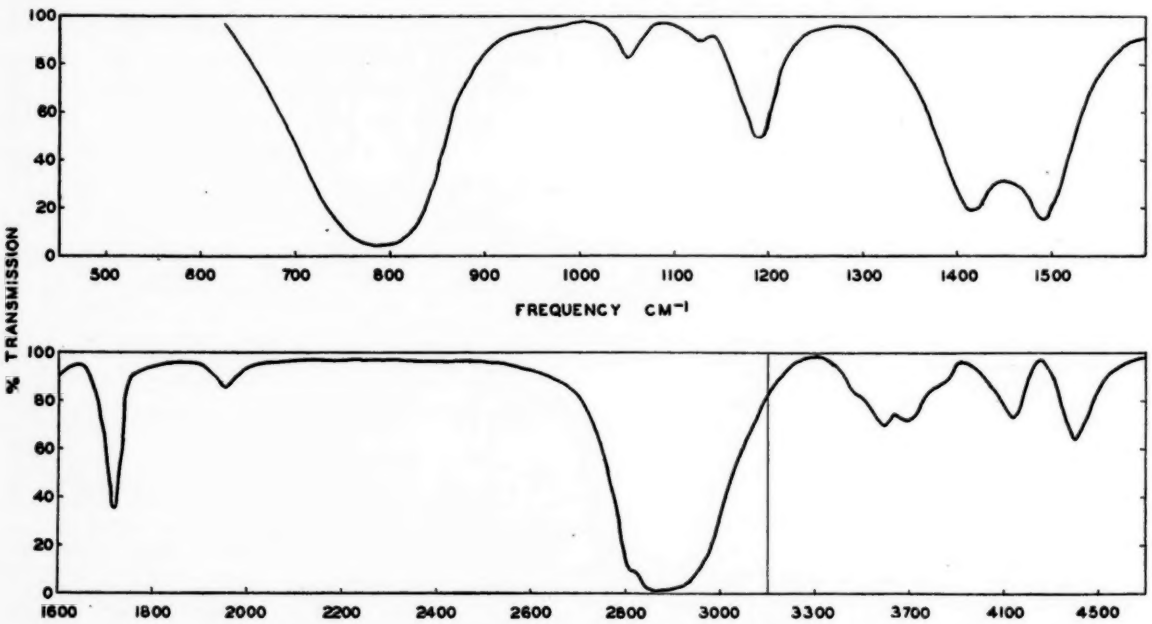


FIG. 2. Infra-red absorption spectrum of $Hg(CH_3)_2$ liquid.

[13] J. T. Edsall and E. B. Wilson, Jr., J. Chem. Phys. **6**, 124 (1938).
[14] B. L. Crawford, Jr. and W. Horwitz, J. Chem. Phys. **15**, 268 (1947).

spectrum represents data from the Baird instrument on the gas at a pressure of 16 cm in a 5-cm NaCl cell.

The sample prepared from $Hg(CH_3)_2$ showed a very weak band at 1135 $cm^{-1}$ which, however, was not present in the other sample, while the latter gave three additional bands readily attributable to $CH_3I$. The data herein presented are those from the "$Hg(CH_3)_2$" sample, minus the 1135-$cm^{-1}$ band, which presumably is from the same impurity mentioned in connection with the infra-red spectrum of dimethyl mercury. The 1450-$cm^{-1}$ band is very weak, and the bands reported by TLW[1] at 1541, 1887, and 2105 $cm^{-1}$ were not observed at all, perhaps because of a smaller effective absorbing path.

TABLE II. The Raman spectrum of dimethyl mercury (*l*).*

| Summary per FKL** $\Delta\nu$ $cm^{-1}$ | | This research $\Delta\nu$ $cm^{-1}$ | |
|---|---|---|---|
| 156 | (1) | grating ghost obscures | |
| 514 | (20b, 0.23) | 515 | (8, 0.5) |
| 700 | (3b, 0.81) | 700 | (3, dp) |
| | | 786 | (0) |
| 1030 | (0, 0.48) | | |
| 1181 | (12, 0.37) | 1184 | (6, 0.4) |
| 1258 | (00) ? | 1246 | (0) ? |
| 1392 | (0, 0.65) | 1402 | (1) |
| 1443 | (0, 0.90) | | |
| 1706 | (00, 0.77) | | |
| 2341 | (0) | | |
| 2869 | (1/2) } (0.21) | 2869 | (2d, dp) |
| 2909 | (6b) } | 2910 | (4, 0.1) |
| 2965 | (1b, 0.26 ?) | 2969 | (3b, dp) |

* d, diffuse; b, broad; dp, depolarized; the numbers after $\Delta\nu$ are intensity and polarization, respectively.
** See reference 4.

## FREQUENCY ASSIGNMENTS

### 1. Introduction

There are two possible structures for the C−M−C skeleton, linear or bent, the latter having $C_{2v}$ symmetry. For a linear model the methyl groups may be staggered, $D_{3d}$; eclipsed, $D_{3h}$; or there may be free rotation $D_{3h}'$. The modes of vibration and the selection rules for these symmetries are available elsewhere;[1,15] $D_{3h}$ and $D_{3h}'$ are governed by the same rules.[16]

It is apparent that the symmetry is probably not $C_{2v}$. Such a bent model allows 21 fundamentals, all of which are active in both infra-red and Raman, while Tables V and VI, which summarize the data and assignments, list only seven coincidences between the Raman and infra-red spectra among over fifty frequencies. This

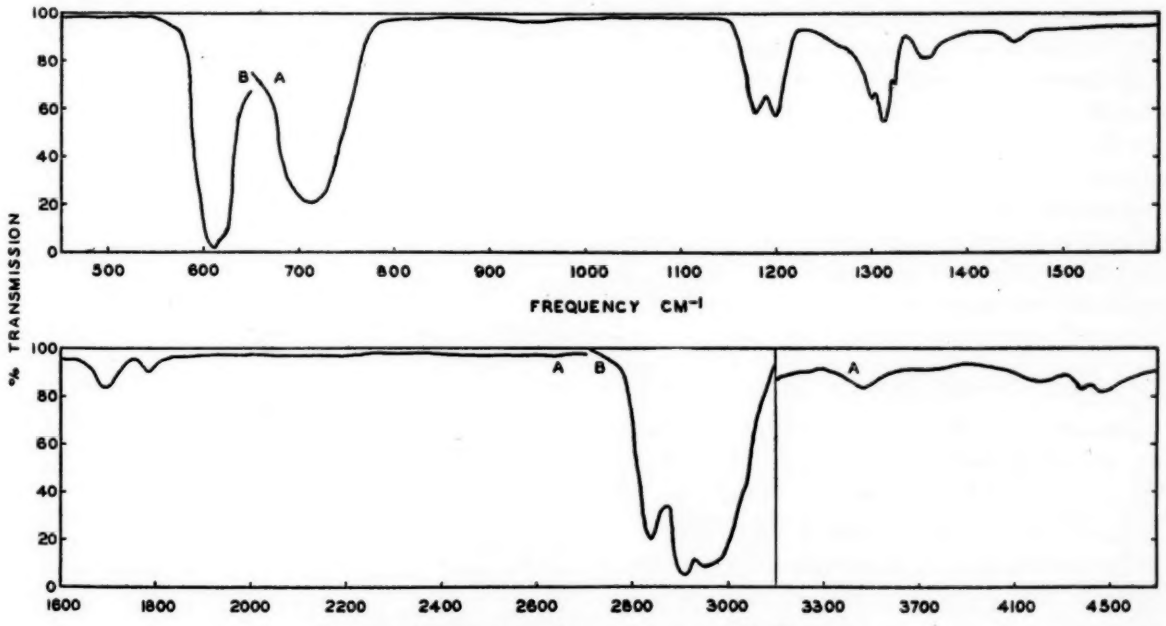


FIG. 3. Infra-red absorption spectrum of $Zn(CH_3)_2$ gas.

[15] G. Herzberg, *Infrared and Raman Spectra of Polyatomic Molecules* (D. Van Nostrand Company, Inc., New York, 1945).
[16] J. B. Howard, J. Chem. Phys. **5**, 442 (1937).

TABLE III. The infra-red spectrum of dimethyl zinc (g).*

| TLW** $\nu$ cm$^{-1}$ | | This research $\nu$ cm$^{-1}$ | |
|---|---|---|---|
| 617 | (vs) | 614 | (10) |
| 704 | (vs) | 710 | (10) |
| 1180 | (s) | 1190 | (5a) |
| 1305 | (m) | 1315 | (5f) |
| 1350 | (w) | 1358 | (2) |
| 1445 | (vw) | 1450 | (0) |
| 1541 | (w) | | |
| 1692 | (m) | 1700 | (2) |
| 1789 | (mw) | 1785 | (1) |
| 1887 | (vw) | | |
| 2105 | (vw) | | |
| | | 2840 | (8c) |
| 2924 | (vs) | 2935 | (10a) |
| 3450 | (s) | 3445 | (2) |
| 4167 | (w) | 4200 | (1) |
| 4386 | (m) | 4400 | (2a) |
| 5781 | (w) | — | |

* a, bimodal; f, has 2 shoulders; c, shoulder; the numbers and other letters after the band frequency indicate relative apparent intensities.
** See reference 1.

conclusion is supported elsewhere,[1,4,15] and therefore a linear model is assumed in all subsequent discussion.

Of the three linear configurations, the eclipsed $D_{3h}$ form is eliminated by the generally accepted nature of the physical interactions restricting rotation. The $D_{3d}$ symmetry differs from the $D_{3h}'$, the selection rules and vibrational modes for which are given in Table IX, in not allowing the $E'$ fundamentals to be Raman active. The coincidences between Raman and infra-red spectra ascribed to $\nu_8$ and $\nu_{10}$ for dimethyl mercury and $\nu_8$, $\nu_9$, and $\nu_{10}$ for dimethyl zinc as well as the appearance of the very low Raman frequencies at about 150 cm$^{-1}$, which seem assignable only as $\nu_{11}$, favor the $D_{3h}'$ model. The rules governing the species of combination bands for this symmetry (also $D_{3h}$) are given in Table IV.

## 2. Frequency Assignment for Dimethyl Mercury

Considering first the fundamental frequencies, the polarized Raman lines at 2910, 1182, and 515 cm$^{-1}$ can be only the $A_1'$ vibrations. The high intensity and sharpness of these bands are in keeping with this assignment. The designation of the frequencies as $\nu_1$, $\nu_2$, and $\nu_3$, respectively, is unambiguous, since the values for $\nu_1$ and $\nu_2$ are typical of the methyl group and $\nu_3$ is in the range expected for the skeletal stretching.

TABLE IV. Combination table for $D_{3h}$ symmetry.

| $A_1'$ | $A_1''$ | $A_2'$ | $A_2''$ | $E'$ | $E''$ |
|---|---|---|---|---|---|
| $A_1''$ | $A_1'$ | $A_2''$ | $A_2'$ | $E''$ | $E'$ |
| $A_2'$ | | $A_1'$ | $A_1''$ | $E'$ | $E''$ |
| $A_2''$ | | | $A_1'$ | $E''$ | $E'$ |
| $E'$ | | | | $A_1'+A_2'+E'$ | $A_1''+A_2''+E''$ |
| $E''$ | | | | | $A_1'+A_2'+E'$ |

The coincidence in Raman and infra-red frequencies at 2966 cm$^{-1}$ is readily assigned as the $E'$ C−H stretching $\nu_8$, excluding Fehér's doubtful finding that the line is polarized. Although the 1475 cm$^{-1}$ vibration appears only in the infra-red, the $E'$ $CH_3$ deformation generally is found very close to this value, and the band is accordingly designated as $\nu_9$. From intensity considerations, both the 788 and 550-cm$^{-1}$ infra-red bands are probably fundamentals. The 550-cm$^{-1}$ band is too low to be a methyl vibration, and since the 786-cm$^{-1}$ Raman line coincides with the 788-cm$^{-1}$ infra-red band, the coincidence is assigned as the $CH_3$ rocking $\nu_{10}$. The only frequency assignable as the C−Hg−C bending $\nu_{11}$ is the 156-cm$^{-1}$ line observed in the Raman. Although Pai[5] observed a Raman line at 255 cm$^{-1}$, this has been shown to be spurious,[4] and hence the 155-cm$^{-1}$ line is the only frequency available in the expected bending range.

The remaining Raman frequencies must be assigned as the $E''$ fundamentals, as combinations, or as overtones. The 2869-cm$^{-1}$ line is probably the C−H stretching $\nu_{12}$. The assignment of the 700-cm$^{-1}$ line as the $CH_3$ rocking $\nu_{14}$ is in accord with its observed depolarization, and the value agrees with the corresponding vibration of $E'$ symmetry. This leaves only the $CH_3$ deformation, $\nu_{13}$, unassigned and the lines at 1030, 1252, 1397, and 1443 cm$^{-1}$ from which to choose. The 1030-cm$^{-1}$ line is low for $\nu_{13}$ and has a polarization of 0.48 which confirms the assignment of it as the overtone $2\nu_3$ (1030 cm$^{-1}$). The 1252-cm$^{-1}$ line is of doubtful reality and furthermore could be attributed readily to $\nu_7+\nu_{14}$ (1250 cm$^{-1}$). The choice between 1397 and 1443 cm$^{-1}$ is a more difficult one. Both can be assigned as combinations: 1397 cm$^{-1}$ as $2\nu_{14}$ (1400 cm$^{-1}$) and 1443 cm$^{-1}$ as $\nu_7+\nu_{10}$ (1437 cm$^{-1}$). Because $\nu_{13}$ is depolarized, the polarization data do recommend to some extent the 1443-cm$^{-1}$ line. Moreover, in general $E'$ and $E''$ $CH_3$ deformation frequencies are not widely separated. Accordingly $\nu_{13}$ is assigned as the 1443-cm$^{-1}$ Raman line.

TABLE V. Observed frequencies, assignments, and calculated frequencies for combination bands of dimethyl mercury.

| Infra-red (*g*) $\nu$ cm$^{-1}$ | Raman (*l*) $\Delta\nu$ cm$^{-1}$ | Assignment | Species for combinations | Calc. Freq. $\nu$ cm$^{-1}$ |
|---|---|---|---|---|
| | 156 (1) | $\nu_{11}$ | | |
| | 515 (20, 0.30) | $\nu_3$ | | |
| 550 (8) | | $\nu_7$ | | |
| 675 (1) | | $\nu_3+\nu_{11}$ | $E'$ | 671 |
| | 700 (5b, 0.81) | $\nu_{14}$ | | |
| 788 (9) | 786 (0) ? | $\nu_{10}$ | | |
| | 1030 (0, 0.48) | $2\nu_3$ | $A_1'$ | 1030 |
| 1070 (2a) | | $\nu_3+\nu_7$ | $A_2''$ | 1065 |
| | 1182 (12, 0.38) | $\nu_2$ | | |
| 1205 (2a) | | $\nu_6$ | | |
| | 1252 (00) ? | $\nu_7+\nu_{14}$ | $E'$ | 1250 |
| | 1397 (0, 0.65) | $2\nu_{14}$ | $A_1'+A_2'+E'$ | 1400 |
| | 1443 (0, 0.90) | $\nu_{13}$ | | |
| 1475 (6a) | | $\nu_9$ | | |
| | 1706 (00, 0.77) | $\nu_2+\nu_3$ | $A_1'$ | 1697 |
| 1735 (3) | | $\nu_2+\nu_7$ | $A_2''$ | 1732 |
| | 2341 (0) | $\nu_{10}+\nu_{11}+\nu_{13}$ | $A_1''+A_2''+3E''$ | 2340 |
| 1980 (0a) | | $\nu_2+\nu_{10}$ | $E'$ | 1969 |
| 2390 (5) | | $\nu_2+\nu_6$ | $A_2''$ | 2387 |
| 2660 (0) | | $\nu_2+\nu_9$ | $E'$ | 2657 |
| | 2869 (2d, dp) | $\nu_{12}$ | | |
| (2880) (6) | | $\nu_5$ | | |
| | 2910 (6, 0.1) | $\nu_1$ | | |
| 2970 (10a) | 2965 (3b, dp?) | $\nu_8$ | | |
| 3660 (1a) | | $\nu_{10}+\nu_{12}$; $\nu_8+\nu_{14}$ | $A_1''+A_2''+E''$ | 3656; 3666 |
| 3855 (0) | | $\nu_1+\nu_{10}+\nu_{11}$ | $A_1'+A_2'+E'$ | 3853 |
| 4150 (1) | | $\nu_2+\nu_8$ | $E'$ | 4148 |
| 4435 (1) | | $\nu_8+\nu_9$ | $A_1'+A_2'+E'$ | 4441 |

The $A_2''$ fundamentals are to be drawn from the remaining infra-red bands. The value of the C−H stretching, $\nu_5$, is complicated by the overlapping of it with $\nu_8$, and possibly with $2\nu_{13}$. The band maximum at 2835 cm$^{-1}$ is hardly $\nu_5$, since the latter is a || type band which should show definite $P$, $Q$, and $R$ branches. The $\perp$ band, $\nu_8$, is a band formed by the unresolved $Q$ branches of the sub-bands against the weaker background of scattered $P$ and $R$ lines; this results from $I_A/I_B$ being small. It appears possible that the shoulder at 2835 cm$^{-1}$ is the $P$ branch of $\nu_5$, with the $Q$ and $R$ branches overlapping $\nu_8$. Such an interpretation gives an estimated value of 2880 cm$^{-1}$ for $\nu_5$. The $CH_3$ deformation, $\nu_6$, might be either the 1070 or 1205-cm$^{-1}$ band, which are the only unassigned bands in the appropriate range. The 1070-cm$^{-1}$ band is interpretable as the combination $\nu_3+\nu_7$ (1065 cm$^{-1}$), whereas no such interpretation presents itself for the 1205-cm$^{-1}$ band; assignment of it as $\nu_3+\nu_{14}$ (1215 cm$^{-1}$) violates the selection rules. This, as well as the higher intensity of the 1205-cm$^{-1}$ band, suggests its assignment as $\nu_6$. The chief objection to this assignment is that the 1205-cm$^{-1}$ band does not exhibit a $Q$ branch which is predicted for a || type band in symmetric top molecules.[17] However, $I_A/I_B$ is small in dimethyl mercury, and the $Q$ branch should be correspondingly less intense though perhaps not completely missing. Moreover, the separation of the maxima of the $P$ and $R$ branch band envelopes is 14 cm$^{-1}$, which agrees well with the value of 13.5 cm$^{-1}$ computed for $\nu_6$ at room temperature from $I_B$, so $\nu_6$ is assigned as 1205 cm$^{-1}$. The strong band at 550 cm$^{-1}$ must be the C−Hg−C stretching, $\nu_7$, which value agrees well with the assigned value for the corresponding symmetrical stretching, $\nu_3$. All other observed bands have been readily assigned as combinations or overtones, obeying the selection rules, for which the calculated frequencies agree well with the experimental values as listed in Table V.

### 3. Frequency Assignment for Dimethyl Zinc

Initial normal coordinate calculations, as well as a qualitative comparison of the dimethyl mercury spectra with the frequency assignment proposed earlier for dimethyl zinc,[1] suggested

[17] See G. Herzberg, reference 15, p. 414 *et seq.* for a detailed description of the band envelopes expected.

TABLE VI. Observed frequencies, assignments, and calculated frequencies for combination bands of dimethyl zinc.

| Infra-red (g) $\nu$ cm$^{-1}$ | Raman (l) $\Delta\nu$ cm$^{-1}$ | Assignment | Species for combinations | Calc. freq. $\nu$ cm$^{-1}$ |
|---|---|---|---|---|
| | 144 (1) | $\nu_{11}$ | | |
| | 488 (1) ? | $\nu_{14}-\nu_{11}$ | $A_1''+A_2''+E''$ | 476 |
| | 504 (20b, 0.18) | $\nu_3$ | | |
| 615 (10) | | $\nu_7$ | | |
| | 620 (3b, 0.80) | $\nu_{14}$ | | |
| 707 (10) | | $\nu_{10}$ | | |
| | 898 (00) ? | $\nu_{13}-(\nu_{14}-\nu_{11})$ | $A_1'+A_2'+3E'$ | 899 |
| | 1013 (00) | $2\nu_3$ | $A_1'$ | 1008 |
| | 1135 (0) | $\nu_3+\nu_{14}$ | $E''$ | 1124 |
| | 1158 (15, 0.32) | $\nu_2$ | | |
| 1185 (5a) | | $\nu_6$ | | |
| | 1189 (0) | $\nu_3+\nu_{10}$ | $E'$ | 1211 |
| | 1244 (0) | $\nu_7+\nu_{14}$; $2\nu_{14}$ | $E'$; $A_1'+A_2'+E'$ | 1235; 1240 |
| 1310 (5f) | 1313 (00) ? | $\nu_2+\nu_{11}$ | $E'$ | 1304 |
| 1354 (2) | | $\nu_3+\nu_{10}+\nu_{11}$ | $A_1'+A_2'+E'$ | 1355 |
| | 1388 (0) | $\nu_{13}$ | | |
| 1448 (0) | 1440 (00) | $\nu_9$ | | |
| 1541 (0) ? | | $\nu_{11}+\nu_{13}$ | $A_1''+A_2''+E''$ | 1532 |
| | 1648 (00) ? | $\nu_2+\nu_3$ | $A_1'$ | 1662 |
| 1696 (2) | | $\nu_3+\nu_6$ | $A_2''$ | 1689 |
| 1787 (1) | | $\nu_2+\nu_7$ | $A_2''$ | 1773 |
| 1887 (00) ? | | $\nu_2+\nu_{10}$ | $E'$ | 1865 |
| 2105 (00) ? | | $\nu_{13}+\nu_{10}$ | $A_1''+A_2''+E''$ | 2095 |
| | 2833 (1/2b) | $\nu_{12}$ | | |
| (2870) (8) | | $\nu_5$ | | |
| | 2898 (4, 0.05) | $\nu_1$ | | |
| 2935 (10a) | 2948 (1b, 0.61) | $\nu_8$ | | |
| 3448 (2) | | $\nu_3+\nu_8$ | $E'$ | 3444 |
| 4185 (1) | | $2\nu_{14}+\nu_8$; $\nu_7+\nu_8+\nu_{14}$ | $A_1'+A_2'+E'$; $A_1'+A_2'+3E'$ | 4175; 4180 |
| 4393 (2a) | | $\nu_8+\nu_9$ | $A_1'+A_2'+E'$ | 4384 |
| 5781 (1) | | $\nu_1+\nu_5$ | $A_2''$ | 5772 |

that the latter required revision. The infra-red spectrum of dimethyl zinc was reinvestigated primarily to determine if any band was present in the observable region below 600 cm$^{-1}$, which is the limit of the earlier work.[1] Table VI summarizes the various available data and gives the assignments arrived at herein.

The general criteria for the frequency assignment are the same as for dimethyl mercury, and only the specific arguments will be considered here. Regarding the fundamentals, the absence of any infra-red band in the 430 to 615-cm$^{-1}$ region requires that the 615-cm$^{-1}$ infra-red band be assigned as $\nu_7$, the $A_2''$ C−Zn stretching, in order to obtain a C−Zn force constant consistent with that from $\nu_3$, the assignment of which can hardly be questioned. The coincidence with the 620-cm$^{-1}$ Raman frequency is ascribed as an accidental degeneracy, and the assignment of the latter to the $E''$ $CH_3$ rocking $\nu_{14}$ is indicated. The 707-cm$^{-1}$ infra-red band originally assigned to $\nu_7$ is transferred to the $E'$ $CH_3$ rocking $\nu_{10}$. The $A_1'$ Raman assignments of TLW[1] are confirmed by the later polarization measurements.[4] These assignments and also $\nu_6$ and $\nu_{11}$ are unchanged. It appears preferable to change the assignment for the $E'$ $CH_3$ deformation $\nu_9$. This vibration, involving the H−C−H angular distortion, usually appears in the 1450–1475-cm$^{-1}$ region and can be assigned to the coincidence between Raman and infra-red spectra at 1447 cm$^{-1}$. $\nu_{13}$ should be in the region 12–1400 cm$^{-1}$, and of the four Raman lines reported therein, the 1388-cm$^{-1}$ value appears most likely. As in dimethyl mercury, the assignment of the $A_2''$ C−H stretching frequency is complicated by the overlapping of the infra-red bands. Employing identical arguments in this case, $\nu_5$ is assigned the value 2870 cm$^{-1}$. The resolution of the C−H stretches in Fehér's Raman data and his polarization measures permit the assignment of $\nu_1$, $\nu_8$, and $\nu_{12}$ as 2898, 2940, and 2833 cm$^{-1}$, though the value for $\nu_{12}$ seems low. As a matter of fact, the 2833-cm$^{-1}$ line is interpretable as $\nu_9+\nu_{13}$ (2832-cm$^{-1}$) but is assigned as $\nu_{12}$ for the lack of anything better.

TABLE VII. $G$ matrix for $CH_3-M-CH_3$.*

$A_1'$ and $A_2''$

$$\begin{vmatrix} \mu_H+\mu_C & -\frac{4}{3}\rho\mu_C & -\frac{\sqrt{3}}{3}\mu_C \\ & 2\rho^2\mu_H+\frac{16}{3}\rho^2\mu_C & \frac{4\sqrt{3}}{3}\rho\mu_C \\ & & \mu_C+2a\mu_M \end{vmatrix}$$

$E'$ and $E''$

$$\begin{vmatrix} \mu_H+\frac{4}{3}\mu_C & -\frac{2\sqrt{2}}{3}\rho\mu_C & -\sqrt{2}\left(\epsilon+\frac{\rho}{3}\right)\mu_C & -\frac{2\sqrt{6}}{3}\epsilon a\mu_C \\ & \frac{5}{2}\rho^2\mu_H+\frac{8}{3}\rho^2\mu_C & -\frac{\rho^2}{4}\mu_H+\rho\left(\epsilon+\frac{\rho}{3}\right)\mu_C & \frac{2\sqrt{3}}{3}\epsilon\rho a\mu_C \\ & & \rho^2\mu_H+\frac{3}{2}\left(\epsilon+\frac{\rho}{3}\right)^2\mu+3\epsilon^2a\mu_{CM} & \sqrt{3}\epsilon\left(\epsilon+\frac{\rho}{3}\right)a\mu_C+2\sqrt{3}\epsilon^2a\mu_M \\ & & & 2\epsilon^2a(\mu_C+2\mu_M) \end{vmatrix}$$

* $\rho=(1/C-H)=(1/d)$; $\epsilon=(1/C-M)=(1/D)$; $a=\begin{cases}1 \text{ for } A_2'', E' \\ 0 \text{ for } A_1', E''\end{cases}$.

The remaining bands have all been assigned as combinations or overtones which obey the selection rules and for which the computed frequencies agree fairly well with the observed values. The calculated frequencies for several of the doubtful combination bands is not very good, suggesting that some of them might not be real.

## NORMAL COORDINATE ANALYSIS

The methods developed by Wilson[18] have been used throughout this section. The internal coordinates $\alpha$, $\beta$, $\gamma$, $r$, and $\eta$ are defined as small displacements in the H−C−H, H−C−M, C−M−C bond angles and C−H, C−M bond distances. Symmetry coordinates, normalized, orthogonal, linear combinations of these internal coordinates, transforming according to the appropriate irreducible representations of the group $D_{3h}$, were obtained by a simple extension of the method used by Meister and Cleveland.[19] The redundancies resulting in the $A_1'$ and $A_2''$ factors were removed by setting one symmetry coordinate in each factor identically equal to zero, expressing the condition that the sum of the angle changes in each methyl group is zero. The general factored $G$ matrix, obtained for $D_{3h}$ symmetry, is given in Table VII, and the diagonal terms of the corresponding valence force $F$ matrix in Table VIII. In the $F$ matrix subscript 2 refers to methyl-methyl interactions, and the primes indicate those interactions involving staggered atoms. As a check, the $F$ and $G$ matrices were determined independently using Lippman's method.[20]

In computing the numerical values of the $G$ matrix, tetrahedral bond angles were assumed for the methyl groups. 1.10A was adopted as the C−H bond distance, $d$,[21] and 2.20A was used for the C−Hg distance, $D$.[22] No direct measurement of the C−Zn bond distance appears to be available, and an estimated value of 2.05A was introduced. This was obtained by taking the sum of the covalent radius of zinc in the metal crystal and the covalent radius of carbon[23] and estimating a correction for the higher covalent radius of zinc in the metal crystals by analogy to mercury. The 1942 values of the International Committee on Atomic Weights were used. The conversion factor 5.8905 $\times 10^{-2}$ used in transforming $cm^{-1}$ to $\lambda$ corresponds to Birge's 1941 table of fundamental constants.

The computed and observed fundamental frequencies are listed in Table IX; the numerical $F$ matrix elements used in the calculations, as well as the force constants identified therewith, are given in Table VIII. Considering the probable effects of anharmonicity and the differences between the vibrational frequencies in the liquid

[18] E. B. Wilson, Jr., J. Chem. Phys. **7**, 1047 (1939); *ibid.* **9**, 76 (1941).

[19] A. G. Meister and F. F. Cleveland, Am. J. Phys. **14**, 13 (1946).

[20] Caro W. Lippman, Jr., unpublished. See reference 26 for a synopsis of the method.

[21] J. W. Simmons, W. Gordy, and A. G. Smith, Phys. Rev. **74**, 243 (1948).

[22] L. O. Brockway and H. O. Jenkins, J. Am. Chem. Soc. **58**, 2036 (1936).

[23] L. Pauling, *Nature of the Chemical Bond* (Cornell University Press, Ithaca, New York, 1940), second edition.

TABLE VIII. *F* matrix and force constants.*

| | | General diagonal terms | Numerical values $Hg(CH_3)_2$ | Numerical values $Zn(CH_3)_2$ |
|---|---|---|---|---|
| $A_1'$ | $F_{11}$ | $f_r+2f_{rr}+f_{rr_2}+2f_{rr_2'}$ | $4.79\times10^5$ | $4.79\times10^5$ |
| | $F_{22}$ | $(d^2/2)\{(f_\alpha+f_\beta)+2(f_{\alpha\alpha}+f_{\beta\beta})+c\}$ | $0.390\times10^{-11}$ | $0.375\times10^{-11}$ |
| | $F_{33}$ | $f_\eta+f_{\eta\eta}$ | $2.45\times10^5$ | $2.39\times10^5$ |
| $A_2''$ | $F_{55}$ | $f_r+2f_{rr}-f_{rr_2}-2f_{rr_2'}$ | $4.79\times10^5$ | $4.79\times10^5$ |
| | $F_{66}$ | $(d^2/2)\{(f_\alpha+f_\beta)+2(f_{\alpha\alpha}+f_{\beta\beta})-c+d\}$ | $0.406\times10^{-11}$ | $0.390\times10^{-11}$ |
| | $F_{77}$ | $f_\eta-f_{\eta\eta}$ | $2.45\times10^5$ | $2.39\times10^5$ |
| $E'$ | $F_{88}$ | $f_r-f_{rr}+f_{rr_2}-f_{rr_2'}$ | $4.55\times10^5$ | $4.55\times10^5$ |
| | $F_{99}$ | $d^2(f_\alpha-f_{\alpha\alpha}+f_{\alpha\alpha_2}-f_{\alpha\alpha_2'})$ | $0.573\times10^{-11}$ | $0.550\times10^{-11}$ |
| | $F_{10-10}$ | $d^2(f_\beta-f_{\beta\beta}+f_{\beta\beta_2}-f_{\beta\beta_2'})$ | $0.417\times10^{-11}$ | $0.331\times10^{-11}$ |
| | $F_{11-11}$ | $D^2f_\gamma$ | $0.457\times10^{-11}$ | $0.276\times10^{-11}$ |
| $E''$ | $F_{12-12}$ | $f_r-f_{rr}-f_{rr_2}+f_{rr_2'}$ | $4.55\times10^5$ | $4.55\times10^5$ |
| | $F_{13-13}$ | $d^2(f_\alpha-f_{\alpha\alpha}-f_{\alpha\alpha_2}+f_{\alpha\alpha_2'})$ | $0.549\times10^{-11}$ | $0.508\times10^{-11}$ |
| | $F_{14-14}$ | $d^2(f_\beta-f_{\beta\beta}-f_{\beta\beta_2}+f_{\beta\beta_2'})$ | $0.333\times10^{-11}$ | $0.258\times10^{-11}$ |
| | | *Force constants* | | |
| | | $f_r$ dynes/cm | $4.63\times10^5$ | $4.63\times10^5$ |
| | | $f_{rr}$ | 0.08 | 0.08 |
| | | $f_\eta$ | 2.45 | 2.39 |
| | | $d^2f_\alpha$ dyne cm/radian | $0.530\times10^{-11}$ | $0.530\times10^{-11}$ |
| | | $d^2f_\beta$ | 0.359 | 0.274 |
| | | $D^2f_\gamma$ | 0.457 | 0.276 |
| | | $d^2f_{\alpha\alpha}$ | −0.031 | 0.001 |
| | | $d^2f_{\beta\beta}$ | −0.016 | −0.021 |
| | | $d^2(f_{\alpha\alpha_2}+f_{\beta\beta_2})$ | 0.031 | 0.033 |
| | | $d^2(f_{\alpha\alpha_2}-f_{\alpha\alpha_2'})$ | 0.012 | 0.021 |
| | | $d^2(f_{\beta\beta_2}-f_{\beta\beta_2'})$ | 0.042 | 0.037 |

* $C=(f_{\alpha\alpha_3}+f_{\beta\beta_3})+2(f_{\alpha\alpha_3'}+f_{\beta\beta_3'})$; $d=-2(2f_{\alpha\beta}+f_{\alpha\beta'}-2f_{\alpha\beta_3}-f_{\alpha\beta_3'})$.

Raman spectrum and the gaseous infra-red spectrum, the number of significant figures given for several of the force constants is too large. They are given as being the actual values used. In the determination of the force constants, the higher frequencies were successively split out of a given factor. These constants were then substituted in the expanded secular equation and the frequencies computed. Successive approximations were made to the force constant, till the computed frequencies agreed with the observed values.

There are insufficient data to evaluate many of the interaction constants explicitly. In view of this it seemed preferable to disregard all off-diagonal elements in the *F* matrix. The off-diagonal element $f_{\alpha\eta}-f_{\beta\eta}$ appears in the $A_1'$ and $A_2''$ factors and is usually considered to be of physical significance. Its evaluation depends on first assigning values to the diagonal elements, for which in this case there appear no *a priori* means. The introduction of typical values found in other cases for $f_{\alpha\eta}-f_{\beta\eta}$[24] has little effect on $f_\eta$ and increases $F_{22}$ and $F_{66}$ by only about 2 percent. Analogous reasons led to the neglect of the $f_{\alpha\beta}$ terms in $F_{66}$. The $A_1'$ C−H $F_{11}$ value of $4.79\times10^5$ dynes/cm is from ethane,[25] and the value of $0.530\times10^{-11}$-dyne cm/radian for $d^2f_\alpha$ is from the results of Decius for the methyl halides.[26] The C−H frequencies are fitted moderately well by using the diagonal element $f_{rr}$. The remaining systematic deviations indicate the fit could be improved somewhat by introducing small $f_{rr_2}$ and $f_{rr_2'}$ terms of dubious physical significance. Similarly, $f_{\eta\eta}$ is neglected because of its small magnitude, although values could be assigned by fitting $\nu_3$ and $\nu_4$ exactly. Subject to the effects of omitting $f_{\alpha\eta}-f_{\beta\eta}$, $f_{\alpha\beta}$, and the off-diagonal elements, several of the methyl vibration interaction terms were evaluated. The end-end interactions are determinable only as the combinations given in Table VIII.

## DISCUSSION

On the basis of a simple bond orbital analysis[23] the C−Hg−C skeleton of dimethyl mercury would be expected to be linear because of hybridization of the 6*s* mercury orbital with the 6*p* orbitals to give the two bond orbitals of maximum strength $1/\sqrt{2}(S+P_z)$, $1/\sqrt{2}(S-P_z)$

[24] B. L. Crawford, Jr. and S. R. Brinkley, Jr., J. Chem. Phys. 9, 69 (1941).

[25] F. Stitt, J. Chem. Phys. 7, 297 (1939).

[26] J. C. Decius, J. Chem. Phys. 16, 214 (1948).

TABLE IX. Observed and computed fundamental frequencies.

| | $D_{3h}'$ | | Dimethyl mercury Obs. | Comp. | % Dev. | Dimethyl zinc Obs. | Comp. | % Dev. |
|---|---|---|---|---|---|---|---|---|
| $A_1'$ | C−H stretching | $\nu_1$ | 2910 cm$^{-1}$ | 2882 cm$^{-1}$ | −0.96 | 2898 cm$^{-1}$ | 2883 cm$^{-1}$ | −0.65 |
| RP | $CH_3$ bending | $\nu_2$ | 1182 | 1181 | * | 1158 | 1158 | * |
| | C−M−C stretching | $\nu_3$ | 515 | 512 | −0.58 | 504 | 505 | * |
| $A_1''$ | torsion | $\nu_4$ | — | — | — | — | — | — |
| $A_2''$ | C−H stretching | $\nu_5$ | 2880 | 2883 | +0.10 | 2870 | 2884 | +0.49 |
| IR, ∥ | $CH_3$ deformation | $\nu_6$ | 1205 | 1205 | * | 1185 | 1185 | * |
| | C−M−C stretching | $\nu_7$ | 550 | 549 | * | 615 | 610 | −0.81 |
| $E'$ | C−H stretching | $\nu_8$ | 2966 | 2921 | −1.52 | 2940 | 2920 | −0.68 |
| R | $CH_3$ deformation | $\nu_9$ | 1475 | 1475 | * | 1444 | 1444 | * |
| IR, ⊥ | $CH_3$ rocking | $\nu_{10}$ | 787 | 787 | * | 707 | 707 | * |
| | C−M−C bending | $\nu_{11}$ | 156 | 156 | * | 144 | 144 | * |
| $E''$ | C−H stretching | $\nu_{12}$ | 2869 | 2921 | +1.85 | 2833? | 2921 | +3.23 |
| R | $CH_3$ deformation | $\nu_{13}$ | 1443 | 1443 | * | 1388 | 1388 | * |
| | $CH_3$ rocking | $\nu_{14}$ | 700 | 700 | * | 620 | 620 | * |

* Used in computing force constants.

which are linear along the $x$ axis. The same reasoning applies to zinc where the hybridization is between the $4s$ and $4p$ orbitals. Brockway and Jenkins[22] were not able to draw any conclusions regarding the linearity of dimethyl mercury from their electron diffraction investigations because of the high background of atomic scattering. The generally accepted linear configurations for the mercury, cadmium, and zinc halides[27] is indirect support for the linearity of the dimethyl compounds. However, the strongest evidence bearing on the linearity of these molecules comes from the lack of any appreciable number of coincidences between the infra-red and Raman spectra. A bent model requires that all fundamentals be active in both infra-red and Raman spectra, yet, among over fifty observed frequencies, there are only seven coincidences. TLW[1] conclude in their frequency assignment for dimethyl zinc that it is linear, and the additional data obtained since then confirm their conclusion. Moreover, the results of the normal coordinate analysis provide further corroboration of the linear structure.

The low values assigned the skeletal bending are perhaps a bit surprising. Indeed, Kohlrausch[28] assumes the Raman lines in the vicinity of 150 cm$^{-1}$ do not belong to the vibrational spectrum. However, the bending frequencies must lie below 400 cm$^{-1}$, and no other values are available for the assignment. A $D_{3d}$ configuration would give the molecules a center of symmetry and make the bending inactive in the Raman, but the other observed coincidences preclude this possibility. The lines may be interpreted as combination bands: $\nu_2-2\nu_3$ for both dimethyl mercury and zinc, and also as $\nu_{14}-\nu_7$ for dimethyl mercury. The normal coordinate analysis suggests that the low frequencies do correspond to the bending, for the values of $D^2f_\gamma$ are of the same magnitude as $d^2f_\beta$. Verification of the assignments could be made by observing the region in the infra-red with the aid of residual rays; the suggested combination for dimethyl zinc is only Raman active.

The extent of the rotational freedom of the methyl groups is an intriguing problem. The coincidences between the Raman and infra-red spectra in $E'$ and the proposed interpretation of the low Raman frequency as the skeletal bending require $D_{3h}'$ or $D_{3h}$ symmetry. The latter is ruled out by the generally accepted views regarding the nature of the interactions restricting rotation,[29] leaving essentially free rotation as the most likely interpretation. The questionable appearance of $\nu_9$ and $\nu_{10}$ in the Raman spectra may result from either the inherently low intensity of $E'$ Raman lines or from only partial relaxation of the selection rules because of small, but still finite, hindrance to free rotation. The fine structure of the ⊥ infra-red bands is another possible means of investigating the

[27] See G. Herzberg, reference 15, p. 287 for references to the pertinent literature.

[28] K. W. F. Kohlrausch, *Ramanspectren* (Becker and Erler, Leipzig, 1943), p. 182.

[29] E. N. Lassettre and L. B. Dean, Jr., J. Chem. Phys. **16**, 151 (1948).

rotational restrictions.[30] Heat capacity data might also profitably be obtained.

The results of the normal coordinate analysis appear to be satisfactory, bearing in mind the reservations made in the frequency assignments. Nineteen force constants, two of which are from other molecules, are used in computing twenty-six frequencies, with a root-mean-square deviation of 1 percent for the ten frequencies not directly used in determining the force constants. A comparison of the force constants $d^2f_\beta$ and $D^2f_\gamma$ suggests that dimethyl zinc is a more readily deformable molecule than dimethyl mercury, a result perhaps of greater ionic character in the C−Zn bonds. $d^2f_{\alpha\alpha}$ is also appreciably smaller for dimethyl zinc perhaps for the same reason. The magnitudes of the interaction terms are of the same order as values reported for similar interactions elsewhere, except $f_{rr}$, which in methane derivatives appears to have a lower value of about $0.03\times10^5$ dynes/cm.[26]

In more complicated molecules it often becomes expeditious to consider groups as units in deriving force constants or assigning frequencies, and a comparison of the more exact values for $f_\gamma$ and $f_\eta$, obtained from the normal coordinate analysis, with the results from such an approximation affords a check on the accuracy of the approximation methods. Using the general formulae for a linear $XY_2$ molecule[15] and $M_y=15$, values for $f_\gamma$ and $f_\eta$ were computed from the corresponding assigned frequencies. The results in units of $10^5$ dynes/cm are tabulated below along with the normal coordinate values for comparison. The agreement is surprisingly good, with the $XY_2$ values consistently low.

| | | $Hg(CH_3)_2$ | | $Zn(CH_3)_2$ | |
|---|---|---|---|---|---|
| | | $XY_2$ | n.c. | $XY_2$ | n.c. |
| $F_\eta$ | $\nu_3$ | 2.35 | — | 2.26 | 2.39 |
| $F_\eta$ | $\nu_7$ | 2.32 | 2.45 | 2.29 | — |
| $f_\gamma$ | $\nu_{11}$ | 0.094 | 0.095 | 0.063 | 0.066 |

[30] J. B. Howard, J. Chem. Phys. **5**, 451 (1937).

The correlation of force constants with atomic parameters is of considerable interest. Recently, Gordy[3] has suggested a semi-empirical expression that appears to have fairly wide applicability. The stretching force constant $k$, in $10^5$ dynes/cm is given as $k=aN(X_AX_B/d^2)^{\frac{3}{4}}+b$, where $a$ and $b$ are empirical constants having the values 1.67 and 0.30 for stable molecules in their normal covalent state. $N$ is the bond order, $X_A$ and $X_B$ are the electronegativities of the bonded atoms, and $d$ the bond distance in angstroms. Using Gordy's values for $X$ (Hg 1.0, Zn 1.2, C 2.55) and 2.20 and 2.05A for the C−Hg and C−Zn bond distances, and $N=1$, his equation gives 1.33 and 1.62 for the C−Hg and C−Zn force constants, contrasting with the directly obtained values 2.45 and 2.39. A partial explanation is available in that the electronegativities Gordy uses for Hg and Zn may be incorrect. Substituting the observed force constants in Gordy's equation, electronegativities of 2.66 and 2.22 are computed for Hg and Zn, respectively. These values agree better with those from thermal data, 1.9 and 1.5 for Hg and Zn,[31] than with those proposed by Gordy, but appear definitely to be too high, suggesting the possible importance of other factors in the poor fit between the experimental and predicted force constants.

## ACKNOWLEDGMENT

I am deeply indebted to Professor E. Bright Wilson, Jr. for his valuable advice and encouragement throughout this research. Also, I wish to thank Dr. E. L. King for several discussions concerning the Hg and Zn electronegativities and for his assistance with the Raman spectrograph. I am grateful to W. L. Hyde and W. E. Keller for their help with the infra-red spectrometers.

[31] M. Haissinsky, J. phys. radium **7**, 7 (1946).

THE JOURNAL OF CHEMICAL PHYSICS VOLUME 17, NUMBER 2 FEBRUARY, 1949

# The Infra-Red Spectrum of $C_2H_6$

LINCOLN G. SMITH
*Palmer Physical Laboratory, Princeton, New Jersey, and University of Michigan, Ann Arbor, Michigan*
(Received August 10, 1948)

The infra-red spectrum of $C_2H_6$ gas has been studied in the region between 1.6 and 13$\mu$ with a spectrometer of high resolving power. From measurements on four resolved $\parallel$ bands the value $I_{B0}=(42.234\pm0.011)\times10^{-40}$ g cm$^2$ has been obtained for the large moment of inertia in the ground state. From measurements on the three fundamental $\perp$ bands the best value at present available for the small moment of inertia is $I_A=10.81\times10^{-40}$ g cm$^2$. Because of uncertainties concerning the perturbations of degenerate state $\nu_8$, of which a semi-quantitative explanation which is apparently basically correct has been obtained, this value is provisional but appears to be fairly reliable. With these values of $I_{B0}$ and $I_A$, if one assumes C$-$C$=$1.55A, one obtains C$-$H$=$1.098A and $\measuredangle$HCC $=109°\,3'$. From the considerations of the perturbations of state $\nu_8$ and of the frequencies and line spacings of the combination $\perp$ bands, spectroscopic evidence indicating that the configuration of $C_2H_6$ is staggered (point group $D_{3d}$) has for the first time been obtained. Also from these considerations the reliable value $\nu_8=1472.2$ cm$^{-1}$ and the values $\nu_4=290$ cm$^{-1}$ for the torsion frequency and $\nu_{12}=1190$ cm$^{-1}$ for the "uncertain" frequency have been obtained. The latter two values are perhaps somewhat more reliable and not inconsistent with values obtained previously by other methods. These and other results are summarized in Figs. 1 and 14 and in Tables XII–XV.

## I. INTRODUCTION

THIS report deals with the results of experiments on the near infra-red spectrum between 1.6 and 13$\mu$ of $C_2H_6$ gas performed at Princeton University before the recent war with a spectrometer of high resolving power. A preliminary account of some of these results was given at the Princeton meeting of The American Physical Society in December 1941 by Smith and Woodward.[1] Also, some of the results were recalculated for inclusion in Professor Herzberg's latest book.[2] All values reported here have been re-examined and analyzed more thoroughly than previously and are slightly different from those reported in either reference 1 or reference 2.

Previous investigations of the Raman and infra-red spectra and of the heat capacity of $C_2H_6$ and $C_2D_6$ have yielded values of the twelve fundamental frequencies of each molecule, which are for the most part quite reliable, but have failed to determine whether the configuration of each is staggered (point group $D_{3d}$) or eclipsed (point group $D_{3h}$). These results are well summarized by Herzberg[3] who points out that some chemical evidence favors the staggered configuration.[4] The experiments described here add considerable detailed data to these results because of the greater resolution employed than by others, particularly in the case of weaker combination bands, because many spectra of $C_2H_6$ gas at temperatures between $-80$°C and $-100$°C were obtained for the first time and because atmospheric absorptions were for the most part effectively removed from the spectrometer.

A level diagram of the twelve fundamental vibration states of $C_2H_6$ based both on the results of previous investigations and on those to be described here is shown in Fig. 1 wherein the states are divided into five symmetry classes which are designated at the bottom of the diagram by the usual symbols for both point groups $D_{3d}$ and $D_{3h}$. In Fig. 1 and throughout this paper the notation for the twelve vibrations given in reference 3 is employed. The frequency values in Fig. 1 are essentially the same as those given in reference 3 except in the cases of $\nu_4$, $\nu_8$ and $\nu_{12}$.

## II. EXPERIMENTAL

The ethane used in these experiments was very kindly prepared by Professor John Turkevich of the Princeton Chemistry Department by hydrogenation of ethylene. Unfortunately no record of the purity of the ethane was kept but

[1] L. G. Smith and W. M. Woodward, Phys. Rev. **61**, 386A (1942).
[2] G. Herzberg, *Infrared and Raman Spectra of Polyatomic Molecules* (D. Van Nostrand Company, Inc., New York, 1945).
[3] Reference 2, p. 342.
[4] The staggered configuration is also favored by the recent theoretical considerations of E. N. Lassettre and Laurence B. Davis (J. Chem. Phys. **16**, 151 (1948)).

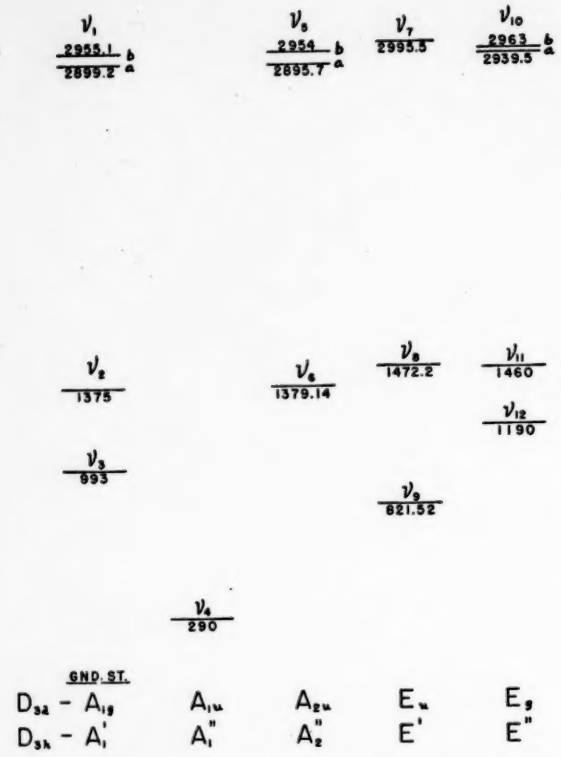


FIG. 1. Level diagram of the twelve fundamental vibrational states of $C_2H_6$. The wave number values (in $cm^{-1}$) are considered the best now available in the light of previous results and those reported here.

no evidences of the strong absorptions of any likely impurities were found.

The prism-grating spectrometer and associated carbon rod source and fixed absorption cell (133 mm long) together with the methods employed for removing water vapor and $CO_2$ from the optical path, for cooling the cell, for obtaining automatic photographic records of galvanometer deflection *vs.* angular position of the divided circle and hence *vs.* wave number and for periodically recording the zero position of the galvanometer on these records have been previously described.[5] Spectrograms of nearly all regions in which infra-red absorption by ethane gas has been reported by other investigators as well as of a region between 5700 and 6000 $cm^{-1}$ not previously studied have been obtained with this equipment and these techniques with the gas at room temperature. In addition spectrograms of the regions below 1600 $cm^{-1}$ and those between 2600 and 3500 $cm^{-1}$ have been obtained with the gas at a temperature near −100°C. Spectrograms of each region studied are reproduced in Figs. 2–12 from tracings made from the original photographs.[6] The value of pressure recorded in each of Figs. 2–12 represents that of the gas in the cell at room temperature (not, in the cases of the low temperature runs, of this gas at the reduced temperature). The 7200 line/inch and 1800 line/inch, replica, echelette gratings used throughout this work were made by Professor R. W. Wood and each had a ruled surface 4 inches high by 6 inches wide. Each grating was calibrated with the third and fourth doublets in the *P* branch of the fundamental H Cl band at 3.46$\mu$ observed in the first order with the 7200 line/inch grating and in the third order with the 1800 line/inch grating. The wave numbers of the four lines were obtained from smooth curves for the entire H Cl band fitted to the data of Meyer and Levin[7] in the manner described by Herzberg.[8]

It is evident on comparison of Fig. 3a with Fig. 3b and of Fig. 9 with a spectrogram (not shown) of the same region with the gas at room temperature that reliable measurements of the wave numbers of the rotation lines of the fundamental || bands $\nu_6$ at 1379 and $\nu_{5a}$ at 2896 $cm^{-1}$ can only be obtained with the gas at low temperature. This is undoubtedly due to appreciable population at room temperature of the lowest excited states of the low lying torsional vibration $\nu_4$. By undergoing transitions from states $n\nu_4$ to states $\nu_6+n\nu_4$ and $\nu_{5a}+n\nu_4$ molecules cause absorption at frequencies very nearly but not exactly the same as those undergoing transitions from the ground state to states $\nu_6$ and $\nu_{5a}$. Except in the case of ⊥ band $\nu_8$ where a few isolated peaks appear to be strongly temperature sensitive, the fine structures in other regions below 1600 $cm^{-1}$ and between 2600 and 3500 $cm^{-1}$ were not found to be markedly different at the two temperatures, though in general the absorption peaks were sharper at the lower temperatures.

[5] L. G. Smith, Rev. Sci. Inst. **13**, 54, 63 and 65 (1942).

[6] In the case of Fig. 2b the curve was replotted from the original photograph which was marred by bad zero drift. Hence in this figure the dashed zero line is straight and horizontal.

[7] C. F. Meyer and A. Levin, Phys. Rev. **34**, 44 (1929).

[8] G. Herzberg, *Molecular Spectra and Molecular Structure* I. *Diatomic Molecules* (Prentice-Hall Inc., New York, 1939), p. 60.

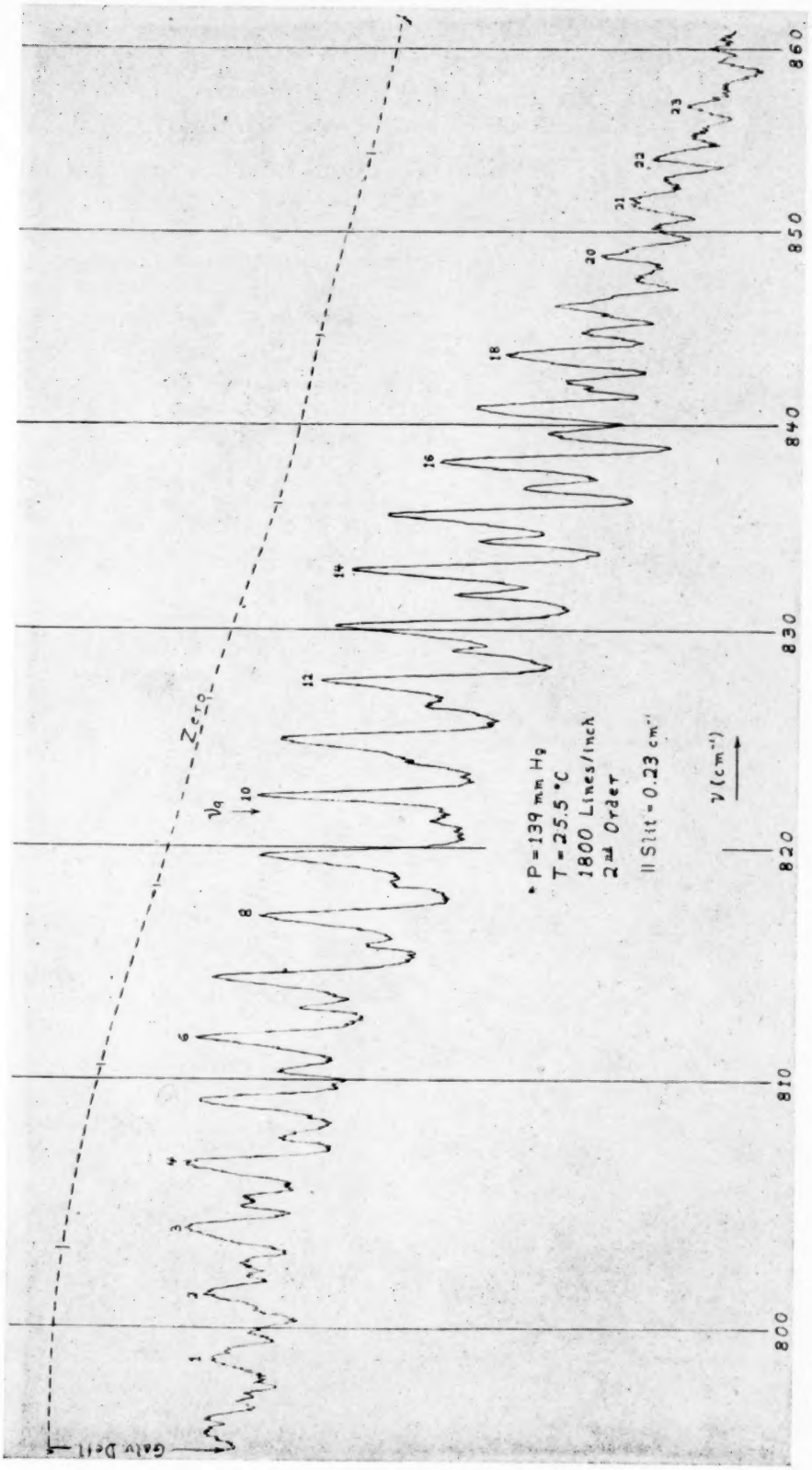


FIG. 2a. Record of fundamental ⊥ band $\nu_9$ with gas at room temperature.

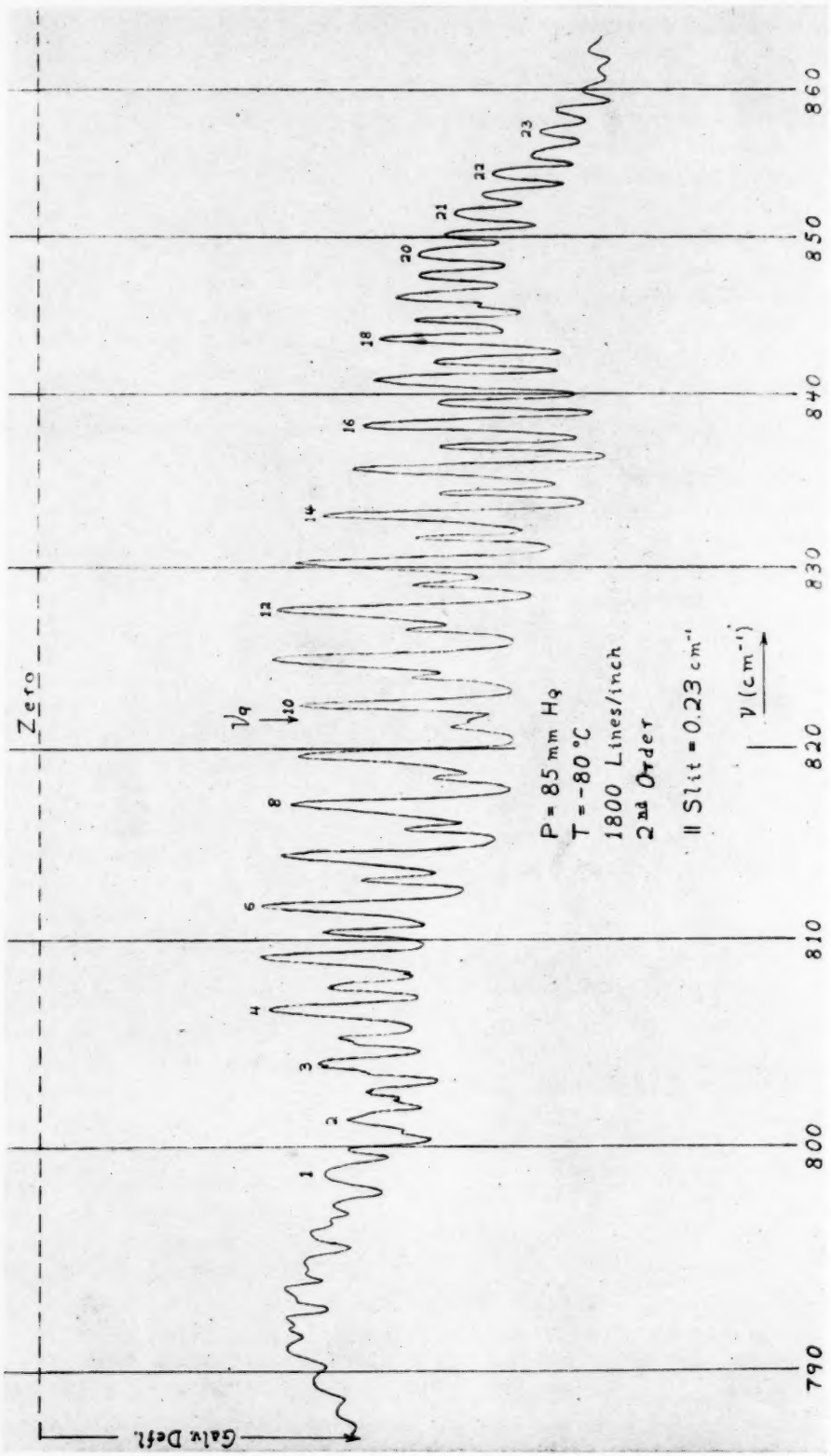


FIG. 2b. Record of fundamental ⊥ band $\nu_9$ with gas at low temperature.

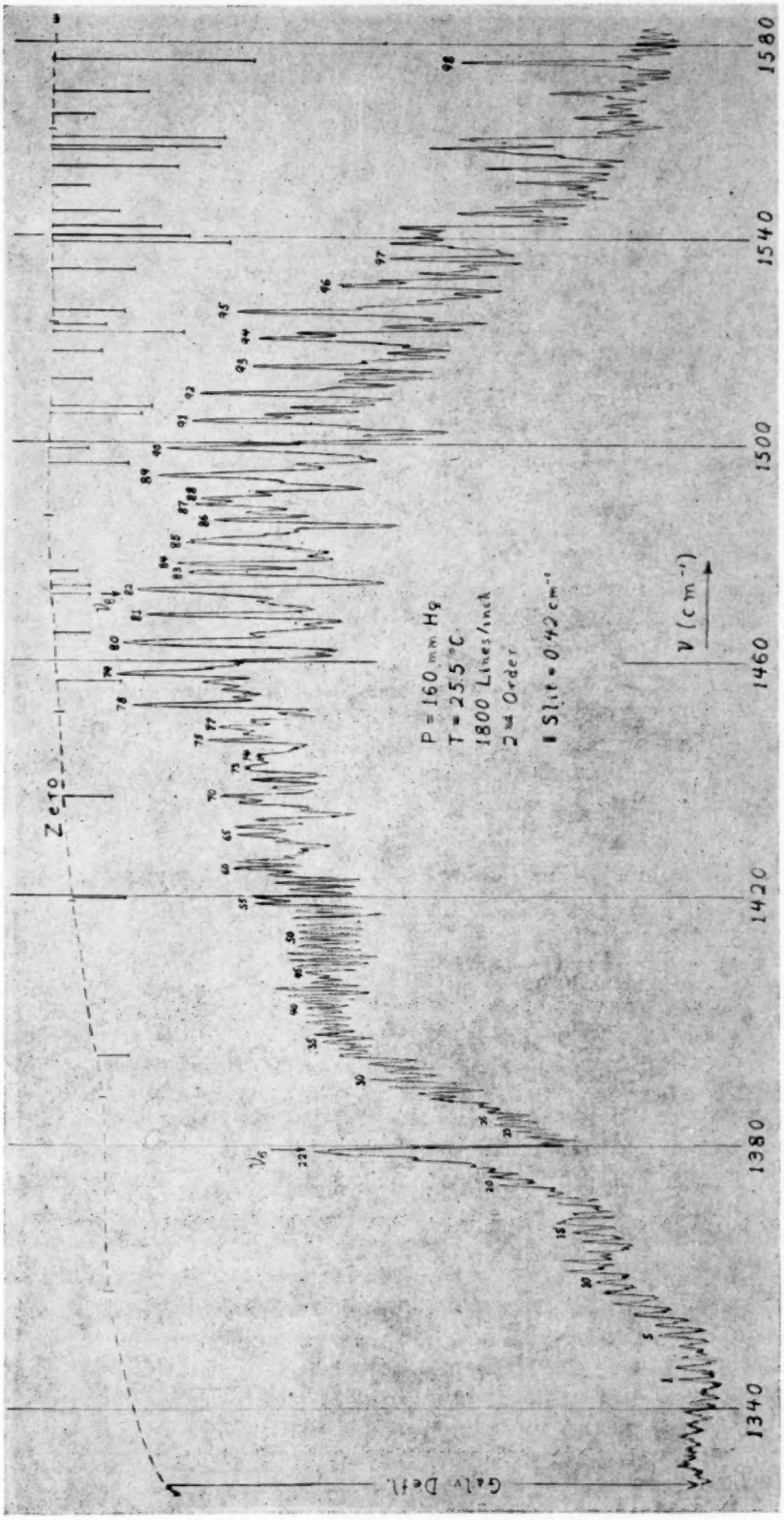


FIG. 3a. Record of fundamental || band $\nu_8$ and fundamental ⊥ band $\nu_9$ with gas at room temperature. Lines drawn down from the zero line show the positions and roughly the correct intensities of interfering water vapor lines which have not been subtracted from the record.

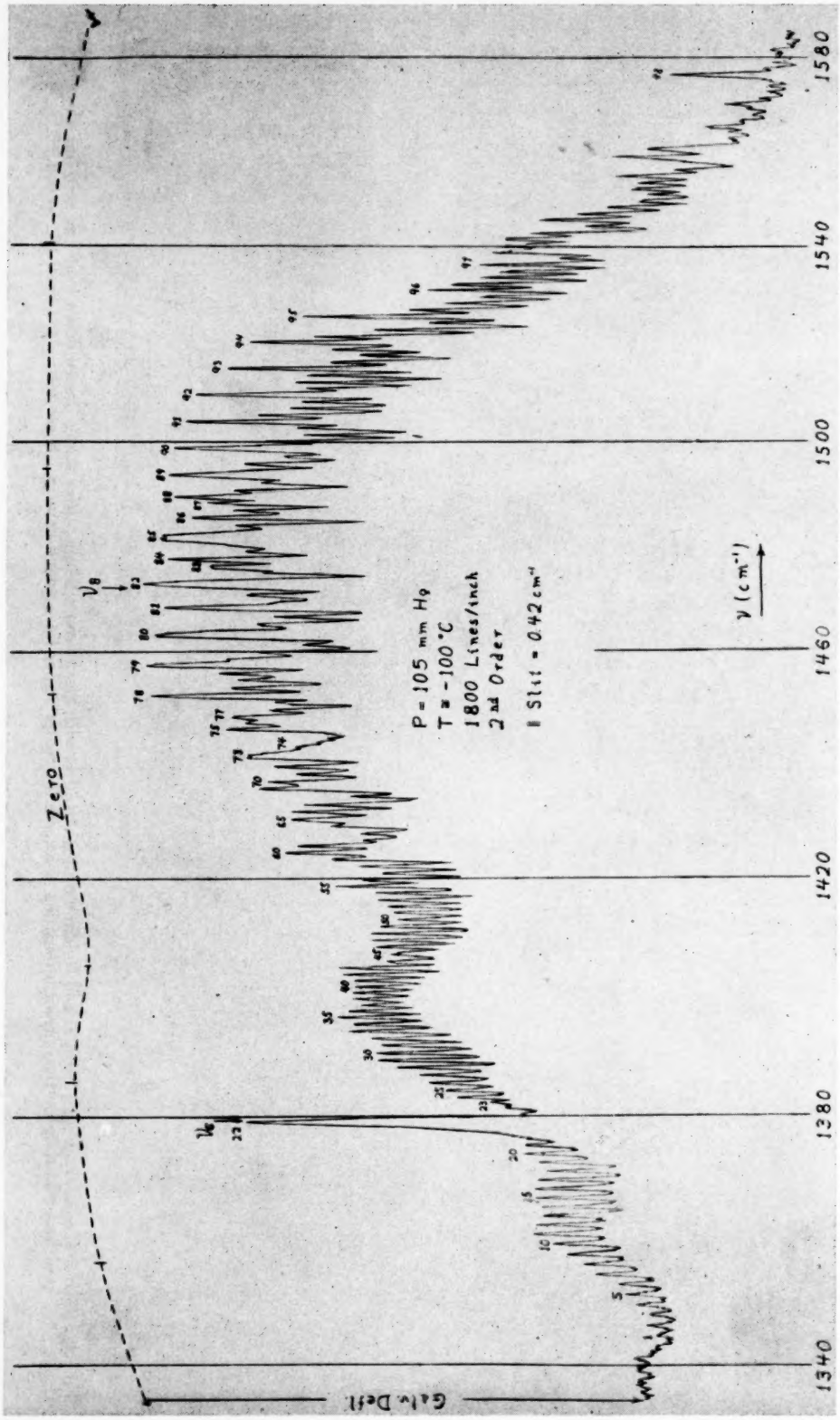


FIG. 3b. Record of fundamental || band $\nu_8$ and fundamental ⊥ band $\nu_9$ with gas at low temperature. Water vapor absorption, as indicated by peak 98, is appreciably less than in Fig. 3a.

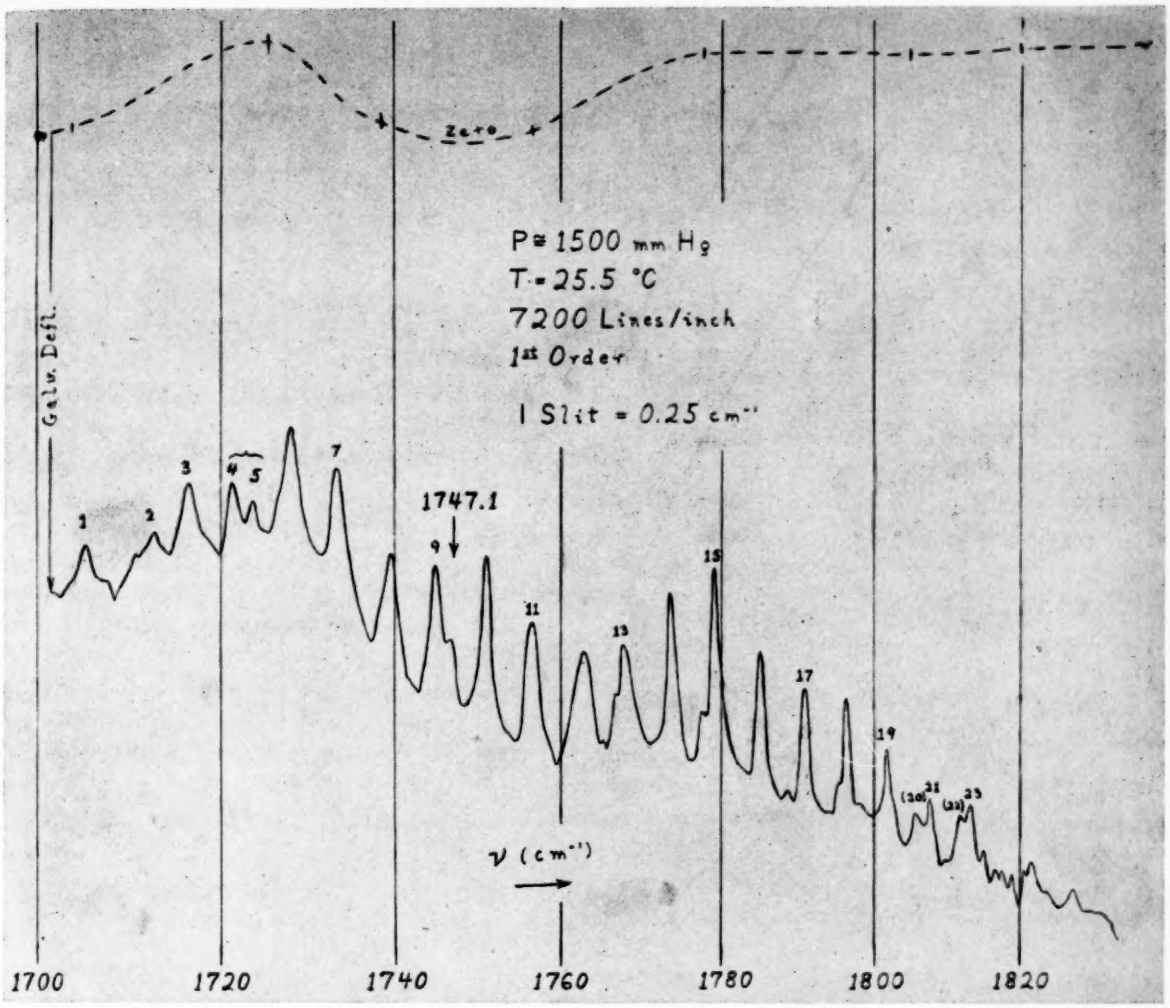


FIG. 4. Record of combination ⊥ band at 1747.1 $cm^{-1}$. A few water vapor peaks, present because the spectrometer was not well dried when this record was taken, have been subtracted from the original record of absorption due to both $C_2H_6$ and water vapor.

It is further evident from Fig. 6, wherein is shown a background run with no gas in the cell, that measurement of the || band at 2369 $cm^{-1}$ would be impossible without very complete removal from the spectrometer of atmospheric $CO_2$. Studies of the bands $\nu_6$ and $\nu_8$, both shown in Fig. 3, require not only low temperature (at least in the case of $\nu_6$) but also thorough removal of water vapor, as a comparison of Fig. 4 of reference 5, which was obtained over the same spectral region, will show. Water vapor absorption is practically negligible in the case of Fig. 3b, though it is not completely negligible in Fig. 3a wherein lines drawn down from the zero line indicate the correct positions and roughly the correct intensities of interfering water lines. (No correction of the observed spectra for water vapor absorption has been made in Fig. 3a or Fig. 3b.) Absorption by water vapor caused some interference in the region shown in Fig. 4. In this case the water lines have been subtracted from the absorption resulting from both water vapor and ethane.

In Tables I–XI are given values of the wave numbers (all corrected to vacuum) of the absorption peaks shown in Figs. 2–12 measured from the original photographic records. Also given where possible are values of $J''$ and $J'$ for the lower and upper states respectively of || bands and of $K''$ and $K'$ for ⊥ bands assigned

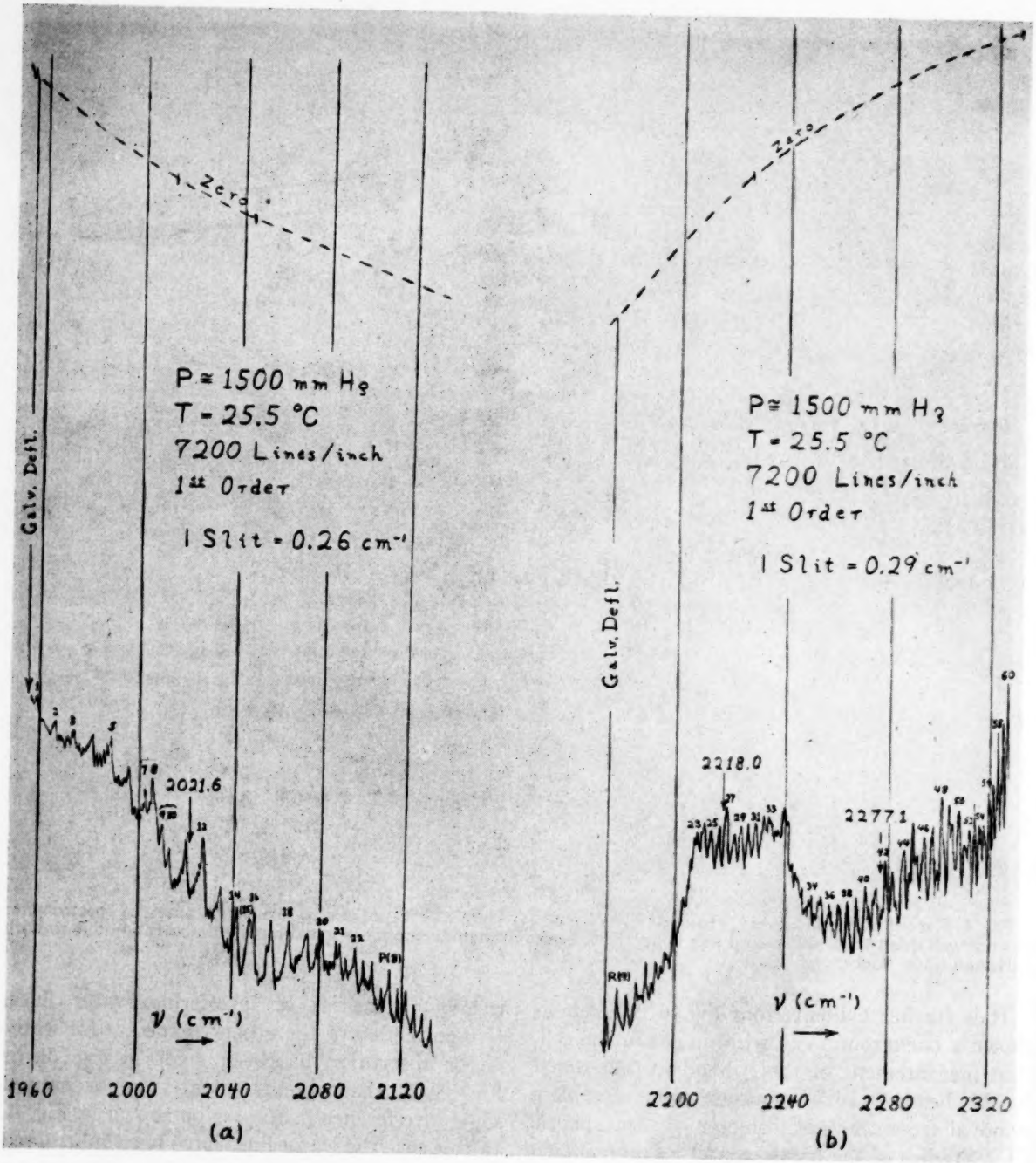


FIG. 5. Record of combination ⊥ bands at 2021.6, 2218.0 and 2277.1 $cm^{-1}$. Some lines of the fundamental band of CO are present because of a slight leak in the carbon rod source. Of these lines, $P(8)$ and $R(9)$ are marked.

in accordance with the reasonings discussed below. In the cases of the absorption regions shown in Figs. 4, 5 and 12, of which unfortunately only preliminary records were made, the calibration lines were placed on the photographic records by an automatic contactor and hence the wave numbers given in Tables III, IV and XI are somewhat less reliable than in other cases where calibration lines were put on manually, because of errors in the worm wheel that drove the divided circle. This plus the fact that in Fig. 5b the angular interval between calibration lines was quite large

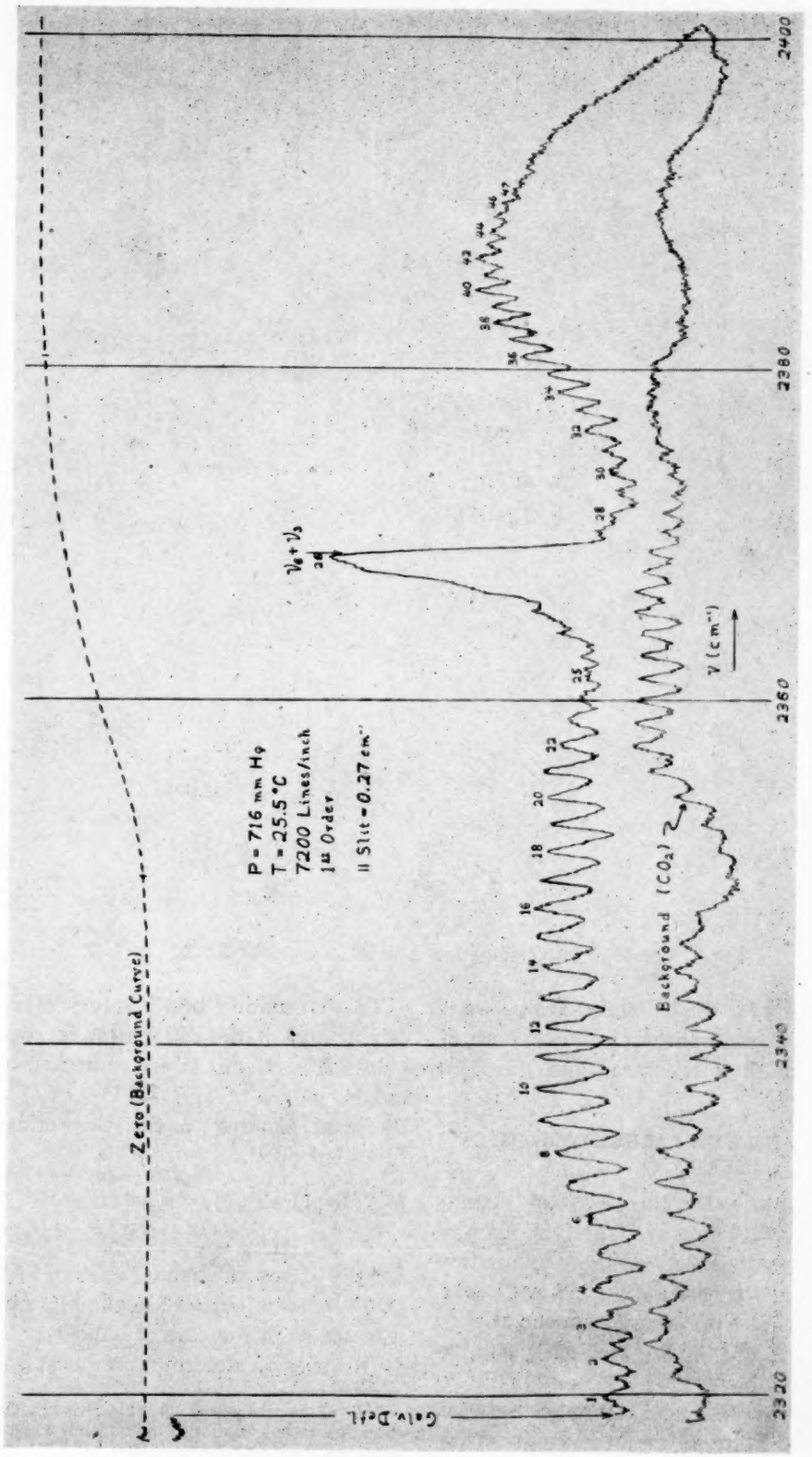


FIG. 6. Record of the combination || band $\nu_1+\nu_3$. $CO_2$ absorption is less intense in the upper record than in the background record because the former was taken first, immediately after the circulating fans (see reference 5) had been turned off.

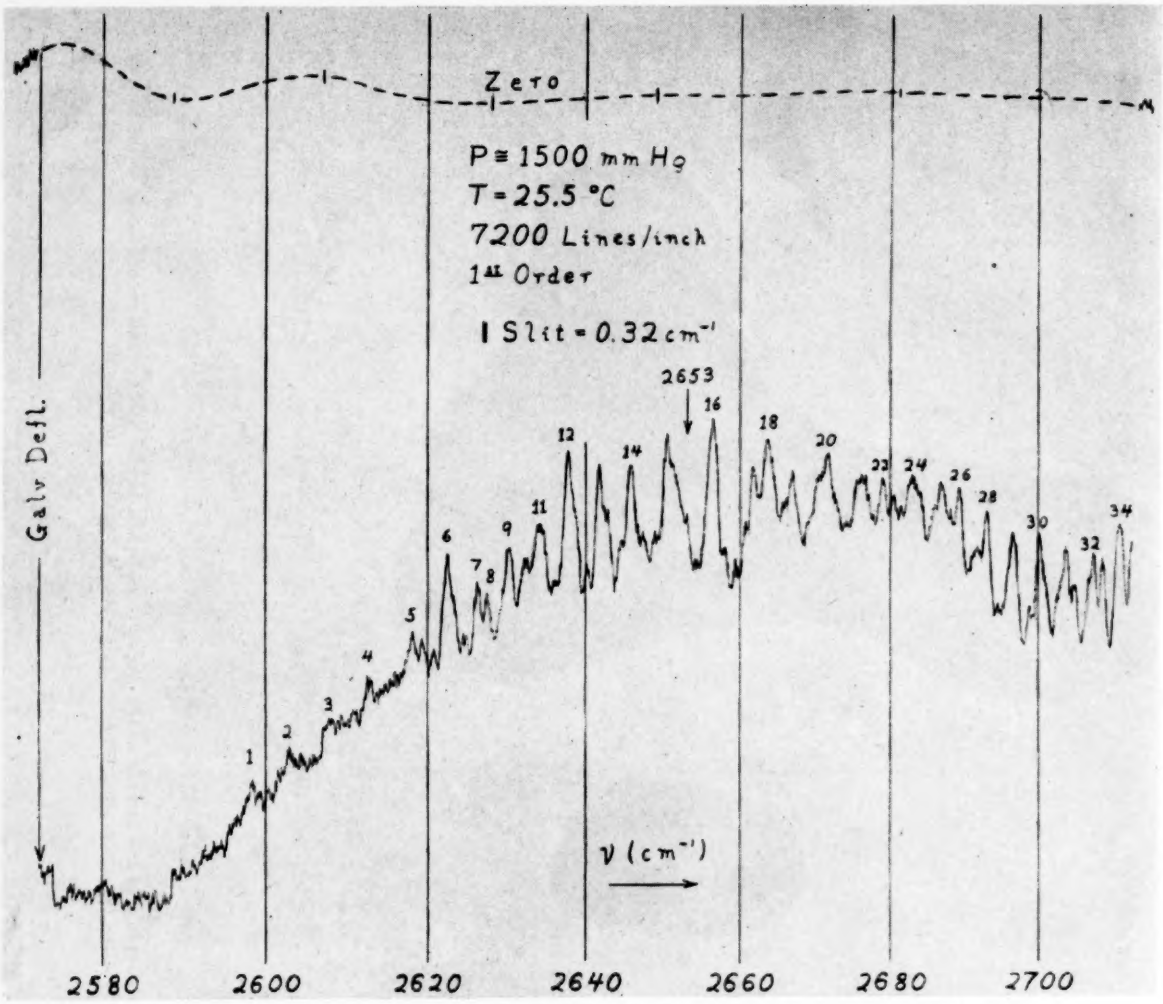


FIG. 7. Record of the combination ⊥ band (or bands) near 2653 cm$^{-1}$.

doubtless accounts for the discrepancies between values of the wave numbers of lines 57–60 in Table IV and those of the same lines (2–5) in Table V.

### III. || BANDS AND THE LARGE MOMENT OF INERTIA $I_B$

The rotational fine structures of four || bands have been resolved. These are: the fundamental band $\nu_6$ at 1379 cm$^{-1}$ (Fig. 3); the combination bands at 2369 cm$^{-1}$ (Fig. 6) and 2753 cm$^{-1}$ (Fig. 8) which doubtless correspond respectively to $\nu_3+\nu_6$ and $\nu_2+\nu_6$; and the low frequency component $\nu_{5a}$ of the doublet 2896−2955 cm$^{-1}$ (Fig. 9) generally attributed to Fermi resonance between the fundamental state $\nu_5$ and the combination state $\nu_8+\nu_{11}$.

To determine "best" values of $\nu_0$, the band origin, and of the differences in rotational constants $B'-B_0$ and $D'-D_0$ for each of the four || bands, values of $\frac{1}{2}[R(J-1)+P(J)]$ were fitted by least squares to the theoretical quadratic function[9] of $J^2$,

$$\tfrac{1}{2}[R(J-1)+P(J)]=\nu_0+[(B'-B_0)-(D'-D_0)]J^2-(D'-D_0)J^4. \quad (1)$$

In the cases of bands $\nu_6$, $\nu_3+\nu_6$ and $\nu_2+\nu_6$, $(D'-D_0)$ was entirely negligible. However, this was not so in the case of band $\nu_{5a}$.

In order to determine a "best" value of $B_0$,

[9] Here, as elsewhere in this report, the notation is essentially that used throughout references 2 and 8, the subscript 0 instead of the superscript " is used on rotational constants of the ground state and $J \equiv J''$.

a value of $D_0$ was first calculated with the aid of the potential function involving three force constants given by Howard.[10] This constant $D_0$, which measures the degree of centrifugal stretching of the rotating, non-vibrating molecule, is given in general for a linear or symmetric top molecule by the expression

$$D_0=\frac{16\pi^2c^2B_0^3}{I_{B0}}\left(\frac{\delta I_{B0}}{\omega^2}-\frac{2V}{\omega^4}\right), \quad (2)$$

where $I_{B0}$ is the moment of inertia of the non-rotating (and non-vibrating) molecule about an axis perpendicular to the symmetry axis, $c$ is the velocity of light, and $\omega$ is the angular rotation frequency, and where $\delta I_{B0}$ is the change in $I_{B0}$ and $V$ the potential energy, both caused by the centrifugal stretching. For the particular case of ethane and Howard's potential function this becomes

$$\begin{aligned}D_0=\frac{4\pi^2c^2B_0^3}{I_{B0}}\Bigg\{&\frac{M^2a^2}{K_3}\\&+\frac{m^2\sin^2\alpha(1+3\cos^2\alpha)}{K_2(1+15\cos^2\alpha)}\\&\times[6(a+b\cos\alpha)^2\\&+b^2(1+3\cos^2\alpha)]\\&+\frac{3m^2}{K_1}[2a^2\cos^2\alpha\\&+b^2(3+2\cos^2\alpha+3\cos^4\alpha)\\&+4ab\cos\alpha(1+\cos^2\alpha)]\Bigg\}, \quad (3)\end{aligned}$$

where, $M$ and $m$ are respectively the masses of the carbon and hydrogen atoms, $a$, $b$ and $\alpha$ are

[10] J. B. Howard, J. Chem. Phys. **5**, 442 (1937).

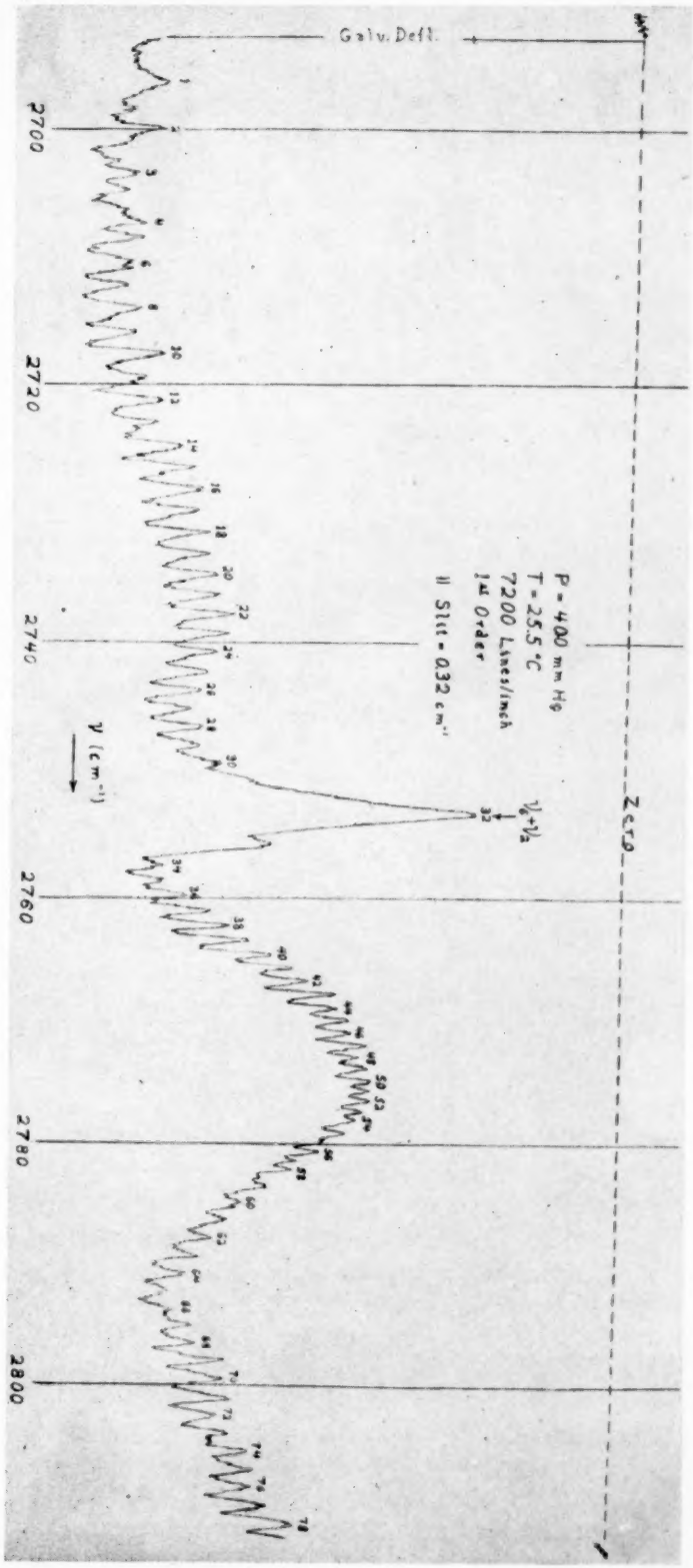


FIG. 8. Record of the combination || band $\nu_2+\nu_6$ and the combination ⊥ band near 2800 cm$^{-1}$.

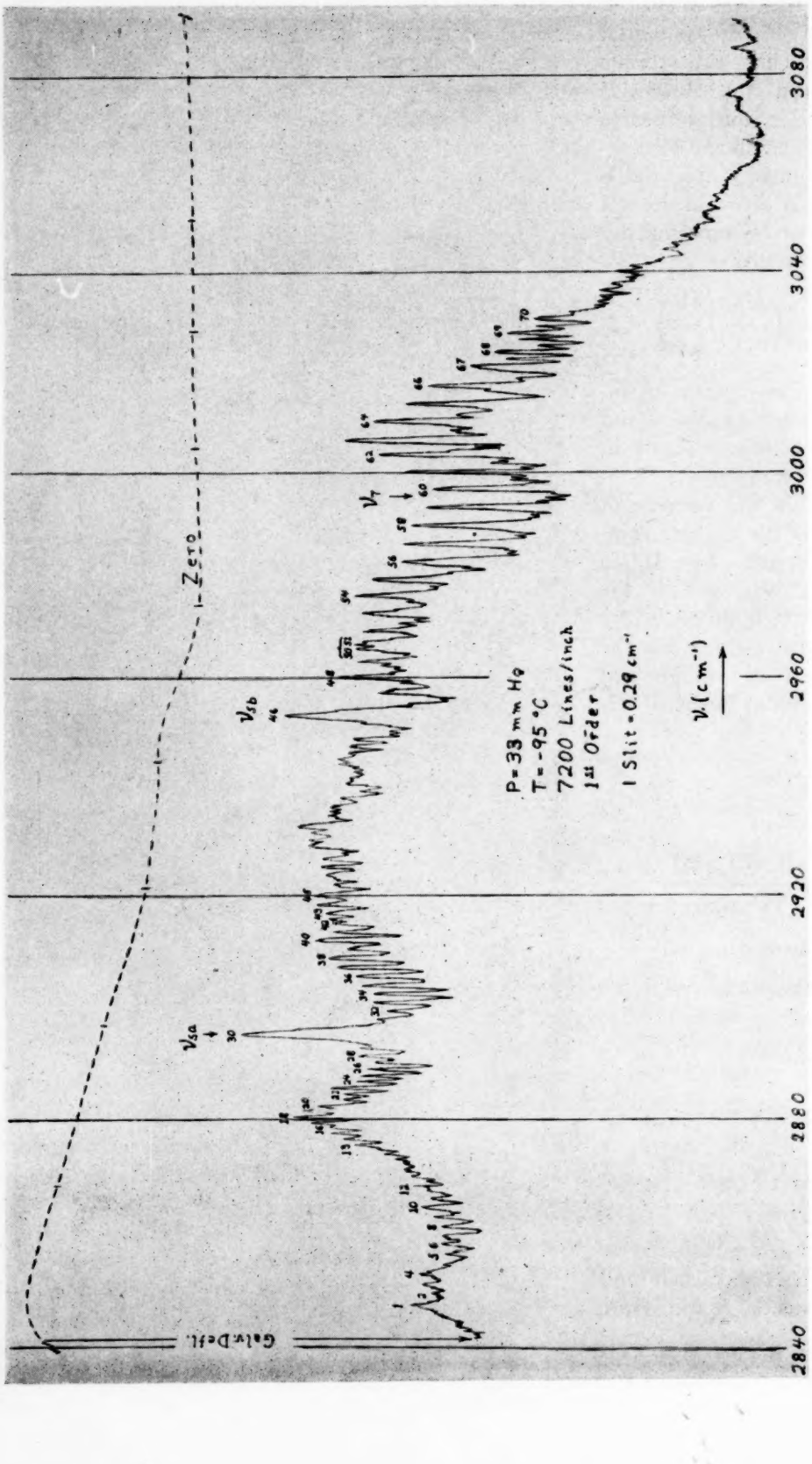


FIG. 9. Record of the combination ⊥ band near 2860 cm$^{-1}$, the fundamental double || band $\nu_{5a}$ and $\nu_{5b}$ and the fundamental ⊥ band $\nu_7$.

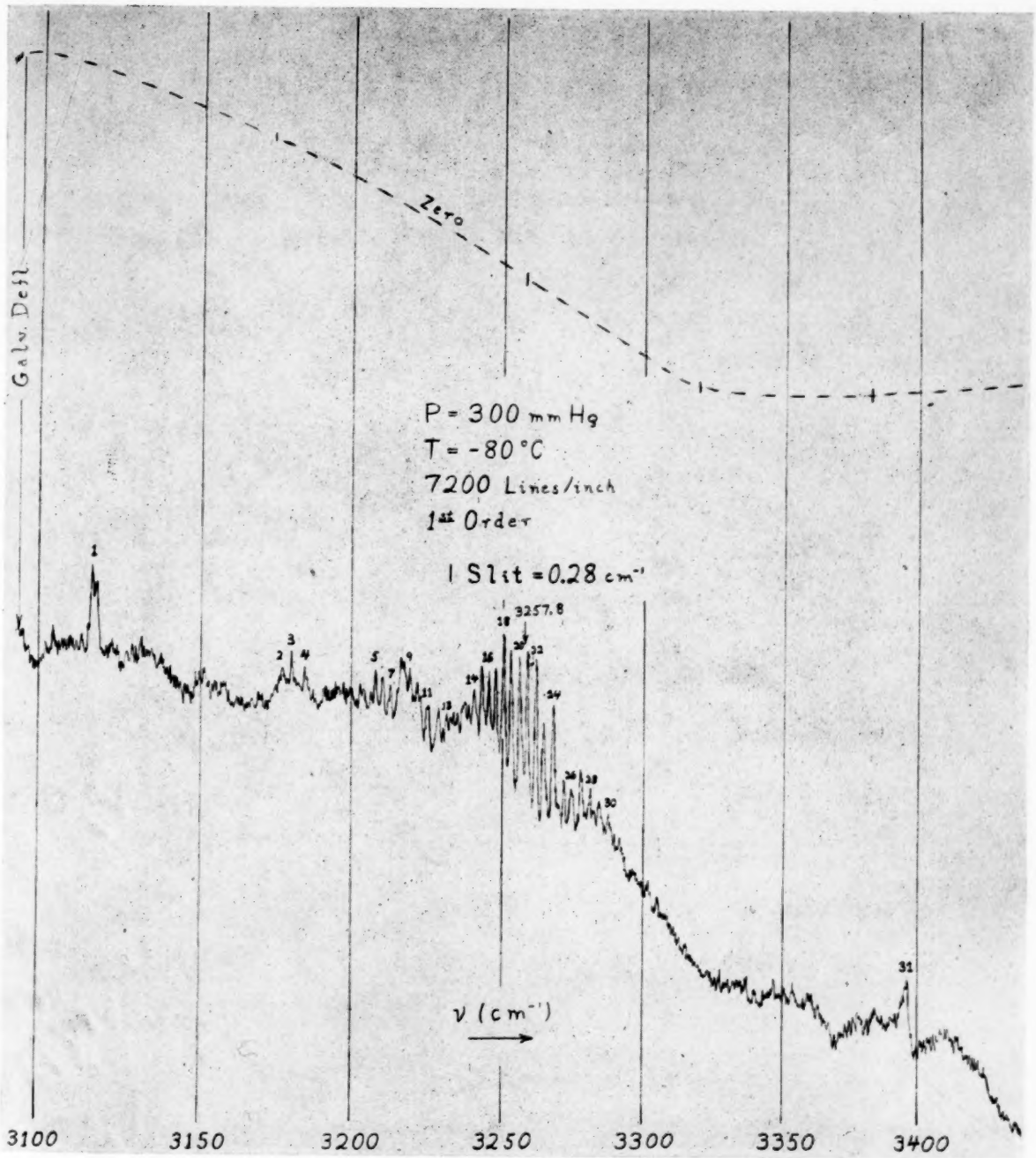


FIG. 10. Record of the combination ⊥ band at 3257.8 $cm^{-1}$ showing in addition what may be combination || bands (peaks 1 and 31) as well as other peaks which may be due to combination ⊥ bands.

respectively the equilibrium values of the C−C distance, the C−H distance and the supplement of the HCC angle, and $K_1$, $K_2$, $K_3$ are the force constants given by Howard. Since $D_0 \ll B_0$, only approximate values of the parameters need be used to determine $D_0$. Hence it was assumed that the HCC and HCH angles are tetrahedral ($\cos\alpha = \frac{1}{3}$), that $a = 1.55$A, $b = 1.10$A, $K_1$, $K_2$ and $K_3$ have the values given by Howard, $B_0 = 0.6626$ $cm^{-1}$ and $I_{B0} = 42.23 \times 10^{-40}$ g $cm^2$. These values are consistent with the final results of the measurements.

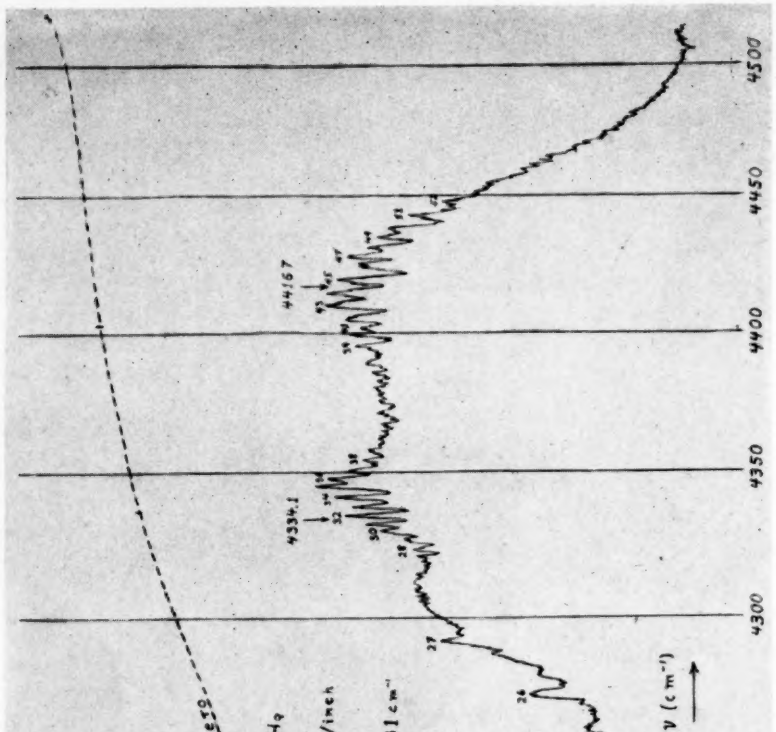


FIG. 11. Record of absorption between 4000 and 4500 cm$^{-1}$.

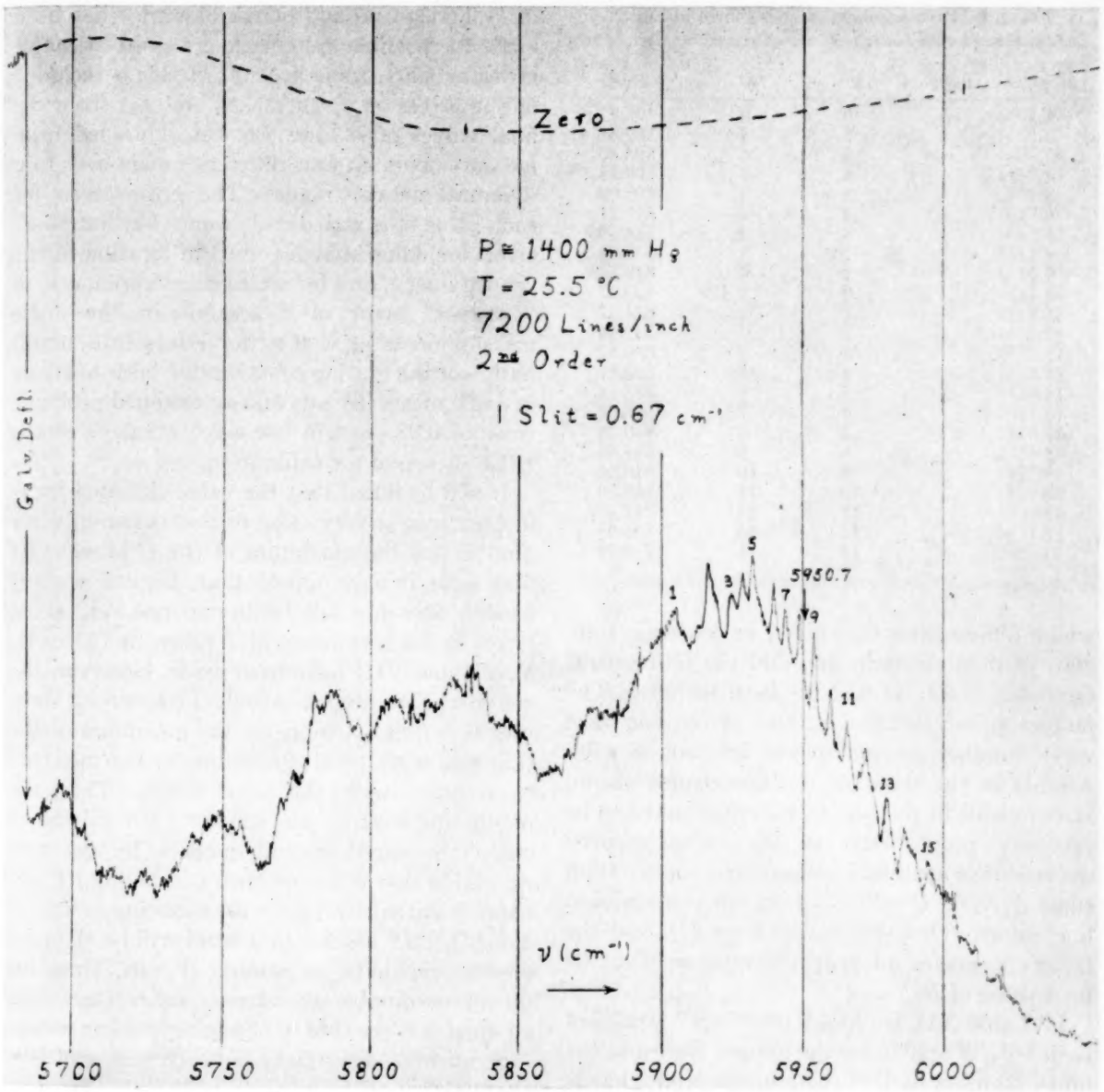


FIG. 12. Record of absorption between 5700 and 6000 $cm^{-1}$.

With the value of $D_0$ obtained thus a "best" value of $B_0$ was determined by fitting by least squares values of $\Delta_2F_0(J)/2(2J+1)$, determined from measurements on all four || bands, to the theoretical linear function of $(2J+1)^2$,

$$\frac{\Delta_2F_0(J)}{2(2J+1)}=\frac{R(J-1)-P(J+1)}{2(2J+1)}$$

$$=(B_0-\tfrac{3}{2}D_0)-\frac{D_0}{2}(2J+1)^2. \quad (4)$$

The measured values of these quantities together with the least squares regression line are shown plotted as a function of $(2J+1)^2$ in Fig. 13. The intercept of the regression line was determined from the relation

$$(B_0-\tfrac{3}{2}D_0)=\frac{\sum_{i=1}^{4}g_i\{\sum(2J+1)\Delta_2F_0+D_0\sum(2J+1)^4\}_i}{2\sum_{i=1}^{4}g_i\{\sum(2J+1)^2\}_i}, \quad (5)$$

TABLE I. Wave numbers of lines shown in Fig. 2.

| Line No. | Band | $K''$ | $K'$ | $\nu$ (cm$^{-1}$) |
|---|---|---|---|---|
| 1 | $\nu_8$ | 9 | 8 | 798.77 |
| 2 | | 8 | 7 | 801.31 |
| 3 | | 7 | 6 | 803.88 |
| 4 | | 6 | 5 | 806.53 |
| 5 | | 5 | 4 | 809.09 |
| 6 | | 4 | 3 | 811.71 |
| 7 | | 3 | 2 | 814.29 |
| 8 | | 2 | 1 | 816.94 |
| 9 | | 1 | 0 | 819.58 |
| 10 | | 0 | 1 | 822.27 |
| 11 | | 1 | 2 | 824.82 |
| 12 | | 2 | 3 | 827.49 |
| 13 | | 3 | 4 | 830.12 |
| 14 | | 4 | 5 | 832.81 |
| 15 | | 5 | 6 | 835.51 |
| 16 | | 6 | 7 | 838.14 |
| 17 | | 7 | 8 | 840.78 |
| 18 | | 8 | 9 | 843.46 |
| 19 | | 9 | 10 | 846.06 |
| 20 | | 10 | 11 | 848.79 |
| 21 | | 11 | 12 | 851.50 |
| 22 | | 12 | 13 | 854.05 |
| 23 | | 13 | 14 | 856.79 |

which differs from that given in reference 8 (p. 200) in that the term $\frac{3}{2}D_0$ and the four weight factors $g_i$ ($i=1, \cdots 4$) have been included. The factors $g_i$, which take account of the fact that wave number measurements are not equally reliable in the cases of the four bands (being least reliable in the case of $\nu_{5a}$), were taken to be inversely proportional to the mean squared deviations of measured values of the combination sums $\frac{1}{2}[R(J-1)+P(J)]$ from their regression line values. (Omission of the term $\frac{3}{2}D_0$ and the factors $g_i$ makes an insignificant change in the final value of $B_0$.)

In Table XII are listed the "best" values of $\nu_0$, $B-B_0$, $B$ and $I_B$ for the ground state and the upper states of each of the four resolved || bands as well as $D$ for the ground state and the state $\nu_{5a}$. The values of $I_B$ were obtained from the $B$ values by use of the latest value of Planck's constant recommended by DuMond and Cohen,[11] namely $h=(6.6234\pm0.0011)\times10^{-27}$ erg sec. The errors given for the values of $B-B_0$, $B$ and $D$ are probable errors estimated by standard statistical methods from the scatter of the measured combination sums and differences about their regression line values while those for the values of $I_B$ include in addition allowance for the uncertainty in $h$. Though no additional allowance has been made for possible systematic errors in the angle measurements, some account of this is included in the errors as given for $B_0$ and $I_{B0}$ since the final values of $B_0$ and $I_{B0}$ were obtained from measurements on four different bands over four different angular ranges. The error given for each value of $\nu_0$ includes allowance for "internal" error, including that involved in location of the central image, and for an assumed systematic or "external" error of 5 seconds in the angle measurements as well as for errors in determination of the grating constant due both to errors in angle measurements and an assumed probable error of 0.05 cm$^{-1}$ in the wave numbers of the H Cl lines used for calibration.

It will be noted that the value obtained for $\nu_0$ in each case is very close to the measured wave number for the maximum of the $Q$ branch. At first sight it may appear that, because each $Q$ branch does not fall farther to one side of $\nu_0$, errors in the assignment of $J$-values in Tables II, V, VII and VIII have been made. However, the considerations on page 416 ff. of reference 2 show that it is quite possible for the maximum of the $Q$ branch of a || band of a symmetric top molecule to coincide with the band origin. That the numbering scheme adopted for each || band is correct is placed beyond question by the consideration that if the assigned numbering for any band is shifted by 1 unit the resulting values of $\Delta_2F_0(J)/2(2J+1)$ for that band will be changed on the average by an amount $B'-B_0$. Thus, for no set of numbering schemes other than that adopted is it possible to obtain agreement within experimental uncertainty between values of this quantity for all four bands such as is shown in Fig. 13.

The fact that $B$ for state $\nu_{5a}$ is greater than $B_0$ so that $I_B$ for this state is less than $I_{B0}$ leads to the conclusion that $\nu_{5a}$ is a perturbed state, because the symmetry of any || vibration of $C_2H_6$ involving a change of dipole moment is such that the instantaneous value of $I_B$ is a minimum when all atoms are in their equilibrium positions so that $I_B$ for the unperturbed upper state of any || band must be greater than $I_{B0}$. Furthermore, this fact cannot be explained on the basis of a perturbation of the Fermi type, which almost certainly occurs between states $\nu_{5a}$

[11] J. W. M. DuMond and E. R. Cohen, Rev. Mod. Phys. 20, 82 (1948).

TABLE II. Wave numbers of lines shown in Fig. 3.

| Line No. | Band | $J''$ | $J'$ | $\nu$ (cm$^{-1}$) |
|---|---|---|---|---|
| 1 | $\nu_6$ | 23 | 22 | 1345.03 |
| 2 | | 22 | 21 | 1346.70 |
| 3 | | 21 | 20 | 1348.26 |
| 4 | | 20 | 19 | 1349.88 |
| 5 | | 19 | 18 | 1351.49 |
| 6 | | 18 | 17 | 1353.06 |
| 7 | | 17 | 16 | 1354.65 |
| 8 | | 16 | 15 | 1356.17 |
| 9 | | 15 | 14 | 1357.73 |
| 10 | | 14 | 13 | 1359.23 |
| 11 | | 13 | 12 | 1360.81 |
| 12 | | 12 | 11 | 1362.28 |
| 13 | | 11 | 10 | 1363.75 |
| 14 | | 10 | 9 | 1365.20 |
| 15 | | 9 | 8 | 1366.77 |
| 16 | | 8 | 7 | 1368.05 |
| 17 | | 7 | 6 | 1369.61 |
| 18 | | 6 | 5 | 1370.96 |
| 19 | | 5 | 4 | 1372.31 |
| 20 | | 4 | 3 | 1373.74 |
| 21 | | 3 | 2 | 1375.07 |
| 22 | | 0 | 0 | 1379.01 |
| 23 | | 1 | 2 | 1382.21 |
| 24 | | 2 | 3 | 1383.06 |
| 25 | | 3 | 4 | 1384.25 |
| 26 | | 4 | 5 | 1385.47 |
| 27 | | 5 | 6 | 1386.89 |
| 28 | | 6 | 7 | 1387.99 |
| 29 | | 7 | 8 | 1389.17 |
| 30 | | 8 | 9 | 1390.47 |
| 31 | | 9 | 10 | 1391.60 |
| 32 | | 10 | 11 | 1392.75 |
| 33 | | 11 | 12 | 1393.99 |
| 34 | | 12 | 13 | 1395.07 |
| 35 | | 13 | 14 | 1396.24 |
| 36 | | 14 | 15 | 1397.38 |
| 37 | | 15 | 16 | 1398.32 |
| 38 | | 16 | 17 | 1399.35 |
| 39 | | 17 | 18 | 1400.58 |
| 40 | | 18 | 19 | 1401.46 |
| 41 | | 19 | 20 | 1402.48 |
| 42 | | 20 | 21 | 1403.63 |
| 43 | | 21 | 22 | 1404.70 |
| 44 | | 22 | 23 | 1405.77 |

TABLE II.—*Continued.*

| Line No. | Band | $K''$ | $K'$ | $\nu$ (cm$^{-1}$) |
|---|---|---|---|---|
| 45 | $\nu_8$ | | | 1407.07 |
| 46 | | | | 1408.27 |
| 47 | | | | 1409.32 |
| 48 | | | | 1410.53 |
| 49 | | | | 1411.71 |
| 50 | | | | 1412.89 |
| 51 | | | | 1414.13 |
| 52 | | | | 1415.18 |
| 53 | | | | 1416.30 |
| 54 | | | | 1417.50 |
| 55 | | | | 1418.71 |
| 56 | | | | 1419.75 |
| 57 | | | | 1421.00 |
| 58 | | | | 1422.20 |
| 59 | | | | 1423.37 |
| 60 | | | | 1424.56 |
| 61 | | | | 1425.83 |
| 62 | | | | 1426.73 |
| 63 | | | | 1427.92 |
| 64 | | | | 1429.38 |
| 65 | | | | 1430.34 |
| 66 | | | | 1431.62 |
| 67 | | | | 1433.17 |
| 68 | | | | 1434.25 |
| 69 | | | | 1435.65 |
| 70 | | | | 1436.85 |
| 71 | | | | 1438.21 |
| 72 | | | | 1439.63 |
| 73 | | | | 1441.36 |
| 74 | | | | 1443.40 |
| 75 | | | | 1446.38 |
| 76 | | | | 1447.45 |
| 77 | | | | 1448.52 |
| 78 | | 4 | 3 | 1452.41 |
| 79 | | 3 | 2 | 1457.91 |
| 80 | | 2 | 1 | 1463.48 |
| 81 | | 1 | 0 | 1468.45 |
| 82 | | 0 | 1 | 1472.95 |
| 83 | | 0 | 1 | 1475.87 |
| 84 | | 1 | 2 | 1477.48 |
| 85 | | 2 | 3 | 1481.49 |
| 86 | | 1 | 2 | 1485.64 |
| 87 | | 2 | 3 | 1488.28 |
| 88 | | 2 | 3 | 1489.29 |
| 89 | | 3 | 4 | 1493.68 |
| 90 | | 4 | 5 | 1498.90 |
| 91 | | 5 | 6 | 1504.13 |
| 92 | | 6 | 7 | 1509.47 |
| 93 | | 7 | 8 | 1514.65 |
| 94 | | 8 | 9 | 1519.85 |
| 95 | | 9 | 10 | 1525.14 |
| 96 | | 10 | 11 | 1530.51 |
| 97 | | 11 | 12 | 1535.80 |
| 98 | $H_2O$ | | | 1576.04 |

and $\nu_{5b}$, because in such a perturbation the $B$ values of both perturbed states lie between those of the perturbing states, which, by the symmetry argument, are both less than $B_0$. For these reasons and also because of the abnormally large value of $D$ of state $\nu_{5a}$, we conclude that a Coriolis perturbation of this state by a nearby vibrational state exists in addition to the Fermi perturbation. If, as appears virtually certain, the matrix elements of this Coriolis perturbation depend primarily on $J$, the other state involved must be of the same species as the upper states of active $\perp$ bands, since the product of this species with that of $\nu_{5a}$ must be the species of a rotation ($R_x$, $R_y$) about an axis perpendicular to the symmetry axis of the molecule.[12] Furthermore, because the rotational levels for which $J>0$ of $\nu_{5a}$ lie higher relative to the level $J=0$ than they would in the absence of a Coriolis perturbation, the perturbing state evidently lies below $\nu_{5a}$. Though there is evidence in Figs. 8

[12] Jahn's rule, cf. reference 2, p. 276 and Tables 20, 22 and 31.

TABLE III. Wave numbers of lines shown in Fig. 4.

| Line No. | Band | $K''$ | $K'$ | $\nu$ (cm$^{-1}$) |
|---|---|---|---|---|
| 1 | 1747.1 | 8 | 7 | 1705.25 |
| 2 | | 7 | 6 | 1712.25 |
| 3 | | 6 | 5 | 1716.57 |
| 4 | | 5 | 4 | 1721.38 |
| 5 | | | | 1723.67 |
| 6 | | 4 | 3 | 1727.97 |
| 7 | | 3 | 2 | 1733.21 |
| 8 | | 2 | 1 | 1739.38 |
| 9 | | 1 | 0 | 1744.87 |
| 10 | | 0 | 1 | 1750.87 |
| 11 | | 1 | 2 | 1756.36 |
| 12 | | 2 | 3 | 1762.71 |
| 13 | | 3 | 4 | 1767.81 |
| 14 | | 4 | 5 | 1773.66 |
| 15 | | 5 | 6 | 1779.29 |
| 16 | | 6 | 7 | 1785.11 |
| 17 | | 7 | 8 | 1790.89 |
| 18 | | 8 | 9 | 1796.44 |
| 19 | | 9 | 10 | 1801.80 |
| 20 | | | | 1805.79 |
| 21 | | 10 | 11 | 1807.54 |
| 22 | | | | 1811.67 |
| 23 | | 11 | 12 | 1813.18 |

and 9 of states of the proper species just below $\nu_{5a}$, no attempt to identify the state in question or to investigate the perturbations of $\nu_{5a}$ in further detail has been made to date.

## IV. FUNDAMENTAL ⊥ BANDS AND THE SMALL MOMENT OF INERTIA $I_A$

Spectrograms of the three fundamental ⊥ bands of $C_2H_6$ ($\nu_9$, $\nu_8$ and $\nu_7$) are shown in Figs. 2, 3 and 9. These spectrograms show the same principal absorption peaks as did those of Levin and Meyer,[13] which peaks Howard[14] has demonstrated are to be identified with the strong, regularly spaced $^PQ$ and $^RQ$ "lines" (actually groups of superposed lines) that theory predicts should be the most prominent features of the ⊥ bands of a symmetric top molecule with out free rotation whose two equal moments of inertia ($I_B$) are greater than its third ($I_A$). Figs. 2, 3 and 9 also reveal much more clearly than the spectrograms of Levin and Meyer the presence and nature of absorption peaks other than those corresponding to the $^PQ$ and $^RQ$ lines. These other absorptions may at first sight appear to arise in part from coincidence of other bands with $\nu_7$, $\nu_8$, and $\nu_9$. In fact, in each case the existence of one or more such other bands has been suggested by other workers. The present results together with the following interpretations indicate that most of these suggestions are invalid.

In band $\nu_9$ (Fig. 2) there is, between each pair of adjacent major peaks, a minor peak, whose existence was first reported by Smith and Woodward.[1] Owens and Barker,[15] who also reported their existence, suggested that the minor peaks might be due to absorptions by molecules initially in a low lying excited vibrational state. However, the low temperature spectrogram reported on by Smith and Woodward and reproduced here in Fig. 2b shows that at −100°C the intensities of the minor relative to the major peaks are not less than at room temperature but, in fact, appear to be slightly greater. This result indicates strongly that the minor as well as the major peaks arise from absorptions by molecules initially in the ground state. The apparent small increase in intensity of the minor peaks as the temperature is lowered is doubtless because of sharpening of all peaks and consequent improvement of resolution.

An entirely reasonable explanation of these minor peaks appears when one notes the fact that the spacing of the major peaks is almost exactly twice the mean spacing ($2B_0$) of the lines of the fundamental || band $\nu_6$. In such a case the $^PP$, $^PR$, $^RP$ and $^RR$ sub-band lines would be expected to be grouped in lines, one of which should occur approximately half way between each adjacent pair of $^PQ$ and $^RQ$ lines, instead of forming an unresolved background to the latter as they usually do in such ⊥ bands. This explanation allows us to state with a high degree of confidence that the origin of $\nu_9$ lies between line 9 and line 10 (Fig. 2 and Table I) since it should lie between the same two major peaks as the weakest minor peak. Thus there is little question concerning the correctness of the assignment of values of $K$ given in Table I for $\nu_9$. This assignment of $K$ values agrees with that of Owens and Barker[15] which these authors based on the slight enhancement of every third line near the middle of the band.

[13] A. Levin and C. F. Meyer, J. Opt. Soc. Amer. **16**, 137 (1928).

[14] J. B. Howard, J. Chem. Phys. **5**, 451 (1937).

[15] R. G. Owens and E. F. Barker, J. Chem. Phys. **10**, 146 (1942). The wave number values reported by these authors are systematically lower than those in Table I by about 0.1 cm$^{-1}$.

TABLE IV. Wave numbers of lines shown in Fig. 5.

| Line No. | Band | $K''$ | $K'$ | $\nu$ ($cm^{-1}$) |
|---|---|---|---|---|
| 1 | 2021.6 | 9 | 8 | 1959.40 |
| 2 | | 8 | 7 | 1966.41 |
| 3 | | 7 | 6 | 1973.75 |
| 4 | | 6 | 5 | 1981.05 |
| 5 | | 5 | 4 | 1988.83 |
| 6 | | 4 | 3 | 1996.03 |
| 7 | | 3 | 2 | 2002.83 |
| 8 | | | | 2006.47 |
| 9 | | | | 2009.86 |
| 10 | | 2 | 1 | 2013.16 |
| 11 | | 1 | 0 | 2020.17 |
| 12 | | 0 | 1 | 2027.37 |
| 13 | | 1 | 2 | 2034.75 |
| 14 | | 2 | 3 | 2042.46 |
| 15 | | | | 2047.85 |
| 16 | | 3 | 4 | 2050.26 |
| 17 | | 4 | 5 | 2057.41 |
| 18 | | 5 | 6 | 2065.55 |
| 19 | | 6 | 7 | 2073.49 |
| 20 | | 7 | 8 | 2080.43 |
| 21 | | 8 | 9 | 2088.43 |
| 22 | | 9 | 10 | 2095.96 |
| 23 | 2218.0 | 4 | 3 | 2207.69 |
| 24 | | 3 | 2 | 2210.67 |
| 25 | | 2 | 1 | 2213.18 |
| 26 | | 1 | 0 | 2216.25 |
| 27 | | 0 | 1 | 2218.95 |
| 28 | | 1 | 2 | 2221.92 |
| 29 | | 2 | 3 | 2224.20 |
| 30 | | 3 | 4 | 2226.73 |
| 31 | | 4 | 5 | 2229.56 |
| 32 | | 5 | 6 | 2232.42 |
| 33 | | 6 | 7 | 2234.76 |
| 34 | 2277.1 | 8 | 7 | 2249.63 |
| 35 | | 7 | 6 | 2253.67 |
| 36 | | 6 | 5 | 2257.38 |
| 37 | | 5 | 4 | 2260.95 |
| 38 | | 4 | 3 | 2264.13 |
| 39 | | 3 | 2 | 2267.71 |
| 40 | | 2 | 1 | 2271.21 |
| 41 | | 1 | 0 | 2274.98 |
| 42 | | 0 | 1 | 2278.60 |
| 43 | | 1 | 2 | 2281.70 |
| 44 | | 2 | 3 | 2286.23 |
| 45 | | 3 | 4 | 2289.48 |
| 46 | | 4 | 5 | 2293.91 |
| 47 | | 5 | 6 | 2297.41 |
| 48 | | 6 | 7 | 2300.91 |
| 49 | | 7 | 8 | 2304.43 |
| 50 | | 8 | 9 | 2307.75 |
| 51 | | 9 | 10 | 2310.12 |
| 52 | | 10 | 11 | 2311.94 |
| 53 | | 11 | 12 | 2313.93 |
| 54 | | 12 | 13 | 2316.18 |
| 55 | | 13 | 14 | 2318.18 |
| | | $J''$ | $J'$ | |
| 56 | $\nu_3+\nu_6$ | 29 | 28 | 2319.86 |
| 57 | | 28 | 27 | 2321.42 |
| 58 | | 27 | 26 | 2323.17 |
| 59 | | 26 | 25 | 2325.36 |
| 60 | | 25 | 24 | 2327.34 |

In band $\nu_7$ (Fig. 9) the $^PQ$ and $^RQ$ absorption maxima are superposed on an unresolved background which has maxima of intensity at about 2970 and 3005 $cm^{-1}$ and a minimum at about 2995 $cm^{-1}$. The maximum of background absorption at about 2970 $cm^{-1}$ is evidently due at least in part to overlapping of the unresolved $R$ branch of the || band $\nu_{5b}$ centered at 2955 $cm^{-1}$. That at about 3005 $cm^{-1}$ doubtless corresponds to the absorption maximum observed under considerably lower dispersion by Bartholomé and Karweil[16] and attributed by them to the $Q$ branch of a || band, a suggestion maintained by subse-

TABLE V. Wave numbers of lines shown in Fig. 6.

| Line No. | Band | $J''$ | $J'$ | $\nu$ ($cm^{-1}$) |
|---|---|---|---|---|
| 1 | $\nu_3+\nu_6$ | 29 | 28 | 2319.87 |
| 2 | | 28 | 27 | 2322.16 |
| 3 | | 27 | 26 | 2324.08 |
| 4 | | 26 | 25 | 2326.13 |
| 5 | | 25 | 24 | 2328.08 |
| 6 | | 24 | 23 | 2330.12 |
| 7 | | 23 | 22 | 2331.98 |
| 8 | | 22 | 21 | 2333.92 |
| 9 | | 21 | 20 | 2335.77 |
| 10 | | 20 | 19 | 2337.48 |
| 11 | | 19 | 18 | 2339.28 |
| 12 | | 18 | 17 | 2341.04 |
| 13 | | 17 | 16 | 2342.76 |
| 14 | | 16 | 15 | 2344.55 |
| 15 | | 15 | 14 | 2346.21 |
| 16 | | 14 | 13 | 2348.02 |
| 17 | | 13 | 12 | 2349.55 |
| 18 | | 12 | 11 | 2351.29 |
| 19 | | 11 | 10 | 2353.00 |
| 20 | | 10 | 9 | 2354.38 |
| 21 | | 9 | 8 | 2355.92 |
| 22 | | 8 | 7 | 2357.50 |
| 23 | | 7 | 6 | 2358.92 |
| 24 | | 6 | 5 | 2360.26 |
| 25 | | 5 | 4 | 2362.05 |
| 26 | | 0 | 0 | 2368.59 |
| 27 | | 0 | 1 | 2370.25 |
| 28 | | 1 | 2 | 2371.33 |
| 29 | | 2 | 3 | 2372.42 |
| 30 | | 3 | 4 | 2373.77 |
| 31 | | 4 | 5 | 2375.11 |
| 32 | | 5 | 6 | 2376.32 |
| 33 | | 6 | 7 | 2377.39 |
| 34 | | 7 | 8 | 2378.57 |
| 35 | | 8 | 9 | 2379.72 |
| 36 | | 9 | 10 | 2380.76 |
| 37 | | 10 | 11 | 2381.76 |
| 38 | | 11 | 12 | 2382.70 |
| 39 | | 12 | 13 | 2383.69 |
| 40 | | 13 | 14 | 2384.72 |
| 41 | | 14 | 15 | 2385.56 |
| 42 | | 15 | 16 | 2386.43 |
| 43 | | 16 | 17 | 2387.33 |
| 44 | | 17 | 18 | 2388.10 |
| 45 | | 18 | 19 | 2389.00 |
| 46 | | 19 | 20 | 2389.88 |
| 47 | | 20 | 21 | 2390.60 |

[16] E. Bartholomé and J. Karweil, Zeits. f. physik. Chemie **B39**, 1 (1938).

TABLE VI. Wave numbers of lines shown in Fig. 7.

| Line No. | Band | $K''$ | $K'$ | $\nu$ (cm$^{-1}$) |
|---|---|---|---|---|
| 1 | 2653 | | | 2598.28 |
| 2 | | | | 2603.26 |
| 3 | | | | 2608.25 |
| 4 | | | | 2612.84 |
| 5 | | | | 2618.12 |
| 6 | | | | 2622.75 |
| 7 | | | | 2626.52 |
| 8 | | | | 2627.78 |
| 9 | | | | 2630.45 |
| 10 | | | | 2632.55 |
| 11 | | | | 2634.40 |
| 12 | | | | 2637.89 |
| 13 | | | | 2641.72 |
| 14 | | | | 2645.70 |
| 15 | | | | 2650.77 |
| 16 | | | | 2656.62 |
| 17 | | | | 2662.05 |
| 18 | | | | 2663.99 |
| 19 | | | | 2667.10 |
| 20 | | | | 2671.79 |
| 21 | | | | 2676.31 |
| 22 | | | | 2679.04 |
| 23 | | | | 2680.30 |
| 24 | | | | 2682.79 |
| 25 | | | | 2686.87 |
| 26 | | | | 2689.15 |
| 27 | | | | 2691.51 |
| 28 | | | | 2692.81 |
| 29 | | | | 2696.44 |
| 30 | | | | 2700.21 |
| 31 | | | | 2703.49 |
| 32 | | | | 2707.26 |
| | | $J''$ | $J'$ | |
| 33 | $\nu_2+\nu_6$ | 28 | 27 | 2708.43 |
| 34 | | 27 | 26 | 2710.55 |

quent authors.[3] Figure 9 shows no trace of such a $Q$ branch, the width of the intensity maximum being considerably too large to be explained thus. This figure suggests rather that the background absorption, while caused in part by the $R$ branch of $\nu_{5b}$ is otherwise due entirely to the sub-band lines of $\nu_7$ itself. Because the spacing of the $Q$ lines of $\nu_7$ is about 2.5 times $2B_0$, these sub-band lines should form an unresolved background and not give rise to minor peaks as in $\nu_9$.

The intensity distribution of background absorption due to unresolved sub-bands in $\perp$ bands of symmetric top molecules has been treated by Gerhard and Dennison.[17] Though their computations are not strictly applicable since they did not take account of the then unknown phenomenon of rotation-vibration interaction in degenerate vibrational states, it happens, as will be shown below, that in level $\nu_7$ the vibrational angular momentum is quite small so that one can compare qualitatively the background intensity distribution of band $\nu_7$ with that computed according to these authors for a value of $\beta=(\Delta\nu_\perp/\Delta\nu_{||})$ of about 2.5. The computed intensity distribution of background absorption for such a value of $\beta$ shows a minimum at the band center flanked by two maxima. Though the calculations do not show a larger maximum of background under the ${}^RQ$ branch than under the ${}^PQ$ branch this is to be expected from the intensity distribution of the minor peaks of band $\nu_9$. These considerations indicate that the origin of $\nu_7$ lies near the minimum of background absorption. The assignment of $K$ values given in Table VIII is based on the assumption that the origin lies between lines 59 and 60. This assignment is considerably less certain than that of band $\nu_9$ and the $K$ values may well be in error by $\pm 1$.

Figures 3a and 3b show that band $\nu_8$ (at least in part) consists of 20 major peaks (lines 78 to 97) extending from 1452 to 1536 cm$^{-1}$ superposed on a background of which much fine structure is resolved. The spacings of major peaks throughout the region above 1493 cm$^{-1}$ (line 89) are evidently highly regular and have an average value almost exactly four times $2B_0$. Hence the existence of three minor peaks between each adjacent pair of major peaks in this region is readily explained in the same manner as the existence of the minor peaks in band $\nu_9$. However, the fine structure of absorption below 1493 cm$^{-1}$ is highly anomalous, particularly between lines 82 and 89 and on the low frequency side of line 78. In the former region there appear to be some "extra" $Q$ lines as a plot of the measured wave numbers of the 20 major peaks *vs.* their ordinal number indicates. In the latter region several major peaks appear to be missing, for the background absorption just below line 78 is nearly maximum and $\nu_8$ in Fig. 3b should show a few more recognizable $Q$ lines than $\nu_9$ in Fig. 2b since the maximum overall absorption in Fig. 3b is greater than in Fig. 2b. Furthermore, below peak 73 and extending down at least to peak 45 there is a long series of minor peaks with a regular spacing of 1.17 cm$^{-1}$ which certainly do not belong to $||$ band $\nu_6$.

[17] S. L. Gerhard and D. M. Dennison, Phys. Rev. **43**, 197 (1933).

TABLE VII. Wave numbers of lines shown in Fig. 8.

| Line No. | Band | $K''$ | $K'$ | $\nu$ (cm$^{-1}$) |
|---|---|---|---|---|
| 1 | 2653 | | | 2696.40 |
| 2 | | | | 2699.91 |
| 3 | | | | 2703.38 |
| 4 | | | | 2707.22 |
| | | $J''$ | $J'$ | |
| 5 | $\nu_2+\nu_8$ | 28 | 27 | 2708.45 |
| 6 | | 27 | 26 | 2710.40 |
| 7 | | 26 | 25 | 2712.07 |
| 8 | | 25 | 24 | 2714.01 |
| 9 | | 24 | 23 | 2715.82 |
| 10 | | 23 | 22 | 2717.52 |
| 11 | | 22 | 21 | 2719.40 |
| 12 | | 21 | 20 | 2721.35 |
| 13 | | 20 | 19 | 2722.95 |
| 14 | | 19 | 18 | 2724.76 |
| 15 | | 18 | 17 | 2726.48 |
| 16 | | 17 | 16 | 2728.12 |
| 17 | | 16 | 15 | 2729.70 |
| 18 | | 15 | 14 | 2731.33 |
| 19 | | 14 | 13 | 2733.04 |
| 20 | | 13 | 12 | 2734.63 |
| 21 | | 12 | 11 | 2736.11 |
| 22 | | 11 | 10 | 2737.69 |
| 23 | | 10 | 9 | 2739.20 |
| 24 | | 9 | 8 | 2740.80 |
| 25 | | 8 | 7 | 2742.13 |
| 26 | | 7 | 6 | 2743.64 |
| 27 | | 6 | 5 | 2745.08 |
| 28 | | 5 | 4 | 2746.65 |
| 29 | | 4 | 3 | 2747.95 |
| 30 | | 3 | 2 | 2749.37 |
| 31 | | 2 | 1 | 2750.52 |
| 32 | | 0 | 0 | 2753.35 |
| 33 | | 1 | 2 | 2755.71 |
| 34 | | 2 | 3 | 2757.17 |
| 35 | | 3 | 4 | 2758.46 |
| 36 | | 4 | 5 | 2759.66 |
| 37 | | 5 | 6 | 2760.90 |
| 38 | | 6 | 7 | 2762.01 |
| 39 | | 7 | 8 | 2763.20 |
| 40 | | 8 | 9 | 2764.47 |
| 41 | | 9 | 10 | 2765.49 |
| 42 | | 10 | 11 | 2766.72 |
| 43 | | 11 | 12 | 2767.69 |
| 44 | | 12 | 13 | 2768.74 |
| 45 | | 13 | 14 | 2769.68 |
| 46 | | 14 | 15 | 2770.71 |
| 47 | | 15 | 16 | 2771.74 |
| 48 | | 16 | 17 | 2772.80 |
| 49 | | 17 | 18 | 2773.76 |
| 50 | | 18 | 19 | 2774.73 |
| 51 | | 19 | 20 | 2775.54 |
| 52 | | 20 | 21 | 2776.35 |
| 53 | | 21 | 22 | 2777.19 |
| 54 | | 22 | 23 | 2777.88 |
| 55 | | 23 | 24 | 2779.03 |

TABLE VII.—*Continued.*

| Line No. | Band | $K''$ | $K'$ | $\nu$ (cm$^{-1}$) |
|---|---|---|---|---|
| 56 | 2800 | | | 2780.55 |
| 57 | | | | 2781.30 |
| 58 | | | | 2782.02 |
| 59 | | | | 2783.38 |
| 60 | | | | 2784.81 |
| 61 | | | | 2786.29 |
| 62 | | | | 2787.83 |
| 63 | | | | 2789.24 |
| 64 | | | | 2790.71 |
| 65 | | | | 2792.16 |
| 66 | | | | 2793.83 |
| 67 | | | | 2795.05 |
| 68 | | | | 2796.46 |
| 69 | | | | 2797.81 |
| 70 | | | | 2799.40 |
| 71 | | | | 2801.08 |
| 72 | | | | 2802.23 |
| 73 | | | | 2803.61 |
| 74 | | | | 2805.07 |
| 75 | | | | 2806.66 |
| 76 | | | | 2808.12 |
| 77 | | | | 2809.56 |
| 78 | | | | 2810.95 |

The fine structure in the neighborhood of line 85 strongly suggests that some rotational levels of vibrational state $\nu_8$ with low $K$ values are perturbed by levels of another nearly coincident vibrational state of $C_2H_6$. This perturbation, because of its limited extent and the fact that major peaks are recognizable though their intensities and positions are anomalous, appears to be a "rotational" perturbation of the Fermi type in which interacting levels have the same $K$ value ($\Delta K=0$) and the elements of the energy matrix are independent of $K$ or $J$. Furthermore, it would appear that the difference in energy of unperturbed levels of the two states with the same $J$ and $K$ values, which difference, for any given value of $J$, is a linear function of $K$ with slope proportional to the difference in $\zeta$ values of the two states, passes through zero at a low value of $K$, the levels of state $\nu_8$ being lower for smaller values of $K$.[18]

The fine structure on the low frequency side of line 78 indicates that those $-l$ levels of $\nu_8$ with $K$ values greater than that corresponding to line 78 are also strongly perturbed by levels of another vibrational state of $C_2H_6$. This perturbation appears to be of the Coriolis type for which $\Delta K=\pm 1$, and for which a dependence of the energy matrix on $J$ as well as $K$ is to be expected, since, in this region, major peaks are not recognizable, though broad intensity maxima, the intervals between which are about equal to

[18] It is assumed here that the energies of each set of levels are represented by a single-valued function of $K$ in which $K$ is taken positive for $+l$ levels (transitions to which give rise to $^RQ$ lines) and negative for $-l$ levels (cf. reference 2, p. 403).

TABLE VIII. Wave numbers of lines shown in Fig. 9.

| Line No. | Band | $K''$ | $K'$ | $\nu$ (cm$^{-1}$) |
|---|---|---|---|---|
| 1 | 2860 | | | 2847.69 |
| 2 | | | | 2849.75 |
| 3 | | | | 2851.19 |
| 4 | | | | 2853.06 |
| 5 | | | | 2856.57 |
| 6 | | | | 2858.16 |
| 7 | | | | 2859.58 |
| 8 | | | | 2861.33 |
| 9 | | | | 2863.04 |
| 10 | | | | 2864.60 |
| 11 | | | | 2866.12 |
| 12 | | | | 2867.93 |
| | | $J''$ | $J'$ | |
| 13 | $\nu_{5a}$ | 18 | 17 | 2875.63 |
| 14 | | 17 | 16 | 2876.80 |
| 15 | | 16 | 15 | 2877.78 |
| 16 | | 15 | 14 | 2878.88 |
| 17 | | 14 | 13 | 2879.60 |
| 18 | | 13 | 12 | 2880.68 |
| 19 | | 12 | 11 | 2881.83 |
| 20 | | 11 | 10 | 2882.69 |
| 21 | | 10 | 9 | 2884.02 |
| 22 | | 9 | 8 | 2885.01 |
| 23 | | 8 | 7 | 2886.00 |
| 24 | | 7 | 6 | 2886.95 |
| 25 | | 6 | 5 | 2888.09 |
| 26 | | 5 | 4 | 2889.23 |
| 27 | | 4 | 3 | 2890.62 |
| 28 | | 3 | 2 | 2891.78 |
| 29 | | 2 | 1 | 2893.27 |
| 30 | | 0 | 0 | 2895.60 |
| 31 | | 1 | 2 | 2898.34 |
| 32 | | 2 | 3 | 2899.84 |
| 33 | | 3 | 4 | 2901.31 |
| 34 | | 4 | 5 | 2902.69 |
| 35 | | 5 | 6 | 2904.16 |
| 36 | | 6 | 7 | 2905.89 |
| 37 | | 7 | 8 | 2907.52 |
| 38 | | 8 | 9 | 2909.13 |
| 39 | | 9 | 10 | 2910.71 |
| 40 | | 10 | 11 | 2912.33 |
| 41 | | 11 | 12 | 2913.91 |
| 42 | | 12 | 13 | 2915.48 |
| 43 | | 13 | 14 | 2917.20 |
| 44 | | 14 | 15 | 2918.76 |
| 45 | | 15 | 16 | 2920.49 |
| 46 | $\nu_{5b}$ | 0 | 0 | 2954.05 |

TABLE VIII.—*Continued.*

| Line No. | Band | $K''$ | $K'$ | $\nu$ (cm$^{-1}$) |
|---|---|---|---|---|
| 47 | $\nu_7$ | 12 | 11 | 2958.35 |
| 48 | | 11 | 10 | 2961.36 |
| 49 | | 10 | 9 | 2964.22 |
| 50 | | 9 | 8 | 2966.87 |
| 51 | | | | 2967.77 |
| 52 | | 8 | 7 | 2970.19 |
| 53 | | 7 | 6 | 2973.49 |
| 54 | | 6 | 5 | 2976.98 |
| 55 | | 5 | 4 | 2980.00 |
| 56 | | 4 | 3 | 2983.44 |
| 57 | | 3 | 2 | 2986.79 |
| 58 | | 2 | 1 | 2990.09 |
| 59 | | 1 | 0 | 2993.57 |
| 60 | | 0 | 1 | 2996.88 |
| 61 | | 1 | 2 | 3000.49 |
| 62 | | 2 | 3 | 3003.79 |
| 63 | | 3 | 4 | 3006.84 |
| 64 | | 4 | 5 | 3010.38 |
| 65 | | 5 | 6 | 3013.81 |
| 66 | | 6 | 7 | 3017.28 |
| 67 | | 7 | 8 | 3020.83 |
| 68 | | 8 | 9 | 3023.93 |
| 69 | | 9 | 10 | 3027.60 |
| 70 | | 10 | 11 | 3030.52 |

those between the regularly spaced major peaks, are visible.

The fact that serious structural irregularities are exhibited by only part of band $\nu_8$ leads to the conclusion that the perturbations are of the "rotational" type and that the perturbing state or states must lie very close to state $\nu_8$. A review of our present knowledge of the locations of the 12 fundamental vibrational states of $C_2H_6$ shows beyond reasonable doubt that the only states sufficiently close to $\nu_8$ to cause such perturbations are $\nu_{11}$ and $\nu_{12}+\nu_4$. Of these only $\nu_{12}+\nu_4$ is of the same species as $\nu_8$ and is thus the only one which could interact with $\nu_8$ by means of a Fermi perturbation. According to Jahn's rule,[14] if $C_2H_6$ belongs to point group $D_{3h}$, a Coriolis perturbation in which $\Delta K=\pm 1$ is possible between $\nu_8$ and $\nu_{11}$ but none is possible between $\nu_8$ and $\nu_{12}+\nu_4$, while, if $C_2H_6$ belongs to $D_{3d}$, a Coriolis perturbation in which $\Delta K=0$ as well as one in which $\Delta K=\pm 1$ is possible between $\nu_8$ and $\nu_{12}+\nu_4$ but none is possible between $\nu_8$ and $\nu_{11}$.

Now Nielsen[19] has shown that to second order of approximation, wherein vibrational functions are assumed to be of the harmonic oscillator variety, Coriolis perturbations can occur between two vibrational states only if the difference between the quantum numbers of each vibration in the two states is unity for two vibrations and zero for all others. Thus, to this approximation, state $\nu_8$ can be perturbed as a result of Coriolis forces only by $\nu_{11}$ and hence only if $C_2H_6$ belongs to $D_{3h}$. However, as Howard[14] has pointed out, a Coriolis perturbation between $\nu_8$ and $\nu_{11}$ should be vanishingly small because in executing these two vibrations each atom moves in very nearly the same straight line. Moreover, as will be shown in the Section V below, the $\zeta$ values of states $\nu_8$ and $\nu_{11}$ are very probably so nearly

[19] H. H. Nielsen, Phys. Rev. 60, 794 (1941).

equal that if a Coriolis perturbation occurred between them effecting strongly the $-l$ levels of $\nu_8$ it should also effect strongly the $+l$ levels of $\nu_8$. Further evidence that a perturbation of $\nu_8$ by $\nu_{11}$ does not exist is provided by the regular structure of a band at 1747.1 $cm^{-1}$ for which, as we shall see in Section V, the only reasonable assignment is $\nu_{11}+\nu_4$. The assumption that a perturbation between $\nu_8$ and $\nu_{11}$ exists would almost certainly require a nearly equally strong perturbation between states $\nu_{11}+\nu_4$ and $\nu_8+\nu_4$.

An attempt to obtain a quantitative explanation of the irregular structure of band $\nu_8$ on the assumption that state $\nu_8$ is perturbed in both a Fermi and a Coriolis perturbation by state $\nu_{12}+\nu_4$ (and hence on the assumption that $C_2H_6$ belongs to $D_{3d}$) has been recently undertaken by Mr. Gordon Hansen of the University of Michigan under Professor Dennison's direction. These considerations have shown that a small Coriolis coupling between rotational levels of $\nu_8$ and $\nu_{12}+\nu_4$ whose $K$ values differ by unity may occur in third order of approximation but that none can occur between levels of the same $K$ value in any approximation. A good account of the relative intensities of both the major and minor peaks above line 89 in Fig. 3b has been given which has led to the adoption of the $K$ values given in Table II for these lines and shows beyond any reasonable doubt that not only these $K$ values but also the explanation of the minor peaks above line 89 given above are correct. Furthermore, a good account of the relative intensities and positions of all the numbered peaks above line 78 has been obtained on the assumptions: (1) of resonable values of $\zeta$ for states $\nu_8$ and $\nu_{12}+\nu_4$; (2) that state $\nu_{12}+\nu_4$ lies about 8 $cm^{-1}$ above state $\nu_8$; and (3) that in the absence of the perturbations considered the wave numbers of the lines of band $\nu_8$ would be given (in $cm^{-1}$) by the formula

$$\nu_8(m)=1475.84+5.550m-0.0125m^2, \quad (6)$$

where $m\equiv K''$ for ${}^RQ$ lines and $-K''$ for ${}^PQ$ lines.

From the theoretical formula for the $Q$ lines of a $\perp$ band of a symmetric top molecule, namely[20]

[20] Cf. reference 2, p. 429 and footnote 9.

TABLE IX. Wave numbers of lines shown in Fig. 10.

| Line No. | Band | $J''$ | $J'$ | $\nu$ ($cm^{-1}$) |
|---|---|---|---|---|
| 1 | ∥? | 0 | 0 | 3116.71 |
| | | $K''$ | $K'$ | |
| 2 | ⊥? | | | 3177.00 |
| 3 | | | | 3179.68 |
| 4 | | | | 3183.71 |
| 5 | ⊥? | | | 3207.00 |
| 6 | | | | 3209.26 |
| 7 | | | | 3211.80 |
| 8 | | | | 3215.87 |
| 9 | | | | 3218.34 |
| 10 | | | | 3220.59 |
| 11 | | | | 3224.59 |
| 12 | | | | 3228.14 |
| 13 | | | | 3230.82 |
| 14 | 3257.8 | 7 | 6 | 3240.30 |
| 15 | | 6 | 5 | 3242.58 |
| 16 | | 5 | 4 | 3245.26 |
| 17 | | 4 | 3 | 3247.45 |
| 18 | | 3 | 2 | 3250.13 |
| 19 | | 2 | 1 | 3252.88 |
| 20 | | 1 | 0 | 3255.90 |
| 21 | | 0 | 1 | 3258.85 |
| 22 | | 1 | 2 | 3261.82 |
| 23 | | 2 | 3 | 3264.69 |
| 24 | | 3 | 4 | 3267.86 |
| 25 | | 4 | 5 | 3271.60 |
| 26 | | 5 | 6 | 3274.26 |
| 27 | | 6 | 7 | 3277.28 |
| 28 | | 7 | 8 | 3280.58 |
| 29 | | 8 | 9 | 3283.92 |
| 30 | | 9 | 10 | 3287.40 |
| | | $J''$ | $J'$ | |
| 31 | ∥? | 0 | 0 | 3396.15 |

$$\nu(m)=\nu_0+[(A'-B')-2A'\zeta] +2[(A'-B')-A'\zeta]m +[(A'-B')-(A_0-B_0)]m^2, \quad (7)$$

where again $m\equiv K''$ for ${}^RQ$ lines and $-K''$ for ${}^PQ$ lines, it is evident that the band origin ($\nu_0$) is given by

$$\nu_0=\nu(m=-1)+(A_0-B_0), \quad (8)$$

that the mean line spacing ($\Delta\nu$), which we shall define as $(d\nu/dm)_{m=-1}$, is given by

$$\Delta\nu\equiv(d\nu/dm)_{m=-1}=2[(A_0-B_0)-A'\zeta], \quad (9)$$

and therefore that

$$A_0-B_0=\tfrac{1}{6}(\Delta\nu_7+\Delta\nu_8+\Delta\nu_9) +\tfrac{1}{3}(A_7\zeta_7+A_8\zeta_8+A_9\zeta_9). \quad (10)$$

The latter relation allows us to determine values of the $A$'s and hence of the $\nu_0$'s and $\zeta$'s in the fairly good approximation that the dependences

TABLE X. Wave numbers of lines shown in Fig. 11.

| Line No. | Band | $K''$ | $K'$ | $\nu$ (cm$^{-1}$) |
|---|---|---|---|---|
| 1 | ⊥? | | | 4073.85 |
| 2 | | | | 4098.07 |
| 3 | | | | 4120.57 |
| 4 | | | | 4127.05 |
| 5 | | | | 4130.67 |
| 6 | | | | 4132.75 |
| 7 | | | | 4134.42 |
| 8 | | | | 4137.04 |
| | | $J''$ | $J'$ | |
| 9 | ‖? | 0 | 0 | 4143.27 |
| | | $K''$ | $K'$ | |
| 10 | 4178.9 | 5 | 4 | 4147.74 |
| 11 | | | | 4150.30 |
| 12 | | 4 | 3 | 4155.10 |
| 13 | | | | 4156.51 |
| 14 | | 3 | 2 | 4163.27 |
| 15 | | 2 | 1 | 4170.38 |
| 16 | | 1 | 0 | 4176.48 |
| 17 | | 0 | 1 | 4183.88 |
| 18 | | 1 | 2 | 4190.86 |
| 19 | | 2 | 3 | 4197.79 |
| 20 | | 3 | 4 | 4204.71 |
| 21 | | 4 | 5 | 4211.14 |
| 22 | | 5 | 6 | 4219.49 |
| 23 | | 6 | 7 | 4226.50 |
| 24 | | 7 | 8 | 4233.74 |
| 25 | | 8 | 9 | 4240.89 |
| | | $J''$ | $J'$ | |
| 26 | ‖? | 0 | 0 | 4274.35 |
| 27 | ‖? | 0 | 0 | 4292.53 |
| | | $K''$ | $K'$ | |
| 28 | 4334.1 | 4 | 3 | 4323.26 |
| 29 | | 3 | 2 | 4326.37 |
| 30 | | 2 | 1 | 4329.45 |
| 31 | | 1 | 0 | 4331.95 |
| 32 | | 0 | 1 | 4334.84 |
| 33 | | 1 | 2 | 4337.68 |
| 34 | | 2 | 3 | 4341.24 |
| 35 | | 3 | 4 | 4344.95 |
| 36 | | 4 | 5 | 4347.62 |
| 37 | | 5 | 6 | 4350.28 |
| 38 | | 6 | 7 | 4353.94 |
| 39 | 4416.7 | 6 | 5 | 4394.87 |
| 40 | | 5 | 4 | 4498.86 |
| 41 | | 4 | 3 | 4401.85 |
| 42 | | 3 | 2 | 4404.54 |
| 43 | | 2 | 1 | 4409.84 |
| 44 | | 1 | 0 | 4413.95 |
| 45 | | 0 | 1 | 4419.05 |
| 46 | | 1 | 2 | 4424.44 |
| 47 | | 2 | 3 | 4427.41 |
| 48 | | 3 | 4 | 4430.69 |
| 49 | | 4 | 5 | 4434.45 |
| 50 | | 5 | 6 | 4437.68 |
| 51 | | 6 | 7 | 4442.59 |
| 52 | | 7 | 8 | 4447.86 |

of (1) the $\zeta$'s and (2) the $A$'s on vibrational quantum numbers are neglected: i.e., in the approximation (1) that the $\zeta$-sum rule, shown by Howard[14] to be

$$\zeta_7+\zeta_8+\zeta_9=0 \tag{11}$$

is valid and (2) that $A_7=A_8=A_9=A_0\equiv A$. Thus in this approximation we may write in place of (8), (9) and (10) the relations:

$$\nu_0=\nu(m=-1)+(A-B_0), \tag{8a}$$

$$\Delta\nu\equiv(d\nu/dm)_{m=-1}=2[(A-B_0)-A\zeta], \tag{9a}$$

$$A-B_0=\tfrac{1}{6}(\Delta\nu_7+\Delta\nu_8+\Delta\nu_9). \tag{10a}$$

Values of $[(A'-B')-(A_0-B_0)]$ and $\Delta\nu$ obtained from relation (6) for band $\nu_8$ and similar empirical relations (wherein the coefficients were determined by least squares) for bands $\nu_7$ and $\nu_9$ as well as values of $A-B_0$, $A$, $I_A$, $\nu_0$ and $\zeta$ obtained from the empirical coefficients with the aid of (8a), (9a) and (10a) are given in Table XIII. Errors given for $\Delta\nu$ and $[(A'-B')-(A_0-B_0)]$ for $\nu_7$ and $\nu_9$ are probable errors computed from the data. Those given for $\nu_0$ include an assumed probable error of 0.06 cm$^{-1}$ for $A-B_0$ in addition to the same allowances made in estimating the errors of values of the origins of the ‖ bands (Table XII). The value of $\Delta\nu_8$ obtained by Hansen is appreciably larger than the mean spacing of lines 89–97 of band $\nu_8$ on which the value of $I_A$ given in reference 2 was based. Hence the value of $I_A$ given here is appreciably less than that given in reference 2 and yields, together with the value of $I_{B0}$ in Table XII what are perhaps more reasonable relationships between the three structural parameters of the $C_2H_6$ molecule than did the previously determined value. Thus with the present values of $I_{B0}$ and $I_A$, if we take C−C=1.55A as determined by Pauling and Brockway,[21] we obtain C−H=1.098A and $\measuredangle$HCC=109° 3′. The rather large negative values of $[(A'-B')-(A_0-B_0)]$ for $\nu_8$ also obtained by Hansen may possibly be due to a second Coriolis perturbation of state $\nu_8$ of the type for which $\Delta K=0$ by a state lying above $\nu_8$.

## V. COMBINATION ⊥ BANDS

It appears from Figs. 4–12 that nearly all the fine structures in the regions of weaker absorption not so far discussed correspond to combina-

[21] L. Pauling and L. O. Brockway, Jr., J. Am. Chem. Soc. 59, 1223 (1937).

tion bands of the ⊥ type, there being in addition a few scattered peaks, some of which are doubtless $Q$ branches of combination || bands. For each group of lines which apparently comprises a ⊥ band values of mean line spacing ($\Delta\nu$), band origin ($\nu_0$) and $\zeta$ are given in Table XIV. These were determined in the same fashion as for the fundamental ⊥ bands $\nu_7$ and $\nu_9$ except that the "regression" line on a graph of wave number *vs.* ordinal number of the lines of each group was determined "by eye" instead of by least squares. The points on each such graph were found to fit on a straight line within experimental uncertainty except those for the group of lines near 2653 $cm^{-1}$ where the structure is so irregular (even at low temperature) that no single value of $\Delta\nu$ can be determined and those for the groups at 3257.8 and 5950.7 $cm^{-1}$. In the latter two cases the points fit on curved lines indicating large positive values of $[(A'-B')-(A_0-B_0)]$ for these bands. The assignment of $K$ values for each combination ⊥ band was guided by the assumption that, as in the case of band $\nu_9$, about 3/5 of the observed lines are $^RQ$ lines and about 2/5 are $^PQ$ lines and by evidence in the spectrograms of alternating intensities, which evidence, however, is fairly definite only in the case of the band at 3257.8 $cm^{-1}$. Thus some values of $\nu_0$ may be in error by one or two line intervals.

A survey of information concerning the twelve fundamental vibrational states of $C_2H_6$ as given in reference 3 leads to the conclusion that the only reasonable assignment for the band at 1747.1 $cm^{-1}$ is $\nu_{11}+\nu_4$. This assignment is supported by the fact that $\Delta\nu$ for this band is nearly the same as for band $\nu_8$, as $\Delta\nu$ of band $\nu_{11}+\nu_4$ should be, since the $\zeta$ values of states $\nu_8$ and $\nu_{11}$ as well as their frequencies should be approximately equal.[22] Also, the most reasonable assignment for the band at 3257.8 $cm^{-1}$ is $\nu_4+a$ component of the multiple level $\nu_{10}$ (probably $\nu_{10b}$)[23] since there is no other binary combination in the neighborhood and such a combination should have roughly the same spacing as band $\nu_7$.

[22] The $\zeta$ value of a combination state and hence $\Delta\nu$ of the corresponding band are independent of what non-degenerate vibrations are excited in the state. (Cf. reference 30 below.)

[23] It is possible that the group of lines 5 to 13 of Fig. 10 near 3217 $cm^{-1}$ whose spacings are rather irregular, but roughly the same as for the band at 3257.8 $cm^{-1}$, corresponds to a combination of $\nu_4$ and another component of $\nu_{10}$.

TABLE XI. Wave numbers of lines shown in Fig. 12.

| Line No. | Band | $J''$ | $J'$ | $\nu$ ($cm^{-1}$) |
|---|---|---|---|---|
| 1 | \|\|? | | | 5904.35 |
| 2 | | 0 | 0 | 5916.28 |
| | | $K''$ | $K'$ | |
| 3 | 5950.7 | 6 | 5 | 5924.50 |
| 4 | | 5 | 4 | 5928.65 |
| 5 | | 4 | 3 | 5932.12 |
| 6 | | 3 | 2 | 5939.49 |
| 7 | | 2 | 1 | 5943.76 |
| 8 | | 1 | 0 | 5948.73 |
| 9 | | 0 | 1 | 5954.13 |
| 10 | | 1 | 2 | 5959.75 |
| 11 | | 2 | 3 | 5965.82 |
| 12 | | 3 | 4 | 5972.60 |
| 13 | | 4 | 5 | 5980.23 |
| 14 | | 5 | 6 | 5986.50 |
| 15 | | 6 | 7 | 5994.73 |

Subject to the validities of these two assignments and of the values of the two band origins, we may combine the latter with values of $\nu_{11}$ and $\nu_{10}$ obtained from Raman data to determine a value of $\nu_4$. From Raman investigations of $C_2H_6$ gas it is fairly well established[24] that $\nu_{11}=1460$ $cm^{-1}$, whence we obtain $\nu_4=287.1$ $cm^{-1}$, while from Raman spectra of liquid $C_2H_6$[25] it appears that $\nu_{10b}=2963$ $cm^{-1}$ from which we obtain $\nu_4=294.8$ $cm^{-1}$. In Fig. 1 the value $\nu_4=290$ $cm^{-1}$ has been adopted as being not inconsistent with and perhaps somewhat more reliable than the value $\nu_4=275$ $cm^{-1}$ determined from heat capacity data.[26] From the former value

TABLE XII. Results obtained from || bands.

| State | $\nu_0$ ($cm^{-1}$) | $B-B_0$ ($cm^{-1}$) | $B$ ($cm^{-1}$) | $D$ ($10^{-7}$ $cm^{-1}$) | $IB^*$ ($10^{-40}$ g $cm^2$) |
|---|---|---|---|---|---|
| $\nu_{8a}$ | 2895.66 ±0.16 | 0.0176 ±0.0006 | 0.6801 ±0.0006 | 165 ±28 | 41.14 ±0.04 |
| $\nu_3+\nu_8$ | 2753.39 ±0.13 | −0.01031 ±0.00006 | 0.65227 ±0.00014 | — | 42.901 ±0.011 |
| $\nu_3+\nu_8$ | 2368.88 ±0.10 | −0.01321 ±0.00010 | 0.64937 ±0.00016 | — | 43.093 ±0.012 |
| $\nu_8$ | 1379.14 ±0.07 | −0.00722 ±0.00005 | 0.65536 ±0.00014 | — | 42.699 ±0.011 |
| Ground | 0 | 0 | 0.66258 ±0.00013 | 6.00† | 42.234 ±0.011 |

* $h=(6.6234\pm0.0011)\times10^{-27}$ erg sec.
† Calculated.

[24] S. Bhagavantam, Ind. J. Phys. 6, 596 (1931) and B. L. Crawford, Jr., W. H. Avery and J. W. Linnett, J. Chem. Phys. 6, 682 (1938).

[25] G. Glockler and M. M. Renfrew, J. Chem. Phys. 6, 295 (1938).

[26] G. B. Kistiakowsky, J. R. Lacher and F. Stitt, J. Chem. Phys. 7, 289 (1939).

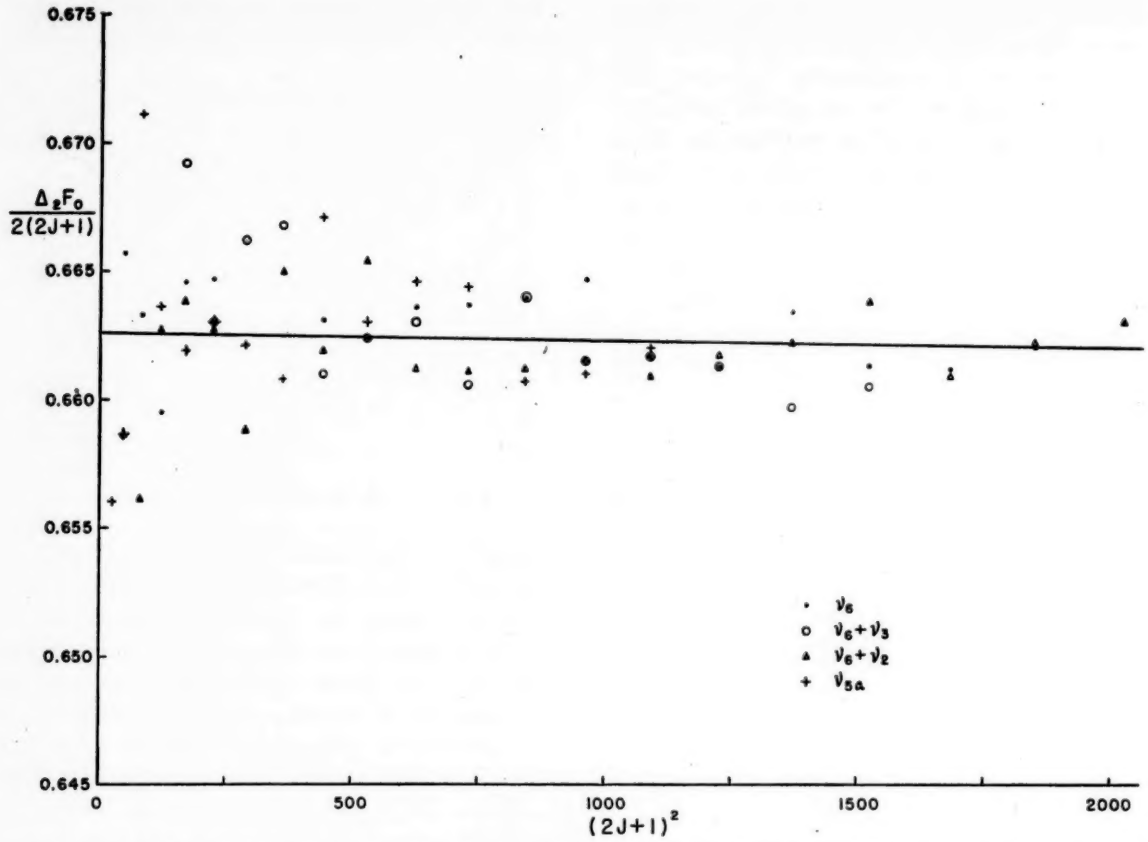


FIG. 13. $\Delta_2 F_0(J)/2(2J+1)$ *vs.* $(2J+1)^2$ showing experimental points for each of the four resolved || bands and the regression line determined by least squares.

and the value $\nu_{12}+\nu_4=1480$ cm$^{-1}$ determined by Hansen in his consideration of the perturbation of state $\nu_8$ the value $\nu_{12}=1190$ cm$^{-1}$ has also been adopted here. This is in fairly good agreement with the value $\nu_{12}=1170$ cm$^{-1}$ determined by Stitt.[27]

Subject also to the validities of these assignments, we may determine $\zeta$ values for states $\nu_{10}$ and $\nu_{11}$ respectively from the values of $\Delta\nu$ for the bands at 3257.8 and 1747.1 cm$^{-1}$ by substituting these in Eq. (9a). $\zeta_{12}$ may then be obtained from $\zeta_{10}$ and $\zeta_{11}$ by use of the $\zeta$-sum rule for states $\nu_{10}$, $\nu_{11}$ and $\nu_{12}$, which may readily be shown to be[28]

$$\zeta_{10}+\zeta_{11}+\zeta_{12}=I_A/2I_{B0}=B_0/2A=0.128. \quad (12)$$

The $\zeta$ values thus obtained together with the present best estimates of the wave numbers of states $\nu_{10}$, $\nu_{11}$ and $\nu_{12}$ are given in Table XV. Also given are values of $\Delta\nu$ for bands[29] $\nu_{10}$, $\nu_{11}$ and $\nu_{12}$. As is evident from Eqs. (9a), (10a) and (12), $\Delta\nu_{12}$ is given in terms of the experimentally measured quantities $\Delta\nu_7-\Delta\nu_{11}$ and $B_0$ by the equation:

$$\Delta\nu_{12}=\Delta\nu_7+\Delta\nu_8+\Delta\nu_9-B_0-\Delta\nu_{10}-\Delta\nu_{11}. \quad (13)$$

TABLE XIII. Results obtained from fundamental ⊥ bands.

| Band | $\nu_0$ (cm$^{-1}$) | $\Delta\nu$ (cm$^{-1}$) | $\zeta$ | $[(A'-B')-(A_0-B_0)]$ (cm$^{-1}$) |
|---|---|---|---|---|
| $\nu_7$ | 2995.5 ±0.2 | 3.362 ±0.006 | 0.095 | 0.0021 ±0.0009 |
| $\nu_8$ | 1472.2 ±0.1 | 5.563 | −0.331 | −0.0125 |
| $\nu_9$ | 821.52 ±0.07 | 2.6285 ±0.0012 | 0.236 | 0.00213 ±0.00015 |

$A-B_0=1.926$ cm$^{-1}$; $A=2.588$ cm$^{-1}$; $I_A=10.81\times10^{-40}$ g cm$^2$

[27] F. Stitt, J. Chem. Phys. **7**, 297 (1939).

[28] Herzberg (reference 2, p. 405) citing Howard (see reference 14), who does not consider this sum, erroneously states that this sum is zero.

[29] We speak in this section of the $\Delta\nu$ of a band even though such a band is inactive.

The value of $\zeta_{12}$ in Table XV and that of $\zeta_8$ in Table XIII are approximately equal to the values employed by Hansen in his considerations of the perturbations of $\nu_8$ by $\nu_{12}+\nu_4$.

In an attempt to determine reasonable assignments for as many as possible of the observed combination $\perp$ bands and hence possibly to obtain more evidence as to the point group to which $C_2H_6$ belongs, two charts, Fig. 14a for $D_{3d}$ and Fig. 14b for $D_{3h}$, have been prepared in which a $\perp$ band is represented by a point whose abscissa gives the origin ($\nu_0$) and whose ordinate gives the mean line spacing ($\Delta\nu$) of the band. The observed bands are represented by crosses in each chart while the circles represent possible combination bands. In the region below 3500 $cm^{-1}$ all possible active binary and ternary combinations exclusive of difference bands with lower states higher than $\nu_4$ are represented, while between 3500 and 6000 $cm^{-1}$ all possible active binary combinations are represented. The wave numbers of the possible combinations were determined as simple sums or differences of those for the fundamental states given in Fig. 1. Their mean spacings were determined from the values of $\Delta\nu$ for the fundamental bands given in Tables XIII and XV with the aid of the rules given by Johnston and Dennison.[30] These authors showed that, for molecules with three-fold axes such as the methyl halides and ethane, the appropriate $\zeta$ value for any state in which one and only one degenerate vibration $\nu_i$ is either singly or triply excited is $\zeta_i$. Hence the line spacing of the corresponding band is $\Delta\nu_i$. They also showed that, for such molecules, the appropriate $\zeta$ values, for a state in which one and only one degenerate vibration $\nu_i$ is doubly excited and for a state in which two and only two degenerate vibrations $\nu_i$ and $\nu_j$ are each singly excited, are respectively $-2\zeta_i$ and $-(\zeta_i+\zeta_j)$. Hence the line spacings of the corresponding bands are, according to Eqs. (9a) and (10a),

$$\Delta\nu(2\nu_i)=\Delta\nu_7+\Delta\nu_8+\Delta\nu_9-2\Delta\nu_i, \qquad (14)$$

and

$$\Delta\nu(\nu_i+\nu_j)=\Delta\nu_7+\Delta\nu_8+\Delta\nu_9-\Delta\nu_i-\Delta\nu_j. \qquad (15)$$

[30] M. Johnston and D. M. Dennison, Phys. Rev. **48**, 868 (1935).

TABLE XIV. Results obtained from combination $\perp$ bands.

| $\nu_0$ ($cm^{-1}$) | $\Delta\nu$ ($cm^{-1}$) | $\zeta$ |
|---|---|---|
| 1747.1 | 5.69 | −0.354 |
| 2021.6 | 7.64 | −0.732 |
| 2218.0 | 2.70 | +0.222 |
| 2277.1 | 3.65 | +0.039 |
| 2653 | ? | ? |
| 2800 | 1.46 | +0.463 |
| 2860 | 1.63 | +0.429 |
| 3257.8 | 3.00 | +0.164 |
| 4178.9 | 7.02 | −0.612 |
| 4334.1 | 3.09 | +0.147 |
| 4416.7 | 4.05 | −0.039 |
| 5950.7 | 5.03 | −0.228 |

It is evident from Fig. 14 that it is not possible on the basis of either point group to account well for any of the observed combination $\perp$ bands, except perhaps that at 2218.0 $cm^{-1}$ and, of course, those at 1747.1 and 3257.8 $cm^{-1}$, without revising or adding to the assumptions that have gone into the determinations of the values of $\nu_0$ or $\Delta\nu$ or both of some of the possible combination bands. This is not very surprising in view of all the possibilities for perturbations of either fundamental or combination states and for appreciable dependence of some $\zeta$ values on vibrational quantum numbers which have been neglected. Moreover, it appears that no less reasonable additions to or revisions of the assumptions on the basis of $D_{3h}$ than on the basis of $D_{3d}$ are required to account well for any of the observed bands with the outstanding exception of that at 2021.6 $cm^{-1}$.

To account for the band at 2021.6 $cm^{-1}$ on the basis of $D_{3h}$, one must assume either: (1) that this band is due to an impurity, which seems most unlikely since it is evidently a $\perp$ band of a symmetric top molecule and does not correspond to a strong band of any likely impurity and since absorption in this region by $C_2H_6$ gas has also been observed by Avery and Ellis;[31] or

TABLE XV. Values of $\nu_0$, $\Delta\nu$ and $\zeta$ for inactive fundamental $\perp$ bands (see reference 29).

| Band | $\nu_0$ ($cm^{-1}$) | $\Delta\nu$ ($cm^{-1}$) | $\zeta$ |
|---|---|---|---|
| $\nu_{10}$ | {2963 / 2939.5} | 3.00 | 0.164 |
| $\nu_{11}$ | 1460 | 5.69 | −0.354 |
| $\nu_{12}$ | 1190 | 2.20 | 0.318 |

[31] W. H. Avery and C. F. Ellis, J. Chem. Phys. **10**, 10 (1942).

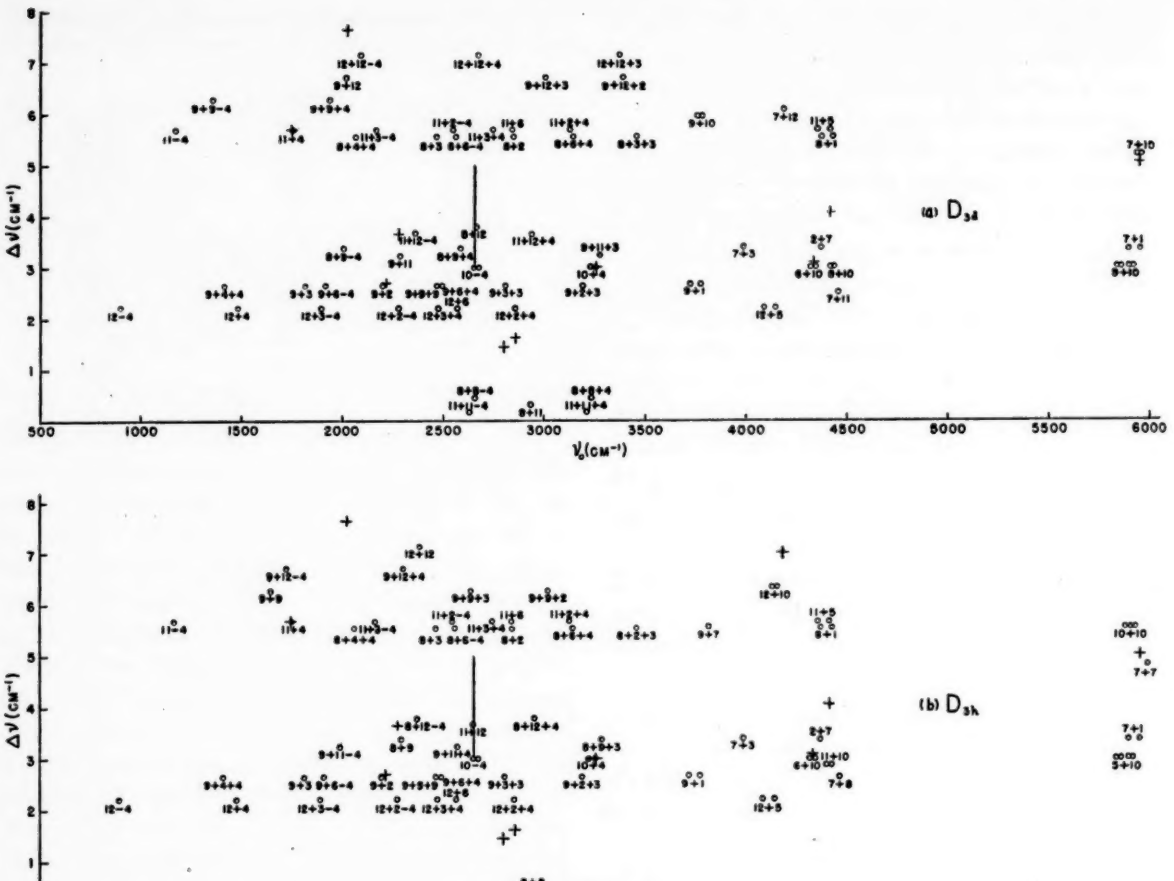


FIG. 14. Mean line spacing ($\Delta\nu$) *vs.* band origin ($\nu_0$) for combination $\perp$ bands. Crosses represent observed bands, except in the case of the band near 2653 cm$^{-1}$ where a vertical line is used because $\Delta\nu$ for this band is uncertain, while circles represent possible active combination bands according as $C_2H_6$ belongs (a) to $D_{3d}$ or (b) to $D_{3h}$. All possible binary and ternary combinations below 3500 cm$^{-1}$ whose lower states are not higher than $\nu_4$ are represented, while between 3500 and 6000 cm$^{-1}$ all possible binary combinations are shown. Combinations involving $\nu_1$, $\nu_5$ and $\nu_{10}$ are represented by multiple points. Combination $\nu_{12}+\nu_3+\nu_4$ is represented by 12+3+4, etc.

(2) that this band is to be assigned to $2\nu_{12}$, which would lead to the very improbable conclusion that $\nu_{12}=1010$ cm$^{-1}$; or (3) that it is to be assigned either to $\nu_9+\nu_{12}+\nu_4$ or $\nu_9+\nu_{12}-\nu_4$, either of which assumptions would require an even less acceptable value of $\nu_{12}$; or (4) that it is to be assigned to some combination such as $\nu_8+2\nu_4$ or $\nu_9+\nu_{11}-\nu_4$, for none of which could the spacing conceivably be as great as 7.64 cm$^{-1}$. On the other hand this band can be accounted for on the basis of $D_{3d}$ if one makes a far less drastic assumption. Thus, as is perhaps most reasonable, one may assign this band as $\nu_9+\nu_{12}$ and assume that the discrepancy in $\Delta\nu$ is due to the fact that state $\nu_{10b}$ is perturbed or that the band at 3257.8 cm$^{-1}$ has been wrongly assigned so that the true value of $\Delta\nu_{10}$ is greater by about 1 cm$^{-1}$ than the value in Table XV. Alternatively we might assign this band as $2\nu_{12}-\nu_4$ and assume the value of $\Delta\nu_{10}$ in Table XV to be low by about 0.25 cm$^{-1}$, though this assignment is less likely because $2\nu_{12}-\nu_4$ is a ternary difference band.

It is perhaps significant that, if we do assume the staggered configuration for $C_2H_6$ and also postulate that the value of $\Delta\nu_{10}$ in Table XV is low by about 1 cm$^{-1}$, then not only may we assign the band at 2021.6 as $\nu_9+\nu_{12}$ but we may

also assign that at 4178.9 $cm^{-1}$ as $\nu_7+\nu_{12}$. Furthermore, on the basis of $D_{3d}$ the group of lines near 2653 $cm^{-1}$ may be assigned as a band $\nu_8+\nu_{12}$ whose structure would be expected to be about as irregular as that of band $\nu_8$ because of a perturbation between states $\nu_8+\nu_{12}$ and $2\nu_{12}+\nu_4$. Thus we could account for three of the bands as combinations of the vibration $\nu_{12}$ with each of the three infra-red active vibrations. It should be noted that changing $\Delta\nu_{10}$ affects only the spacings of combination bands involving the vibrations $\nu_{10}$ or $\nu_{12}$.

Concerning possible assignments for the remainder of the observed combination $\perp$ bands very little can be said that is not highly speculative. Possibly it is worth while to point out that better agreement between the spacing of the band at 2277.1 $cm^{-1}$ and that of $\nu_9+\nu_{11}$ would result if a value of $\Delta\nu_8$ larger than 5.563 $cm^{-1}$ were adopted.

## VI. CONCLUSION

The measurements on the fine structures of the infra-red bands of $C_2H_6$ described here have yielded an accurate value of the moment of inertia $I_{B0}$ and a fairly reliable value of $I_A$. They have also yielded some very puzzling results from considerations of which new estimates of the values of the fundamental vibration frequencies $\nu_4$ and $\nu_{12}$ and a reliable value of $\nu_8$ have been obtained. Finally, from considerations of the apparent perturbations of state $\nu_8$ and an analysis of combination $\perp$ bands, definite spectroscopic evidence that $C_2H_6$ belongs to point group $D_{3d}$ has for the first time been obtained. Though not conclusive, this evidence carries considerable weight. Further high resolution work including obtaining of better records of some of the combination bands and a search for bands $\nu_{12}-\nu_4$, near 900 $cm^{-1}$ and $\nu_{11}-\nu_4$ near 1170 $cm^{-1}$ with a cell including a long absorbing path would be very desirable.[32] Also, the results of high resolution measurements on the spectrum of $C_2D_6$ now being undertaken by Mr. Gordon Hansen at the University of Michigan should prove highly enlightening.

The author wishes to express sincere thanks to Professor John Turkevich for providing the ethane used, to Drs. Van Zandt Williams and William Woodward for much assistance in gathering the data and to Mr. Gordon Hansen and Professor D. M. Dennison for many valuable suggestions concerning the interpretation of the results, particularly those on the band $\nu_8$, on which many of the values obtained depend.

[32] Very weak absorption near 1216 $cm^{-1}$ has been observed under low dispersion by Avery and Ellis (see reference 31) and attributed by them to band $\nu_{11}-\nu_4$.

THE JOURNAL OF CHEMICAL PHYSICS VOLUME 17, NUMBER 2 FEBRUARY, 1949

# The Exchange Reaction between Bromine and Bromotrichloromethane

A. A. MILLER AND J. E. WILLARD
*Department of Chemistry, The University of Wisconsin, Madison, Wisconsin*

(Received August 13, 1948)

Thermal exchange of the bromine in $CCl_3Br$ with $Br_2$ has been measured in the temperature range from 100° to 135°C in liquid $CCl_3Br$, in the range from 135° to 170°C in $CCl_4$ solution, and in the range from 150° to 220°C in the gas phase. The activation energy has been found to be approximately 29 kcal. mole$^{-1}$ in each phase. The rate of exchange has been found to be proportional to the first power of the $CCl_3Br$ concentration and to the square root of the bromine concentration, indicating an atomic mechanism. The values of the rate constants obtained in the liquid and gas phases are approximately equal. From the results it may be deduced that the activation energy for the step which initiates the exchange, i.e., either $CCl_3Br+Br\rightarrow CCl_3+Br_2$ or the reaction $CCl_3Br+Br^*\rightarrow CCl_3Br^*+Br$ is about[7] kcal. mole$^{-1}$. This value is in the range of values of 5–10 kcal. mole$^{-1}$ indicated by previous experiments on the analogous photochemical reaction in carbon tetrachloride solution. The thermal reaction has been found to be much less sensitive to oxygen than various previously studied photo-chemical halogenation reactions. Analysis of the results suggests that the "cage" effect may appreciably lower the quantum yield of the photo-chemical reaction in the liquid phase.

## INTRODUCTION

MANY reactions of halogens with halogenated hydrocarbons have been studied for the purpose of establishing the reaction mechanisms and determining the activation energies of the elementary steps involving atoms or radicals.[1] Probably the simplest reactions of this type are those which involve only the exchange of atoms between elementary halogen molecules and the same halogen in organic combination. In such reaction systems only two molecular species are present and there is no change in the chemical composition of the system. The number of possible elementary reaction steps involving atoms and free radicals is smaller than in systems containing more species and consequently the possibility of certainty in assigning activation energies to these steps is increased. Several investigations[2] of such reactions have been reported but only in a very few have activation energies or quantum yields been determined.

In studying a variety of reactions of halogens with halogenated hydrocarbons we have obtained information on the thermal and photochemical exchange of bromine with bromotrichloromethane. This reaction may be represented by the over-all equation $CCl_3Br+BrBr^*\rightarrow CCl_3Br^*+BrBr$, where Br* is used to denote radioactive bromine tracer, which is used as a means of observing the exchange. Evidence for the existence of a reaction of this type was first reported by Wilson and Dickinson.[2b,3] As might be expected, the results for the thermal reaction are consistent with a mechanism involving the following steps:

$$Br_2\rightarrow 2Br \qquad k_1, \qquad (1)$$

$$CCl_3Br+Br\rightarrow CCl_3+Br_2 \qquad k_2, \qquad (2)$$

$$CCl_3+Br_2\rightarrow CCl_3Br+Br \qquad k_3, \qquad (3)$$

$$2Br\rightarrow Br_2 \qquad k_4, \qquad (4)$$

where the steady state concentration of bromine atoms is controlled solely by the thermal dissociation equilibrium for which the equilibrium constant is $K_c=k_1/k_4$. The rate law for this mechanism is simply: $R$=rate of exchange of halogen $=k_2[CCl_3Br](k_1[Br_2]/k_4)^{\frac{1}{2}}=k[CCl_3Br][Br_2]^{\frac{1}{2}}$. The same rate law will hold if the exchange occurs by the step $CCl_3Br+Br^*\rightarrow CCl_3Br^*+Br$ (having a rate constant

[1] See for example, E. W. R. Steacie, *Atomic and Free Radical Reactions* (Reinhold Publishing Corporation, New York, 1946). Chapters IX, X, and XI.

[2] See, for example; a. G. K. Rollefson and W. F. Libby, J. Chem. Phys. 5, 569 (1937); b. J. N. Wilson and R. G. Dickinson, J. Am. Chem. Soc. 61, 3519 (1939); c. L. C. Liberatore and E. O. Wiig, J. Chem. Phys. 8, 349 (1940); d. J. H. Hodges and A. S. Miceli, J. Chem. Phys. 9, 725 (1941); e. L. B. Seely, Jr. and J. E. Willard, J. Am. Chem. Soc. 69, 2061 (1947).

[3] A study of the kinetics of the gas phase reaction has recently been made by N. Davidson and J. H. Sullivan of the California Institute of Technology (see article in this issue). We learned of this just as our work was being completed.

again designated as $k_2$) rather than by reactions 2 and 3 above. The over-all activation energy, which may be determined with the aid of the Arrhenius equation from the dependence of $k$ on the temperature, is related to the activation energies of the elementary steps by the equation: $E_{\text{over-all}}=E_2+\frac{1}{2}(E_1-E_4)$ since $k=k_2(k_1/k_4)^{\frac{1}{2}}$. Since $E_4$ may be assumed to be zero and $E_1$ equal to the heat of dissociation of bromine the value of the activation energy for the elementary reaction $Br+CCl_3Br\rightarrow CCl_3+Br_2$ may be calculated from the experimental data.

In an exchange reaction of this type the measured rate of change of the radiobromine from one chemical form to the other becomes progressively slower, as the equilibrium distribution of radioactivity is approached, although the true exchange reaction continues at a constant rate. Regardless of the mechanism of the exchange reaction the observed rate of equilibration of the radiobromine will follow a first order rate law[4] for which the observed rate constant is $k'=(2.3/t)\log(1/1-F)$ where $F$ equals the concentration of radioactivity in the $CCl_3Br$ relative to that at equilibrium and $t$ equals the time of reaction. Equilibrium will be attained when the activity per gram atom of bromine in the $CCl_3Br$ and $Br_2$ fractions is equal. It can be shown that if the true rate of the exchange reaction is given by: $R=k[Br_2]^m\times[CCl_3Br]^n$ where $k$ is the true velocity constant that

$$k'=R\frac{(2[Br_2]+[CCl_3Br])}{2[Br_2][CCl_3Br]}.$$

If, as in the case of the present work, the bromotrichloromethane concentration is much greater than the bromine concentration,

$$k=2k'([Br_2]^{1-m}/[CCl_3Br]^n).$$

The over-all activation energy can be determined from the temperature coefficient of $k$ or, if the concentration of each reactant is constant in a series of experiments at different temperatures, can be obtained directly from the temperature coefficient of the experimental velocity constant, $k'$.

## EXPERIMENTAL

In order to minimize the possibility that the results of these experiments would be affected by air, water, or other impurities the reactants were degassed, dried and distilled into the reaction tubes on the vacuum system illustrated in Fig. 1. Radiobromine, $Br^{82}$(34 hr.), was prepared from active KBr[5] by reaction with the stoichiometric equivalent of $KBrO_3$ and an excess of 85 percent $H_3PO_4$ in tube $A$ of Fig. 1. With the aid of heat the $Br_2$ was driven into trap $B$; tube $A$ was removed from the system and outlet $C$ was closed with a flame. The system was then evacuated while the bromine was frozen in $B$, following which the bromine was distilled from the $P_2O_5$ in $B$ through a train of $P_2O_5$ on glass wool and condensed in the tube $D$ where it was further degassed by several cycles of alternate freezing and evacuation. From a knowledge of the vapor pressure-temperature curve of bromine it was then possible to obtain a desired pressure of bromine gas in the bulb $E$

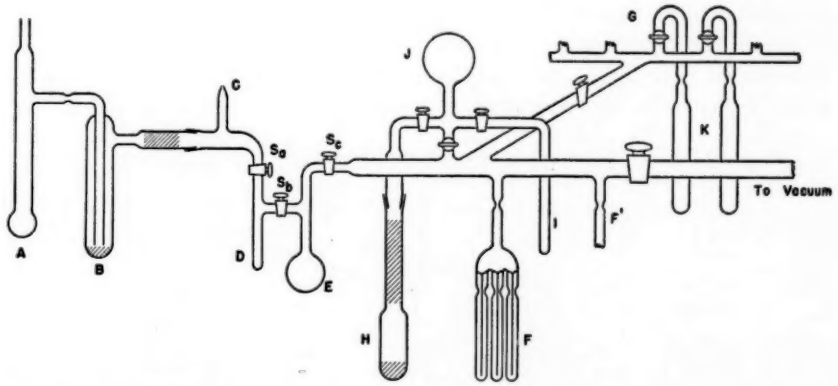


FIG. 1. Apparatus for filling reaction tubes in study of $CCl_3Br$-$Br_2$ reaction.

[4] a. H. A. C. McKay, Nature 142, 997 (1938); b. S. Z. Roginsky, Acta Physicochemica URSS 14, 1 (1941); c. R. B. Duffield and M. Calvin, J. Am. Chem. Soc. 68, 557 (1946).

[5] U. S. Atomic Energy Commission, Item No. 11, Radioisotopes Catalogue No. 2, September 1947.

TABLE I. $CCl_3Br$-$Br_2$ exchange in liquid $CCl_3Br$.

| Tube | Temp., °C | Time, hours | $[CCl_3Br]$, mole/l | $[Br_2]$, mole/l | $F \times 100$ | $k'$, hr.$^{-1}$ | $k_{AV.}$ (mole/l)$^{-\frac{1}{2}}$ hr.$^{-1}$ |
|---|---|---|---|---|---|---|---|
| A1 | 100 | 2.0 | 9.3 | 0.0293 | 15.8 | 0.087 | |
| A2 | 100 | 4.0 | 9.3 | 0.0293 | 30.8 | 0.092 | 0.0034 |
| A3 | 100 | 8.0 | 9.3 | 0.0293 | 78.5 | 0.090 | |
| A4 | 125 | 0.5 | 8.95 | 0.0282 | 49.0 | 1.35 | |
| A5 | 125 | 0.75 | 8.95 | 0.0282 | 60.5 | 1.24 | 0.050 |
| A6 | 125 | 1.0 | 8.95 | 0.0282 | 78.5 | 1.53 | |
| A7 | R.T. | 70 | 10 | 0.030 | 0.7 | — | — |
| C1 | 100 | 2 | 9.3 | 0.0785 | 12.4 | 0.066 | |
| C2 | 100 | 4 | 9.3 | 0.0785 | 22.0 | 0.062 | 0.0038 |
| C3 | 100 | 8 | 9.3 | 0.0785 | 39.8 | 0.063 | |
| C4 | 100 | 12 | 9.3 | 0.0785 | 52.5 | 0.062 | |
| B1 | 115 | 1 | 9.1 | 0.0735 | 26.9 | 0.315 | 0.0184 |
| B2 | 115 | 2 | 9.1 | 0.0735 | 45.0 | 0.300 | |
| B3 | 125 | 0.5 | 8.95 | 0.0720 | 32.1 | 0.770 | |
| B4 | 125 | 1.0 | 8.95 | 0.0720 | 56.6 | 0.830 | 0.048 |
| B5 | 125 | 1.5 | 8.95 | 0.0720 | 70.8 | 0.820 | |
| B6 | 125 | 2.0 | 8.95 | 0.0720 | 80.2 | 0.810 | |
| C5 | 135 | 0.33 | 8.8 | 0.0745 | 46.5 | 1.89 | 0.118 |
| C6 | 135 | 0.66 | 8.8 | 0.0745 | 72.2 | 1.94 | |

by regulating the temperature of $D$ and allowing the vapor to fill the system between stopcocks $S_A$ and $S_C$. The volume of the bulb $E$ together with its connecting tubes was known. By introducing bromine at a known pressure from $D$, then closing $S_B$ and opening $S_C$ it was therefore possible to introduce variable known amounts of bromine into the liquid phase reaction tubes $F$ and $F'$ or into the gas phase tubes attached to the manifold $G$.

Bromotrichloromethane, prepared by the photo-bromination of boiling chloroform in a nitrogen atmosphere,[6] and subsequent fractional distillation, was degassed by alternate freezings and evacuations in the bulb $H$, and distilled from $P_2O_5$ through a train of $P_2O_5$ on glass wool into the metering tube $I$ of which the volume per unit length was known.

To fill the liquid phase reaction tubes a known amount of bromotrichloromethane was distilled from $I$ into the six tubes in the cluster at $F$ cooled with liquid air. (Each of these tubes was made of 2.5 mm I.D., 9 mm O.D. Pyrex capillary tubing and contained 0.3 ml of solution when half-filled.) The stopcock $S_C$ was then opened and the known amount of bromine from bulb $E$ was condensed with the bromotrichloromethane in $F$. Following further degassing cycles, continued until no Tesla coil discharge was obtained while the liquid was frozen, the cluster of six tubes was sealed off from the system, the liquid was thawed, mixed and refrozen, and the individual tubes were sealed off from the manifold. From the total amounts of $Br_2$ and $CCl_3Br$ the concentration, which was the same in each tube, could be calculated. Since no data were found on the coefficient of thermal expansion of liquid $CCl_3Br$, this information, which was needed for use in calculating the concentrations in the reaction tubes at different temperatures, was estimated from data for carbon tetrachloride. Final calculations of the amount of bromine were based on the total radioactive counting rate obtained when the tubes were opened and the contents analyzed. The counting rate per unit weight of bromine was determined for each shipment by counting an aliquot of the stock KBr solution and weighing the solid KBr from a second aliquot.

TABLE II. Effect of bromine concentration on the $CCl_3Br$-$Br_2$ exchange in liquid $CCl_3Br$.

| Temp. 0°C | $[Br_2]$, mole/l | $k'$, hr.$^{-1}$ | $k'[Br_2]$ | $k'[Br_2]^{\frac{1}{2}}$ | $k'[Br_2]^{-1}$ |
|---|---|---|---|---|---|
| 100 | 0.0293 | 0.090 | 0.0026 | 0.015 | 3.07 |
| | 0.0785 | 0.063 | 0.0049 | 0.018 | 0.80 |
| 125 | 0.0282 | 1.37 | 0.40 | 0.23 | 48.5 |
| | 0.0720 | 0.81 | 0.58 | 0.22 | 11.2 |

The reaction tubes in which carbon tetrachloride was used as a solvent were filled in the same manner using a second calibrated tube similar to $I$ (Fig. 1) to introduce the desired amount of $CCl_4$ into the system. The carbon tetrachloride was purified by the method described by Dickinson and Leermakers.[7]

In the preparation of the gas phase reaction tubes a known amount of bromine vapor from the bulb $E$ was allowed to expand into the system including the twelve reaction tubes $K$ on the manifold $G$, after which the stopcocks were closed. These tubes had a uniform volume of 20 ml; it was thus possible to obtain approximately equal amounts of bromine in each. Equal amounts of bromotrichloromethane were then metered into each of the tubes by maintaining the liquid in $I$ at 20°C, allowing the vapor to expand into the known volume of bulb $J$ and then condensing it from this volume into one of

[6] E. G. Bohlmann and J. E. Willard, J. Am. Chem. Soc. 64, 1342 (1942).

[7] R. G. Dickinson and J. A. Leermakers, J. Am. Chem. Soc. 54, 3853 (1932).

the tubes by cooling the tube in liquid air and opening the corresponding stopcock. After degassing, the tube was sealed off at the constriction below the stopcock. The exact amount of bromine in each vapor phase tube was determined from the measured counting rate following reaction. The exact amount of bromotrichloromethane was determined from the weight of the tube following reaction before it was opened (a buoyancy correction was applied) and the weight of the clean dry pieces after it was emptied. About 0.06 to 0.08 gram of bromotrichloromethane was normally used in each tube.

In all cases the reaction tubes were kept at 0° in the dark until they were reacted, and were wrapped in aluminum foil to exclude light during heating and subsequent handling. The reactions were carried out in an oil bath with temperature controlled to within ±0.5°. After removal from the bath each tube was rapidly cooled in an air blast and frozen in dry ice until it was analyzed.

All stopcocks on the system shown in Fig. 1 were lubricated with silicone high vacuum stopcock grease, tests with radiobromine having demonstrated that this grease is much less reactive toward bromine than other common types. All reaction tubes were prepared by boiling in fuming nitric acid and rinsing with triply distilled water. The reaction tubes and all other parts of the apparatus for which it was feasible were degassed prior to use by flaming while evacuated.

In order to determine the extent of reaction in a tube, the contents were frozen in the bottom with dry ice. The top was broken off, carbon tetrachloride was added, and the contents were transferred together with the carbon tetrachloride rinses to a separatory funnel containing 20 percent aqueous sodium iodide. The aqueous and carbon tetrachloride layers were separated, made up to 10 ml each and counted in a Technical Associates solution-type Geiger-Mueller tube. Preliminary experiments showed that under our conditions of measurement the counting rate of radiobromine in carbon tetrachloride was 90 percent of that of the same amount of bromine in 20 percent aqueous sodium iodide solution. This correction and corrections for background and decay were applied where necessary. The fraction of the radiobromine which had exchanged was then given by the ratio of the count in the carbon tetrachloride to the total count. A total count of 5000 was usually measured giving a probable statistical counting error of about 1 percent.

TABLE III. $CCl_3Br$-$Br_2$ exchange in $CCl_4$ solution.

| Tube | Temp., °C | Time, hours | $[CCl_3Br]$, mole/l | $[Br_2]$, mole/l $\times 10^3$ | $F \times 100$ | $k'$, $hr.^{-1}$ | $k$, $(mole/l)^{-1}$ $hr.^{-1}$ |
|---|---|---|---|---|---|---|---|
| A1 | 135 | 1.0 | 0.207 | 2.84 | 18.5 | 0.21 | 0.110 |
| A2 | 135 | 2.0 | 0.207 | 2.84 | 28.9 | 0.17 | 0.090 |
| A3 | 150 | 1.0 | 0.201 | 2.93 | 42.7 | 0.56 | 0.30 |
| A4 | 150 | 2.0 | 0.201 | 2.93 | 73.6 | 0.66 | 0.34 |
| A5 | 170 | 0.25 | 0.194 | 2.74 | 57.0 | 3.36 | 1.82 |
| A6 | 170 | 0.50 | 0.194 | 2.74 | 86.2 | 3.96 | 2.12 |
| B1 | 135 | 1.0 | 0.942 | 7.90 | 43.5 | 0.59 | 0.112 |
| B2 | 135 | 2.0 | 0.942 | 7.90 | 66.6 | 0.51 | 0.096 |
| B3 | 150 | 0.5 | 0.916 | 7.68 | 44.8 | 1.14 | 0.22 |
| B4 | 150 | 1.0 | 0.916 | 7.68 | 64.5 | 1.10 | 0.20 |

## RESULTS

The conditions and results of exchange experiments carried out with liquid phase mixtures of bromine and bromotrichloromethane are given in Table I, where $F$ is the fraction of radiobromine equilibrium attained and $k'$ is the observed first order velocity constant for the transfer of radiobromine from $Br_2$ to $CCl_3Br$. The letters $A$, $B$, and $C$ each indicate a separate series of reaction tubes prepared as a unit. Series $B$ and $C$ were prepared from a single bromine shipment under conditions as nearly identical as possible while $A$ was prepared from a different bromine shipment and with a much lower bromine concentration.

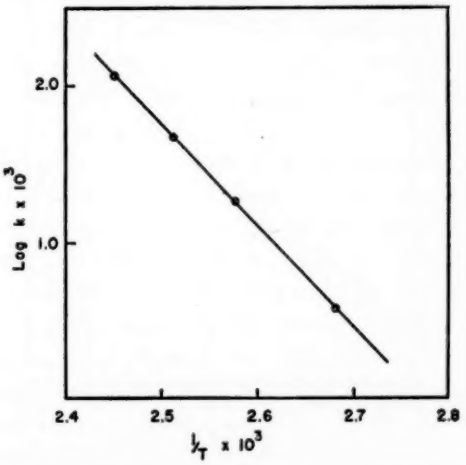


FIG. 2. Temperature dependence of rate of $CCl_3Br$-$Br_2$ exchange in liquid $CCl_3Br$.

TABLE IV. $CCl_3Br$-$Br_2$ exchange in the gas phase.

| Tube | Temp., °C | Time, hours | $[CCl_3Br]$, mole/l $\times 10^3$ | $[Br_2]$, mole/l $\times 10^3$ | $F' \times 100$ | $F_\infty \times 100$ | $F \times 100$ | $k$, (mole/l)$^{-\frac{1}{2}}$ hr.$^{-1}$ | $k_{Av}$, (mole/l)$^{-\frac{1}{2}}$ hr.$^{-1}$ |
|---|---|---|---|---|---|---|---|---|---|
| 1 | 150 | 0.5 | 5.5 | 0.33 | 2.0 | 89.3 | 2.2 | 0.26 | 0.26 |
| 2 | 170 | 0.5 | 7.2 | 0.34 | 9.6 | 91.3 | 10.5 | 1.16 | |
| 3 | 170 | 2.0 | 4.2 | 0.37 | 17.4 | 84.5 | 20.6 | 1.06 | 1.11 |
| 4 | 170 | 4.75 | 20.3 | 0.41 | 86.6 | 96.0 | 90.4 | 1.12 | |
| 5 | 200 | 0.5 | 3.9 | 0.36 | 34.8 | 84.4 | 41.2 | 10.30 | |
| 6 | 200 | 1.0 | 6.9 | 0.36 | 76.4 | 90.5 | 84.5 | 10.26 | 10.28 |
| 7 | 220 | 0.25 | 3.9 | 0.47 | 43.2 | 80.5 | 53.6 | 34.2 | 34.2 |
| 8 | 220 | 0.50 | 10.6 | 0.37 | 92.8 | 93.5 | 99.4 | | |

Experiment A7, in which a reaction mixture was allowed to stand for 70 hours at room temperature and then analyzed, shows that reaction is negligible at this temperature.

In Table II data from Table I for experiments made at two different bromine concentrations at each of two temperatures are tabulated, together with the values of $k'$ multiplied by different powers of the bromine concentration. From the equations stated in the Introduction, $R = k[Br_2]^m \times [CCl_3Br]^n$ and $k = 2k'[Br_2]^{1-m}/[CCl_3Br]^n$ it is evident that if the $CCl_3Br$ concentration is held constant and $k'$ is determined at different concentrations of bromine then the value of $m$ which gives a constant value of the product $k'[Br_2]^{1-m}$ will be equal to the order of the bromine dependency of the exchange reaction. The results of Table II indicate that the rate of exchange of bromine with liquid bromotrichloromethane is proportional to the square root of the bromine concentration.

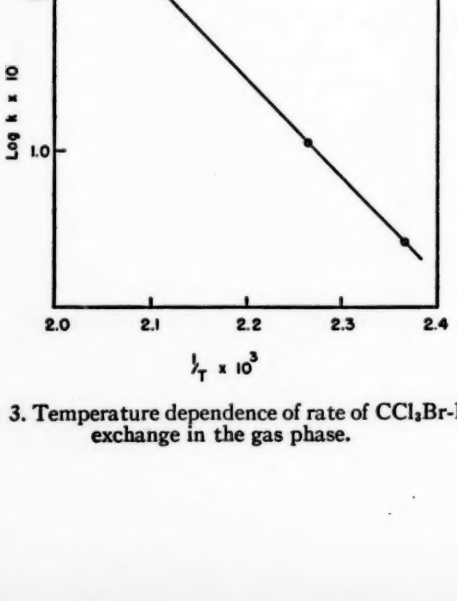


FIG. 3. Temperature dependence of rate of $CCl_3Br$-$Br_2$ exchange in the gas phase.

The first power dependency of the rate on the concentration of $CCl_3Br$ is indicated by the results listed in Table III for experiments in $CCl_4$ as a solvent[8] and by the results of the gas phase experiments listed in Table IV. Except for the discrepancy of unknown origin shown by the results at 150°C in Table III, the values of $k$ calculated using the formula for first order dependency on $CCl_3Br$ concentration, $k = (2k' \times [Br_2]^{\frac{1}{2}})/([CCl_3Br])$, are essentially constant over three and fourfold variations in $CCl_3Br$ concentration.

A calculation of the activation energy of the reaction on the basis of the two temperatures of Table I, series $A$ gives a value of 32 kcal. mole$^{-1}$. The data of Table I, series $B$ and $C$, for four temperatures, plotted in Fig. 2, give 29.8 kcal. mole$^{-1}$. The latter is probably a more accurate value since the experiments of series $A$ were exploratory in nature and run under less carefully controlled conditions. The data of Table III for $CCl_4$ solutions give a value of about 29 kcal. mole$^{-1}$.

In the gas phase experiments (Table IV) the $CCl_3Br$-$Br_2$ ratio was usually less than 100, so that, in contrast to the liquid phase runs, where the excess of bromotrichloromethane was greater, a measurable fraction of the activity would have remained in the form of elemental bromine at equilibrium. In Table IV the observed fraction of the activity in the organic layer is denoted by $F'$, the calculated equilibrium fraction by $F_\infty$, and the fraction of equilibrium achieved

[8] We have found that the rate of the reaction of $Br_2$ with the solvent is negligible even at the highest temperature used in this work. The reaction between $CCl_4$ and $Br_2$ does take place with an easily measurable rate above 200°C, the activation energy being about 40 kcal./mole.

by $F$

$$F=F'/F_\infty;\quad F_\infty=1/1+r;\quad r=2[Br_2]/[CCl_3Br].$$

Fig. 3 shows the plot of $\log k$ *vs.* $1/T$ for the gas phase experiments. The slope of this line yields a value of 28.7 kcal. mole$^{-1}$ for the activation energy.

In order to prove the identity of the organic radiobromine compound resulting from these experiments the organic fractions from one series of tubes were combined and fractionally distilled with carriers covering a wide boiling point range and including $CCl_3Br$. The separate fractions were counted with a Geiger-Mueller counter. Essentially all of the activity was found in the $CCl_3Br$ fraction.

A series of experiments was made to determine whether or not added constituents affect the rate of the $CCl_3Br$-$Br_2$ exchange reaction in the gas phase at 170° and at concentrations similar to those used in the experiments of Table IV. The results indicate that a pressure of $O_2$ 15 percent as great as that of the $Br_2$, of $H_2O$ 12 percent as great as that of the $Br_2$, or of $Cl_2$ 40 percent as great as that of the $Br_2$ causes a decrease in the rate constant of approximately 50 percent. A test in which a quartz tube was used in place of the usual Pyrex tube showed no change in the rate constant. These results are of qualitative rather than quantitative significance but are adequate to indicate that the reaction is not extremely sensitive to any of the variables tested.

Day[9] has shown that a bromine-sensitized photo-chemical formation of $C_2Cl_6$ from $CCl_3Br$ ($2CCl_3Br \xrightarrow[h\nu]{Br_2} C_2Cl_6+Br_2$) occurs at very low bromine concentrations. We have determined qualitatively that this reaction also occurs as a thermal reaction but is not observable at bromine concentrations as high as those used in the work of this paper.

## DISCUSSION

The results presented above establish the fact that the rate of equilibration of the radiobromine between the inorganic and organic phases in a mixture of $Br_2$ and $CCl_3Br$ follows a first order law, in agreement with the belief that it is a simple exchange reaction. This belief is further established by the distillation experiment showing the organically bound activity to be in the form of bromotrichloromethane.

[9] W. U. Day, Ph.D. thesis, University of Wisconsin (1942).

TABLE V. Comparison of rate constants of $CCl_3Br$-$Br_2$ exchange in liquid and gas phase.

| Table | Series | Temp., °C | Conditions | $k$, (mole/l)$^{-\frac{1}{2}}$ hr.$^{-1}$ |
|---|---|---|---|---|
| I | *C* | 135 | Liquid Phase | 0.118 |
| III | *A* | 135 | $CCl_4$ Solution | 0.100 |
| | *B* | 135 | $CCl_4$ Solution | 0.104 |
| III | *A* | 150 | $CCl_4$ Solution | 0.32 |
| | *B* | 150 | $CCl_4$ Solution | 0.22 |
| IV | | 150 | Gas Phase | 0.26 |
| III | *A* | 170 | $CCl_4$ Solution | 1.96 |
| I | *B, C* | 170 | Liquid Phase | 1.92* |
| IV | | 170 | Gas Phase | 1.11 |

* Obtained by extrapolation on Fig. 2.

The fact that the rate of the over-all exchange reaction is proportional to the square root of the bromine concentration is strong evidence that the exchange occurs through the medium of bromine atoms whose concentration is controlled by the thermal equilibrium $Br_2 \rightleftharpoons 2Br$. This suggests that the mechanism of the exchange is either

$$CCl_3Br+Br \rightarrow CCl_3+Br_2, \qquad (2)$$

$$CCl_3+BrBr^* \rightarrow CCl_3Br^*+Br, \qquad (3)$$

or

$$CCl_3Br+Br^* \rightarrow CCl_3Br^*+Br. \qquad (2')$$

It is impossible to distinguish between these two mechanisms on the basis of the results reported in this paper.

Selected rate constants which afford the best comparison of the exchange reaction in liquid $CCl_3Br$, in $CCl_4$ solution, and in the gas phase have been taken from Tables I, III, and IV and listed in Table V.

The near equivalence of the activation energy (Figs. 1 and 2) and of the rate constants (Table V) in the gas and liquid phases suggests that the elementary steps are the same in the two phases and that at the same temperature the steady state concentration of the bromine atom intermediate is the same in the two cases.

The over-all activation energy for the thermal $CCl_3Br$-$Br_2$ exchange may be expected to be derived from the activation energies of the primary steps by the relation $E_{\text{over-all}}=E_2+\frac{1}{2}(E_1-E_4)$. Substituting the average experi-

TABLE VI. Photo-chemical exchange of $Br_2$ with $CCl_3Br$ in $CCl_4$ solution.[9] $[CCl_3Br]=0.47$ m/l.

| | $[Br_2]$, mole/l $\times 10^3$ | $T$, °C | % of Equilib. exchange | Quanta abs sec.$^{-1}$ cc$^{-1}$, $\times 10^{-16}$ | Quantum yield | Activation energy, kcal. moles$^{-1}$ |
|---|---|---|---|---|---|---|
| 1a | 0.335 | 28 | 25 | 4.37 | 0.63 | 5.1 |
| 1b | 0.335 | 50 | 42 | 3.74 | 1.27 | |
| 2a | 0.370 | 28 | 8.6 | 3.90 | 0.26 | 9.7 |
| 2b | 0.370 | 50 | 20.5 | 3.71 | 0.68 | |

mental value of 29.2 kcal. mole$^{-1}$ for $E_{\text{over-all}}$; 45.2 kcal. for $E_1$, the heat of dissociation of $Br_2$; and 0 for $E_4$, the activation energy of combination of bromine atoms, gives a value of 7 kcal. mole$^{-1}$ for $E_2$. This appears to be the activation energy for either the reaction $CCl_3Br+Br\rightarrow CCl_3+Br_2$ or $CCl_3Br+Br^*\rightarrow CCl_3Br^*+Br$, whichever accounts for the observed bromine exchange. This result is in agreement with results of Day which gave a value of 5–10 kcal. mole$^{-1}$ for the activation energy of the photo-chemical exchange based on the data reproduced in Table VI and also with the deductions of Franke and Schumacher[10] from a study of the bromine-sensitized photo-oxidation of $CCl_3Br$. Determinations 1a and 1b of Table VI were made on two cells filled from the same reaction mixture, and 2a and 2b on two filled from another reaction mixture. In both cases considerable care was taken to have the system free from oxygen, moisture and other impurities.

The difference in the quantum yields of the two sets of experiments and the variation in the temperature coefficient may mean that this reaction, like the photo-chemical exchange of $Br_2$ with $CBr_4$[2e], is very sensitive to impurities. If so, the mechanisms of the photo-chemical and thermal exchange reaction are different, or possibly oxygen-bromine complexes which use up bromine atoms at the temperature of the photo-chemical studies are unstable at the temperatures of the thermal studies. Further experiments should be made to clarify this question.

If the activation energy of 7 kcal. mole$^{-1}$ is correctly ascribed to the elementary reaction $CCl_3Br+Br\rightarrow CCl_3+Br_2$ it may be concluded that the heat of dissociation of the carbon-bromine bond in bromotrichloromethane is equal to or less than 52 kcal. mole$^{-1}$, i.e., the heat of formation of the bromine molecule formed plus this energy of activation.

A calculation of the rate of collisions between Br atoms and $CCl_3Br$ molecules leads to the result that the rate of collisions involving an energy of at least 7 kcal. mole$^{-1}$ is about 20 times the observed rate of exchange. In this calculation the collision diameter of Br is assumed to be 2.2A[11] and that of $CCl_3Br$ is assumed to be equal to 6.4A, the diameter of a $CCl_4$ molecule in the liquid phase,[12] and the bromine atom concentration is determined from $K_p$[13] for the $Br_2\rightleftharpoons 2Br$ equilibrium.

In the work reported in this paper the maximum activity of the radiobromine used in any experiment was about $4\times 10^{10}$ disintegrations liter$^{-1}$ hour$^{-1}$. If it is assumed as a limiting case that all of the energy of the $\beta$-radiations from these disintegrations was absorbed in the reaction mixture and resulted in the cleavage of C—Br bonds in $CCl_3Br$, it may be estimated that the rate of breaking of C—Br bonds by this means is only $10^{-6}$ of the observed rate of exchange of $Br_2$ with $CCl_3Br$. This indicates that the effect of the beta- (and also the gamma-) radiations on the rate of the exchange can be neglected. This conclusion is in accord with the experimental observation that the rate of the $CCl_3Br$-$Br_2$ exchange is independent of the specific activity of the bromine in the 10-fold range ($4\times 10^{10}$ dis/1 hr.$^{-1}$ down to $4\times 10^{9}$ dis/1 hr.$^{-1}$) covered in these experiments.

## SOLVENT EFFECTS

By comparing the data for the thermal and photo-chemical $CCl_3Br$-$Br_2$ exchange in the liquid phase it is possible to deduce that only one out of every 400 bromine molecules which absorb a photon in solution produces atoms which escape primary recombination. The steps of reasoning involved are in part similar to those used by Bodenstein and Lütkemeyer[14] in calculating the

[10] W. Franke and H. J. Schumacher, Zeits. f. physik. Chemie B42, 297 (1939).

[11] E. Rabinowitch and W. C. Wood, Trans. Faraday Soc. 32, 907 (1936).

[12] E. E. Bray and N. S. Gingrich, J. Chem. Phys. 11, 351 (1943).

[13] A. R. Gordon and Colin Barnes, J. Chem. Phys. 1, 693 (1933).

[14] M. Bodenstein and H. Lütkemeyer, Zeits. f. Physik. Chemie 114, 208 (1924).

rate constants for the dissociation of $Br_2$ molecules and recombination of Br atoms in the gas phase and in part related to problems of determining the primary photo-chemical yield in solution which have been discussed by Dickinson[15] and others.

The conclusion is in agreement with the "cage" hypothesis originally proposed by Franck and Rabinowitch.[16] Attempts to verify the existence of the process of primary recombination and determine its quantitative significance have in general supported the hypothesis but have not been conclusive.[15] Perhaps the most conclusive evidence of the effect of solvent in favoring the combination of atoms and radicals which are formed in the same solvent envelope is furnished by a study of reactions activated by nuclear processes.[6]

The method and assumptions involved in the present discussion are outlined below.

(1) The equilibrium constant for the reaction $Br_2 \rightleftharpoons 2Br$ is assumed to be the same in solution as in the gas phase. This assumption is a plausible one, since it is probable that $k_2$ is the same in the liquid phase as in the gas phase and since it has been observed that the rate constants in gas, solution, and liquid $CCl_3Br$ are approximately the same, implying equal Br atom concentrations at equal $Br_2$ concentrations.

(2) The collision frequency between Br atoms in solution is assumed to be given by the expression for the rate of collisions in the gas phase: $Z_{Br\text{-}Br}=2n^2\sigma^2\cdot(\pi RT/M)^{\frac{1}{2}}$, and this is assumed to be equal to the maximum possible rate of combination of Br atoms.

(3) The thermal equilibrium concentration of Br atoms (at a specified temperature and $Br_2$ concentration) calculated by $[Br]=(K_c[Br_2])^{\frac{1}{2}}$ is employed in (2) to calculate the maximum rate of recombination of Br atoms which must equal the rate of dissociation of $Br_2$ molecules, that is to say, $k_4[Br]^2=k_1[Br_2]$ where $k_1/k_4=K_c$.

(4) Assuming that the elementary reaction steps and the corresponding velocity constants, except for the initial step which produces Br atoms, are the same in the photo-chemical and thermal reactions, we have

$$\frac{R'}{R}=\left(\frac{2\beta Q}{k_1[Br_2]}\right)^{\frac{1}{2}},$$

where $R'$ and $R$ represent the rates of the photo-chemical and thermal reactions, respectively, at the same temperature and concentrations, $Q$ is the rate of light absorption in the photo-chemical reaction, and $\beta$ is the fraction of the absorbed quanta which produce dissociation of the bromine molecules without primary recombination within the solvent cage.

The numerical data used in determining the value of $\beta$ by the method outlined above are as follows. From Table VI, Experiment 1b, $[CCl_3Br]=0.47$ mole/l; $[Br_2]=0.00335$ mole/l; $t=50°C$; $Q=0.225$ Einsteins/l hr.$^{-1}$; $R'=0.352$ mole/l hr.$^{-1}$. For the thermal reaction, $k=7.6\times10^{-6}$ (mole/l)$^{-\frac{1}{2}}$ hr.$^{-1}$ at 50°C by extrapolation on Fig. 2, giving $R=2.1\times10^{-7}$ mole/l hr.$^{-1}$ for the concentrations listed above. At 50°C, $K_c=9.4\times10^{-23}$ mole/l, this value being derived from $K_p$ for the gaseous equilibrium.[13]

The value of $\beta$ obtained is 0.0025. Subject to the validity of the assumptions and to an uncertainty of a factor of at least 2 in the experimental value of the rate of the photo-chemical reaction, this means that only one bromine molecule in 400 which absorbs photons in $CCl_4$ solution escapes primary recombination and yields free bromine atoms to the solution. If the number of encounters between bromine atoms in solution is less than in the gas phase the value calculated for $\beta$, i.e., the quantum yield for dissociation of $Br_2$, would be even lower than 0.0025. Since the observed quantum yield for the exchange of bromine with $CCl_3Br$ is about unity the chain length of the observed photo-chemical reaction must be at least 400 and the quantum yield of the exchange in the gas phase, where negligible primary recombination may be assumed, should be about $(400)^{\frac{1}{2}}$ at 50°C and a light absorption rate of $4\times10^{16}$ quanta sec.$^{-1}$ cc$^{-1}$, if the calculated value for $\beta$ is correct.


## ACKNOWLEDGMENT

This research was supported, in part, by the Research Committee of the Graduate School from funds supplied by the Wisconsin Alumni Research Foundation.


[15] R. G. Dickinson, J. Phys. Chem. **42**, 740 (1938).
[16] J. Franck and E. Rabinowitch, Trans. Faraday Soc. **30**, 120 (1934).

# The Kinetics of the Vapor Phase Exchange of Radioactive Bromine between Trichlorobromomethane and Bromine

NORMAN DAVIDSON AND JOHN H. SULLIVAN
*Gates and Crellin Laboratories of Chemistry,* California Institute of Technology, Pasadena, California*

(Received July 30, 1948)

The rate of exchange of radioactive bromine between trichlorobromomethane and bromine in the vapor phase in the temperature range 420–455°K has been determined. The rate is equal to $k[Br_2]^{\frac{1}{2}}[CCl_3Br]$, where $\log_{10}k(\text{moles/liter})^{-\frac{1}{2}}(\text{sec.})^{-1} = (-33{,}100(\pm 400))/(4.574T) + 12.75(\pm 0.20)$. The energy of activation for the elementary reaction between bromine atoms and trichlorobromomethane molecules is 10.3 kcal., and the frequency factor is $7.9\times 10^{10}$. It is proposed that the reaction proceeds via the sequence: $Br^* + BrCCl_3 \rightarrow BrBr^* + -CCl_3$, and $Cl_3C- + Br_2^* \rightarrow Cl_3CBr^* + Br^*$, rather than by a Walden inversion mechanism. The observation that chloroform is formed when hydrogen bromide, bromine, and trichlorobromomethane are heated is cited as evidence for the presence of $-CCl_3$ radicals and for the reaction $Cl_3C- + HBr \rightarrow Cl_3CH + Br$. The $-CCl_3$ radical is then more stable than the $-CH_3$ radical by 10 kcal. or more.

The vapor pressures of liquid trichlorobromomethane are given by the equation: $\log_{10}p(\text{mm}) = (-8240/4.574T) + 7.64$. The exchange reaction $Br_2(g) + AgBr^* \rightarrow Br_2^*(g) + AgBr$ readily goes to completion and is the basis for a convenient semi-micro method for the preparation of radioactive elementary bromine.

## INTRODUCTION

THE investigation of the kinetics and mechanism of the exchange of radioactivity between atoms and molecules may be expected to contribute to an understanding of free radical reactions in general in much the same ways that the study of exchange reactions between ions and molecules in solution has contributed to the theory of ionic displacement reactions in organic chemistry.[1]

Wilson and Dickinson[2] observed a photochemically induced exchange between bromine and trichlorobromomethane in carbon tetrachloride solution at 76°C, suggesting that the exchange reaction is between bromine atoms and trichlorobromomethane molecules. In order to avoid the complications in the interpretation of photo-chemical reactions because of non-uniform intensity of light along the light path and because of uncertainties as to the rate of recombination of bromine atoms, we have chosen to investigate the thermal vapor phase exchange between bromine and trichlorobromomethane.[3]

Hodges and Miceli[4] have very briefly reported that the exchange between bromine and carbon tetrabromide in the gas or liquid phase proceeds by a bromine atom mechanism, and that the activation energy for the elementary reaction is 0–3 kcal.

## EXPERIMENTAL

### (a) Preparation of Materials

The trichlorobromomethane was prepared by the reaction of carbon tetrachloride and aluminum bromide.[5] A sample boiling at 104.2°C at 745 mm was obtained by fractional distillation in an all-glass apparatus.

The vapor tensions of the substance were measured using a mercury manometer in a glass vacuum apparatus. These values, $p(0°) = 11 \pm 1$ mm, $p(22°) = 35 \pm 1$ mm, $p(24°) = 38 \pm 1$ mm, in conjunction with the boiling point at atmospheric pressure, imply the vapor pressure equation, $\log_{10}p(\text{mm}) = (-8240)/(4.574T) + 7.64$, and a Trouton constant of 21.8. The measured density of 1.99 g/ml at 25°C agrees with the literature values.

Hydrogen bromide was prepared by the reaction of hydrogen and bromine over a heated

* Contribution No. 1232 from the Gates and Crellin Laboratories of Chemistry.

[1] L. P. Hammett, *Physical Organic Chemistry*, (McGraw-Hill Book Company, Inc., New York, 1940), p. 164.

[2] J. N. Wilson and R. G. Dickinson, J. Am. Chem. Soc. **61**, 3519 (1939).

[3] Just at the conclusion of our experimental work we learned that Professor J. Willard and Mr. A. Miller of the University of Wisconsin were independently engaged in a study of the same problem. J. Chem. Phys. **17**, 168 (1949).

[4] J. H. Hodges and A. S. Miceli, J. Chem. Phys. **9**, 725 (1941).

[5] H. G. Vesper and G. K. Rollefson, J. Am. Chem. Soc. **56**, 1456 (1934).

platinum filament, and purified by repeated bulb to bulb distillation in vacuum.

The radioactive isotope used was the 34.5-hr. $Br^{82}$. It was prepared by irradiation of 12 liters of ethylene dibromide with neutrons from a 250-mc radon-beryllium source, extracted with 400 ml of water containing 20 mg of sodium bromide, and precipitated as silver bromide, which was washed and dried. Radioactive molecular bromine was obtained by the reaction: $AgBr^* + Br_2 \rightarrow AgBr + Br_2^*$. A quantity of 100–200 microliters of reagent grade bromine was distilled in vacuum into a Y-shaped vessel of *ca.* 50-ml volume containing the silver bromide. The tube was sealed off and heated to 160°C for several hours with occasional shaking. The radioactive bromine was then condensed in one arm of the tube. Under these conditions, there was 100 percent exchange of activity. Kolthoff and O'Brien[6] report 60 percent exchange between bromine vapor and freshly precipitated silver bromide at room temperature. This method of isolation on the semi-micro scale of radioactive bromine was selected and developed because of its convenience and because it was believed to be a method that was unlikely to introduce impurities, particularly the oxygen bearing impurities that are often troublesome in free radical chemistry.

### (b) Procedure for the Exchange Reactions

Aliquots of $Br_2^*$ (15–75 microliters) and trichlorobromomethane (100–300 microliters) were mixed in a test tube that could be attached to a vacuum apparatus by a ground joint. The mixture was distilled in vacuum through $P_2O_5$ and condensed in liquid air with constant pumping, and then distilled into an evacuated reaction vessel of known volume. The reaction vessels had been treated with hot sulfuric acid-dichromate solution, rinsed with hot water, treated with boiling nitric acid, rinsed four times with boiling, distilled water, and outgassed by flaming in vacuum. The volumes (*ca.* 80 ml) of the reaction vessels were determined by observing the weights of water required to fill them to the seal-off constriction.

The exchange reactions took place in the dark in an oil bath, the temperature being constant to ±0.07°C. Temperatures were measured with a Chromel-Alumel thermocouple and a Leeds and Northrup portable precision potentiometer with a precision of ±0.05°C. The thermocouple was calibrated against standard thermometers to an accuracy of 0.5°C.

In order to avoid possible photo-chemical exchange, reaction mixtures were stored in liquid air when not being handled. An experiment showed that there was no exchange in unheated reaction mixtures.

### (c) Radio-Assay Procedure

After reaction, the bromine was extracted from the trichlorobromomethane with sodium nitrite solution. Mercurous bromide was precipitated from aliquots of the solution which contained an amount of bromide equivalent to 15 microliters of bromine. Reproducible counting samples were obtained by suction filtration of the precipitate through disks of S. and S. No. 576 filter paper mounted on a sintered glass plate. The area on which the smooth mercurous bromide mats were formed was defined with a glass tube pressed against the filter paper. In cases where analyses were run on two aliquots of the same solution, the results agreed within the statistical counting error, usually about 1 percent. The activity of the bromine before exchange was determined in the same way from solutions obtained by reducing measured volumes of the liquid radioactive bromine with sodium nitrite. That the transfer of bromine into the reaction vessels by distillation was quantitative was shown by radioactive assay of a reaction mixture which had not been heated.

### (d) Chemical Analyses of Reaction Mixtures

For the semi-quantitative chemical analyses of the reaction products reported in the discussion, the components of reaction mixtures were separated and identified using a small glass column and the general type of vacuum techniques described by Stock[7] and Burg.[8]

[6] I. M. Kolthoff and A. S. O'Brien, J. Chem. Phys. **7**, 401 (1939).

[7] A. Stock, *Hydrides of Boron and Silicon* (Cornell University Press, Ithaca, 1933).

[8] A. B. Burg, J. Am. Chem. Soc. **56**, 499 (1934).

TABLE I. Exchange reaction between $Br_2$ and $CCl_3Br$.

| Expt. | | 2[$Br_2$] (moles/liter) $\times 10^3$ | [$CCl_3Br$] $\times 10^3$ | $t$ sec. $\times 10^{-3}$ | $T$ °K | $\frac{x}{c}$ | $k$(expt.) (moles/liter)$^{-\frac{1}{2}}$ sec.$^{-1}$ $\times 10^5$ | $k$(calc.) sec.$^{-1}$ |
|---|---|---|---|---|---|---|---|---|
| 1 | a | 6.77 | 33.45 | 194.3 | 419.10 | 0.282 | 2.98 ± .04 | 2.97 |
| | b | 6.38 | 31.60 | | | 0.286 | 3.00 ± .04 | |
| | c | 11.90 | 35.35 | | | 0.383 | 2.92 ± .08 | |
| | d | 11.57 | 34.30 | | | 0.382 | 2.99 ± .08 | |
| 2 | a | 7.71 | 35.65 | 36.0 | 432.00 | 0.427 | 9.18 ± .14 | 9.63 |
| | b | 6.55 | 11.30 | | | 0.730 | 10.05 ± .29 | |
| 3 | a | 7.30 | 36.05 | 36.1 | 433.80 | 0.346 | 11.30 ± .2 | 11.43 |
| | b | 12.42 | 36.85 | | | 0.457 | 11.09 ± .2 | |
| | c | 11.84 | 35.20 | | | 0.466 | 11.05 ± .3 | |
| 4 | a | 33.50 | 33.00 | 8.95 | 442.85 | 0.770 | 27.1 ±1.3 | 25.1 |
| | b | 6.62 | 32.65 | | | 0.548 | 26.0 ± .6 | |
| | c | 6.59 | 32.50 | | | 0.534 | 27.2 ± .6 | |
| | d | 15.17 | 26.15 | | | 0.720 | 27.7 ± .8 | |
| 5 | a | 7.00 | 24.10 | 8.74 | 444.25 | 0.594 | 32.8 ±1.0 | 28.2 |
| | b | 7.61 | 13.12 | | | 0.754 | 33.8 ±1.5 | |
| 6 | a | 7.38 | 36.55 | 17.05 | 445.07 | 0.287 | 31.6 ± .4 | 30.3 |
| | b | 6.94 | 34.25 | | | 0.294 | 31.7 ± .4 | |
| 7 | a | 13.00 | 38.50 | 4.14 | 455.52 | 0.576 | 63.5 ±1.4 | 71.4 |
| | b | 12.50 | 25.80 | | | 0.685 | 65.2 ±1.9 | |
| | c | 10.15 | 34.95 | | | 0.535 | 70.1 ±1.2 | |
| 8 | a | 6.58 | 32.50 | 7.08 | 455.75 | 0.312 | 72.8 ±1.3 | 72.6 |
| | b | 6.82 | 32.70 | | | 0.310 | 73.3 ±1.7 | |
| | c | 10.37 | 30.75 | | | 0.436 | 69.5 ±1.3 | |
| | d | 12.42 | 36.80 | | | 0.408 | 71.1 ±1.3 | |

## RESULTS AND DISCUSSION

### (a) Analysis of the Kinetic Data

An integrated form of the expression for the decrease of the activity of radioactive bromine due to exchange with trichlorobromomethane that is originally inactive is

$$\ln\left[\left(\frac{a}{b}+1\right)\frac{x}{c}-\frac{a}{b}\right]=-R(a,b)\frac{a+b}{ab}t.$$

In this relation

$a$ = concentration of elementary bromine, in units of atoms per unit volume,
$b$ = concentration of trichlorobromomethane,
$c$ = initial activity of bromine,
$x$ = activity of bromine after reaction for time $t$, and
$R(a, b)$ is the rate of exchange.

This result is a consequence of the general analysis due to McKay[9] of the rate of exchange between two components in chemical equilibrium.

We have tested the hypothesis that the exchange is a reaction between bromine atoms in thermal equilibrium with bromine gas and trichlorobromomethane molecules, i.e., $R(a, b)=k\times(a/2)^{\frac{1}{2}}b$. Table I exhibits the analysis of the experiments on this basis. It is evident, particularly from experiments 2, 4, 5, that the rate constant derived in this way is essentially constant for fivefold and threefold variations in the concentrations of bromine and trichlorobromomethane, respectively.

An experiment in a vessel packed with glass beads, in which the surface area was *ca.* 12 times that in an unpacked vessel, established that the rate of reaction was not dependent on surface area; the rate constants of Table I refer to a homogeneous, gas phase reaction.

It was also established that there were no significant side reactions taking place. The following observations bear on this point:

(1) The weight of the mercurous bromide precipitate from a reaction mixture was the same within 2 percent as that from the unreacted bromine, and in agreement with the expected value. Thus, there was no consumption or formation of bromine during the reaction.

(2) A mixture of bromine and trichlorobromomethane at concentrations of $5.1\times10^{-3}$ and $17.5\times10^{-3}$ moles/liter, respectively, in a two-liter bulb was heated to 456°K for a time such that more than 75 percent of the trichlorobromomethane would have undergone exchange. After extraction of the bromine, the organic layer was dried and fractionally distilled in vacuum. The substance was pure trichlorobromomethane with the vapor pressures reported above; there was less than ½ percent $CCl_4$ or other more volatile products and less than 1 percent of less volatile products ($CCl_2Br_2$, $C_2Cl_6$). Distillation of a known mixture showed that less than ½ percent of carbon tetrachloride could be detected by this means.

The variation of $k$ with temperature is described by the equation

$$\log_{10}k=(-33{,}120(\pm400))/(4.574T)+12.75(\pm0.20).$$

The values of the parameters were obtained by a least squares analysis of the data of Table I. For this treatment it was assumed that the temperatures were known with certainty. The standard deviations in $k$ given in the table were obtained from the assumption that the error was due to statistical error of counting by using an analysis of errors in an exchange reaction that will be published separately.[10] The comparison

[9] H. A. C. McKay, Nature **142**, 997 (1938).

[10] N. Davidson and J. H. Sullivan, to be published.

of calculated and observed rate constants indicates that other sources of error were significant.

### (b) The Mechanism of the Reaction

The dependence of the rate of exchange on concentrations implies that the exchange proceeds via the sequence:

$$Br_2^* \rightleftarrows 2Br^* \quad \text{(fast)}, \tag{1}$$

$$Br^* + CCl_3Br \xrightarrow{k_0} \text{exchange}. \tag{2}$$

The bromine atoms liberated in reaction (2) are assumed to come rapidly into radioactive equilibrium with the rest of the elementary bromine. For $k_0$, the rate constant of the elementary reaction (2), we have $k_0 = kK_c^{-\frac{1}{2}}$, where $K_c = [Br]^2/[Br_2]$ is the equilibrium constant (in concentration units) for the dissociation of bromine.

For reaction (1), $\Delta H_{291°K} = 46{,}110$ cal.,[11] taking $\Delta C_v = 0.6$,[12] $\Delta E_{435°K} = 45{,}620$. In addition, $\Delta S_{298°K} = 25.00$ e.u.,[13] $\Delta S_{435°K} = 26.00$ e.u. For the equilibrium constant of reaction (1) in a small temperature range around 435°K, $K_p = \exp(26.00/R) \times \exp(-(45{,}620 + RT)/(RT))$ and $K_c = K_p/RT = (1/R \times 435°) \exp((26.00 - R)/(R)) \exp(-45{,}620/RT) = (10^{3.69} \times 10^{-(45,620)/(4.574T)})$. Since $k_0 = kK_c^{-\frac{1}{2}}$, $k_0 = 7.9 \times 10^{10(\pm 0.20)} \times 10^{-(10,310(\pm 400))/(4.574T)}$ moles/liter×sec. The activation energy of reaction (2) is 10,310 cal. The frequency factor corresponds to a mean collision diameter of 3.3A. This frequency factor is but slightly larger than the value of *ca.* $3 \cdot 10^{10}$, which holds for several similar reactions of bromine atoms as tabulated by Kistiakowsky and Van Artsdalen.[14]

The possible specific elementary exchange reactions are

$$Br^* + Cl_3CBr \rightarrow Br^*CCl_3 + Br \text{ (Walden inversion)}, \tag{2a}$$

$$Br + Br^*CCl_3 \rightarrow Br - Br^* + -CCl_3, \tag{2b1}$$

$$Cl_3C- + Br_2^* \rightarrow Cl_3CBr^* + Br^*. \tag{2b2}$$

Other possible reactions of interest here are

$$Cl_3C- + BrCCl_3 \rightarrow Cl_3CBr + -CCl_3 \text{ (no net effect)}, \tag{3}$$

$$Cl_3C- + Cl_3CBr \rightarrow CCl_4 + -CCl_2Br, \tag{4a}$$

$$Cl_2BrC- + Br_2 \rightarrow Cl_2CBr_2 + Br, \tag{4b}$$

$$Cl_3C- + -CCl_3 + M \rightarrow C_2Cl_6 + M, \tag{5}$$

$$Cl_3C- + Cl_3CBr \rightarrow C_2Cl_6 + Br, \tag{6}$$

$$Br + Cl_3CBr \rightarrow BrCl + -CCl_2Br, \tag{7a}$$

$$Cl_2BrC- + Br_2 \rightarrow CCl_2Br_2 + Br. \tag{7b}$$

The observation that there were no significant side reactions implies that reactions (4)–(7) are not of importance for the present research.

The heat of the Walden inversion reaction (2a) is zero, so that it is not impossible for it to have an activation energy of 10 kcals. However, there seem to be no certain examples of the Walden inversion type of reaction in the free radical reactions of organic compounds. There is no evident way of proving or disproving this mechanism except by the examination of all the other possible mechanisms.

The value of the C—H bond strength of methane of 102 kcal. determined by Kistiakowsky and Van Artsdalen (see reference 14, p. 478) implies that for the $-CH_3$ radical, $\Delta H(f)_{291°K} = 32$ kcal.[15] For the reaction of methyl bromide analogous to (2b):

$Br + BrCH_3 = Br_2 + -CH_3$, $\Delta H_{291°} = 21$ kcal.[15] *If the reaction scheme (2b) is responsible for the exchange, the C—Br bond in trichlorobromomethane must be at least 11 kcal. weaker than the C—Br bond of methyl bromide. Nevertheless, the experiment described below strongly supports the hypothesis that the exchange proceeds via this mechanism.*

Braunworth and Schumacher[16] have studied the photo-chemical bromination of chloroform. The following reactions were of importance in

---

[11] F. R. Bichowsky and F. D. Rossini, *The Thermochemistry of the Chemical Substances* (Reinhold Publishing Corporation, New York, 1936).

[12] G. N. Lewis and M. Randall, *Thermodynamics* (McGraw-Hill Book Company, Inc., New York, 1923), p. 80.

[13] K. K. Kelley, *The Entropies of Inorganic Substances* (1940), Bulletin 434 of the United States Department of the Interior, Bureau of Mines.

[14] G. B. Kistiakowsky and E. R. Van Artsdalen, J. Chem. Phys. **12**, 475 (1944), Table V. (The values of $A$ in Table V should be multiplied by $(575)^{\frac{1}{2}}/1000$ to make them comparable to the frequency factor quoted here.)

[15] Using the values for the heats of formation of $CH_4$, H, Br, $Br_2$, and $CH_3Br$ given in reference 11.

[16] V. V. Braunworth and H. J. Schumacher, Kolloid Zeits, **89**, 184(1939).

their discussion of the results:

| | $E_a$(k cal.) | $\Delta H$(k cal.) | |
|---|---|---|---|
| $Cl_3CH+Br\rightarrow Cl_3C-+HBr,$ | 10 | 4 | (8a) |
| $Cl_3C-+HBr\rightarrow Cl_3CH+Br,$ | 6 | | (8b) |
| $Br+BrCCl_3\rightarrow Br_2+-CCl_3,$ | 6 | | (2b1) |
| $Cl_3C-+Br_2\rightarrow Cl_3CBr+Br.$ | 6 | 0 | (2b2) |

Reactions (8a) and (2b2) are the direct sequence for the bromination. Reaction (8b) accounts for the inhibition of the reaction by hydrogen bromide, and reaction (2b1) for the inhibition of the reaction by trichlorobromomethane. The temperature coefficient of the rate of reaction gives the activation energy for reaction (8a). The values for (2b) were obtained from a study of the bromine sensitized photochemical oxidation of trichlorobromomethane.[17] The inhibiting effect of hydrogen bromide corresponded to a rate constant for reaction (8b) of *ca.* $\frac{1}{10}$ that of (2b2); this ratio was independent of temperature, so that the activation energies of the two reactions must be the same. The values of $\Delta H$ were obtained as differences of activation energies, they imply that

$$CCl_3H+Br_2\rightarrow CCl_3Br+HBr \quad \Delta H=4. \quad (9)$$

This conslusion that the bromination of chloroform is endothermic is somewhat surprising. Since the entropy of the reaction is probably quite small, it implies that the equilibrium in the reaction should lie largely to the left. Actually the reaction has been used for the synthesis of trichlorobromomethane in a sealed tube.[18]

The conclusions of Schumacher and Braunworth may not therefore be entirely correct. They contain, however, the interesting suggestion that reaction (8b) takes place at a rate comparable to that of (2b2) and that the formation of chloroform in the presence of hydrogen bromide be used to detect $-CCl_3$ radicals.

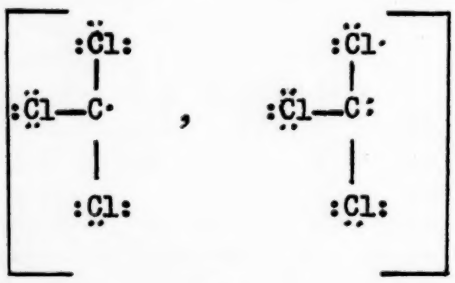

FIG. 1.

In an experiment in a two-liter flask the initial concentrations (in moles/liter) were: $[Br_2]=1.85\times10^{-3}$, $[HBr]=3.80\times10^{-2}$, $[CCl_3Br]=3.37\times10^{-2}$. The mixture was heated to 460°K for a time of about a half-time for the exchange reaction of the trichlorobromomethane with bromine. After extraction of the hydrogen bromide and bromine, the organic layer was examined in a Beckmann infra-red spectrophotometer and by vacuum distillation.

The infra-red study revealed the absorption bonds of chloroform; the optical density of the 3.3$\mu$-CH fundamental corresponded to a mole ratio of chloroform to trichlorobromomethane of 0.10. In the vacuum distillation, the only fractions isolated were chloroform and trichlorobromomethane in a mole ratio of 0.19. The chloroform was identified by its vapor tension; its vapor density corresponded to a molecular weight of 118.4 (th. 119.4).

The observation that the rate of formation of chloroform is comparable to the rate of the exchange reaction strongly suggests that the exchange proceeds via the reaction sequence (2b) involving the $-CCl_3$ radical. We are now engaged in a precise study of the kinetics of the formation of chloroform definitely to settle this point.

It is noteworthy that as part of the recent developments in free radical chain reactions in organic chemistry, $-CCl_3$ radicals, generated either from chloroform or from trichlorobromomethane, have been used as chain carriers.[19,20] The results of the present research suggest that the carbon bromine bond in trichlorobromomethane is weaker than the carbon bromine bond in methyl bromide. Braunworth and Schumacher's values for the activation energy and heat of reaction (8a) are much smaller than Kistiakowsky and Van Artsdalen's[14] values for

[17] W. Franke and H. J. Schumacher, Zeits. f. physik. Chemie **B42**, 297 (1939).
[18] E. Paterno, Jahresb. Forts. Chemie **24**, 259 (1871).
[19] M. S. Kharasch, E. V. Jensen, and W. H. Urry, J. Am. Chem. Soc. **69**, 1100 (1947).
[20] M. S. Kharasch, O. Reinmuth, and W. H. Urry, J. Am. Chem. Soc. **69**, 1105 (1947).

the corresponding reaction of methane, *viz.*,

$CH_4+Br=(-CH_3)+HBr$, $E_A=17.8$, $\Delta H=15.8$.

There is, therefore, evidence that the carbon hydrogen bond in chloroform is weaker than the carbon hydrogen bond in methane. If it is in general true that the C—X bond in $CCl_3X$ is weaker than the C—X bond in $CH_3X$, we may say that the $-CCl_3$ radical is relatively more stable than the $-CH_3$ radical. It may be that this is because of either: (a) steric repulsion of the chlorine atoms in $Cl_3CX$ compounds, which is partly relieved in the $Cl_3C-$ radical because the chlorine atoms are further apart; (b) resonance stabilization involving the structures shown in Fig. 1.

This latter type of stabilization will be more important the more readily an electron can be removed from the ligands attached to the carbon. Judging from the present research, the extent of the stabilization of the $-CCl_3$ radical is greater than 10 kcal.

**ACKNOWLEDGMENT**

We are indebted to Professor R. M. Badger and Mr. S. Burket for their cooperation in the infra-red analysis for chloroform.

THE JOURNAL OF CHEMICAL PHYSICS VOLUME 17, NUMBER 2 FEBRUARY, 1949

# The Infra-Red Absorption Spectrum of Mono-Deutero-Ethane under High Resolution

L. R. Posey, Jr.* and E. F. Barker
*Harrison M. Randall Laboratory of Physics, University of Michigan, Ann Arbor, Michigan*
(Received August 16, 1948)

The infra-red spectrum of $C_2H_5D$ has been investigated under high resolution. As expected, the bands corresponding to degenerate vibrations of $C_2H_6$ are split into two components with oscillations in the symmetry plane and normal to the symmetry plane respectively. Analogues of several of the inactive $C_2H_6$ frequencies have also been observed, including a pair at 1122 $cm^{-1}$ and 1159 $cm^{-1}$ corresponding to a Raman line of ordinary ethane which has been predicted at about 1170 $cm^{-1}$ but has not as yet been found.

ALTHOUGH the infra-red and Raman spectra of ethane have been examined on a number of occasions,[1] several uncertainties remain. $\nu_{12}$, sometimes called the "uncertain frequency" has never been observed in the Raman spectrum and its value has had to be ascertained by indirect methods. The frequency of the internal torsional motion and the height of the barrier hindering free rotation remain open to question. Furthermore, there is not sufficient experimental evidence to decide definitely whether ethane belongs to the point group $D_{3h}$ or to the point group $D_{3d}$.

The infra-red spectrum of the slightly asymmetrical mono-deutero-ethane molecule here reported, has been investigated as a means of acquiring more information regarding the existing uncertainties. The only previously published work on $C_2H_5D$ was done by E. Bartholome and H. Sachsse.[2] They used low dispersion and considered only the 12$\mu$ and 6.8$\mu$ regions. Benedict, Morikawa, Barnes, and Taylor[3] have also published some work on deutero-ethanes but made no attempt to prepare and analyze specific ones.

The replacement of one of the hydrogen atoms in the ethane molecule by a deuterium atom results in the formation of the asymmetric $C_2H_5D$ molecule. This molecule possesses only one element of symmetry which is a plane containing the deuterium atom, the two carbon atoms, and one hydrogen atom. It belongs to the point group $C_s$ and the symmetry type of a vibration is called $A'$ or $A''$ depending on whether the vibration is symmetric or antisymmetric with respect to the plane of symmetry. It can be shown that eleven of the eighteen fundamental frequencies belong to symmetry class $A'$ while the remaining seven belong to the class $A''$.

The reduction in symmetry removes the degeneracy of the perpendicular bands of $C_2H_6$ and allows the possibility of certain bands which are active only in the Raman spectrum of ethane to become observable in the infra-red spectrum of mono-deutero-ethane.

The mono-deutero-ethane was prepared by the well-known Grignard reaction:

$$C_2H_5Br+Mg\rightarrow C_2H_5MgBr, \quad (1)$$

$$C_2H_5MgBr+D_2O\rightarrow C_2H_5D+Mg\begin{matrix}OD\\Br\end{matrix}. \quad (2)$$

Precautions were taken to assure the absence of ether and water vapor in the final product. The mono-deutero-ethane was found quite free of impurity except for a trace of ethylene which had probably been left in the system when it was previously used for the preparation of that gas. Only the 950 $cm^{-1}$ band of ethylene, which is indeed a very intense one, appeared in the infra-red spectrum of the final product. It is certain that the amount of $C_2H_6$ was small though the heavy water was not of the highest purity.

* Now at Morgan State College, Baltimore, Maryland.

[1] A. Levin and C. F. Meyer, J. Opt. Soc. Am. **16**, 137 (1928); E. Bartholome and J. Karweil, Zeits. f. physik. Chemie **B39**, 1 (1938); J. Karweil and K. Schafer, ibid. **B40**, 382 (1938); B. L. Crawford, W. H. Avery, and J. W. Linnett, J. Chem. Phys. **6**, 682 (1938); P. Daure, Ann. de physique **12**, 375 (1929); C. M. Lewis and W. V. Houston, Phys. Rev. **49**, 903 (1933); G. Glocker and M. W. Renfrew, J. Chem. Phys. **6**, 295 and 409 (1935); G. Goubeau and J. Karweil, Zeits. f. physik. Chemie **B40**, 376 (1938).

[2] E. Bartholome and H. Sachsse, Zeits. f. physik. Chemie **B30**, 40 (1935).

[3] Benedict, Morikawa, Barnes, and Taylor, J. Chem. Phys. **5**, 1 (1937).

Throughout the experimental observations a grating spectrometer with a rocksalt foreprism was used. This instrument has been described by Barker and Meyer.[4] The individual points used for plotting were obtained as the result of several deflections of the galvanometer with and without the gas cell in the beam. Table I lists the experimental conditions under which various regions of absorption were studied. The observed bands are shown in Figs. 1–5. Recent observations on the perpendicular bands of $C_2H_6$ are also shown for comparison with their counterparts in $C_2H_5D$.

The slight asymmetry of the $C_2H_5D$ molecule will result in the splitting of the doubly degenerate perpendicular bands of $C_2H_6$ into two components of the types called *C* and *B* depending on whether the change of electric moment takes place along the major or intermediate axis of inertia. The general nature of the appearance of the infra-red bands of an asymmetric rotator has been discussed by Nielsen[5] for planar molecules and by Badger and Zumwalt[6] in the more general non-planar case. Generally speaking, the *C* type bands show a central maximum, as a result of a tendency of the *K* structure to converge toward the center, while the *B* type bands show a central minimum or gap caused by the tendency of the *K* structure to diverge from the center. The $C_2H_5D$ bands whose centers are at 804.62 $cm^{-1}$ and 715.18 $cm^{-1}$ are excellent examples of the *C* and *B* type bands respectively. These two bands are the components into which the 821 $cm^{-1}$ band ($\nu_9$) of ethane is split because of the asymmetry of the $C_2H_5D$ molecule. The two bands observed at 1159.00 $cm^{-1}$ and 1121.95 $cm^{-1}$ are also typical examples of such bands.

TABLE I. Experimental conditions used in observations.

| Region ($\mu$) | Center ($cm^{-1}$) | Grating (lines per inch) | Interval of readings ($cm^{-1}$) | Effective slit width ($cm^{-1}$) | Pressure (cm Hg) | Cell length (cm) |
|---|---|---|---|---|---|---|
| 13.98 | 715.18 | 2400 | 0.24 | 0.44 | 35 | 10 |
| 12.44 | 804.62 | 2400 | 0.17 | 0.34 | 18 | 10 |
| 8.8 | 1121.95<br>1159.00 | 2400 | 0.36 | 0.60 | 70 | 18 |
| 7.63 | 1309.76<br>1311.73 | 2400 | 0.5, 0.25 | 0.67 | 18 | 10 |
| 6.81 | 1468.55 | 2400 | 0.65 | 0.87 | 10 | 10 |
| 4.59 | 2180.55 | 4800 | 0.33 | 0.89 | 10 | 10 |
| 4.38 | 2281 | 4800 | 0.38 | 0.90 | 70 | 18 |
| 3.85 | 2596 | 4800 | 0.97 | 1.3 | 70 | 18 |
| 3.63 | 2753.53 | 4800 | 1.1, 0.55 | 1.5 | 70 | 10 |
| 3.37 | 2981.07 | 7200 | 0.4 | 1.1 | 1 | 10 |

It seems probable that this pair is the counterpart of the "uncertain frequency" ($\nu_{12}$) in ethane, for the observations show this to be the only remaining pair having pure *C* and *B* type structure. This frequency, which is Raman active in

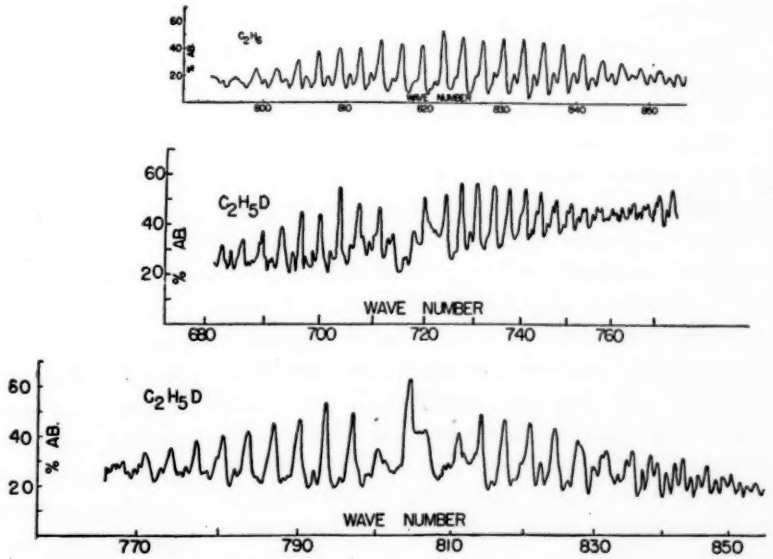


FIG. 1. The $\nu_9$ band of $C_2H_6$ and the corresponding pair of bands for $C_2H_5D$.

[4] E. F. Barker and C. F. Meyer, Trans. Faraday Soc. **25**, 912 (1929).
[5] H. H. Nielsen, Phys. Rev. **38**, 1432 (1931).
[6] R. M. Badger and L. R. Zumwalt, J. Chem. Phys. **6**, 711 (1938).

$C_2H_6$ but has never been observed, could be active in the infra-red spectrum of $C_2H_5D$, and one would expect it to appear with low intensity, which is the case. Since in general the replacement of a hydrogen atom by one of deuterium removes the degeneracy and two components appear, one in approximately the same position as for $C_2H_6$ and the other at a considerably lower frequency, the value 1170 $cm^{-1}$ calculated by Stitt[7] from his work on $C_2D_6$ is experimentally substantiated.

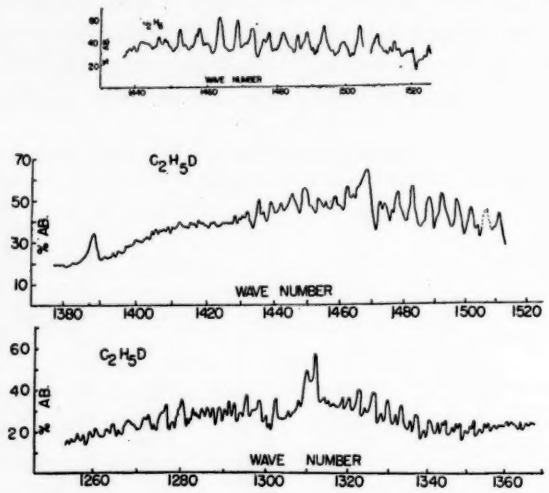


FIG. 2. The $\nu_8$ band of $C_2H_6$ and the corresponding pair of bands for $C_2H_5D$. The $Q$ branch at 1388 $cm^{-1}$ in the middle curve corresponds to the frequency $\nu_6$ in $C_2H_6$.

It may happen in certain vibrations of an asymmetric molecule that the change of electric moment does not take place purely along one of the principal axes, but has components along two or possibly three of the axes, in which case bands of a two- or threefold hybrid character will appear. A superposition of the corresponding pure band structures will result and the observed band will have neither the appearance of a pure $C$ type nor that of a pure $B$ type band. Examples of such bands observed in the infra-red spectrum of $C_2H_5D$ are the pair at 1311.73 $cm^{-1}$ and 1468.55 $cm^{-1}$ which correspond to the doubly degenerate 1480 $cm^{-1}$ band ($\nu_8$) of $C_2H_6$ and the pair at 2981.07 $cm^{-1}$ and 2180.55 $cm^{-1}$ corresponding to the doubly degenerate 2989 $cm^{-1}$ band ($\nu_7$) of $C_2H_6$. It is to be noted that each of the components exhibits a central maximum.

[7] F. Stitt, J. Chem. Phys. 7, 297 (1939).

It is probable that the 1309.76 $cm^{-1}$ band which appears in Fig. 2 as the weaker component of a doublet, is another instance in which the asymmetry of the $C_2H_5D$ molecule allows the appearance of a frequency in the infra-red spectrum the counterpart of which was forbidden in the infra-red spectrum of the symmetrical $C_2H_6$ molecule. If this band at 1309.76 $cm^{-1}$ is one of the components related to the 1463 $cm^{-1}$ Raman-active vibration ($\nu_{11}$) of $C_2H_6$ then it would appear that the 1468.55 $cm^{-1}$ band of $C_2H_5D$ should also show a doublet nature. Not only should the $E_u$** infra-red active band split into two components in going over to $C_2H_5D$ but the $E_g$ Raman-active frequency should do likewise. Again, one of the components will be expected to appear at a frequency only slightly different from the $E_g$ frequency, while the other will be shifted considerably toward lower frequencies. However, in the case of the least shifted frequency, the presence of the deuterium atom has very little effect on the motions of the hydrogen atoms, and if the corresponding frequency in $C_2H_6$ is inactive in the infra-red

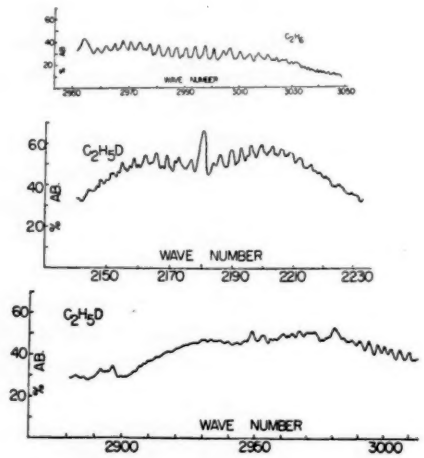


FIG. 3. The $\nu_7$ band of $C_2H_6$ and the corresponding pair of bands for $C_2H_5D$. In the upper curve one of the $Q$ branches of $\nu_5$ appears at 2954 $cm^{-1}$. The low frequency component in the middle curve is a hybrid of types $A$ and $B$. In the lower curve the $Q$ branch of the band corresponding to $\nu_7$ is found at 2981 $cm^{-1}$, with the $Q$ branches of the pairs of resonance doublets corresponding to $\nu_5$ and $\nu_1$ on the lower frequency side.

** Naming the symmetry of the vibrations in accord with a $D_{3d}$ configuration is not to be interpreted as eliminating the $D_{3h}$ possibility.

because it involves no change in electric moment, then the change in electric moment will probably be quite small in the case of $C_2H_5D$. On the other hand, in the component of lower frequency, the deuterium atom has a large effect on the motion of the hydrogen atoms, and the change in electric moment may be correspondingly larger, yielding a greater intensity of absorption. Thus, the 1400 $cm^{-1}$ component which is to be associated with the 1309.16 $cm^{-1}$ frequency is probably obscured by the much greater intensity of the 1468.55 $cm^{-1}$ band while the 1309.16 $cm^{-1}$ component is observed since its intensity is nearly comparable with that of the 1311.37 $cm^{-1}$ band.

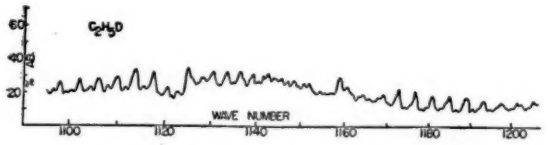


FIG. 4. The *B* type component at 1122 $cm^{-1}$, and the *C* type component at 1159 $cm^{-1}$ of the pair of bands corresponding to $\nu_{12}$ in $C_2H_6$, the uncertain Raman frequency.

The asymmetric rotator also exhibits *A* type bands which correspond to the parallel bands of a symmetric rotator. In the infra-red spectrum of ethane a Fermi-doublet with components at 2954 $cm^{-1}$ and 2894 $cm^{-1}$ is observed. The Raman spectrum exhibits a similar Fermi-doublet with components at 2899 and 2955 $cm^{-1}$. In the corresponding region of absorption in $C_2H_5D$, again a Fermi-doublet appears but each component of it appears to be double. The measurements indicate that parallel *Q* branches appear at 2892.33, 2896.87, 2948.86, and 2952.93 $cm^{-1}$. There is, then, at least an indication that the $C_2H_5D$ vibration which corresponds to the highest frequency Raman active $A_{1g}$ vibration ($\nu_1$) of ethane, appears in infra-red absorption as well as the vibration which corresponds to the $A_{2u}$ infra-red active frequency ($\nu_5$) in the same region.

The *A* type band which appears in $C_2H_5D$ at 1388.42 $cm^{-1}$ is no doubt the counterpart of the 1379 $cm^{-1}$ band ($\nu_6$) in $C_2H_6$. The fact that the frequency is higher in $C_2H_5D$ indicates that the presence of the deuterium atom has the effect of changing the motion of the hydrogen atoms in such a way that a larger restoring force acts upon them in $C_2H_5D$ than in $C_2H_6$.

The Raman active counterpart ($\nu_2$) of the 1379 $cm^{-1}$ infra-red active band has never been

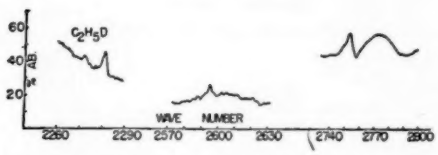


FIG. 5. Observed combination bands in $C_2H_5D$.

observed. However, its value is estimated by means of the moderately strong parallel type combination band at 2753.6 $cm^{-1}$. In the infra-red spectrum of $C_2H_5D$, an almost identical parallel combination band is found at 2753.53

TABLE II. Fundamental frequencies of $C_2H_6$ and $C_2H_5D$ as suggested on basis of present observations.

| Symmetry type in $C_2H_6$ | Assignment | $\nu(cm^{-1})$ | Symmetry type in $C_2H_5D$ | $\nu(cm^{-1})$ |
|---|---|---|---|---|
| $A_{1g}$ | $\nu_1$ | 2927* {2899, 2955} | $A'$ | 2923* {2892, 2953} |
| | $\nu_2$ | 1375** | | 1365** |
| | $\nu_3$ | 993 | | ? |
| $A_{2u}$ | $\nu_5$ | 2924* {2894, 2954} | $A'$ | 2923* {2897, 2949} |
| | $\nu_6$ | 1379 | | 1388 |
| $E_u$ | $\nu_7$ | 2989 | $A''$ | 2981 |
| | | | $A'$ | 2180 |
| | $\nu_8$ | 1480 | $A''$ | 1468 |
| | | | $A'$ | 1312 |
| | $\nu_9$ | 821 | $A''$ | 804 |
| | | | $A'$ | 715 |
| $E_g$ | $\nu_{10}$ | 2960 | $A''$ | ? |
| | | | $A'$ | ? |
| | $\nu_{11}$ | 1460 | $A''$ | 1477** |
| | | | $A'$ | 1310 |
| | $\nu_{12}$ | 1170** | $A''$ | 1159 |
| | | | $A'$ | 1122 |

* Arithmetical mean of resonance doublet shown.
** Calculated by means of observed combination bands.
*** Stitt's value of uncertain frequency.

$cm^{-1}$. No doubt, it is the combination of the 1388 $cm^{-1}$ band and the unobserved parallel fundamental of $C_2H_5D$ in the same region. It

TABLE III. Positions of principal lines of the 715.18 $cm^{-1}$ band of $C_2H_5D$.

| | |
|---|---|
| 682.84 $cm^{-1}$ | 717.80 |
| 686.39 | 719.97 |
| 689.78 | 724.20 |
| 693.22 | 727.30 |
| 696.63 | 730.65 |
| 700.03 | 734.18 |
| 703.62 | 737.35 |
| 707.27 | 740.85 |
| 711.20 | 744.12 |
| 713.77 | 747.47 |
| 715.18 (central minimum) | 750.78 |
| | 754.03 |

can be estimated, therefore, that the frequency of the latter is 1365 $cm^{-1}$.

Two other combination bands have been observed in the infra-red spectrum of $C_2H_5D$. One is the weak band, apparently perpendicular in type, at 2595.63 $cm^{-1}$. The other appears to

TABLE IV. Positions of principal lines of the 804.62 $cm^{-1}$ band of $C_2H_5D$.

| | |
|---|---|
| 771.00 $cm^{-1}$ | 826.36* |
| 772.95* | 827.66 |
| 774.20 | 829.90* |
| 776.08* | 831.32 |
| 777.27 | 831.84 |
| 780.53 | 833.60* |
| 782.04* | 834.84 |
| 783.70 | 835.72 |
| 786.87 | 837.14 |
| 790.18 | 838.42 |
| 791.97* | 839.50 |
| 793.52 | 840.76 |
| 795.33* | 842.02 |
| 796.97 | 843.28 |
| 798.95* | 844.36 |
| 800.38 | 845.56 |
| 804.62 (central maximum) | 846.84 |
| 811.12 | 848.22 |
| 814.08 | 849.32 |
| 817.43 | 850.44 |
| 820.98 | 851.72 |
| 822.50* | 852.84 |
| 824.56 | 854.34 |

* Weak lines.

be a parallel type band with its $Q$ branch at 2281.11 $cm^{-1}$.

If it is assumed that the selection rules for the combination bands of ethane still hold in the slightly modified $C_2H_5D$ molecule, the only reasonable assignment for the 2596 $cm^{-1}$ band is the sum of the 1469 $cm^{-1}$ frequency and the 1120 $cm^{-1}$ frequency. It is gratifying to observe this combination which involves one of the components of the pair of bands at 1120 and 1159 $cm^{-1}$, for its appearance supports the contention that this pair of bands is the counterpart of the "uncertain frequency" ($\nu_{12}$) of $C_2H_6$.

The only reasonable assignment for the parallel combination band at 2281 $cm^{-1}$ appears

TABLE V. Line positions in the 1310 $cm^{-1}$ bands of $C_2H_5D$.

| | |
|---|---|
| 1264.62 $cm^{-1}$ | 1305.33* |
| 1268.03 | 1307.79* |
| 1272.21 | 1309.76 (central |
| 1276.62 | 1311.73 maxima) |
| 1280.21 | 1318.69 |
| 1282.71 | 1320.18 |
| 1284.82 | 1322.70 |
| 1286.00 | 1324.18* |
| 1287.32 | 1326.21 |
| 1288.85 | 1328.25* |
| 1290.21 | 1329.79 |
| 1291.24 | 1331.81* |
| 1292.35 | 1333.33 |
| 1293.88 | 1335.39* |
| 1295.29 | 1336.94 |
| 1298.38 | 1339.00* |
| 1299.91* | 1340.54 |
| 1302.42 | 1342.61* |
| | 1344.19 |

* Weak lines.

TABLE VI. Line positions in the 1468.55 $cm^{-1}$ band of $C_2H_5D$.

| | |
|---|---|
| 1431.94 $cm^{-1}$ | 1468.55 (central maximum) |
| 1435.53 | 1473.20 |
| 1439.13 | 1478.27 |
| 1442.13 | 1482.73 |
| 1445.47 | 1488.42 |
| 1449.10 | 1492.13 |
| 1453.41 | 1496.90 |
| 1458.67 | 1501.48 |
| 1462.48 | — |
| | 1510.70 |

$Q$ branch of parallel band at 1388.42 $cm^{-1}$

to be the sum of the 804 $cm^{-1}$ frequency and the unobserved frequency in the 1400 to 1500 $cm^{-1}$ region, corresponding to the $E_g$ band of ethane in this vicinity. Using the combination band to determine the frequency of the unobserved vibration, its value is approximately 1477 $cm^{-1}$.

Table II gives the suggested set of fundamental frequencies for $C_2H_6$ and $C_2H_5D$. It will be noted that the frequencies of all the $E_u$ bands are slightly different from those given by Stitt.[7]

TABLE VII. Line positions in the 2180.55 $cm^{-1}$ band of $C_2H_5D$.

| | |
|---|---|
| 2148.52 $cm^{-1}$ | 2183.90 |
| 2151.85 | 2185.85 |
| 2155.05 | 2189.68 |
| 2158.80 | 2192.85 |
| 2162.58 | 2195.85 |
| 2165.75 | 2199.53 |
| 2169.00 | 2203.25 |
| 2172.90 | 2206.16 |
| 2176.85 | 2209.21 |
| 2180.55 (central maximum) | 2212.32 |
| | 2216.05 |

TABLE VIII. Line positions in the 2981 $cm^{-1}$ band of $C_2H_5D$.

| | |
|---|---|
| 2981.07 $cm^{-1}$ (central maximum) | 2997.64 |
| 2984.29 | 3000.47 |
| 2987.29 | 3003.07 |
| 2990.53 | 3006.64 |
| 2994.20 | 3010.21 |
| Parallel band doublet | 2892.33 |
| | 2896.87 |
| Parallel band doublet | 2948.86 |
| | 2952.93 |

These differences are based on recent observations in this laboratory of the ethane spectrum under high resolution. In Tables III to IX the positions of the principal lines in the various observed bands are listed.

These frequencies have not been corrected to vacuum.

TABLE IX. Line positions in the 1121.95 and 1159.00 $cm^{-1}$ bands of $C_2H_5D$.

| 1121.95 $cm^{-1}$ band | 1159.00 $cm^{-1}$ band |
|---|---|
| 1098.27 $cm^{-1}$ | 1159.00 $cm^{-1}$ (central maximum) |
| 1102.30 | 1160.49 |
| 1106.03 | 1164.34 |
| 1110.13 | 1169.18 |
| 1113.92 | 1172.81 |
| 1117.74 | 1176.70 |
| 1120.90 | 1180.84 |
| 1121.95 (central minimum) | 1184.97 |
| 1122.82 | 1188.97 |
| 1125.13 | 1193.36 |
| 1128.32 | 1197.40 |
| 1130.63 | 1201.47 |
| 1133.71 | 1205.55 |
| 1136.58 | |
| 1139.60 | |
| 1142.87 | |

# Magnetic Susceptibility, Freezing Point Diagram, Density, and Spectral Absorption of the System Vanadium Tetrachloride-Carbon Tetrachloride

A. GREENVILLE WHITTAKER* AND DON M. YOST**
*Gates and Crellin Laboratories of Chemistry, California Institute of Technology, Pasadena, California*
(Received August 25, 1947)

ON the basis of results of freezing point lowering experiments, it was reported by Simons and Powell[1] that an equilibrium existed between $VCl_4$ and $V_2Cl_8$ in carbon tetrachloride solution. Since vanadium tetrachloride is an odd molecule, it was implied that dimerization could take place, as in nitrogen dioxide, such that the odd electrons become paired. In the present paper are reported the results of a study on the system by means of magnetic susceptibility measurements, freezing point diagram determination, and spectral absorption of the solution, as a function of concentration of vanadium tetrachloride in carbon tetrachloride.

## PREPARATION OF THE MATERIALS

The vanadium tetrachloride was prepared by passing dry chlorine over about 3.4-inch mesh lumps of ferrovanadium in a 4- by 40-cm Pyrex tube at 400° to 450°C. The chlorine was dried by bubbling it through concentrated sulfuric acid; a sintered glass served as a gas disperser. The composition of the ferrovanadium used was: vanadium, 50 to 55 percent; silicon, 4.0 percent; carbon, 1.0 percent; iron, 45 to 50 percent. The large iron content caused the reaction tube to clog readily with the ferric chloride which condensed just outside the heated zone. To minimize the effect, a three-inch bulb was sealed onto the reaction tube at this location, the furnace lining was made of copper to give a more even distribution of heat to the reaction tube to the very end of the furnace, and a reaction temperature was maintained well above the sublimation temperature of ferric chloride.

The chief impurities in the crude product were silicon chlorides, which were easily removed by distillation at atmospheric pressure. It was found that mixing the crude product with an equal volume of dry carbon tetrachloride helped to get rid of the silicon chlorides in the distillation process. The distillation column was 30 cm long, and was packed with glass spirals. When the carbon tetrachloride and silicon chlorides were distilled off and the temperature at the top of the column reached about 148°C, the system was then evacuated to about 30 mm Hg and samples of about 50 cc each were collected. Four large batches were made this way, and each time the analysis of the finished product was about the same: vanadium, 26.38 percent; chlorine, 73.13 percent--the theoretical values are 26.43 percent and 73.57 percent, respectively.

Vanadium was determined by dissolving the sample in water and fuming out the chloride ion with sulfuric acid. The resulting solution was then diluted, the vanadium was reduced with sodium bisulfite, excess $SO_2$ boiled out, and the resulting vanadyl solution was titrated with standardized permanganate solution. Chlorine was determined by carefully placing a sample in water so that the hydrogen chloride formed in the vigorous reaction between vanadium tetrachloride and water could not escape. The chloride ion in the resulting solution was then determined as silver chloride by standard gravimetric methods.

## MAGNETIC STUDIES

### Apparatus

Magnetic measurements were made by the Gouy method.[2-4] The magnet was water cooled and run by large storage batteries. Currents between 10 and 15 amperes which gave fields in the range of 7200 to 8500 gauss were employed. Magnet currents could be held constant to

* du Pont Fellow in chemistry at the California Institute of Technology.

** Some of the material in this paper was presented by one of us (D.M.Y.) in the Julius Stieglitz Memorial lecture at the University of Chicago in April 1946.

[1] J. H. Simons and M. G. Powell, J. Am. Chem. Soc. 67, 75 (1945).

[2] Pierce W. Selwood, *Magnetochemistry* (Interscience Publishers, Inc., New York, 1943), p. 2.

[3] Wilhelm Klemm, *Magnetochemie* (Akademische Verlagsgesellschaft, Leipzig, 1936), p. 50.

[4] L. F. Bates, *Modern Magnetism* (Cambridge University Press, Nottingham, 1939), p, 97.

TABLE I. Susceptibilities and densities of solutions of vanadium tetrachloride in carbon tetrachloride (series 3 and 4 at 25.4°C).

| Conc. $VCl_4$ (mole fract.) | Suscept. solution $\chi \times 10^6$ | Suscept. mole $VCl_4$ $\chi_m \times 10^6$ | $\mu_{eff}$ of $VCl_4$* | Density of solution g/cc |
|---|---|---|---|---|
| 1.000 | 6.031** | 1163** | 1.672** | 1.8255** |
| 0.7625 | 4.689 | 1149 | 1.662 | 1.7702 |
| 0.4983 | 3.104 | 1145 | 1.659 | 1.7078 |
| 0.2542 | 1.474 | 1142 | 1.657 | 1.6490 |
| 0.1331 | 0.5933 | 1137 | 1.654 | 1.6173 |
| 1.000 | 5.923 | 1142 | 1.657 | 1.8198 |
| 0.7615 | 4.653 | 1142 | 1.657 | 1.7695 |
| 0.4639 | 2.849 | 1136 | 1.653 | 1.6984 |
| 0.3188 | 1.896 | 1130 | 1.649 | 1.6632 |
| 0.1772 | 0.9043 | 1129 | 1.648 | 1.6278 |
| 0.0876 | 0.2379 | 1120 | 1.641 | 1.6056 |
| 0.0445 | −0.0918 | 1106 | 1.631 | 1.5947 |

* $\mu_{eff}$ moment in effective Bohr magnetons.
** These may have contained some $VCl_3$.

within 0.02 ampere for sufficient time to make a single measurement. The magnet pole pieces were eight centimeters in diameter at the base and tapered sharply to 4 cm at the faces. Pole faces were 2.5 cm apart. The balance used was capable of measuring weight changes to about 0.2 milligram.

The sample tube was the usual partitioned type with upper and lower sections, except that the upper section was fitted with a specific gravity bottle top plus a cap, so that density and magnetic measurements could be made at the same time. The volume of the upper section was determined with freshly distilled water and was found to be $45.822 \pm 0.002$ cc at 25.3°C. Surrounding the sample tube region was an air thermostat equipped with heaters, fan, and a mercury thermoregulator. The temperature of the thermostat could be held constant to within ±0.1°C.

## Calibration of Apparatus

A nickel chloride solution containing about 28 percent $NiCl_2$ by weight was used to calibrate the apparatus. The solution was prepared by dissolving "reagent grade"*** $NiCl_2 \cdot 6H_2O$ in distilled water. A gravimetric determination of nickel ion was made on the solution by means of dimethylglyoxime. The gram susceptibility of nickel chloride solution[5] was taken as $\chi = [(10030X/T) - 0.720(1-X)] \times 10^{-6}$, where $T$ is the absolute temperature and $X$ the weight fraction of $NiCl_2$ in solution.

It was found more convenient to evaluate an "apparatus constant" rather than attempt to measure absolute values of magnetic fields. This was done by measuring the pull at certain magnet currents on the sample tube to be used when the top half was filled with a nickel chloride solution of known susceptibility and the bottom half contained air at a pressure of one atmosphere. The "apparatus constant" is simply the change in pull divided by the difference between the susceptibility of the solution and air. This gives an apparatus constant corresponding to particular values of magnet current only. It automatically takes into account effects of residual fields, non-uniformity of the tube diameter, absolute field strengths, and the acceleration due to gravity, and lumps them into one constant that is easy to determine. The apparatus constant had to be checked before and after each series of determinations, since the magnet iron appeared to show slight changes with usage. Nickel chloride solutions also appeared to change slightly over a period of several months so that fresh solutions were used for each calibration. It was found that the pull on the tube was not affected by changing the position of the tube with respect to the magnetic field within easily reproducible limits. The empty sample tube showed a slight change in pull with

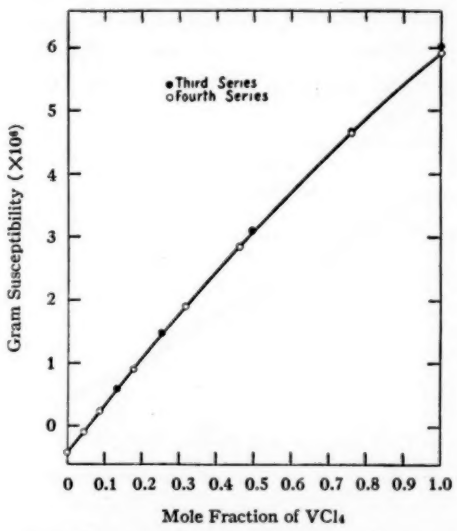


FIG. 1. Gram susceptibility for the system vanadium tetrachloride-carbon tetrachloride at 25.3°.

*** Some reagent grade $NiCl_2 \cdot 6H_2O$ was found to contain intolerable amounts of manganous salts which were not mentioned in the analysis on the label.

[5] H. R. Nettleton and S. Sugden, Proc. Roy. Soc. **A173**, 313 (1939).

field, but the correction was small (0.0003 g) and affected measurements on dilute solutions only.

### Measurements

Magnetic and density measurements on pure vanadium tetrachloride and on the more concentrated solutions (50 percent or greater) were made as soon as possible after each preparation to avoid any errors that might arise due to decomposition; the more dilute solutions were fairly stable. The carbon tetrachloride used was dried for at least one week over anhydrous magnesium perchlorate. Table I shows the results obtained. The values of $\mu_{eff}$ were calculated according to the relation $\mu_{eff}=2.83(\chi_m T)^{\frac{1}{2}}$, where $\chi_m$ is the experimental value given in column three, Table I, and T is the absolute temperature.

Four such series were run, but the first two were not acceptable as quantitatively correct. However, the first two series showed the same general behavior as the last two, and it is believed that the small variation of mole susceptibility with concentration is a real effect even though accurate values are not easy to get as the solutions become more dilute. The susceptibility of the solutions was not precisely a linear function of the concentration, as may be seen in Fig. 1. Each susceptibility value is the average of three (for series 3) or four (series 4) measurements on the same solution at different field strengths; such experiments showed the susceptibility of the solutions to be independent of the field strengths employed. The mass susceptibility and density of the carbon tetrachloride used were found to be $-0.432\times10^{-6}$ and 1.5837 g/cc at 25.3°C, respectively. The corresponding values from the *International Critical Tables*[6] are $-0.429\times10^{-6}$ and 1.58376 g/cc at 25.3°C.

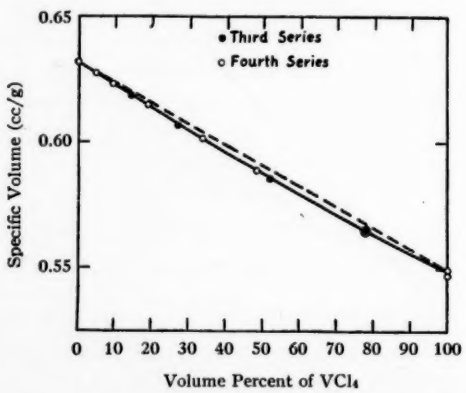


FIG. 2. Specific volume for the system vanadium tetrachloride-carbon tetrachloride at 25.3°.

TABLE II. Effect of temperature on the magnetic susceptibility of vanadium tetrachloride.

| Abs. temp. | $\chi_m(\times10^6)$ | $\chi_m T$ | $\theta$ |
|---|---|---|---|
| 274 ±1 | 1234 | 0.365 | −7 |
| 298.9±0.2 | 1152 | 0.373 | 1 |
| 328.7±0.7 | 1041 | 0.375 | 2 |

The values in Table I were calculated in the following manner:

$$\chi=(1/\rho)[(\Delta W/C)+K_a]$$

and

$$\chi_m=192.78[(1/\rho f)[(\Delta W/C)+K_a]+0.432[(1-f)/f]\times10^{-6}],$$

where $\rho$ is the density of the solution, $f$ is the weight fraction of vanadium tetrachloride in the solution, $\Delta W$ is the change in pull in grams on the sample from zero magnet current to full current, $K_a$ is the volume susceptibility of air, which was taken as $0.027\times10^{-6}$ for the general laboratory conditions of 25° and 750 mm Hg, and $C$ is the apparatus constant calculated as previously described.

The magnitude of $\Delta W$ ranged from 0.7387 gram for pure $VCl_4$ to −0.0124 gram for the most dilute solution at maximum field strength. Apparatus constants ran something as follows: at a magnet current of 10 amperes $C=5.003\times10^4$, at 15 amperes $C=6.878\times10^4$, for the fourth series.

The specific volume of the system (Fig. 2) shows that the volume of the solution is generally slightly less than the sum of the volumes of the pure components. The observed density of pure vanadium tetrachloride was 1.8198 g/cc at 25.3°C and agrees fairly well with the interpolated value of 1.8187 g/cc at 25.3°C from the data given by Roscoe.[7]

### Variation of Susceptibility with Temperature

Magnetic susceptibility measurements were made on a fresh sample of vanadium tetra-

[6] *International Critical Tables* (McGraw-Hill Book Company, Inc., New York, 1930), Vol. 6, p. 361; Vol. 3, p. 28.
[7] K. S. Gibson and M. M. Balcom, J. Opt. Soc. Am. 37, 593 (1947).

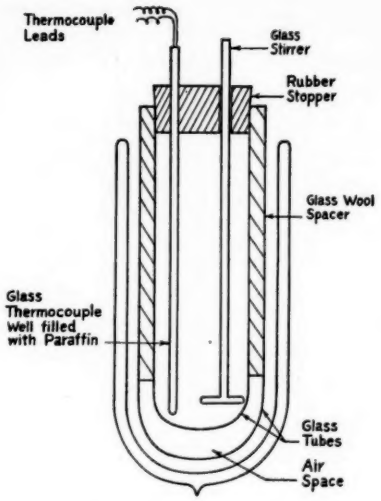


FIG. 3. Freezing point apparatus.

chloride at three different temperatures, Since the apparatus was not well adapted for this type of work, the temperature range was rather narrow. The results are given in Table II. In calculating the values of $\chi_m T$ a diamagnetic correction of $-98\times10^{-6}$ was used. The $\theta$ values were calculated from the Curie-Weiss formula $\chi_m[C/(T-\theta)]$, using 0.372 (assuming the theoretical value for one unpaired electron) as the value of the Curie constant. Experimental errors plus the uncertainty in the diamagnetic correction cause an uncertainty in $\theta$ of a magnitude about equal to the average value of $\theta$.

## FREEZING POINT DIAGRAM

The freezing point diagram of the system, vanadium tetrachloride-carbon tetrachloride, was determined by running cooling and warming curves on solutions of known composition. A diagram of the apparatus used is shown in Fig. 3. Carbon tetrachloride and mercury freezing points were used to determine an apparatus correction. The thermocouple was a calibrated copper constantan couple with the cold junction in crushed clean ice in a small amount of distilled water. A Leeds and Northrup Type K potentiometer and type HS galvanometer arrangement was used to measure to e.m.f. of the couple. The sample was stirred continuously. Each sample was analyzed before and after the cooling and warming curves were taken.

Samples containing 70 percent vanadium tetrachloride by weight or less showed changes in composition of about 0.4 percent during the course of an experiment which lasted about five hours. The 80 percent sample decreased in concentration by about 1.5 percent during a run. All samples showed marked supercooling. In all cases the breaks in the cooling curves occurred at a lower temperature than the corresponding breaks in the warming curves. Each point reported is an arithmetic average of two such temperatures. Figure 4 shows the results obtained. The accuracy claimed for each temperature is not greater than $\pm1$°C, except for the eutectic, which is good to about $\pm0.5$°C. The eutectic temperature was $-64.0$°C; the freezing point of pure vanadium tetrachloride was $-25.7$°C. This latter temperature agrees well with the value $-25.7$°C given by Simons and Powell.[1] The eutectic composition occurs at 0.37 mole fraction, and the solidus lines reach the eutectic temperature at 0.17 and 0.62 mole fraction of vanadium tetrachloride. It was quite difficult to obtain cooling or warming curve breaks corresponding to points on the liquidus curve in the concentration range about 0.23 mole fraction.

## LIGHT ABSORPTION STUDIES

Light absorption data were obtained by means of a Beckman spectrophotometer. Measurements were made over the wave-length range from 4000A to 12,000A, although it was realized that readings beyond about 10,000A are of ques-

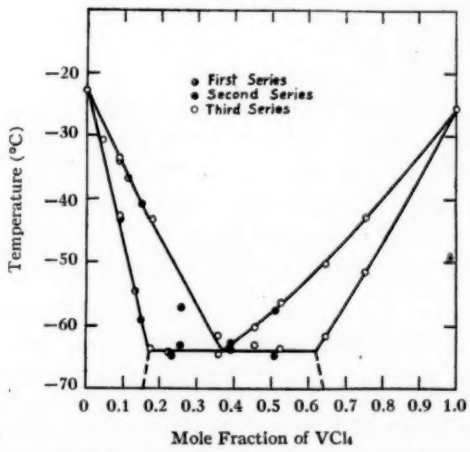


FIG. 4. Freezing point diagram for the system vanadium tetrachloride-carbon tetrachloride.

tionable value.[7] Corex cells were used, and the path length was one centimeter. The cells were sealed shut immediately after filling to avoid introduction of moisture. This was particularly important for the dilute solutions, since a small amount of moisture could change the concentration in the cell considerably from that of the part of the solution actually analyzed. Because of this effect, reliable results could not be obtained on solutions of concentrations less than about 0.01 mole per liter of solution. Some of the absorption curves are shown in Fig. 5. The behavior of these solutions with respect to Beer's law was investigated in various regions of the spectrum. Some such curves are shown in Fig. 6. The character of these curves suggested that a polymerization reaction might be involved. To investigate this, the apparent molal absorption coefficient was calculated at various wave-lengths according to the formula

$$\log_{10}(I_0/I) = (l/2.3)b_m lc,$$

where $\log_{10}(I_0/I)$ is the extinction coefficient, $b_m$ the apparent molal absorption coefficient, $l$ the path length of the light in cm, and $c$ is the concentration of solution in moles/liter of solution. Some of the results are shown in Table III.

The data in Table III seem to indicate that the absorption in the region between 9000A and 12,000A *may* be due largely to a monomer, and the strong absorption starting about 7000A and extending to shorter wave-lengths *may* be due to one or more polymers. Although the values of $b_m$ in the monomer region increase as the concentration decreases, they do not approach a limit at zero concentration in the manner one would ordinarily expect. Indeed, as far as the values are concerned it can be shown empirically that $1/b_m$ appears to be a linear function of the concentration for the more dilute solutions. It may happen, however, that limiting value of $b_m$ will be reached rather suddenly in the concentration range between $6.4\times10^{-3}$ and zero moles per liter.

## HEAT OF SOLUTION

As a side experiment in the course of this work, a single semi-quantitative experiment was performed on the heat of dilution of vanadium tetrachloride by carbon tetrachloride. About 1.4 moles of vanadium tetrachloride were diluted with about 1 mole of carbon tetrachloride; a thermometer immersed in the solution showed a temperature drop of 7°C. This corresponds to the absorption of about 420 calories per mole of vanadium tetrachloride when diluted to about 63 percent by weight.

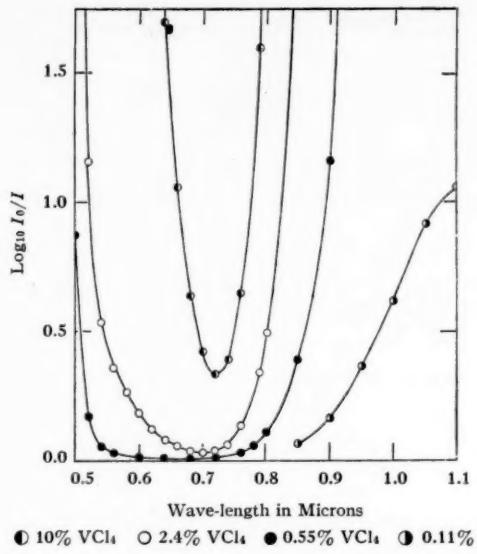


FIG. 5. Absorption spectrum of solutions of vanadium tetrachloride in carbon tetrachloride.

It is interesting to note that this system is anomalous in that the density data indicate a negative deviation from Raoult's law, but the heat of dilution result points to a positive deviation. This situation is not without precedence, however.[8]

## DISCUSSION

Vanadium tetrachloride is a molecule having one odd electron per vanadium atom; hence, on the basis of the formula derived from quantum statistics for non-interacting magnetic dipoles, the paramagnetic susceptibility per mole of this compound could be expected to be $1247\times10^{-6}$ c.g.s. unit at 25.3°C. A diamagnetic correction can be estimated by taking $\chi_m'$ for each chlorine[9] as $-22\times10^{-6}$ and for vanadium[10] $\chi_m'$ as $-10\times10^{-6}$; this gives a diamagnetic susceptibility for the whole molecule of $-98\times10^{-6}$ c.g.s. unit per mole. Hence, the predicted susceptibility of

[8] J. H. Hildebrand, *Solubility* (The Chemical Catalog Company, Inc., New York, 1924), p. 63.
[9] K. Ikenmeyer, Ann. Phys. (5) **1**, 169 (1929).
[10] W. R. Angus, Proc. Roy. Soc. **136A**, 569 (1932).

TABLE III. Apparent molal absorption coefficients of solutions of $VCl_4$ in $CCl_4$.

| Conc. in moles/l of sol. | Wave-length A 12000 | 11000 | 10000 | 9000 | 8000 | 7000 | 6000 |
|---|---|---|---|---|---|---|---|
| $6.41\times10^{-3}$ | 262.0 | 308 | 181 | 45.2 | 8.6 | | |
| $9.05\times10^{-3}$ | 232.0 | 267 | 160 | 42.7 | (10.4) | | |
| $2.63\times10^{-2}$ | 142.0 | 252 | 209* | 63.0* | (7.5) | | |
| $4.52\times10^{-2}$ | 86.4 | | 153 | 59.2 | 5.5 | 0.3 | 0.8 |
| $6.16\times10^{-2}$ | 69.0 | | 105 | 63.8 | 6.2 | 1.0* | 1.8* |
| $9.06\times10^{-2}$ | 48.8 | | | | 5.6 | 0.4 | 1.2 |
| $1.98\times10^{-1}$ | 25.1 | | | | 5.8 | 0.4 | 2.2 |
| $4.81\times10^{-1}$ | | | | | 5.6 | 6.6 | 5.2 |
| $9.19\times10^{-1}$ | | | | | 5.6 | 10.7 | 8.5 |

* Readings on the Beckman were always started in the long wave-length region, and it usually happened that solutions went bad before all readings could be taken. It required about an hour to take a complete set of readings.

vanadium tetrachloride is approximately 1149 $\times10^{-6}$ c.g.s. unit per mole, which is in good agreement with the average experimental value of $1152\times10^{-6}$ c.g.s. unit per mole. From this one may infer that the vanadium tetrachloride molecules act as essentially independent, non-interacting magnetic dipoles, or, at least if a polymer is formed, there is no coupling of the odd electrons as occurs in, say, nitrogen dioxide. Also, the change in mole susceptibility with concentration of vanadium tetrachloride in carbon tetrachloride solution (Fig. 7) shows a small decrease with a decrease in concentration, which is exactly opposite to what would be expected if the odd electron were involved in a polymerization reaction.

Actually, if no reactions or interactions between molecules take place, the mole susceptibility of vanadium tetrachloride should be independent of concentration. However, in paramagnetic solutions this case is rarely observed over a wide range of concentrations. It is interesting to note that solutions of ferric chloride[11] in water behave in very much the same way as the solutions studied here. However, in the water system the decrease in susceptibility is attributed mainly to the hydrolysis of the ferric ion. In the case at hand, reaction with carbon tetrachloride does not seem very likely.

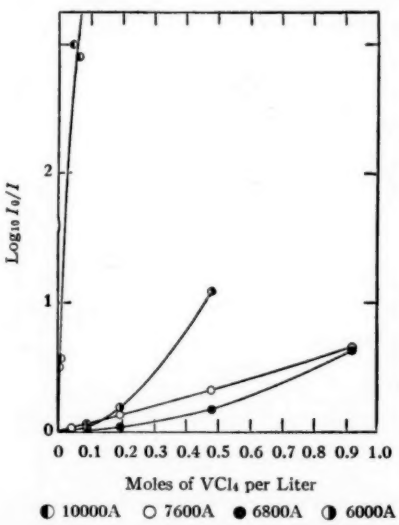


FIG. 6. Beer's law plot for Fig. 5.

The freezing point diagram in Fig. 4 shows clear evidence of the existence of limited solid solution formation in this system. In the treatment of their freezing point lowering data, Simons and Powell[1] assumed pure carbon tetrachloride to be solid phase. It is now clear that conclusions based on such a treatment are not valid. The experimental results of Simons and Powell are in agreement with the phase diagram in Fig. 4 in that their freezing points fall very close to the liquidus curve, and that the freezing point lowering is not as great when the observed solid solutions form as when pure solvent crystallizes out. Hence, the data would have the same general character if a polymerization were involved and pure solvent did crystallize out, as it has when solid solution crystallizes out.

The heat of fusion of vanadium tetrachloride can be calculated approximately from the phase diagram by the use of the equation[12]

$$\Delta H_1/RT^2 = -(dN_2/dT) - (dN'_2/dT),$$

in which $R$ is the gas constant, $T$ the melting point of solvent, $\Delta H_1$ the heat of fusion of solvent, $(dN_2/dT)$ the limiting rate of change of solute in liquid solution with temperature, and $(dN_2'/dT)$ the limiting rate of change of solute in solid solution with temperature. The heat of fusion of vanadium tetrachloride turns out to be about 550 cal./mole. The entropy of fusion is then about 2.2 entropy units per mole which is about right for a normal liquid.

The phase diagram is probably in error because the cooling and warming curves were de-

[11] E. C. Stoner, *Magnetism and Matter* (Methuen and Company, Ltd., London, 1934), p. 326.
[12] G. N. Lewis and M. Randall, *Thermodynamics* (McGraw-Hill Book Company, Inc., New York, 1923), p. 238.

termined over a rather short period, and the solid was annealed for only about 20 minutes. As a result, it can be argued that the region between the liquidus and solidus curves should be narrower than shown. The points on the liquidus curve are probably all right, but the points on the solidus curve may be too far over toward the corresponding pure components. This can come about because the solid solutions are richer in solvent than the corresponding liquid solutions; hence, if the solid solutions do not dissolve and reform as the temperature decreases, the final solution that freezes will correspond to a composition closer to the eutectic than the original composition. This means that all the points should be shifted toward the eutectic composition, which causes a narrowing of the regions between the liquidus and solidus curves. As a result, the phase diagram should give entropy of fusion values that are too large. However, the entropy of fusion of carbon tetrachloride given by Fig. 4 turns out to be 2.1 e.u., but the literature value is 2.56 e.u. Hence, it is more likely that the entropy of fusion found for vanadium tetrachloride is low rather than high, and that other effects were operative which overbalance the effect discussed above.

In order to analyze the light absorption data in a conventional way, it is necessary to find $b_m^0$ monomer. This is obtained by extrapolating the apparent $b_m$ to zero concentration taken at a wave-length at which the principal absorber is monomer. As was pointed out earlier, this is not easy to do in the case at hand. However, reasonable values of $b_m^0$ monomer can be estimated without causing serious difficulties in discussing the data. The absorption values taken at 10000A and 11000A will be taken for discussion. Reasonable extrapolated values of $b_m^0$ monomer at these wave-lengths are 182 and 312, respectively. Now, the concentration of monomer at any total concentration can be obtained from $C_1 = C_m{}^b/b_m{}^0$, where $C_1$ is the concentration of monomer, $C$ the total concentration from analysis, $b_m$ the apparent molal absorption coefficient, and $b_m^0$ the molal absorption coefficient of monomer, provided values of the $b$'s are taken in regions where only monomer absorbs light. For simplicity the polymerization reaction $nA \rightleftharpoons A_n$ was assumed. If this reaction occurs,

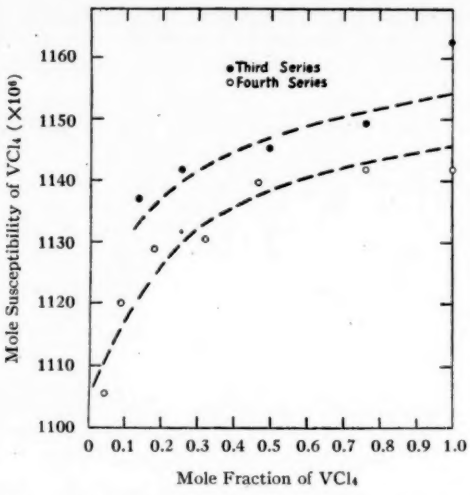


FIG. 7. Mole susceptibility of vanadium tetrachloride in carbon tetrachloride solutions at 25.3°.

then it can be shown that

$$\log(C-C_1) = n\log C_1 + \log C_n K,$$
$$C = C_1 + nC_n; \quad K = (C_n/C_1{}^n),$$

where $C_n$ is the concentration of polymer and $K$ the equilibrium constant for the assumed reaction. In Fig. 8 there is shown a plot of $\log(C-C_1)$ *versus* $\log C_1$. The points appear to follow roughly a linear relation, considering all the approxima-

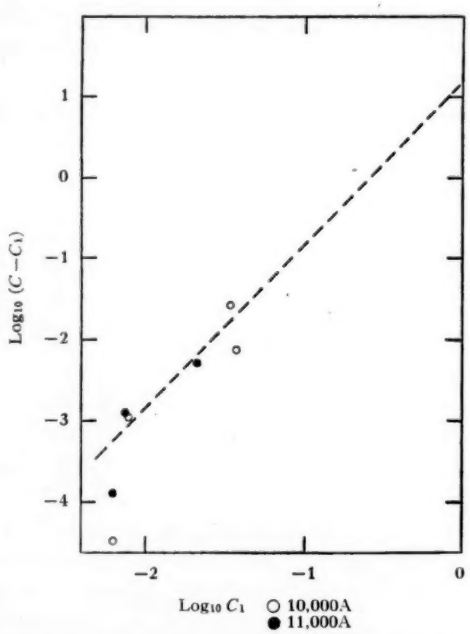


FIG. 8. Relation between the logarithm of the concentration of polymer, and the logarithm of the concentration of monomer at about 25°.

TABLE IV. Variation of the mole absorption coefficient of "dimer" with total concentration.

| Total conc. formality ($\times 10^2$) | Conc. of "monomer" ($\times 10^2$) | Conc. of "dimer" ($\times 10^2$) | Log $I_0/I$ at 6000A | $b_d^0$ |
|---|---|---|---|---|
| 4.52 | 3.07 | 0.73 | 0.0157 | 4.95 |
| 9.06 | 5.12 | 1.97 | 0.0473 | 5.52 |
| 19.8 | 8.60 | 5.60 | 0.189 | 7.76 |
| 48.1 | 14.8 | 16.7 | 1.09 | 15.0 |
| 91.9 | 21.5 | 35.2 | 3.40 | 22.2 |

tions made and the inaccuracies involved in measuring the low concentrations. The dashed straight line has a slope of two and $K=7.6$. However, this relation does not hold as the solutions become more concentrated. This is shown by the data in Table IV. The value of $b_d^0$, the absorption coefficient of "dimer," was calculated assuming the values of $n$ and $K$ given above. It is clear that $b_d^0$ is not constant, but increases with increasing concentration. Unfortunately, not enough data was obtained to identify clearly the source of the observed deviations from Beer's law.

An experimental value for the diamagnetism of vanadium tetrachloride is not available, but values calculated by the method of Angus[11] seem to be rather reliable and the value $-98 \times 10^{-6}$ is probably not in error by more than four or five percent. This makes the measured susceptibility of pure vanadium tetrachloride agree, within experimental error, with the calculated susceptibility of noninteracting magnetic dipoles. Van Vleck[13] has shown that polyatomic molecules should have a paramagnetic susceptibility somewhat greater than this by a term which he calls the high frequency constant paramagnetism, but it may be that the vanadium tetrachloride molecule is sufficiently symmetrical to make this term negligible.[14] This situation makes it difficult to explain the variation of susceptibility with concentration. It may be that the peculiar effects encountered in solids are beginning to show up. The fact that $\theta$ appears to be a function of the temperature is some indication that something out of the ordinary is involved.

Unfortunately, there are not enough experimental data to make it possible to give a definite explanation of the observed variation of susceptibility. The theoretical value of Curie's constant for $J=\frac{1}{2}$ was assumed in order to calculate $\theta$. Actually, the value of Curie's constant may differ from the theoretical value for pure vanadium tetrachloride and it may be a function of concentration. It would be interesting to measure susceptibilities of pure vanadium tetrachloride and its solutions in carbon tetrachloride over a sufficient temperature range to determine Curie's constant and $\theta$ experimentally with reasonable accuracy. In addition, it would be well to know the susceptibility of vanadium tetrachloride in the vapor phase so as to have a value essentially free from possible effects of the interactions between molecules.

Because the thermodynamic properties of vanadium tetrachloride indicate that the liquid is normal, it is not likely that definite polymers are actually formed in the liquid phase. It may be that both the departure from Beer's law and the variation of susceptibilities with concentration result from the same basic cause. However, the light absorption and the magnetic studies would have to be greatly extended in order to establish this.


## ACKNOWLEDGMENTS

We wish to thank Professors V. Schomaker, R. Badger, and J. Hildebrand, and Dr. O. Wulf for many helpful discussions and suggestions. We are also very grateful to the Research Corporation for a grant which aided, in part, the work reported here. Our good friend, Mr. Hal Weis, gave us much valuable technical assistance.


[13] J. H. Van Vleck, *Electric and Magnetic Susceptibilities* (Oxford University Press, Oxford, 1932), p. 195.
[14] Reference 13, p. 277.

# Bipyramidal Pentacovalent Bond Orbitals

GEORGE H. DUFFEY
*Chemistry Department, South Dakota State College, Brookings, South Dakota*

(Received August 23, 1948)

The Pauling-Slater theory of directed valence is applied to the trigonal bipyramid structure. Covalent molecules of the type $AB_5$ are considered. It is assumed that the bonding orbitals are of composition $sp^{1+2n}d^{3-2n}$, and the bond strengths are determined as a function of $n$.

ELECTRON diffraction measurements have indicated that some molecules have the configuration of a trigonal bipyramid. Among these are[1] $PF_5$, $PF_3Cl_2$, $PCl_5$, $Fe(CO)_5$, and $MoCl_5$. It is of interest to apply the method of directed valence bonds as developed by Pauling[1,2] and Slater[3] to this structure.

Consider *spd* hybrid orbitals for bonds directed from a central atom to the corners of a regular trigonal bipyramid. Assume that the two axial bonds are equivalent and that the three other bonds are equivalent to each other but not, in general, to the axial bonds. Also assume that the configuration is $sp^{1+2n}d^{3-2n}$ where $0 \leq n \leq 1$. When it is introduced, this assumption limits the discussion to a set of orbitals having the symmetry[4] $D_{3h}$. Differences in the radial parts of the wave functions will be neglected and the angular parts hybridized to give the desired structure.

The angular parts of the $s$, $p$, and $d$ wave functions, normalized to $4\pi$, are given by the equations

$$s = 1, \tag{1}$$

$$p_x = \sqrt{3}\sin\vartheta\cos\varphi, \tag{2}$$

$$p_y = \sqrt{3}\sin\vartheta\sin\varphi, \tag{3}$$

$$p_z = \sqrt{3}\cos\vartheta, \tag{4}$$

$$d_z = [(5)^{\frac{1}{2}}/2](3\cos^2\vartheta - 1), \tag{5}$$

$$d_{xy} = [(15)^{\frac{1}{2}}/2]\sin^2\vartheta\cos 2\varphi, \tag{6}$$

$$d_{x+y} = [(15)^{\frac{1}{2}}/2]\sin^2\vartheta\sin 2\varphi, \tag{7}$$

$$d_{x+z} = (15)^{\frac{1}{2}}\sin\vartheta\cos\vartheta\cos\varphi, \tag{8}$$

and

$$d_{y+z} = (15)^{\frac{1}{2}}\sin\vartheta\cos\vartheta\sin\varphi, \tag{9}$$

where $\vartheta$ and $\varphi$ are the angles used in polar coordinates. The axis of the bipyramid will be chosen as the $z$ axis.

Three equivalent bonds lying in the $xy$ plane and separated by angles of 120° may be represented by the functions[4]

$$\psi_1 = [(1/\sqrt{3})\sin\alpha]s + [(\sqrt{2}/\sqrt{3})\cos\beta]p_x - [(1/\sqrt{3})\cos\alpha]d_z + [(\sqrt{2}/\sqrt{3})\sin\beta]d_{xy}, \tag{10}$$

$$\psi_2 = [(1/\sqrt{3})\sin\alpha]s - \{[1/(6)^{\frac{1}{2}}]\cos\beta\}p_x + [(1/\sqrt{2})\cos\beta]p_y - [(1/\sqrt{3})\cos\alpha]d_z - \{[1/(6)^{\frac{1}{2}}]\sin\beta\}d_{xy} - [(1/\sqrt{2})\sin\beta]d_{x+y}, \tag{11}$$

$$\psi_3 = [(1/\sqrt{3})\sin\alpha]s - \{[1/(6)^{\frac{1}{2}}]\cos\beta\}p_x - [(1/\sqrt{2})\cos\beta]p_y - [(1/\sqrt{3})\cos\alpha]d_z - \{[1/(6)^{\frac{1}{2}}]\sin\beta\}d_{xy} + [(1/\sqrt{2})\sin\beta]d_{x+y}. \tag{12}$$

If it is assumed that the maxima of the $p$ and $d$ functions for the axial bonds lie on the $z$ axis, the axial bonds may be represented by the

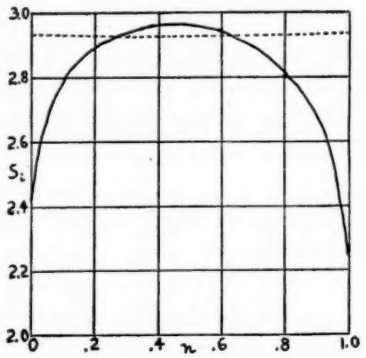


FIG. 1. Trigonal bipyramidal orbitals. The solid line represents $S_1$, the strength of an equatorial bond. The dotted line represents $S_4$, the strength of an axial bond. Each of these is plotted against $n$ where the arrangement is $sp^{1+2n}d^{3-2n}$.

[1] L. Pauling, *The Nature of the Chemical Bond* (Cornell University Press, Ithaca, 1940).
[2] L. Pauling, J. Am. Chem. Soc. **53**, 1367 (1931).
[3] J. C. Slater, Phys. Rev. **37**, 481 (1931).
[4] See G. Kimball, J. Chem. Phys. **8**, 188 (1940).

TABLE I. Results[a] of calculations on trigonal bipyramidal orbitals of type $sp^{1+2n}d^{3-2n}$.

| $n$ | $\cos\beta$ | $\cos\alpha$ | $S_1$, strength of equatorial bond | $S_4$, strength of axial bond |
|---|---|---|---|---|
| 1.0000 | 1.0000 | 0.5424 | 2.249 | 2.937 |
| 0.9000 | 0.9487 | 0.5574 | 2.681 | 2.932 |
| 0.8000 | 0.8944 | 0.5615 | 2.812 | 2.930 |
| 0.4444 | 0.6667 | 0.5659 | 2.963 | 2.928 |
| 0.2000 | 0.4472 | 0.5637 | 2.887 | 2.929 |
| 0.1000 | 0.3162 | 0.5607 | 2.787 | 2.930 |
| 0.0000 | 0.0000 | 0.5485 | 2.418 | 2.935 |

[a] These bond strengths may be compared with the following reported by Pauling (see reference 1). The best bond orbital obtainable from $s-p-d$ hybridization has a strength of 3.000. The best two equivalent orbitals, oppositely directed, obtainable on $s-p-d$ hybridization have a strength of 2.96.

functions[5]

$$\psi_4=[(1/\sqrt{2})\cos\gamma]s+(1/\sqrt{2})p_z+[(\sin\gamma\cos\delta)/\sqrt{2}]d_z+[(\sin\gamma\sin\delta)/\sqrt{2}]d_{xy}, \quad (13)$$

$$\psi_5=[(1/\sqrt{2})\cos\gamma]s-(1/\sqrt{2})p_z+[(\sin\gamma\cos\delta)/\sqrt{2}]d_z+[(\sin\gamma\sin\delta)/\sqrt{2}]d_{xy}. \quad (14)$$

The parameters in Eqs. (10), (11), (12), (13), and (14) are subject to conditions imposed by the orthogonality of the axial bond functions to the other bond functions. Thus if $\sin\delta\neq 0$, $\sin\beta=0$. Also $\sin\alpha\cos\gamma=\cos\alpha\sin\gamma\cos\delta$. The assumption that the configuration is $sp^{1+2n}d^{3-2n}$ gives the relation $\sin^2\alpha+\cos^2\gamma=1$. This gives the relations

$$\alpha=\gamma, \quad (15)$$

$$\cos\delta=1. \quad (16)$$

Four orbitals orthogonal to $\psi_1$, $\psi_2$, $\psi_3$, $\psi_4$, and $\psi_5$ with $\cos\delta=1$ can be set up as follows:

$$\psi_6=[(\sqrt{2}/\sqrt{3})\sin\beta]p_x-[(\sqrt{2}/\sqrt{3})\cos\beta]d_{xy}+(1/\sqrt{3})d_{x+z}, \quad (17)$$

[5] See R. Hultgren, Phys. Rev. **40**, 891 (1932).

$$\psi_7=-\{[1/(6)^{\frac{1}{2}}]\sin\beta\}p_x+[(1/\sqrt{2})\sin\beta]p_y+\{[1/(6)^{\frac{1}{2}}]\cos\beta\}d_{xy}+[(1/\sqrt{2})\cos\beta]d_{x+y}+(1/\sqrt{3})d_{x+z}, \quad (18)$$

$$\psi_8=-\{[1/(6)^{\frac{1}{2}}]\sin\beta\}p_x-[(1/\sqrt{2})\sin\beta]p_y+\{[1/(6)^{\frac{1}{2}}]\cos\beta\}d_{xy}-[(1/\sqrt{2})\cos\beta]d_{x+y}+(1/\sqrt{3})d_{x+z}, \quad (19)$$

$$\psi_9=d_{y+z}. \quad (20)$$

The relation between $n$ and $\beta$ is

$$\cos^2\beta=n. \quad (21)$$

Consider molecules or ions of the type $AB_5$ and assume that the energy of the $A-B$ bond is proportional to the product of the squares of the strengths of the orbitals of the two atoms.[6] The strength of an equatorial bond equals $S_1$, the value of $\psi_1$ when $\vartheta=\pi/2$, $\varphi=0$. The strength of an axial bond equals $S_4$, the value of $\psi_4$ when $\vartheta=0$. The covalent bond energy of the molecule is then proportional to $3S_1^2+2S_4^2$. The results of maximizing this function for various values of $\cos\beta$ are given in Table I and Fig. 1.

If $n$ can change without changing the electronic energy of the central atom, $n$ will equal 4/9 for the most stable structure and the strength of an axial bond will equal 2.928, the strength of an equatorial bond 2.963. In general, however, a change in $n$ will change the electronic energy of the central atom. For example, in $PCl_5$, $n$ would presumably not differ much from 1. When $n$ equals 1, the strength of an axial bond equals 2.937, and the strength of an equatorial bond equals 2.249.

[6] See H. Kuhn, J. Chem. Phys. **16**, 727 (1948). The results obtained are not very sensitive to the form of assumption made at this point. For instance, if we assumed that the energy of the $A-B$ bond is proportional to the product of the strengths of the orbitals of the two atoms, the calculated bond strengths would not differ by more than 0.5 percent from the values reported here.

# Concerning the Work of Polarization In Ionic Crystals of the NaCl Type. I. Polarization around a Single Charge in the Rigid Lattice*

E. S. RITTNER, R. A. HUTNER, AND F. K. DU PRÉ
*Philips Laboratories, Inc., Irvington-on-Hudson, New York*

(Received September 1, 1948)

Previous work is reviewed, and the Mott-Littleton method of treating the rigid lattice case is extended with some modification to higher order approximations. Numerical results are given for their hypothetical monatomic crystal and for NaCl.

QUANTITATIVE calculations of the polarization work which occurs in ionic crystals on removing one or more charges are of great importance in theories of electrolytic conductivity,[1–3] absorption spectra,[4,5] color centers,[6] and electron emission.[4,7] The cases which have been previously considered are (a) the removal of a single charge, treated by Jost,[1] Jost, and Nehlep,[1] and Mott and Littleton;[3] and (b) the removal of two adjacent charges, treated by Klemm[5] and Born.[8] It is the purpose of the present series of papers to review and to extend this work.

## FORMULATION OF THE PROBLEM FOR REMOVAL OF A SINGLE CHARGE

If a charge $-e$ disappears at a lattice point, an effective charge $+e$ will tend to polarize the surrounding medium. It is known from Maxwell's equations that when a charge is placed in a dielectric medium, the electrostatic energy,

$$U=(1/8\pi)\int\int\int(\mathbf{E}\cdot\mathbf{D})dv, \qquad (1)$$

is changed by an amount

$$W=\tfrac{1}{2}e\varphi, \qquad (2)$$

where $\varphi$ is the potential field at the charge $e$ (to be taken as origin) due to the polarized medium and $W$ is the polarization work. If the medium is considered to consist of discrete ions, each with a polarizability $\alpha$ and a distance $r$ from the origin,

$$W=\frac{1}{2}(-e)\sum_i\varphi_i=\frac{1}{2}(-e)\sum_i\frac{\mu_i}{r_i^2}=\frac{1}{2}(-e)\sum_i\alpha_i\frac{F_i}{r_i^2}. \qquad (3)$$

Here $F_i$ is the component directed along $r_i$ of the total electric field on the $i$th ion due to the polarizing charge and to the dipoles on all other ions,** and $\mu_i$ is the corresponding dipole moment. Only this radial component of $\mu_i$ contributes to $\varphi_i$ and $W$.

$$\mu_i=\alpha_iF_i=\alpha_i\left[\frac{e}{r_i^2}+\mathbf{F}_d\cdot\frac{\mathbf{r}_i}{r_i}\right];\quad \mathbf{F}_d=\sum_j{}'\nabla_i\varphi_j,$$

where $\varphi_j$ is the potential field of the $j$th ion dipole on the $i$th ion, and the prime denotes the omission of the origin and the case $i=j$.

$$\varphi_j=-\mu_j\cdot\nabla_i\frac{1}{|\mathbf{r}'|};\quad \mathbf{r}'=\mathbf{r}_i-\mathbf{r}_j.$$

Finally,

$$\mu_i=\alpha_i\left[\frac{e}{r_i^2}-\sum_j{}'\nabla_i\left(\mu_j\cdot\nabla_i\frac{1}{|\mathbf{r}'|}\right)\cdot\frac{\mathbf{r}_i}{r_i}\right]. \qquad (4)$$

This is an exact formulation of the problem. However, Eqs. (3) and (4) lead to an infinite set of equations with an infinite number of unknowns, and attempts to obtain exact solutions

* This work was carried out with the partial support of the Air Materiel Command, under Contract W33-038 ac-15141.

[1] W. Jost, J. Chem. Phys. **1**, 466 (1933); W. Jost and G. Nehlep, Zeits. f. physik. Chemie **B32**, 1 (1936).
[2] W. Schottky, Zeits. f. physik. Chemie **B29**, 335 (1935).
[3] N. F. Mott and M. J. Littleton, Trans. Faraday Soc. **34**, 485 (1938); N. F. Mott and R. W. Gurney, *Electronic Processes in Ionic Crystals* (Oxford University Press, New York, 1940), Ch. II.
[4] See reference 3, Chapters III and IV.
[5] W. Klemm, Zeits. f. Physik **82**, 529 (1933).
[6] F. Seitz, Rev. Mod. Phys. **18**, 384 (1946).
[7] D. A. Wright, Proc. Phys. Soc. **60**, 13 (1948).
[8] J. H. de Boer, *Electron Emission and Adsorption Phenomena* (Cambridge University Press, Teddington, 1935), p. 241.

** The polarization work is sometimes calculated from the expression:

$$W=1/2\Sigma\alpha_iF_i^2.$$

This expression disagrees with Eq. (3) except for the special case: $F_i=e/r_i^2$, which corresponds to neglecting the dipole-dipole interaction.



TABLE I. System of four, seven, and ten simultaneous equations.

TABLE I. System of four, seven, and ten simultaneous equations.

| | | | | | | | | | | | | | | | | | | | | |
|---|---|---|---|---|---|---|---|---|---|---|---|---|---|---|---|---|---|---|---|---|
| 1.00000= | $\left(\frac{1}{\beta_1}+2.3713\right)$ | $m_1+$ | 4.5749 | $m_2+$ | 1.2879 | $m_3-$ | 1.4966 | $m_4$ | $-$ | 0.22001 | $m_5+$ | 0.31057 | $m_6+$ | 0.085827 | $m_7$ | $+$ | 0.068323 | $m_8-$ | 0.15349 | $m_9-$ | 0.043242 | $m_{10}$ |
| 0.50000= | 2.2874 | $m_1+\left(\frac{1}{\beta_2}+2.70745\right)$ | $m_2+$ | 2.2903 | $m_3+$ | 0.80873 | $m_4$ | $+$ | 0.20265 | $m_5+$ | 0.45988 | $m_6-$ | 0.34349 | $m_7$ | $+$ | 0.017680 | $m_8+$ | 0.12157 | $m_9+$ | 0.060969 | $m_{10}$ |
| 0.33333= | 0.98593 | $m_1+$ | 3.4499 | $m_2+\left(\frac{1}{\beta_1}+0.76008\right)$ | $m_3+$ | 0.81341 | $m_4$ | $+$ | 2.6804 | $m_5-$ | 0.24095 | $m_6+$ | 0.29823 | $m_7$ | $-$ | 0.02092 | $m_8+$ | 0.47658 | $m_9+$ | 0.17898 | $m_{10}$ |
| 0.25000= | $-1.4966$ | $m_1+$ | 1.6175 | $m_2+$ | 1.0845 | $m_3+\left(\frac{1}{\beta_2}+0.29042\right)$ | $m_4$ | $+$ | 4.7253 | $m_5+$ | 1.8908 | $m_6+$ | 0.57186 | $m_7$ | $-$ | 0.98202 | $m_8-$ | 0.85640 | $m_9-$ | 0.030186 | $m_{10}$ |
| 0.20000= | $-0.057252$ | $m_1-$ | 0.10132 | $m_2+$ | 0.89647 | $m_3+$ | 1.1813 | $m_4$ | $+\left(\frac{1}{\beta_1}+2.2211\right)$ | $m_5+$ | 3.2005 | $m_6+$ | 0.44497 | $m_7$ | $+$ | 1.1560 | $m_8-$ | 0.88219 | $m_9+$ | 0.035975 | $m_{10}$ |
| 0.16667= | 0.077641 | $m_1+$ | 0.22994 | $m_2-$ | 0.080318 | $m_3+$ | 0.54486 | $m_4$ | $+$ | 3.2005 | $m_5+\left(\frac{1}{\beta_2}+1.7539\right)$ | $m_6+$ | 0.92089 | $m_7$ | $+$ | 1.3701 | $m_8+$ | 0.88966 | $m_9-$ | 0.57982 | $m_{10}$ |
| 0.12500= | $-0.042914$ | $m_1-$ | 0.34349 | $m_2+$ | 0.19215 | $m_3+$ | 0.28593 | $m_4$ | $+$ | 0.88994 | $m_5+$ | 1.8418 | $m_6+\left(\frac{1}{\beta_2}+0.33843\right)$ | $m_7$ | $+$ | 2.8977 | $m_8+$ | 1.2733 | $m_9+$ | 1.0183 | $m_{10}$ |
| 0.11111= | $-0.030800$ | $m_1+$ | 0.071296 | $m_2-$ | 0.010541 | $m_3-$ | 0.82244 | $m_4$ | $+$ | 0.90353 | $m_5+$ | 1.1299 | $m_6+$ | 0.92606 | $m_7$ | $+\left(\frac{1}{\beta_1}+1.2606\right)$ | $m_8+$ | 2.6558 | $m_9+$ | 1.9370 | $m_{10}$ |
| 0.10000= | $-0.040085$ | $m_1+$ | 0.060785 | $m_2+$ | 0.15886 | $m_3+$ | 0.13653 | $m_4$ | $-$ | 0.88219 | $m_5+$ | 0.88717 | $m_6+$ | 0.63665 | $m_7$ | $+$ | 2.0749 | $m_8+\left(\frac{1}{\beta_2}+1.2257\right)$ | $m_9+$ | 2.4500 | $m_{10}$ |
| 0.09091= | $-0.010810$ | $m_1+$ | 0.030485 | $m_2+$ | 0.059660 | $m_3-$ | 0.0075464 | $m_4$ | $+$ | 0.060325 | $m_5-$ | 0.58065 | $m_6+$ | 0.52108 | $m_7$ | $+$ | 1.5932 | $m_8+$ | 2.4500 | $m_9+\left(\frac{1}{\beta_1}+0.67456\right)$ | $m_{10}$ |

$\beta_i=\alpha_i/a^3$

have been unsuccessful. All solutions heretofore obtained represent approximations of various orders.

## APPROXIMATE SOLUTIONS FOR THE RIGID LATTICE

One of the simplest approximations that can be made is to neglect the dipole-dipole interaction, as has been done by Landshoff in a paper dealing mainly with another problem.[9] This leads to

$$W=e^2/2\sum\alpha_i/r_i^4, \tag{5}$$

where the summation is of the type evaluated by Jones and Ingham.[10] The polarization work calculated in this manner is certainly too high.

The method of Jost[1] (applied to a rigid lattice) is to consider the hole produced by the removal of an ion from the crystal as a spherical cavity of radius $R$ in a continuous medium of optical dielectric constant $\kappa_0$. The polarization work is then given by

$$W=e^2(1-1/\kappa_0)/2R. \tag{6}$$

This method includes the dipole-dipole interactions by way of the dielectric constant concept, avoids the structure sensitive lattice summations, and has the advantage of extreme simplicity. The great disadvantage, however, is the uncertainty in the value to be chosen for $R$.

Jost and Nehlep[1] have improved somewhat this earlier work by considering the first shell of six ions surrounding the origin in the manner of Eq. (5), and the rest of the crystal in the manner of Eq. (6).

The most nearly exact solution of the problem yet presented is that of Mott and Littleton,[3] which represents a series of approximations of varying order up to the fourth. In their zero-order approximation, in order to include dipole-dipole interactions, the concept of a dielectric constant is employed in calculating the dipole moment on each of the ions, but the crystal is not treated as a continuum. Instead, the total polarization is considered as constituted of an array of induced point dipoles at lattice sites.

$$P=(\mu_1+\mu_2)/2a^3, \tag{7}$$

[9] R. Landshoff, Phys. Rev. **55**, 631 (1939).
[10] J. E. Jones and A. E. Ingham, Proc. Roy. Soc. London (A) **107**, 636 (1925).

where:

$P$ = polarization,
$a$ = interionic distance,
$2a^3$ = volume/ion pair,

which leads to

$$\mu_1 = \frac{M_1 a^3 e}{r^2}, \tag{8}$$

where:

$$M_1 = \frac{2\alpha_1}{\alpha_1+\alpha_2}\frac{1}{4\pi}\left(1-\frac{1}{\kappa_0}\right)$$

with similar expressions for $\mu_2$ and $M_2$. It has been tacitly assumed in the derivation of Eq. (8) that the field $F_i$ at any point is independent of the type of ion at $i$.

The potential at the origin due to all the induced dipoles is

$$\varphi = ea^3\left[M_1\sum_1\frac{1}{r^4}+M_2\sum_2\frac{1}{r^4}\right]; \tag{9}$$

the indicated summations are again those evaluated by Jones and Ingham.[10] It will be noted that the polarization work, $\frac{1}{2}e\varphi$, is identical with Eq. (5) if $\alpha_i$ is replaced by $M_i a^3$. The zero-order approximation, Eq. (9), avoids the uncertainty in $R$ inherent in the Jost treatment, but it cannot be stated at this stage that it necessarily yields more exact answers than the latter.

In their higher order approximations, Mott and Littleton consider the first few shells surrounding the origin in a more nearly exact way while continuing to consider the rest of the medium in the manner of the zero-order approximation. In their first-order approximation, for example, the first shell of six ions is considered in detail. The dipole moment, $\mu_1$, on each of these ions is determined as the resultant of three electric fields:

(a) the field resulting from the polarizing charge,
(b) the dipole field of the other five ions in the first shell,
(c) the field resulting from the dipoles on all the ions outside the first shell, the moments of which are given by Eq. (8).

In their second-, third-, and fourth-order approximations, Mott and Littleton repeat this process for the first two, first three, and first four shells of ions, respectively. On comparing the final numerical results for the potential field, they find that, except for a slight oscillation, all the values derived from approximations of higher order than the zero are about constant. This leads them to the conclusion that the first-order approximation is a satisfactory one.

It is interesting to compare the values of the dipole moments on all of the ions in the first

TABLE II. Values of $\mu$ and $\mu r^2$ in the hypothetical monatomic crystal.*

| | Number of equations solved | | | | |
|---|---|---|---|---|---|
| | $1(M-L)$ | $4(M-L)$ | 4 | 7 | 10 |
| $\mu_1$ | 0.850 | 0.916 | 0.932 | 0.914 | 0.921 |
| $\mu_2$ | | 0.236 | 0.220 | 0.235 | 0.229 |
| $\mu_3$ | | 0.138 | 0.170 | 0.136 | 0.138 |
| $\mu_4$ | | 0.314 | 0.406 | 0.305 | 0.331 |
| $\mu_5$ | | | | 0.128 | 0.126 |
| $\mu_6$ | | | | 0.097 | 0.087 |
| $\mu_7$ | | | | 0.119 | 0.072 |
| $\mu_8$ | | | | | 0.090 |
| $\mu_9$ | | | | | 0.067 |
| $\mu_{10}$ | | | | | 0.072 |
| $\mu_1 r_1^2$ | 6.73 | 7.25 | 7.37 | 7.23 | 7.29 |
| $\mu_2 r_2^2$ | | 3.74 | 3.48 | 3.72 | 3.62 |
| $\mu_3 r_3^2$ | | 3.28 | 4.04 | 3.23 | 3.28 |
| $\mu_4 r_4^2$ | | 9.93 | 12.9 | 9.66 | 10.4 |
| $\mu_5 r_5^2$ | | | | 5.05 | 4.97 |
| $\mu_6 r_6^2$ | | | | 4.60 | 4.14 |
| $\mu_7 r_7^2$ | | | | 7.54 | 4.58 |
| $\mu_8 r_8^2$ | | | | | 6.44 |
| $\mu_9 r_9^2$ | | | | | 5.30 |
| $\mu_{10} r_{10}^2$ | | | | | 6.30 |

$\mu r^2 = Ma^3e = 5.02$

* The units of $\mu$ are such that $W$ is in electron volts in the equation $W=(e/2)(\mu/r^2)$ when $e$ has the value 3.7815 and $r$ is in A units.

It is interesting to compare the values of the dipole moments on all of the ions in the first

TABLE III. Values of $\mu$ and $\mu r^2$ for ten shells in NaCl.*

| | Removal of positive ion | | Removal of negative ion | |
|---|---|---|---|---|
| $\mu_1$ | 1.09 | | | 0.059 |
| $\mu_2$ | | 0.015 | 0.501 | |
| $\mu_3$ | 0.246 | | | 0.011 |
| $\mu_4$ | | 0.021 | 0.216 | |
| $\mu_5$ | 0.194 | | | 0.010 |
| $\mu_6$ | | 0.005 | 0.147 | |
| $\mu_7$ | | 0.003 | 0.136 | |
| $\mu_8$ | 0.100 | | | 0.005 |
| $\mu_9$ | | 0.005 | 0.093 | |
| $\mu_{10}$ | 0.099 | | | 0.004 |
| $\mu_1 r_1^2$ | 8.59 | | | 0.46 |
| $\mu_2 r_2^2$ | | 0.24 | 7.93 | |
| $\mu_3 r_3^2$ | 5.83 | | | 0.25 |
| $\mu_4 r_4^2$ | | 0.67 | 6.83 | |
| $\mu_5 r_5^2$ | 7.66 | | | 0.38 |
| $\mu_6 r_6^2$ | | 0.25 | 6.97 | |
| $\mu_7 r_7^2$ | | 0.20 | 8.62 | |
| $\mu_8 r_8^2$ | 7.12 | | | 0.38 |
| $\mu_9 r_9^2$ | | 0.42 | 7.32 | |
| $\mu_{10} r_{10}^2$ | 8.61 | | | 0.37 |

$\mu_+ r^2 = M_+ a^3 e = 0.36$; $\mu_- r^2 = M_- a^3 e = 7.29$

* The units of $\mu$ are such that $W$ is in electron volts in the equation $W=(e/2)(\mu/r^2)$, when $e$ has the value 3.7815 and $r$ is in A units.

TABLE IV. Constants for use in Eq. (10).

| Order of approx. $n$ | $f_n$ | $g_n$ | $h_n$ |
|---|---|---|---|
| 0 | 0 | 10.1977 | 6.3346 |
| 1 | 6.0000 | 4.1977 | 6.3346 |
| 2 | 6.0000 | 4.1977 | 3.3346 |
| 3 | 2.6667 | 3.3088 | 3.3346 |
| 4 | 1.5000 | 3.3088 | 2.9596 |
| 5 | 4.8000 | 2.3488 | 2.9596 |
| 6 | 4.0000 | 2.3488 | 2.2929 |
| 7 | 1.5000 | 2.3488 | 2.1054 |
| 8 | 3.3333 | 1.9784 | 2.1054 |

TABLE V. Values of $\varphi$ in the monatomic crystal for various orders of approximation.*

| $n$ | $\varphi_d$ | $\varphi_c(J)$ | $\varphi_c(M-L)$ | $\frac{\varphi_d+\varphi_c(J)}{\varphi_0}$ | $\frac{\varphi_d+\varphi_c(M-L)}{\varphi_0}$ | $\frac{\varphi}{\varphi_0}(M-L)^3$ |
|---|---|---|---|---|---|---|
| 0 | 0.0 | 2.016 | 1.326 | 25.13 | 16.53 | 16.53 |
| 1 | 0.699 | 0.835 | 0.845 | 19.12 | 19.24 | 18.57 |
| 2 | 0.872 | 0.641 | 0.604 | 18.86 | 18.40 | 18.15 |
| 3 | 0.919 | 0.540 | 0.533 | 18.18 | 18.09 | 18.03 |
| 4 | 0.981 | 0.476 | 0.503 | 18.16 | 18.50 | 18.5 |
| 5 | 1.057 | 0.430 | 0.426 | 18.54 | 18.49 | |
| 6 | 1.101 | 0.382 | 0.372 | 18.49 | 18.37 | |
| 7 | 1.115 | 0.346 | 0.357 | 18.21 | 18.35 | |
| 8 | 1.153 | 0.327 | 0.328 | 18.45 | 18.46 | |

$\varphi_0 = 0.08023$

* The units of $\varphi$ are such that $W$ is in electron volts in the equation $W = \frac{1}{2}e\varphi$, when $e = 3.7815$.

four shells calculated in this more exact way with the corresponding $\mu$'s obtained from the zero-order treatment. Actually, it is more convenient to compare the values of $\mu_i r_i^2$ as, for the zero-order case, this quantity is a constant equal to $M_i a^3 e$. The $\mu_i r_i^2$ values, which are not listed in reference (3), are contained in the second column of Table II below for a hypothetical crystal with $\alpha_1 = \alpha_2$, $\kappa_0 = 4$, and $a = 2.813$A. It will be seen that the deviations from the zero-order $\mu r^2$ value, given at the bottom of the table, are quite pronounced even beyond the first shell. These deviations arise essentially from the irregular change of the number of ions in each shell with distance from the origin, i.e., from the necessity of treating in spherical coordinates a problem where the symmetry is better described by Cartesian coordinates. The $\mu r^2$ zero-order value represents an average of these fluctuating values over a very large number of shells. Hence, the justification for considering the first-order approximation as a satisfactory solution resides solely in the numerical constancy obtained in the final potential field results.

Moreover, it will be noted that the value of $\mu_1$ obtained from the first-order approximation (Table II, column 1) is seven percent lower than the more accurate value of $\mu_1$ obtained from the fourth-order approximation. This can probably be accounted for by the fact that the nearest neighbors contribute most heavily to field ($c$) and that the exact $\mu_2$ and $\mu_3$ values are appreciably lower than the corresponding zero-order values actually used in determining this field, which is depolarizing in the present case. In view of the disparity in the values of $\mu_1$ obtained in these two ways for the monatomic crystal considered, and in view of the large contribution of $\mu_1$ to the potential field, the excellent agreement between the first-($\varphi/\varphi_0 = 18.57$) and fourth-($\varphi/\varphi_0 = 18.5$) order approximations of Mott-Littleton[3] is quite surprising.

In order to gain more insight into the problem, we have carried out higher order approximations in the spirit of the Mott-Littleton method with an important exception. The evaluation by their method of the field corresponding to field ($c$) is subject to the objection raised in the previous paragraph and also requires performing tedious lattice sums. We have avoided these difficulties by solving Eq. (4) for a convenient number of shells, neglecting the remainder of the crystal in this part of the problem. Consequently, the values of $\mu$ for the last few shells will be in error, and they have been discarded in calculating the potential field, $\sum_i \varphi_i$. To obtain the latter, these last few shells and the remainder of the crystal were treated in the manner of the Mott-Littleton zero-order approximation and also, for comparison, in the manner of the Jost approach. The disadvantage of the latter method, namely, the uncertainty in $R$, becomes less important as $R$ increases because the percentage uncertainty in $R$ decreases and the total contribution of that portion of the crystal considered in this way also decreases.

In the present work a system of ten equations for $m_i = \mu_i/ea$ was derived from Eq. (4). (See Table I for equations and the Appendix for the method of deriving the numerical coefficients.)

These ten equations were applied to the hypothetical monatomic crystal ($\alpha_1 = \alpha_2$, $\kappa_0 = 4$, $a = 2.813$A) and to NaCl ($\alpha_1/\alpha_2 = 20.3$, $\kappa_0 = 2.33$, $a = 2.813$A) for the removal of both a positive

and a negative ion. In addition, the sets of four and seven equations outlined in Table I by solid lines were also examined in the case of the monatomic crystal to gain information as to the uncertainty in the $\mu$'s on the ions in the last few shells. Solutions were kindly obtained for us by the R.C.A. Laboratories with the use of their recently developed "Electronic Simultaneous Equation Solver."[11] Final results for $\mu$ and $\mu r^2$ are shown in Tables II and III.

It will be noted that, as before, appreciable variations in the $\mu r^2$ values from the zero-order value still obtain at the larger distances. Also, comparing the third and fourth columns of Table II with the last column, it appears that the last two values of $\mu$ obtained from a set of equations are sufficiently in error to warrant their discard.

The total potential at the origin is the sum of the contributions of the shells treated "exactly," $\varphi_d$, and of the rest of the crystal, $\varphi_c$. A general expression for the potential field at the origin due to all the induced dipoles for the $n$th order approximation is

$$\sum_i \varphi_i = (f_1\mu_1 + f_2\mu_2 + \cdots + f_n\mu_n)/a^2 + \varphi_{cn}, \quad (10)$$

where, in the spirit of the method of Mott-Littleton,

$$\varphi_{cn}(M-L) = e(g_nM_1 + h_nM_2)/a.$$

$M_1$ refers to the same type of ion as that in the first shell and $M_2$ to the type of ion in the second shell. Values of the constants, $f$, $g$, and $h$, for various orders of approximation up to and including $n=8$, are given in Table IV. In the Jost approach

$$\varphi_{cn}(J) = e(1-1/\kappa_0)/R_n.$$

We have taken for $R_n$ the distance from the origin to a point halfway between the center of the last shell treated as discrete, and the center of the first shell in the continuum.

The values of $\varphi_d$ and $\varphi_c$ obtained for various orders of approximation, using only the $\mu$'s on the ions in the first eight shells obtained from the solution of all ten equations, are shown in Table V for the monatomic crystal, and in Tables VI and VII for removing a positive ion and negative ion from NaCl, respectively. Values of $\varphi/\varphi_0$ are included to permit comparison with the Mott-Littleton results. ($\varphi_0 = e(1-1/\kappa_0)/4\pi a$.) Finally, in Table VIII are shown the values of the polarization work in NaCl calculated by the various methods discussed.

It will be seen that rapid convergence of the quantity $\varphi_d+\varphi_c(M-L)$ occurs in all cases for approximations of higher order than the third. The convergence in $\varphi_d+\varphi_c(J)$ is less satisfactory, but the eighth-order approximations, where $\frac{1}{2}e\varphi_d$ is roughly 75 percent of the total polarization work, yield closely similar results by both methods.

Tables V, VI, and VII also show that the polarization work calculated by a first-order approximation, using a very nearly exact value of $\mu_1$, is in error by several percent (compare $\varphi_d+\varphi_c(M-L)/\varphi_0$ for $n=1$ and $n=8$). The original Mott-Littleton first-order approximation, which employs approximate values of $\mu_1$, yields excellent results (see Table VIII) because in the cases considered the errors in the $\mu$'s

TABLE VI. Values of $\varphi$ in NaCl for removing a positive ion.*

| $n$ | $\varphi_d$ | $\varphi_c(J)$ | $\varphi_c(M-L)$ | $\frac{\varphi_d+\varphi_c(J)}{\varphi_0}$ | $\frac{\varphi_d+\varphi_c(M-L)}{\varphi_0}$ | $\frac{\varphi}{\varphi_0}(M-L)^3$ |
|---|---|---|---|---|---|---|
| 0 | 0.0 | 1.535 | 1.223 | 25.13 | 20.03 | 20.03 |
| 1 | 0.823 | 0.636 | 0.525 | 23.88 | 22.07 | 21.88 |
| 2 | 0.834 | 0.488 | 0.508 | 21.65 | 21.97 | 21.83 |
| 3 | 0.917 | 0.411 | 0.404 | 21.75 | 21.63 | 21.62 |
| 4 | 0.921 | 0.362 | 0.402 | 21.01 | 21.66 | 21.69 |
| 5 | 1.038 | 0.328 | 0.290 | 22.37 | 21.76 | |
| 6 | 1.041 | 0.291 | 0.287 | 21.81 | 21.74 | |
| 7 | 1.042 | 0.263 | 0.285 | 21.37 | 21.73 | |
| 8 | 1.085 | 0.249 | 0.242 | 21.83 | 21.72 | |

$\varphi_0 = 0.06106$

TABLE VII. Values of $\varphi$ in NaCl for removing a negative ion.*

| $n$ | $\varphi_d$ | $\varphi_c(J)$ | $\varphi_c(M-L)$ | $\frac{\varphi_d+\varphi_c(J)}{\varphi_0}$ | $\frac{\varphi_d+\varphi_c(M-L)}{\varphi_0}$ | $\frac{\varphi}{\varphi_0}(M-L)^3$ |
|---|---|---|---|---|---|---|
| 0 | 0.0 | 1.535 | 0.796 | 25.13 | 13.03 | |
| 1 | 0.044 | 0.636 | 0.761 | 11.14 | 13.20 | 13.21 |
| 2 | 0.424 | 0.488 | 0.412 | 14.94 | 13.70 | |
| 3 | 0.428 | 0.411 | 0.407 | 13.74 | 13.67 | |
| 4 | 0.469 | 0.362 | 0.363 | 13.61 | 13.63 | |
| 5 | 0.475 | 0.328 | 0.358 | 13.14 | 13.63 | |
| 6 | 0.549 | 0.291 | 0.280 | 13.75 | 13.58 | |
| 7 | 0.575 | 0.263 | 0.259 | 13.72 | 13.64 | |
| 8 | 0.577 | 0.249 | 0.256 | 13.53 | 13.65 | |

$\varphi_0 = 0.06106$

* The units of $\varphi$ are such that $W$ is in electron volts in the equation $W = \frac{1}{2}e\varphi$, when $e = 3.7815$.

[11] E. A. Goldberg and G. W. Brown, J. App. Phys. **19**, 339 (1948).

TABLE VIII. Polarization work in NaCl calculated by various methods, ev.

| Removal of | No dip.-dip. Eq. (5) | Jost $R=a/2$ | Jost-Nehlep | $M-L$ 0 order | $M-L$ 1st order | $M-L$ 4th order | $\frac{1}{2}e[\varphi_d+\varphi_e(M-L)]$ $n=8$ | $\frac{1}{2}e[\varphi_d+\varphi_e(J)]$ $n=8$ |
|---|---|---|---|---|---|---|---|---|
| $Na^+$ | 3.73 | 2.90 | 3.20 | 2.31 | 2.53 | 2.50 | 2.51 | 2.52 |
| $Cl^-$ | 2.43 | 2.90 | 1.66 | 1.50 | 1.53 | — | 1.57 | 1.56 |
| Sum | 6.16 | 5.80 | 4.86 | 3.81 | 4.06 | — | 4.08 | 4.08 |

happen to compensate those in $W$. It is not certain that in other cases these errors will be mutually compensatory. To be completely certain of accurate results, higher order approximations should be carried out; this can be readily accomplished for other crystals of the NaCl type by the use of Table I and Eq. (10).


## ACKNOWLEDGMENTS

We wish to express our appreciation to Professor G. E. Uhlenbeck for many valuable discussions, and to Dr. O. S. Duffendack for his encouragement and interest in this work. We are greatly indebted to Dr. Zworykin for making the R.C.A. "Electronic Simultaneous Equation Solver" available, and to E. A. Goldberg and R. Serrell for the solutions of the simultaneous equations.


## APPENDIX

Equation (4) can be written in the form

$$\mu_i=\alpha_i\left[\frac{e}{r_i^2}-\sum_j{}'\mathbf{A}_{ij}\cdot\frac{\mathbf{r}_i}{r_i}\right],$$

where

$$\mathbf{A}_{ij}=\nabla_i\left(\mathbf{u}_j\cdot\nabla_i\frac{1}{|\mathbf{r}'|}\right),$$

and

$$|\mathbf{r}'|=[(x_i-x_j)^2+(y_i-y_j)^2+(z_i-z_j)^2]^{\frac{1}{2}}.$$

The summation over all the $j$ ions in the crystal can be rewritten so as to bring out explicitly the summation over each shell individually, and leads to the following equation:

$$\mu_i=\alpha_i\left[\frac{e}{r_i^2}-\sum_{k=1}^{\infty}\left(\sum_{\substack{\text{all ions in}\\ k\text{th shell}}}{}'\mathbf{A}_{ik}\cdot\frac{\mathbf{r}_i}{r_i}\right)\right],$$

where the index $k$ refers to the number of the shell, $\sum_{k=1}^{\infty}$ represents the summation over all shells, and the $\sum'$ within the parentheses is the sum over all the ions in the $k$th shell.

Using the simplifying notation,

$$r_i^2/a^2=l_i^2+m_i^2+n_i^2=p_i,$$

$$r_k^2/a^2=l_k^2+m_k^2+n_k^2=p_k,$$

$$\mathbf{r}_i\cdot\mathbf{r}_k/a^2=l_il_k+m_im_k+n_in_k=q,$$

it can be shown that

$$\sum_{k\text{th shell}}{}'\mathbf{A}_{ik}\cdot\frac{\mathbf{r}_i}{r_i}=\frac{\mu_k}{a^3}\sum_{k\text{th shell}}{}'b_{ik},$$

where

$$b_{ik}=\frac{1}{(p_ip_k)^{\frac{1}{2}}}\left[\frac{q(p_i+p_k-2q)+3(p_i-q)(p_k-q)}{(p_i+p_k-2q)^{5/2}}\right].$$

Thus,

$$\mu_i=\alpha_i\left[\frac{e}{r_i^2}-\sum_{k=1}^{\infty}\frac{\mu_k}{a^3}\sum_{k\text{th shell}}{}'b_{ik}\right]$$

$$=\frac{\alpha_i}{a^3}\left[\frac{ea}{p_i}-\sum_{k=1}^{\infty}\mu_k\sum_{k\text{th shell}}{}'b_{ik}\right].$$

In the notation of Mott-Littleton,

$$\mu_i=eam_i \quad\text{and}\quad \frac{\alpha_i}{a^3}=\beta_i.$$

Then,

$$m_i=\beta_i\left[\frac{1}{p_i}-m_1\sum_{1\text{st shell}}{}'b_{i1}-m_2\sum_{2\text{nd shell}}{}'b_{i2}-m_3\sum_{3\text{rd shell}}{}'b_{i3}-\cdots\right]$$

and

$$\frac{1}{p_1}=\left(\frac{1}{\beta_1}+\sum_{1\text{st shell}}{}'b_{11}\right)m_1+\sum_{2\text{nd shell}}b_{12}m_2+\sum_{3\text{rd shell}}b_{13}m_3+\cdots,$$

$$\frac{1}{p_2}=\sum_{1\text{st shell}}b_{21}m_1+\left(\frac{1}{\beta_2}+\sum_{2\text{nd shell}}{}'b_{22}\right)m_2+\sum_{3\text{rd shell}}b_{23}m_3+\cdots,\ \text{etc.}$$

These are the equations used to derive Table I

# Concerning the Work of Polarization in Ionic Crystals of the NaCl Type. II. Polarization around Two Adjacent Charges in the Rigid Lattice*

R. A. HUTNER, E. S. RITTNER, AND F. K. DU PRÉ
*Philips Laboratories, Inc., Irvington-on-Hudson, New York*

(Received September 1, 1948)

The method of the Mott-Littleton first-order approximation for the polarization work is extended to the case of the removal of two adjacent charges from a rigid lattice of the NaCl type. Numerical results are given for NaCl and RbCl.

IN the first paper[1] (Part I) of this series previous calculations of the polarization work resulting from the removal of a single charge from an ionic crystal were reviewed, and still higher order approximations were carried out. It is the purpose of the present paper similarly to review and to extend previous work for the case of the removal of two adjacent charges.

### A. KLEMM-BORN APPROXIMATION

The only[2] treatment of this problem that has been heretofore presented appears to be that of Klemm[3] and Born.[4] By neglecting dipole-dipole interaction, Klemm derived the following expression for the polarization work:

$$W' = Ce^2(\alpha_1+\alpha_2)/a^4. \qquad (1)$$

The constant $C$ is a lattice sum evaluated as 1.8 by Klemm using only a few terms, and improved by Born, Jansen, and Mangelsdorf,[3,4] who obtained $C=2.027$. The approximation leading to Eq. (1) is equivalent to that used in deriving Eq. (5) of Part I, and again gives rise to numerically high results.

### B. JOST[5]-LIKE APPROXIMATION

We have made several attempts to solve the problem by applying the Jost idea of scooping out an appropriate cavity in a continuous dielectric medium. However, the polarization work was found to be so highly sensitive to the shape, as well as to the size of the cavity about the two adjacent charges that this approach was discarded.

### C. MOTT-LITTLETON[6]-LIKE ZERO ORDER APPROXIMATION

On the other hand, the method of the Mott-Littleton zero-order approximation can be readily applied to the problem. As pointed out in Part I, this method uses the dielectric concept to determine the dipole moment, $\mu$, on each ion, but in the final calculation of the polarization work treats the crystal as an array of induced point dipoles at lattice sites rather than as a continuum.

In Fig. 1, the circled points *1* and *2* indicate the adjacent charges which are to be removed. The final dipole moment, $\mu_i$, induced on the $i$th ion is the resultant of $\mu_{1i}$, due to the fields of the effective negative polarizing charge at *1* and of all the other dipoles induced by *1*, and $\mu_{2i}$, due to the corresponding fields created by *2*. These components have been treated separately in finding their contributions to the total potential fields $\Phi_1$ and $\Phi_2$ back at positions *1* and *2*, respectively.

The equation for the total work of polarization is

$$W' = \tfrac{1}{2}e\Phi_1 + \tfrac{1}{2}(-e)\Phi_2, \qquad (2)$$

where

$$\Phi_1 = \sum_i{}' \{(\mu_{1i})/(r_{1i}^2) - (\mu_{2i}\cos\gamma_i)/(r_{1i}^2)\}, \qquad (3)$$

$$\Phi_2 = \sum_i{}' \{(-\mu_{2i})/(r_{2i}^2) + (\mu_{1i}\cos\gamma_i)/(r_{2i}^2)\}. \qquad (4)$$

* This work was carried out with the partial support of the Air Materiel Command, under Contract W33-038 ac-15141.

[1] E. S. Rittner, R. A. Hutner, and F. K. du Pré, J. Chem. Phys. **16**, 197 (1948).

[2] R. Landshoff (Phys. Rev. **55**, 631 (1939)) has considered the more general problem in which an electron is transferred from one ion to an adjacent neighbor, but is then strongly drawn back towards the original ion because of polarization forces. Klemm has treated the same problem, but divided it into two parts, the first of which is that discussed above.

[3] W. Klemm, Zeits. f. Physik **82**, 529 (1933).

[4] J. H. de Boer, *Electron Emission and Adsorption Phenomena* (Cambridge University Press, Teddington, 1935), p. 241.

[5] W. Jost, J. Chem. Phys. **1**, 466 (1933).

[6] N. F. Mott and M. J. Littleton, Trans. Faraday Soc. **34**, 485 (1938).

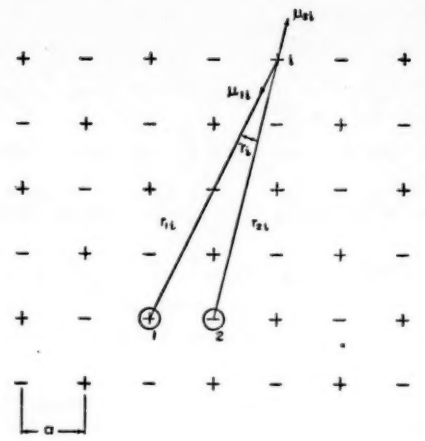

FIG. 1. Dipole moments induced on $i$th ion by the adjacent polarizing charges, *1* and *2*.

The prime indicates the omission of points *1* and *2* in the sums.

In accordance with the Mott-Littleton idea, Eq. (8) of Part I is used to determine the dipole moments, *viz.*,

$$\mu_{1i}=M_+a^3e/r_{1i}^2;\quad \mu_{2i}=M_+a^3e/r_{2i}^2 \tag{5}$$

in the directions shown in Fig. 1.

By substituting Eqs. (3)–(5) in (2), the polarization work becomes

$$W'=\tfrac{1}{2}e^2a^3\Big[\sum_{\substack{i\\ \text{odd}}}{}' M_-\{1/r_{1i}^4+1/r_{2i}^4-(2\cos\gamma_i)/(r_{1i}^2r_{2i}^2)\}+\sum_{\substack{i\\ \text{even}}}{}' M_+\{1/r_{1i}^4+1/r_{2i}^4-(2\cos\gamma_i)/(r_{1i}^2r_{2i}^2)\}\Big], \tag{6}$$

where $M_-$ refers to the negative (odd) ions, and $M_+$ to the positive (even) ions, and where it is seen from Fig. 1 that

$$\cos\gamma_i=(r_{1i}^2+r_{2i}^2-a^2)/(2r_{1i}r_{2i}). \tag{7}$$

Note that if

$$r_{1i}^2=a^2(l^2+m^2+n^2), \tag{8}$$

then

$$r_{2i}^2=a^2[(l-1)^2+m^2+n^2],$$

and when $(l^2+m^2+n^2)$ is even, $[(l-1)^2+m^2+n^2]$ is odd. Since $(1/r_{1i}^4+1/r_{2i}^4-2\cos\gamma_i/r_{1i}^2r_{2i}^2)$ is symmetric in $r_{1i}$ and $r_{2i}$, the sum over odd values is equal to the sum over even values.

Thus Eq. (6) becomes

$$W'=\frac{1}{2}\frac{e^2}{a^4}(M_-a^3+M_+a^3)\sum_{\text{even}}{}' a^4\{1/r_{1i}^4+1/r_{2i}^4-(2\cos\gamma_i)/(r_{1i}^2r_{2i}^2)\}, \tag{9}$$

where the quantity to be summed is a constant corresponding to $2C$ in Eq. (1). A comparison of Eqs. (1) and (9) shows that they become identical if $\alpha_1$ is replaced by $M_-a^3$ and $\alpha_2$ by $M_+a^3$. (See also discussion of Eq. (9), Part I.)

Let

$$l^2+m^2+n^2=p; \tag{10}$$

then

$$(l-1)^2+m^2+n^2=p-2l+1,$$

and

$$2C=\sum_{\text{even}}{}' a^4\{1/r_{1i}^4+1/r_{2i}^4-(2\cos\gamma_i)/(r_{1i}^2r_{2i}^2)\}$$

$$=\sum_{\substack{l\\ (\text{even }p)}}\sum_{m}\sum_{n}{}'\{1/p^2+1/(p-2l+1)^2-(2(p-l))/[p(p-2l+1)]^{\frac{1}{2}}\}. \tag{11}$$

The constant $C$ was first checked by direct summation, but the rate of convergence was found to be so slow** (see Table I) that it became necessary to resort to the expedient of adding and subtracting a convenient expression to Eq. (11) to make the series converge more rapidly.

$$2C=(2C-A)+A,$$

TABLE I. Values of summation constant $C$ *vs.* number of shells summed.

| No. of shells | $C(p=\text{odd})$ | $C(p=\text{even})$ |
|---|---|---|
| 1 | 1.367 | 1.464 |
| 2 | 1.613 | 1.781 |
| 3 | 1.905 | 1.909 |
| 5 | 1.952 | |
| 10 | 1.996 | |
| 15 | 2.008 | |
| 20 | 2.011 | |

** While the manuscript was in preparation, an article by S. J. Dienes appeared in J. Chem. Phys. **16**, 620 (1948), in which a calculation was made of the difference in polarization energy between two configurations, one of which is that considered here. Dienes has apparently included only two rings in the summation and has neglected most of the dipole-dipole interactions. However, since the errors so introduced are mutually compensatory and since he is dealing with differences, it is possible that his final results may not be seriously in error.

where $A$ was taken as

$$A=\sum_{(\text{even } p)}\sum\sum'\left(\frac{2}{p^3}+\frac{3}{p^4}+\frac{4}{p^5}\right). \quad (12)$$

(See Appendix I for the choice of this function and the evaluation of $A$ as 7.55272.) Thus $C$ was obtained from the expression

$$2C=\sum_{(\text{even } p)}\sum\sum'\{1/p^2-2/p^3-3/p^4-4/p^5 +1/(p-2l+1)^2 -(2(p-l))/[p(p-2l+1)]^4\} +7.55272. \quad (13)$$

The summation over 17 rings yielded the value $C=2.0285$, in good agreement with that cited in Section A.

Returning now to Eq. (9), note that

$$(M_-+M_+)=\frac{2\alpha_-}{(\alpha_-+\alpha_+)}\frac{1}{4\pi}\left(1-\frac{1}{\kappa_0}\right) +\frac{2\alpha_+}{(\alpha_-+\alpha_+)}\frac{1}{4\pi}\left(1-\frac{1}{\kappa_0}\right) =(1-1/\kappa_0)/2\pi. \quad (14)$$

Hence, the polarization work for the Mott-Littleton-like zero-order approximation can finally be expressed in the form

$$W'=0.3228e^2(1-1/\kappa_0)/a. \quad (15)$$

### D. MOTT-LITTLETON-LIKE FIRST-ORDER APPROXIMATION

This approximation improves on that of the previous section by considering in a more nearly exact way the dipole moment on each of the ten ions immediately adjacent to points *1* and *2*, while continuing to treat the rest of the crystal in the zero-order manner.

An enlarged picture of points *1* and *2*, and six of the ten surrounding nearest ions, is given in Fig. 2. Among these ten ions there are four different values of $\mu$ arising from the two types of ions and their positions relative to *1* and *2*; there is one ion corresponding to the charge and position $a+$, four ions to $b+$, four to $b-$, and one to $a-$.

The electric fields which determine each of these four dipole moments arise from the polarizing charges *1* and *2*, the dipoles on the other nine ions, and the dipoles (given by Eq. (5)) on all the remaining ions of the crystal. The detailed consideration (see Appendix II) of these fields leads to the two sets of four simultaneous linear equations with four unknowns shown in Table II. As in Part I, the Mott-Littleton notation $\mu_i=eam_i$ and $\beta_i=\alpha_i/a^3$ is used, and the simultaneous equations are given in terms of $m_i$. Solutions of these equations yield the dipole moments on the ten nearest ions.

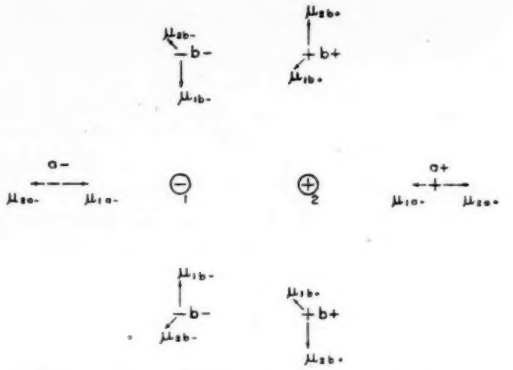


FIG. 2. Enlargement of Fig. 1, showing the dipole moments induced on the ten ions nearest to points *1* and *2*.

It can be seen from Fig. 2 that the potential fields at points *1* and *2* are related to these dipole moments by the following expressions:

$$\Phi_1=(\mu_{1a+})/((2a)^2)-(\mu_{2a+})/((2a)^2) +(4\mu_{1b+})/(2a^2)-(4\mu_{2b+}\cos 45°)/(2a^2) +(4\mu_{1b-})/(a^2)-(4\mu_{2b-}\cos 45°)/(a^2) +(\mu_{1a-})/(a^2)-(\mu_{2a-})/(a^2)+\varphi_{1\text{ lat}}, \quad (16)$$

where $\varphi_{1\text{ lat}}$ represents the contribution of the rest of the lattice beyond the set of ten nearest neighbors to the potential field at point *1*, and

$$\Phi_2=(\mu_{1a+})/(a^2)-(\mu_{2a+})/(a^2)+(4\mu_{1b+}\cos 45°)/(a^2) -(4\mu_{2b+})/(a^2)+(4\mu_{1b-}\cos 45°)/(2a^2) -(4\mu_{2b-})/(2a^2)+(\mu_{1a-})/((2a)^2) -(\mu_{2a-})/((2a)^2)+\varphi_{2\text{ lat}}, \quad (17)$$

where $\varphi_{2\text{ lat}}$ is the contribution corresponding to $\varphi_{1\text{ lat}}$ to the potential at *2*.

When Eqs. (16) and (17) are substituted in Eq. (2), the term $\frac{1}{2}e(\varphi_{1\text{ lat}}-\varphi_{2\text{ lat}})$ appears; this can be expressed as (see Appendix III)

$$0.1053e^2(1-1/\kappa_0)/a.$$

The polarization work for the Mott-Littleton-

TABLE II. Two sets of four simultaneous linear equations.

| | | | | | | | | |
|---|---|---|---|---|---|---|---|---|
| $0.25000-1.20752\,M_--0.82491\,M_+=$ | $\frac{1}{\beta_+}$ | $m_{1a+}+$ | | $m_{1b+}+$ | $0.42933$ | $m_{1b-}+0.074074$ | $m_{1a-}$ |
| $0.50000-0.73014\,M_--1.00211\,M_+=0.25000$ | $m_{1a+}+\left(\frac{1}{\beta_+}+1.07138\right)$ | | | $m_{1b+}+$ | $1.41588$ | $m_{1b-}+0.16444$ | $m_{1a-}$ |
| $1.00000-0.38810\,M_-1.23040\,M_+=0.10733$ | $m_{1a+}+$ | $1.41588$ | | $m_{1b+}+\left(\frac{1}{\beta_-}+1.31066\right)$ | | $m_{1b-}+0.53033$ | $m_{1a-}$ |
| $1.00000-0.38810\,M_--1.61778\,M_+=0.074074$ | $m_{1a+}+$ | $0.65775$ | | $m_{1b+}+$ | $2.12132$ | $m_{1b-}+\frac{1}{\beta_-}$ | $m_{1a-}$ |
| $1.00000-1.61778\,M_--0.38810\,M_+=$ | $\frac{1}{\beta_+}$ | $m_{2a+}+$ | $2.12132$ | $m_{2b+}+$ | $0.65775$ | $m_{2b-}+0.074074$ | $m_{2a-}$ |
| $1.00000-1.23040\,M_--0.38810\,M_+=0.53033$ | $m_{2a+}+\left(\frac{1}{\beta_+}+1.31066\right)$ | | | $m_{2b+}+$ | $1.41588$ | $m_{2b-}+0.10733$ | $m_{2a-}$ |
| $0.25000-1.00211\,M_--0.73014\,M_+=0.16444$ | $m_{2a+}+$ | $1.41588$ | | $m_{2b+}+\left(\frac{1}{\beta_-}+1.07138\right)$ | | $m_{2b-}+0.25000$ | $m_{2a-}$ |
| $0.25000-0.82491\,M_--1.20752\,M_+=0.074074$ | $m_{2a+}+$ | $0.42933$ | | $m_{2b+}+$ | | $m_{2b-}+\frac{1}{\beta_-}$ | $m_{2a-}$ |

like first-order approximation finally becomes

$$W'=\frac{0.1053e^2}{a}\left(1-\frac{1}{\kappa_0}\right)$$
$$+\frac{e}{a_2}[0.37500(\mu_{2a+}+\mu_{1a-}-\mu_{1a+}-\mu_{2a-})$$
$$-0.41422(\mu_{1b+}+\mu_{2b-})$$
$$+1.29290(\mu_{2b+}+\mu_{1b-})]. \quad (18)$$

We have evaluated the polarization work for NaCl and RbCl, using the following constants:

(a) NaCl: $\alpha_-/\alpha_+=20.3$, $\kappa_0=2.33$, $a=2.813$A;
(b) RbCl: $\alpha_-/\alpha_+=2.6$, $\kappa_0=2.18$, $a=3.267$A.

The solutions of the sets of four simultaneous equations were obtained for us by the use of the R.C.A. "Electronic Simultaneous Equation Solver."[7] In Table III the results for the first-order approximations are compared with those calculated by the Klemm-Born method, Eq. (1), and by the zero-order approximation, Eq. (15).

TABLE III. Polarization work in e.v. for different degrees of approximation.

| | Klemm-Born | Zero-order | First-order |
|---|---|---|---|
| NaCl | 1.51 | 0.94 | 1.11 |
| RbCl | 1.20 | 0.77 | 0.92 |

[7] E. A. Goldberg and G. W. Brown, J. App. Phys. **19**, 339 (1948).

Note that the zero-order approximation yields results about twenty percent lower than the first-order one and that Klemm-Born values deviate by a much larger percentage in the opposite sense. However, the numerical differences between the various results are small because of the low magnitude of $W'$. In view of this latter consideration and the prohibitive amount of labor required, no attempt has been made to extend the work to higher orders of approximation as was done[1,6] in the calculation of the much larger polarization work attending the removal of a single charge.

## ACKNOWLEDGMENTS

We wish to acknowledge the helpful discussions with Professor G. E. Uhlenbeck, and the continued interest of Dr. O. S. Duffendack. We are very grateful to Dr. Zworykin for permission to use the R.C.A. "Electronic Simultaneous Equation Solver," and to R. Serrell and E. A. Goldberg for providing us with the solutions.

## APPENDIX I

The expression (12) for $A$ was obtained by considering a sphere of radius $r_{1i}$ about the origin and taking the average of the quantity

$$(1/r_{1i}^4+1/r_{2i}^4-(r_{1i}^2+r_{2i}^2-a^2)/(r_{1i}^3r_{2i}^3)) \quad (1A)$$

over this sphere. The subscript $i$ is omitted below for convenience. From Fig. 3

$$r_2^2=r_1^2+a^2-2r_1a\cos\theta$$
$$=r_1^2+a^2-2r_1ay,$$

where $y=\cos\theta$.

$$\text{Area of sphere}=2\pi r_1^2\int_0^{\pi}\sin\theta d\theta=2\pi r_1^2\int_{-1}^{1}dy.$$

$$(1/r_2^4)_{ave}=\left(2\pi r_1^2\int_{-1}^{1}dy/r_2^4\right)\Big/(4\pi r_1^2)=1/(r_1^2-a^2)^2.$$

By similarly averaging each of the remaining terms in Eq. (1A), and converting from the $r$-notation into the $p$-notation, one finally obtains a series, the first three terms of which were chosen as $A$:

$$A=\sum_{(\text{even } p)}\sum\sum(2/p^3+3/p^4+4/p^5).$$

These sums can be evaluated from the Jones and Ingham[8] tables and lead to $A=7.55272$.

## APPENDIX II

The following types of equations are needed to obtain the dipole moments on the ten ions surrounding the pair of vacancies:

$$\mu_{1a+}=\alpha_{a+}(E_{1a+}+4E_{1,a+,b+}+4E_{1,a+,b-}+E_{1,a+,a-}+\Sigma_j L_{1,a+,j}), \quad (2A)$$

with three similar equations for $\mu_{1b+}$, $\mu_{1b-}$, and $\mu_{1a-}$. This forms one set of four equations with four unknowns, where $E_{1a+}$ is the electric field due to the polarizing charge *1*; $E_{1,a+,b+}$ is the electric field due to the dipole moment, $\mu_{1b+}$, on an ion of the kind $b+$; $E_{1,a+,b-}$ is the electric field due to the dipole moment, $\mu_{1b-}$, on an ion of the kind $b-$; $E_{1,a+,a-}$ is the electric field due to the dipole moment, $\mu_{1a-}$, on an ion of the kind $a-$; and $\Sigma_j L_{1,a+,j}$ is the electric field due to the lattice beyond the ten ions, but depending only on the components of the dipole moments induced by charge *1*. All the above electric fields are the components directed toward point *1*.

It can be seen from the derivation in the Appendix of Part I that the general expression for the component of the electric field directed toward the polarizing charge of a $j$th ion dipole on an $i$th ion is

$$E_{1ij}=-b_{ij}\mu_{1j}/a^3,$$

where

$$b_{ij}=\frac{1}{(p_ip_j)^{\frac{1}{2}}}\left[\frac{q(p_i+p_j-2q)+3(p_i-q)(p_j-q)}{(p_i+p_j-2q)^{5/2}}\right],$$

$$p_i=l_i^2+m_i^2+n_i^2, \quad p_j=l_j^2+m_j^2+n_j^2, \quad q=l_il_j+m_im_j+n_in_j,$$

which leads to, for example,

$$E_{1,a+,b+}=-b_{a+,b+}\mu_{1b+}/a^3.$$

To determine the terms of the type $\Sigma_j L_{1ij}$, note that Mott and Littleton have performed these lattice sums for the "whole" (probably 23 shells) lattice, excluding the first four shells. The equations of type (2A) require the sums for the whole lattice, excluding the ten ions under discussion and the points *1* and *2*. Hence, it was necessary to add to the Mott-Littleton sums the contributions of the following $j$ ions:

| | | | | | | |
|---|---|---|---|---|---|---|
| $\bar{1}10$ | $\bar{1}0\bar{1}$ | $01\bar{1}$ | $1\bar{1}1$ | $\bar{1}11$ | $\bar{1}\bar{1}\bar{1}$ | $\bar{2}00$ |
| $\bar{1}01$ | $011$ | $0\bar{1}\bar{1}$ | $11\bar{1}$ | $\bar{1}\bar{1}1$ | $020$ | $0\bar{2}0$ |
| $\bar{1}\bar{1}0$ | $0\bar{1}1$ | $111$ | $1\bar{1}\bar{1}$ | $\bar{1}1\bar{1}$ | $002$ | $00\bar{2}$ |

These contributions are determined from the general expression for an $L_{1ij}$ term:

$$L_{1ij}=-b_{ij}eM_j/p_ja^2,$$

which is derived from the above equation for $E_{1ij}$ when $\mu_{1j}$ is replaced by its zero-order expression, Eq. (5),

$$\mu_{1j}=M_ja^3e/r_{1j}^2=M_jea/p_j.$$

For example, we have

$$L_{1,a+,j}=-b_{a+,j}eM_j/p_ja^2.$$

The second set of four simultaneous equations consists of $\mu_{2a+}=\alpha_{a+}(E_{2a+}+4E_{2,a+,b+}+4E_{2,a+,b-}+E_{2,a+,a-}+\Sigma_j L_{2,a+,j})$, and the three similar expressions for $\mu_{2b+}$, $\mu_{2b-}$, and $\mu_{2a-}$. All the definitions and equations for this set are analogous to those for the first set (exemplified by Eq. (2A)).

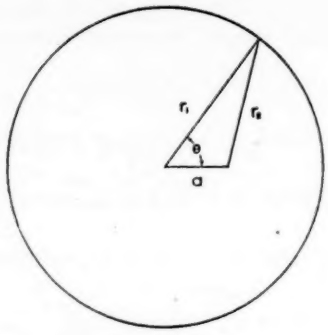


FIG. 3. Definitions of quantities for averaging over a sphere.

## APPENDIX III

It is seen that

$$\tfrac{1}{2}e(\varphi_{1\text{ lat}}-\varphi_{2\text{ lat}})=(2.0285-N_{10\text{ ions}})\frac{e^2}{a}(M_-+M_+),$$

where $N_{10\text{ ions}}$ is the contribution of the ten ions to the sum indicated in Eq. (11).

$$N_{10\text{ ions}}=1.36705 \quad \text{(using only odd or only even values of } p\text{)}.$$

$$\therefore \quad \tfrac{1}{2}e(\varphi_{1\text{ lat}}-\varphi_{2\text{ lat}})=0.6615\frac{e^2}{a}(M_-+M_+)$$

$$=0.1053\frac{e^2}{a}\left(1-\frac{1}{\kappa_0}\right).$$

[8] J. E. Jones and A. E. Ingham, Proc. Roy. Soc. (A) **107**, 636 (1925).

# Letters to the Editor

*THIS section will accept reports of new work, provided these are terse and contain few figures, and especially few halftone cuts. The Editorial Board will not hold itself responsible for opinions expressed by the correspondents. Contributions to this section should not exceed 600 words in length and must reach the office of the Managing Editor not later than the first of the month preceding that of the issue in which the letter is to appear. No proof will be sent to the authors. The usual publication charge (\$4.00 per page) will not be made and no reprints will be furnished free.*

## Note on Transient Pressure Effect in Effusion

R. B. BERNSTEIN*
*Columbia University, New York, New York*
December 20, 1948

IF two different gases at the same initial pressures are allowed to intereffuse at constant temperature through a small orifice, a transient net flux through the opening is anticipated because of the difference in the average molecular velocities of the two gases. Graham (1846) first observed such a transient flux in experiments involving transpiration through a porous plate. For the case of an orifice, the calculation of the resulting transient pressure effect is based on straightforward considerations from the expression for the number of molecules effusing through a small hole.[1]

If $N_{1a}$ = number of molecules of component 1 in vessel $A$ of volume $V_a$ and $N_{1b}$ = number of molecules of component 1 in vessel $B$ of volume $V_b$, with $N_{2a}$ and $N_{2b}$ defined similarly for gas 2, then it is possible to show that

$$[\partial^2/\partial t^2][N_{1a}] = -[S/4]\bar{v}_1[(1/V_a)+(1/V_b)][\partial/\partial t][N_{1a}]$$

and

$$[\partial^2/\partial t^2][N_{2a}] = -[S/4]\bar{v}_2[(1/V_a)+(1/V_b)][\partial/\partial t][N_{2a}],$$

where $S$ = effective cross section of orifice and $\bar{v}_1$, $\bar{v}_2$ = average velocities of components 1 and 2. It is assumed that the mean free path is considerably larger than the orifice diameter.

Solving with the appropriate boundary conditions, the composition and pressure in either vessel may be obtained as a function of time. The solution for the ratio of the pressure in vessel $A$ at time $t$ to the initial pressure is

$$P_a(t)/P(0) = \frac{N_{1a}(t)+N_{2a}(t)}{N_a(0)}$$

$$= 1+\left(\frac{1}{(1+\beta)}\right)[\exp(-k\bar{v}_1 t)-\exp(-k\bar{v}_2 t)], \quad (1)$$

where $k$ is a constant of the apparatus defined—

$$k = \frac{S}{4V_a}(1+\beta) \quad \text{and} \quad \beta = V_a/V_b.$$

Thus the ratio $P(t)/P(0)$ is seen to go through a maximum (or minimum) at a time $t_m$ which may be shown to be given by the relation

$$t_m = \frac{\ln(\bar{v}_2/\bar{v}_1)}{k(\bar{v}_2-\bar{v}_1)} = \left(\frac{\pi}{2RT}\right)^{\frac{1}{2}}\frac{1}{4k}\frac{\ln(M_1/M_2)}{\left(\frac{1}{(M_2)^{\frac{1}{2}}}-\frac{1}{(M_1)^{\frac{1}{2}}}\right)},$$

where $M_1$ and $M_2$ are the molecular weights of the gases 1 and 2.

Several experiments were performed to observe this transient pressure effect. The temperature was 25°±1°C. The region of 100–500 microns pressure was chosen so that the ratio of the mean free path to the orifice dimensions would be large. Four glass orifices in parallel were sealed into a manifold between two vessels provided with large diameter stopcocks. A McLeod gauge was connected to the smaller of the two vessels. The volumes of the bulbs were 4.80 and 1.34 liters. The orifices were designed and constructed by V. H. Dibeler for use as an inlet leak for a mass spectrometer. They were found to be approximately 0.04 mm in diameter and 0.08 mm thick. Applying Clausing's short tube area correction factor[2] to the individual orifice cross sections gave for the total effective orifice area $S = (1.8\pm0.3)\times10^{-5}$ cm².

By measuring the rate of effusion of $N_2$ and $H_2$ from either reservoir through the orifice bank into a vacuum, a more reliable value of $S$ was obtained. Curves of $\ln P$ *vs.* time gave straight lines within the experimental error of ±2 percent in the pressure. Measurements over the range 100–500 microns with both $N_2$ and $H_2$ resulted in the same value for $S$ from the slopes of the lines. The result, $S = (2.1\pm0.1)\times10^{-5}$ cm², may be compared with the above value. By comparing the slopes of curves of effusion from each of the two vessels, the volume ratio $\beta$ was obtained, with a precision of about four percent.

The apparatus constant $k$ was thus determined to be $5.0\times10^{-9}$ cm$^{-1}$. Substitution into Eq. (1) together with the appropriate velocities made it possible to compute the transient pressure effect for a given gas pair.

Figure 1 shows a graph of the pressure ratio $P(t)/P(0)$ as a function of time for $N_2$, $H_2$ and argon, $H_2$. The solid curves were calculated from Eq. (1). The various experimental points were obtained from pressure measurements in the smaller bulb, which initially contained either $H_2$, $N_2$, or argon at indicated pressures from 85–480 microns. The agreement of the experimental points with the calcu-

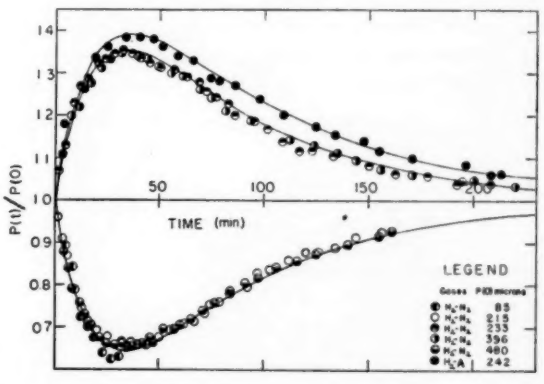


FIG. 1

lated curves is seen to be within ±2 percent. It may be noted that after 3 hours a residual effect of 5–10 percent of the pressure is still observed.

It is hoped to extend measurements of this kind to regions of higher pressure where the transition from molecular to hydrodynamic flow may be evidenced.

The author wishes to thank V. H. Dibeler for kindly supplying the orifices. Thanks are due T. I. Taylor and R. S. Halford for valuable discussions.

* Present address: Illinois Institute of Technology, Chicago 16, Illinois.

[1] L. B. Loeb, *Kinetic Theory of Gases* (McGraw-Hill Book Company, Inc., New York, 1934), p. 302.

[2] P. Clausing, Physica **9**, 65 (1929).

## An Isotope Effect in Photosynthesis*

JOHN W. WEIGL AND M. CALVIN
*Radiation Laboratory and Department of Chemistry, University of California, Berkeley, California*
December 16, 1948

IN the course of some kinetic studies on photosynthesis of barley seedlings, it has been found that plants utilize $C^{12}O_2$ faster than $C^{14}O_2$. The plants were placed in a closed system containing an infra-red absorption-cell for the analysis of total $CO_2$ and an ionization chamber for the determination of $C^{14}O_2$ in the gas phase, both instruments recording continuously.

Carbon dioxide, containing about 2 percent $C^{14}O_2$, was introduced in the dark and the specific activity at this point taken as unity. After a short dark period, the lights were turned on and photosynthesis was allowed to take place. Figure 1 shows the results of a typical experiment.

During the initial dark period the specific activity fell because of dilution by inactive respired $CO_2$. However, as photosynthesis proceeded, the specific activity of the residual $CO_2$ rose until, when only $\frac{1}{6}$ of it remained, the specific activity reached a peak some 20 percent higher than it had been at the start of photosynthesis. At this point the steady respiratory dilution became an appreciable fraction of the total remaining $CO_2$, and the specific activity dropped rapidly.

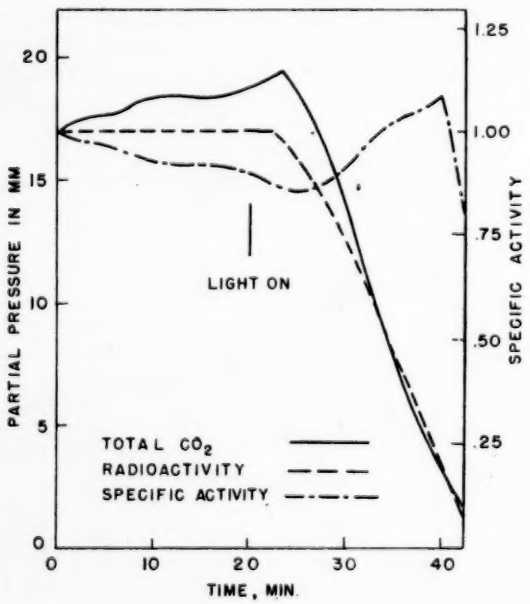


FIG. 1.

Two other possible explanations of the rise in specific activity were

(1) a difference in the response times between the instruments of the order of a minute or two and
(2) the conversion of the $CO_2$ into some other volatile compound.

Independent determinations of the response time to changes in the system revealed no appreciable time lags. The interpretation as an isotope effect was confirmed by removing samples of $CO_2$ during the course of a run and determining its specific activity by counting as $BaCO_3$, reconverting to $CO_2$, and measuring in a separate ionization chamber.

As a further check, a 200-mg "isotope farm" was grown from a 2-mg inoculum in a large quantity of dilute $C^{14}O_2$ (initial pressure, 4 mm). When 70 percent of this carbon had been converted into organic matter, the reaction was stopped, the three phases (air, solution, and algae) separated, and the carbon in each converted into $BaCO_3$ under an inert atmosphere. The carbonate was counted; the resultant specific activities were (a) air phase, 99; (b) water phase, 106; (c) algae, 81. The large difference in the specific activities between the organic and inorganic carbonate fractions further confirms the reality of the isotope effect.

A similar selectivity favoring $C^{12}O_2$ over $C^{13}O_2$ has been observed by Nier[1] and by Urey[2] in steady state systems, in which the net effect is considerably smaller than that reported here.

The authors wish to acknowledge the valuable aid of Mr. Paul M. Warrington in these experiments.

* This paper is based upon work performed under Contract No. W-7405-Eng-48 with the AEC in connection with the Radiation Laboratory, University of California, Berkeley.

[1] A. O. Nier and E. A. Gulbransen, J. Am. Chem. Soc. **61**, 697 (1939); B. F. Murphey and A. O. Nier, Phys. Rev. **59**, 771 (1941).

[2] H. C. Urey, Science **108**, 489 (1948).

## The Strength of the Hydrogen Bond in Water

ALAN W. SEARCY
*Department of Chemistry, University of California, Berkeley, California*
November 24, 1948

THE gaseous polymerization of water molecules appears to be too slight to permit an accurate determination of hydrogen bond energy from a heat of polymerization; however, the energy of formation of the hydrogen bond in ice has been determined by indirect means to be 4.5 and 4.3 kcal.[1,2] Both of these values depend on the assumption that the non-hydrogen bonding energy in water is the heat of sublimation that ice would have if it were not hydrogen bonded. This heat was estimated from the heats of sublimation of $H_2S$, $H_2Se$, and $H_2Te$.

There are two objections to such an assumption: First, the molecule in ice has only four nearest neighbors compared to twelve in $H_2S$, $H_2Se$, and $H_2Te$ crystals. Second, as the critical data for non-hydrogen bonded molecules[3] listed in Table I illustrates, a non-hydrogen bonded water

TABLE I. Critical data for some non-hydrogen bonded molecules.

| | Critical temperature degrees C | Critical density g/cm³ |
|---|---|---|
| Ne | −228.7 | 0.484 |
| $CH_4$ | − 82.5 | 0.162 |
| A | −122 | 0.531 |
| HCl | 51.4 | 0.42 |
| $PH_3$ | 51 | 0.30 |

would have a density at room temperature less than half that of actual water. The non-hydrogen bond energies in an $H_2S$-like ice might be considerably different from those in real ice, particularly if the closer approach of nearest neighbors in real ice makes the repulsive energy large.

If we assume that at absolute zero the simple equation

$$E=a/r^3+b/r^6-c/r^{12} \qquad (1)$$

applies, where $a$, $b$, and $c$ are arbitrary constants, $E$ is the energy of sublimation, and $r$ is the intermolecular distance, we can calculate the dipole energy in ice by a method which eliminates the sources of error mentioned above. In our equation $a/r^3$ is the dipole energy, $b/r^6$ is the London energy, and $c/r^{12}$ is the repulsive energy. We shall consider that the dipole energy is the sum of the energies of the two hydrogen bonds of the molecule.

The derivative of Eq. (1) with respect to $r$ must be equal to zero for a stable crystal, and $E$ can be calculated from known data to be 10.9 kcal. at absolute zero. We need only estimate the London energy to determine both the dipole and repulsive energies. We will find the London energy between a pair of nearest neighbors in a hypothetical non-polar ice and make a sixth power correction for a change of intermolecular distance to that in real ice.

TABLE II. Heats of sublimation and density at 0°K.

| | Heat of sublimation kcal./mole | Density of solid g/cm³ |
|---|---|---|
| Ne | 0.4 | 1.44 |
| $CH_4$ | (2.6) | — |
| $N_2$ | 1.5 | 1.03 |
| $O_2$ | 2.0 | 1.43 |
| A | 1.8 | 1.60 |

In Table II are listed approximate heats of sublimation[4] and density[5] data for non-polar substances near 0°K. From these data we estimate that the density of hypothetical twelve-coordinated, non-polar water would be about 1.3±0.2 g/cm³ and the energy of sublimation, 1.5±0.5 kcal. at absolute zero. Since the dipole energy would be zero, we solve the energy equation and its derivative equation directly, finding 3±1 kcal. for the London energy of a non-polar water. A consideration of the geometry of a close-packed crystal indicates that the London energy per molecule is 7.227 times that binding the molecule to one nearest neighbor.[6] By a similar calculation one finds that in a real ice crystal the London energy is approximately 2.5 times that between two nearest neighbors. A close-packed crystal of density 1.3±0.2 g/cm³ would have a nearest neighbor distance of 3.2±0.2A compared to 2.75A for real ice of density 0.948.[7] The London energy in actual ice is then $3.0(3.2/2.75)^6 \times(2.5/7.2)=2.6\pm1.5$ kcal. Introducing this value into our two equations we find the repulsive energy in real ice to be 4.5±0.5 kcal. and the total dipole energy, 12.8±1 kcal. Since there are two hydrogen bonds per molecule of ice, the dipole energy per bond is 6.4±0.5 kcal.

We conclude that repulsive forces make an important contribution to the energy of ice and that the dipole energy per hydrogen bond is about 2 kcal. per mole greater than previously estimated.

[1] L. Pauling, *Nature of the Chemical Bond* (Cornell University Press, Ithaca, 1944), p. 304.
[2] R. W. Taft, Jr. and H. H. Sisler, J. Chem. Ed. **24**, 175–181 (1947).
[3] *International Critical Tables*, Vol. III, p. 248.
[4] F. R. Bichowsky and F. D. Rossini, *Thermochemistry of Chemical Substances* (Reinhold Publishing Corporation, New York, 1936). Values corrected to absolute zero.
[5] *International Critical Tables*, Vol. I, p. 103; neon and argon values from K. Clusius, Zeits. f. physik. Chemie **B31**, 459 (1936).
[6] J. E. Jones and A. E. Ingham, Proc. Roy. Soc. **A107**, 636 (1925).
[7] N. E. Dorsey, *Properties of Ordinary Water Substance* (Reinhold Publishing Corporation, New York, 1940), p. 466.

## Structure of Ethylene Oxide

G. L. CUNNINGHAM, A. W. BOYD, AND WILLIAM D. GWINN
*Department of Chemistry, University of California, Berkeley, California*
AND
W. I. LEVAN
*Department of Electrical Engineering, University of California, Berkeley, California*
December 6, 1948

THE moments of inertia of ethylene oxide have recently been reported.[1] In order to calculate the bond distances, deuterated ethylene oxide has been prepared, and its microwave spectrum has been measured. The values of the rotational parameters for the zero rotational level are: $(a-c)/2=4427.5\pm0.5$ mc, $\kappa=-0.11615\pm0.00010$, and $(a+c)=31{,}943\pm1$ mc. The transitions observed are listed in Table I with the values of $(a-c)/2$ calculated assuming $\kappa=-0.11615$. The uncertainty of $\kappa$ has very little effect on the uncertainty of the moments of inertia because of the small value of $\kappa$. The recent values of the physical constants[2] have been employed, necessitating a small revision of the moments of inertia of $C_2H_4O$. The values for both molecules are given in Table II.

Since the moments of inertia are very sensitive to the bond distances, it is possible to calculate distances which

TABLE I. Spectrum of $C_2D_4O$.

| Transition | Frequency | $\left(\frac{a-c}{2}\right)$ (calc.) | Δ |
|---|---|---|---|
| $0_0-1_0$ | 31,943 mc | — | — |
| $2_{-1}-2_1$ | 26,565 | 4427.5 | 0.0 |
| $3_{-3}-3_{-1}$ | 24,055 | 4427.9 | +0.4 |
| $3_{-2}-3_0$ | 33,285 | 4427.9 | +0.4 |
| $3_0-3_2$ | 35,341 | 4427.7 | +0.2 |
| $3_1-3_3$ | 29,080 | 4427.9 | +0.4 |
| $4_{-2}-4_0$ | 21,664 | 4427.8 | +0.2 |
| $5_{-1}-5_1$ | 24,668 | 4427.7 | +0.2 |
| $5_1-5_3$ | 39,592 | 4427.7 | +0.2 |
| $6_{-2}-6_0$ | 28,495 | 4427.5 | 0.0 |
| $8_{-2}-8_0$ | 35,068 | 4427.1 | −0.4 |

TABLE II. Moments of inertia.

| | |
|---|---|
| | $C_2H_4O$ |
| $I_A$ | $32.917\times10^{-40}$ g-cm² |
| $I_B$ | $37.920\times10^{-40}$ g-cm² |
| $I_C$ | $59.500\times10^{-40}$ g-cm² |
| | $C_2D_4O$ |
| $I_A$ | $41.123\times10^{-40}$ g-cm² |
| $I_B$ | $54.271\times10^{-40}$ g-cm² |
| $I_C$ | $72.667\times10^{-40}$ g-cm² |

are uncertain by less than ±0.0001A. However, the moments of inertia measured are those of the zero vibrational level, and introduction of a different isotope alters the zero-point energies and may change the effective positions of the atoms. The uncertainty of the bond distance obtained has been estimated[3] as less than 0.01A in OCS. In the case of ethylene oxide, the molecular dimensions are determined by five parameters, so that with six moments of inertia it is possible to remove one of the assumptions about the relative positions of the hydrogen and deuterium atoms. If we assume the direction of the C−H bond does not change, a C−D bond length can be calculated. The bond distances so calculated have an uncertainty which is unknown, but less than 0.01A. They are given in Table III.

It should be noted that although six variables were solved for, it is impossible to obtain equally valid results by making a large change in one and compensating small changes in the other five. The height of the hydrogen atoms above the plane of the molecule is in each case determined directly by the difference between $(I_A+I_B)$ and $I_C$. (The sign of $\kappa$ was determined by this relationship because, when $\kappa$ is small, the Stark coefficients vary only slightly in going from $+\kappa$ to $-\kappa$, making assignment from the observed Stark effect difficult. If $\kappa$ were positive, the C−D distance would be 8 percent smaller than the C−H distance, whereas for negative $\kappa$ the distance increases by only 0.16 percent.) The two values of $I_B$ then determine the C−C distance and one component of the C−H distance, and of $I_A$ determine the distance of the oxygen atom from the C−C bond and the other component of the C−H distance. Each pair of solutions is unique.

It is interesting to note that the normal C−C bond distance is 1.54A and the C−O distance is 1.44A. In ethylene oxide, the C−O distance is nearly 1.44A, while the C−C distance is 0.07A shorter than the normal bond. This seems to indicate that nearly all the strain required to form the C−O−C ring is taken up in the C−C bond.

Three further lines of the $C_2H_4O$ spectrum have been observed. They are in complete agreement with the previously observed spectrum and are given in Table IV. The value predicted[1] for the $4_2-4_4$ transition was somewhat low because of a numerical error in the calculated energy of the $4_4$ level.

TABLE III.

| | |
|---|---|
| C−O distance | 1.4363A |
| C−C distance | 1.4728A |
| C−H distance | 1.0802A |
| C−D distance | 1.0819A |
| H−C−H angle | 116° 51′ |
| $H_2$−C−C angle | 158° 5′ |
| Derived | |
| C−O−C angle | 61° 41.2′ |
| O−C−C angle | 59° 9.4′ |
| $H_2$−CO angle | 142° 45.6′ |

Data differing from ours on ethylene oxide have been published.[4] The discrepancy between our results and those of Shulman, Dailey, and Townes is of the same order of magnitude as the internal consistency of their data as shown in Table V.

TABLE IV. Additional lines for $C_2H_4O$.

| Transition | Frequency | $\left(\frac{a-c}{2}\right)$ (calc.) | Δ |
|---|---|---|---|
| $2_{-1}-2_1$ | 34,158 | 5693.0 | +0.1 |
| $4_2-4_4$ | 34,150 | 5692.7 | −0.2 |
| $4_{-2}-4_0$ | 41,581 | 5692.5 | −0.4 |
| $8_2-8_4$ | 43,398 | 5689.6 | −3.3 |

TABLE V. Data of Shulman, Dailey, and Townes on $C_2H_4O$.

| Transition | Frequency | $\left(\frac{a-c}{2}\right)$ (calc.) assuming $\kappa=0.395$ | Δ |
|---|---|---|---|
| $2_{-2}-2_0$ | 24,948 | 5744.4 | — |
| $3_{-1}-3_1$ | 23,614 | 5727.2 | − 17.2 |
| $3_1-3_3$ | 23,160 | 5611.7 | −132.7 |
| $4_0-4_2$ | 24,855 | 5685.9 | − 58.5 |

We wish to express our appreciation to the Research Corporation for a grant-in-aid support of this research. We also wish to express our appreciation to Mr. James Shoolery for designing and building a part of our electronic equipment.

[1] G. L. Cunningham, W. I. LeVan, and William D. Gwinn, Phys. Rev. **74**, 1537 (1948).
[2] J. W. M. DuMond and E. R. Cohen, Rev. Mod. Phys. **20**, 82 (1948).
[3] C. H. Townes, A. N. Holden, and F. R. Merritt, Phys. Rev. **74**, 1113 (1948).
[4] R. G. Shulman, B. P. Dailey, and C. H. Townes, Phys. Rev. **74**, 846 (1948).

## Vibrational Spectrum of Diiodoacetylene

ARNOLD G. MEISTER AND FORREST F. CLEVELAND
*Department of Physics, Illinois Institute of Technology, Chicago 16, Illinois*
December 15, 1948

RAMAN frequencies and semiquantitative relative intensities have been obtained for diiodoacetylene in alcohol and acetone solutions. The results are compared in Table I with the previous Raman data of Glockler and Morrell[1] and with the infra-red data of Emschwiller and Lecomte.[2] The Raman frequencies agree rather well in the two investigations except that in the present work a value of 2099 $cm^{-1}$ was obtained for the second line in the 2100-$cm^{-1}$ region which Glockler and Morrell observed but did not measure. This line was measured on three separate plates as 2098, 2098, and 2101 $cm^{-1}$ and is visible on the microphotometer tracing in the paper by Glockler and Morrell. Also, no coincidences in Raman and infra-red frequencies were observed in the region for which the infra-red frequencies were determined by Emschwiller and Lecomte (650–1450 $cm^{-1}$).

TABLE I. Raman and infra-red data, calculated frequencies, and assignments for diiodoacetylene ($C_2I_2$).*

| Observed Raman: Glockler, Morrell $\Delta\nu$ | $I$ | Observed Raman: Present results $\Delta\nu$ | $I$ | Observed Infra-red: $CS_2$ soln. $\nu$ | $I$ | Observed Infra-red: Solid $\nu$ | $I$ | Calc. $\nu_c$ | Assignment | Symmetry |
|---|---|---|---|---|---|---|---|---|---|---|
| | | | | — — | | — — | | 115 | $\nu_5$ | $E_{1u}$ |
| 191.3 | 70 | 191 | 11 | | | | | 191 | $\nu_1$ | $A_{1g}$ |
| 310.2 | 50 | 307 | 8 | | | | | 310 | $\nu_4$ | $E_{1g}$ |
| 627.0 | 30 | 621 | 3 | | | | | (620) | $2\nu_4$ | $A_{1g}+E_{2g}$ |
| 688.2 | 20 | 688 | 1 | | | | | (692) | $\nu_4+2\nu_1$ | $E_{1g}$ |
| | | | | 718 | $s$ | 703 | $s$ | 710 | $\nu_3$ | $A_{1u}$ |
| | | | | | | 780 | $m$ | (735) | $\nu_5+2\nu_4$ | $2E_{1u}+E_{2u}$ |
| | | | | | | 1003 | $w$ | (1020) | $\nu_4+\nu_3$ | $E_{1u}$ |
| | | | | | | 1052 | $w$ | (1092) | $\nu_3+2\nu_1$ | $A_{1u}$ |
| | | | | | | 1420 | $m$ | (1402) | $2\nu_1+\nu_3+\nu_4$ | $E_{1u}$ |
| | | | | | | | | (1399) | or $\nu_2-\nu_3$ | $A_{1u}$ |
| | | 2099 | (40) | | | | | (2148) | $2\nu_5+\nu_2-\nu_1$ | $A_{1g}+E_{2g}$ |
| 2109.4 | 100 | 2113 | 100 | | | | | 2109 | $\nu_2$ | $A_{1g}$ |

* $\Delta\nu$ = Raman frequency in $cm^{-1}$; $\nu$ = infra-red frequency in $cm^{-1}$; $\nu_c$ = calculated frequency in $cm^{-1}$; $I$ = relative intensity, on the basis of 100 for the strongest Raman line, $s$ = strong, $m$ = medium, $w$ = weak; values in regard to which there is some uncertainty are enclosed in parentheses; both of the Raman spectra were obtained in solution in acetone and in absolute alcohol.

Since Glockler and Morrell expressed some doubt as to the linearity of the structure of $C_2I_2$, it was felt that a calculation of the fundamental frequencies might be of some help. Accordingly, these frequencies were calculated using the Wilson[3] *FG* matrix method and force constants obtained from a previous investigation of methyliodoacetylene.[4] A linear model was assumed since the observed dipole moment is nearly zero,[5] and electron diffraction results[6] indicate that diiodoacetylene is linear. Six constants were used in the potential energy function. They were $k_a$, the C≡C stretching force constant, $k_i$, the C−I stretching force constant, $k_{ia}$ and $k_{ii}$ stretching interaction constants, $k_\varphi$, the I−C≡C angle bending force constant, and $k_{\varphi\varphi}$, the angle bending interaction constant. The calculated frequencies obtained from the force constants transferred from methyliodoacetylene are given as Set 1 in Table II. The results indicate that there is an unobserved infra-red fundamental frequency near 120 $cm^{-1}$. In order to improve the agreement between the calculated and observed values of the frequencies, the frequencies in Table II enclosed in brackets were used to modify the force constants of Set 1 so that Sets 2 and 3 were obtained. As a result of these modifications, it appears that the unobserved infra-red fundamental should be near 115 $cm^{-1}$. This frequency is further established by its appearance in two of the combination frequencies given in the assignments of the observed frequencies in Table I.

TABLE II. Force constants, corresponding calculated fundamental frequencies, and observed fundamental frequencies for diiodoacetylene.

| Force constants | Numerical values, $10^5$ dynes/cm: Set 1 | Set 2 | Set 3 |
|---|---|---|---|
| $k_a$ | (15.799)* | (15.799) | (15.799) |
| $k_i$ | (3.5707) | [3.2559] | [3.0186] |
| $k_\varphi$ | (0.059671) | (0.05967) | (0.05967) |
| $k_{ia}$ | (0.5320) | [0.8500] | [0.7350] |
| $k_{\varphi\varphi}$ | (0.036945) | [0.02538] | [0.02538] |
| $k_{ii}$ | (0.00000) | (0.00000) | [−0.2372] |

| Frequencies: Type | Designation | Calculated values, $cm^{-1}$: Set 1 | Set 2 | Set 3 | Observed |
|---|---|---|---|---|---|
| $A_{1g}$ | $\nu_1$ | 213 | 206 | [191] | 191 |
| $A_{1g}$ | $\nu_2$ | 2162 | [2109] | [2109] | 2109 |
| $A_{1u}$ | $\nu_3$ | 744 | [710] | [710] | 710 |
| $E_{1g}$ | $\nu_4$ | 252 | [310] | [310] | 310 |
| $E_{1u}$ | $\nu_5$ | 122 | 115 | 115 | — |

* The force constants in parentheses were transferred from methyliodoacetylene; those in brackets were determined from the frequencies in brackets.

In view of the reasonable agreement of the principal Raman and infra-red bands with the frequencies calculated from methyliodoacetylene force constants (Set I of Table I), the satisfactory assignment of the observed frequencies given in Table I, and the dipole moment and electron diffraction evidence, it no longer appears necessary to assume that diiodoacetylene departs from the conventional linear and symmetrical structure of acetylene itself.[7]

[1] G. Glockler and C. Morrell, J. Chem. Phys. **2**, 349 (1934); **4**, 15 (1936).
[2] G. Emschwiller and J. Lecomte, J. de phys. et rad. **8**, 130 (1937).
[3] E. B. Wilson, Jr., J. Chem. Phys. **7**, 1047 (1939); **9**, 76 (1941).
[4] A. G. Meister, J. Chem. Phys. **16**, 953 (1948).
[5] L. E. Sutton, R. G. A. New, and J. B. Bentley, J. Chem. Soc., 652 (1933).
[6] H. de Laszlo, Trans. Faraday Soc. **30**, 825 (1934); Nature **135**, 474 (1935).
[7] A more detailed paper bearing the same title was presented at the international colloquium on Diffusion des radiations électromagnétiques par la matière at Bordeaux, France, in April 1948; this paper is scheduled for later publication as a part of the proceedings of this colloquium.

## The Electronic State of the Methylene Radical

K. J. LAIDLER AND E. J. CASEY
*Department of Chemistry, The Catholic University of America, Washington, D. C.*
December 22, 1948

IN a recent discussion of possible electronic configurations for the methylene radical, A. D. Walsh[1] has tentatively concluded that the C−H bonds have more $sp$-hybrid character than $p$-character. On the other hand, when due regard is paid to the fact that little resonance occurs between states of different multiplicity, it would seem that this conclusion should be reversed: very little hybridization occurs, the bonds being $\sigma p$ with a certain amount of ionic character.

This may be shown as follows. Atomic carbon in its lowest state has the configuration $[(1s)^2(2s)^2(2p_z)(2p_y)]$, and if it forms $CH_2$ by making two pure $p$-bonds with hydrogen atoms, the molecular configuration becomes $CH_2$ $[(1s)^2(2s)^2(2p_z)^2(2p_y)^2]$, the two localized $\sigma$-orbitals[2] being directed at right-angles to each other; this is a singlet covalent state, which we shall denote by $CH_2$ ($c\,^1A$), and the bond angle H−C−H is 90 degrees.

Alternatively, if $sp$-hybridization occurs, following the promotion of an $s$ electron to give the $^5S$ atomic state of carbon $[(1s)^2(2s)(2p_z)(2p_y)(2p_x)]$, the lowest $sp$-hybrid state can be represented as $[(1s)^2(2q)^2(2p_z)(2p_y)]$, where $q$ denotes one $sp$-hybrid bond orbital and the two unshared electrons go into different $p$-orbitals; the state is consequently triplet, and the bond angle is now 180 degrees, owing to the $sp$-hybridization. This triplet state of $CH_2$ with the covalent hybrid bonding can be designated $CH_2$ ($ch\,^3\Pi$), and has the configuration $CH_2$ $[(1s)^2(2q\Omega_1)^2$

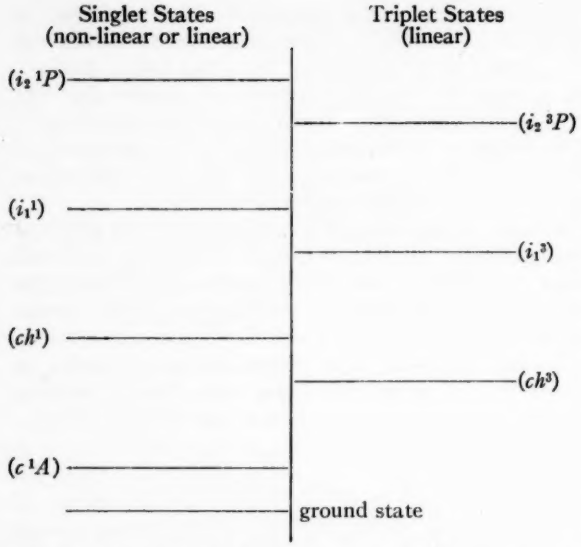


FIG. 1. Schematic representation of energy levels corresponding to various pure ionic and pure covalent states in the $CH_2$ radical. $c$ = pure covalent state; $ch$ = pure covalent-hybrid state; $i_1$ = ionic state corresponding to $HC^-H^+$; $i$ = ionic state corresponding to $H^+C^-H^+$. As explained in the text, the singlet ionic states are slightly higher than the corresponding triplet states, but the covalent singlet state, $CH_2$ $(c\,{}^1A)$, must be lower than $CH_2$ $(ch\,{}^3\Pi)$ to account for the experimental angle of 140 degrees. The bonds are thus formed mainly from pure $p$-orbitals of carbon.

$\times(2q\Omega_2)^2(2p_z)(2p_y)]$, where $\Omega_1$ and $\Omega_2$ represent the molecular orbitals binding the carbon atom to the two hydrogen atoms.

The possible *ionic* states of $CH_2$ $(c\,{}^1A)$ can be shown to be singlet and triplet: single ionization of $CH_2$ $(c\,{}^1A)$ to give $H-C^-H^+$ gives (a) the lowest state of $H-C^-$ to be $[(1s)^2(2s)^2(2p_x)^2(2p_y)(2p_z)]$, an ionic triplet state, to be denoted by $(i_1\,{}^3\Pi)$, and (b) a higher state, $[(1s)^2(2s)^2 \times(2p_z)^2(p_y)^2]$, which is a singlet state and denoted by $(i_1\,{}^1\Pi)$. Similarly, the doubly ionized possibilities are (a) the lowest energy state of $C^-$, $[(1s)^2(2s)^2(2p_z)^2(2p_y)(2p_z)]$ a triplet, denoted by $(i_2\,{}^3P)$, and (b) a higher state $[(1s)^2(2s)^2 \times(2p_z)^2(2p_y)^2]$, a singlet state, denoted by $(i_2\,{}^1P)$. The methylene radical in the state $CH_2$ $(c\,{}^1A)$ can resonate with ionized forms involving the same multiplicity, *viz.*: $(i_1\,{}^1\Pi)$ and $(i_2\,{}^1P)$, both singlets. No resonance can occur with the states $(i_1\,{}^3\Pi)$ and $(i_2\,{}^3P)$.

In a similar manner, it can be shown that $CH_2$ $(ch\,{}^3\Pi)$ can resonate with two triplet, ionized states. The corresponding singlet states also occur, but these cannot resonate with the triplet ground state.

There are therefore two distinct possibilities for the methylene radical in the ground state: (1) it is in a singlet state in which there is resonance mainly between the 90-degree covalent structure, $(c\,{}^1A)$, and the two singlet ionic states, $(i_1\,{}^1\Pi)$ and $(i_2\,{}^1P)$, the effect of the ionic states being to increase the bond angle beyond 90 degrees, and (2) it is in a triplet state involving resonance between the hybridized linear triplet covalent state CH $(ch\,{}^3\Pi)$ and the two corresponding ionic states. Ionic states in this case do not affect the 180-degree bond angle. From a consideration of the ionic states alone, the linear triplet ground state would be favored over the bent singlet ground state since triplet ionic states are lower in energy than corresponding singlet states.

Experimentally, it is found that the bond angle in the lowest state is about 140 degrees. Herzberg[3] has identified certain bands found in the spectra of comets as arising from $CH_2$ and has succeeded in reproducing the bands by passing an electrodeless discharge through methane.[4] The bands have also been obtained by Herman,[5] who passed a discharge between carbon electrodes in an atmosphere of hydrogen, and by Letort and his co-workers[6] from the decomposition of diazomethane, which can be shown by the tellurium mirror technique to give rise to methylene radicals. There would seem, therefore, to be little doubt about Herzberg's identification or about his conclusion as to the angle.

The fact that the angle is less than 180 degrees appears to point unequivocally to the conclusion that the molecule is in a singlet state and that the bonds arise largely from pure $p$-orbitals of carbon, with only a small contribution from $sp$-hybrid orbitals. Since the ionic states favor the triplet state somewhat, the pure covalent state $CH_2$ $(c\,{}^1A)$ must be lower than the pure covalent hybrid $CH_2$ $(ch\,{}^3\Pi)$, indicating that in this case the bonding energy gained by hybridizing after promotion of an electron is more than offset by the energy needed to promote the electron. The relative positions of the energy levels are indicated schematically in Fig. 1.

It may be noted that a certain amount of $sp$-hybridization may occur in the molecule, arising from resonance between $CH_2$ $(c\,{}^1A)$ and singlet *excited* hybrid states of $CH_2$ $(ch\,{}^3\Pi)$, the lowest of these excited hybrid states being designated as $CH_2$ $(ch\,{}^1\Pi)$. However, since these states are less stable than the lowest state, $CH_2$ $(ch\,{}^3\Pi)$, and since the experimental angle shows that $CH_2$ $(ch\,{}^3\Pi)$ is higher than the lowest singlet state $CH_2$ $(c\,{}^1A)$, formed by the bonding of pure $p$-orbitals, it can be concluded that the amount of $sp$ character in the bonding is very small. This being so, the analogy between the C—H bond in methylene and in acetylene (in which $sp$-hybridization occurs to completion) is not as close as has sometimes been supposed.

The above interpretation of the structure of the methylene radical is consistent with the experimental findings of Pearson, Purcell, and Saigh,[7] according to whom the methylene radical is much less reactive than the methyl radical, and who conclude, therefore, that the $CH_2$ radical contains no unpaired electrons, i.e., is in a singlet state. Support is also found in the work of Lennard-Jones,[8] who, by a quantum-mechanical analysis, found that $(c\,{}^1A)$ is the state of lowest energy.

Thanks are due Dr. G. Herzberg and Professor P. Letort for information relative to this problem.

[1] A. D. Walsh, Faraday Soc. Discussions **2**, 18 (1948).
[2] Cf. C. A. Coulson, Quarterly Rev. **1**, 160 (1947).
[3] G. Herzberg, Rev. Mod. Phys. **14**, 195 (1942).
[4] Idem, Astrophys. J. **96**, 314 (1942).
[5] R. Herman, Comptes Rendus **223**, 280 (1946).
[6] M. Letort, private communication.
[7] T. G. Pearson, R. H. Purcell, and G. S. Saigh, J. Chem. Soc., 409 (1948).
[8] J. E. Lennard-Jones, Trans. Faraday Soc. **30**, 70 (1934).

## The Efficiency of the Internal Conversion Process in $Br^{80*}$

WILLIAM H. HAMILL AND J. A. YOUNG
*Department of Chemistry, University of Notre Dame, Notre Dame, Indiana*
December 17, 1948

SEVERAL values for the efficiency of internal conversion of $Br^{80}$ (4.5 hr.) have been reported. Previous studies of chemical effects accompanying this nuclear reaction carried out in condensed phases have given values of 0.85 to 0.90.[1] According to recent physical measurements,[2] the transition proceeds in two steps, one of which is apparently completely internally converted, as evidenced by failure to find the corresponding unconverted gamma-ray. This should lead to chemical activation in every decay, although the ultimate chemical effect will depend upon the environment.

Since we plan to undertake quantitative kinetic studies with $Br^{80}$ (4.5 hr.) in gaseous systems, it is first necessary to measure the conversion efficiency in terms of the chemical effects produced in a gaseous system, and to correlate quantitatively, if possible, chemically and physically measured conversion efficiencies. To achieve maximum separation of parent and daughter activities it is probably necessary to avoid the cage effect of the liquid phase, to introduce the parent into a relatively stable molecular form, and to add an acceptor which will readily combine or exchange with the nascent daughter particles. Finally it must be possible to remove $Br^{80}$ (18 min.) and begin counting $Br^{80}$ (4.5 hr.) within a brief interval since the ratio of the counting rates at zero time (moment of separation) is a measure of conversion efficiency. The following procedure proved to be satisfactory. The total bromine activity, as $AgBr^*$, was converted to $AlBr_3^*$ and exchanged with $CH_3Br^*$; water was added to destroy $AlBr_3$ and $CH_3Br^*$ was then distilled from $P_2O_5$ and HBr (0–50-mole percent) was added. This gaseous mixture remained at room temperature for two hours. The $CH_3Br^*$ was transferred to the cold finger of a gas sample holder surrounding a thin-wall counter within an interval of ten seconds: HBr was removed during the transfer by an interposed soda-lime tube. Counting of the gas sample, at a fraction of its vapor pressure, started within thirty seconds and continued through the decay of $Br^{82}$. In our counting arrangement the counting efficiency of $Br^{80}$ (4.5 hr.) is quite negligible and therefore its activity must be measured through its 18-min. daughter. After correcting for a small $Br^{82}$ (34 hr.) contribution and for background the residual growth and decay curve may be expressed by

$$A_2-A_1{}^0\frac{\lambda_2}{\lambda_2-\lambda_1}e^{-\lambda_1 t}=\left(A_2{}^0-A_1{}^0\frac{\lambda_2}{\lambda_2-\lambda_1}\right)e^{-\lambda_2 t}. \quad (1)$$

TABLE I.

| MeBr cm | HBr cm | $A_1{}^0$ | $A_2{}^0$ | Efficiency |
|---|---|---|---|---|
| 12 | 6 | 1328 | −35 | 1.00 |
| 20 | 12 | 375 | +15 | 0.96 |
| 15 | 0 | 1206 | +45 | 0.96 |
| 45 | 45 | 2238 | +30 | 0.99 |

The 4.5-hr. and 18-min. periods are adequately resolved and represented by

$$A_2=A_1{}^0\frac{\lambda_2}{\lambda_2-\lambda_1}e^{-\lambda_1 t} \quad \text{for} \quad e^{-\lambda_1 t}\gg e^{-\lambda_2 t}, \quad (2)$$

$$A_2+A_1{}^0\frac{\lambda_2}{\lambda_2-\lambda_1}\left(\lambda_1 t+\frac{\lambda_2{}^2 t^2}{2}\right)=A_1{}^0\frac{\lambda_2{}^2}{\lambda_2-\lambda_1}t+A_2{}^0, \quad (3)$$

during the time intervals 180–500 min. and 0–15 min., respectively. In these equations subscripts 1, 2 refer to parent and daughter and $A$, $\lambda$, $t$ refer to activity, decay constant, and time, respectively. Table I summarizes these results. The experimental points agree with the expected slopes of both segments of the growth and decay curve in all cases.

It is interesting that even without addition of HBr there is very little apparent retention of $Br^{80}$ (18 min.) by $CH_3Br$. Although no attempt was made to follow in detail the fate of daughter particles, it was repeatedly observed that about half of the 18-min. activity remained in the counter chamber after removal of the parent $CH_3Br^*$. Unless the half-time for absorption of these particles is short, it might be expected that a time-dependent geometry would be exhibited as a trend in the 18-min. period. Since the latter is correct within the statistical counting error, the effect may be ignored since the conversion efficiency is based upon the ratio of extrapolated $Br^{80}$ (18-min.) activities.

These experiments demonstrate that there is no branching decay of $Br^{80}$ (4.5 hr.), that the chemical effects produced correspond to complete conversion, in agreement with the physical effects, and that quantitative correlation of chemical effects with nuclear phenomena in the liquid phase may be unreliable.

We are grateful to Dr. Russell R. Williams, Jr., for his interest in a helpful discussion of this work.

* This work was supported under ONR contract N6 ori 165 T.O. II.
[1] Devault and Libby, J. Am. Chem. Soc. **63**, 3216 (1941); Willard, J. Am. Chem. Soc. **62**, 3162 (1940).
[2] A. D. Grinberg and L. I. Rossinow, Phys. Rev. **58**, 181 (1940); Berthelot, Ann. de physique **19**, 219 (1944).

## Styrene Polymerization in a Magnetic Field

J. E. LEFFLER AND M. J. SIENKO
*Baker Laboratory of Chemistry, Cornell University, Ithaca, New York*
December 16, 1948

SCHMID *et al.* have reported that a strong external magnetic field decreases the rate of the polymerization of styrene to methanol-insoluble polystyrene.[1] They suggest that the reaction impending influence of the magnetic field is due to the orienting of reacting molecules and the associated restriction of the mobility of the molecules. The Cotton-Mouton effect is probably too small at the temperature of polymerization of styrene to produce the observed decrease in rate by orienting the molecules. Since organic free radicals have been shown to be in a $\Sigma$-state[2] in which the coupling between the spin moment and the axis of figure of the molecule can be neglected, it is likely that an external magnetic field would orient not the radicals but only the spin moments of the odd electrons.

For the thermal polymerization of styrene, Walling has suggested that the rate is proportional to the first power of the rate constant of the radical propagation step.[3] Assuming that the chain propagation step in field-free space occurs by a preliminary uncoupling of the Π-electrons, the process can be represented as follows:

$$\underset{\text{monomer}}{\overset{\uparrow\downarrow}{\underset{\cdot\cdot}{\text{Ph}-\text{CH}-\text{CH}_2}}}+\underset{\text{radical}}{\overset{\uparrow}{\underset{\cdot}{\text{R}}}}\rightleftharpoons\underset{\text{transition state}}{\left[\overset{\uparrow}{\underset{\cdot}{\text{Ph}-\text{CH}}}-\overset{\downarrow}{\underset{\cdot}{\text{CH}_2}}-\overset{\uparrow}{\underset{\cdot}{\text{R}}}\right]}$$

$$\rightleftharpoons\text{Ph}-\overset{\uparrow}{\underset{\cdot}{\text{CH}}}-\underset{\cdot\cdot}{\overset{\downarrow\uparrow}{\text{CH}_2}}-\text{R}.$$
radical

In the presence of a strong external magnetic field the uncoupled state is more probably $\left[\overset{\uparrow}{\underset{\cdot}{\text{Ph}-\text{CH}}}-\overset{\uparrow}{\underset{\cdot}{\text{CH}_2}}-\overset{\uparrow}{\underset{\cdot}{\text{R}}}\right]$ where all three electron spin moments are now oriented with respect to the external field. Such a configuration would not lead to bond formation in either direction.

It is evident that this formulation agrees with the observed deceleration by the external magnetic field. If in the thermal depolymerization of polystyrene, degradation of a radical is involved, the same uncoupled transition state should occur, and an external magnetic field should diminish the rate constant of the radical degradation step.

[1] H. Schmid, G. Muhr, and H. Marek, Zeits. f. Elektrochemie **51**, 37 (1945).
[2] E. Müller, Zeits. f. Elektrochemie **51**, 24 (1945); E. Müller, I. Müller-Rodloff, and W. Bunge, Lieb. Ann. d. Chemie **520**, 235 (1935).
[3] C. Walling, E. R. Briggs, and F. R. Mayo, J. Am. Chem. Soc. **68**, 1145 (1946).

## The Estimation of the Hindering Potential Barrier of Hexachloroethane by Electron Diffraction Investigation

YONEZO MORINO AND MACHIO IWASAKI
*Faculty of Science, Nagoya University, Nagoya, Japan*
December 27, 1948

RECENTLY J. Karle[1] calculated the contribution of hindered rotation to electron diffraction by gaseous molecules and suggested that the hindering potential barrier $V_0$ of hexachloroethane for the rotation of $CCl_3$ groups would be determined by electron diffraction investigation, because the intensity curve of this molecule is sensitive to $V_0/kT$.

One of the present authors and his co-workers[2] interpreted the electron diffraction pattern of hexachloroethane by the rigid staggered model. Their treatment has an imperfection that the intensity relation between the 5th, 6th, and 7th maxima in the theoretical intensity curve do not agree with the observed pattern. It should be of great interest to remark that this disagreement can be removed by considering the effect of the hindering rotation of $CCl_3$ groups by Karle's method.

The curve $V$ in Fig. 1 is the visual curve of the photograph obtained at room temperature, the curve $A$ is the one which is calculated for the rigid staggered model, and the curve $B$ is the one calculated at room temperature for

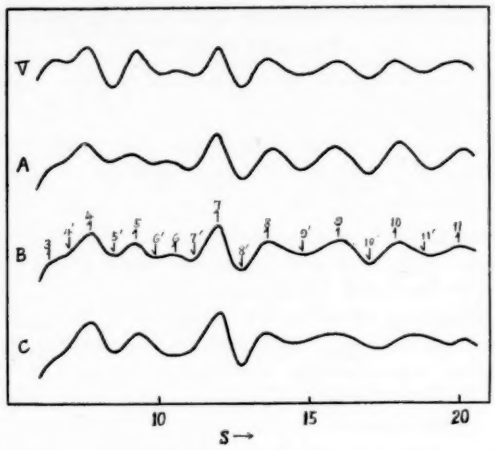


FIG. 1. Comparison of the theoretical intensity curves with the visual curve of hexachloroethane. Curve $V$, the visual curve; Curve $A$, the calculated curve for the rigid staggered model ($V_0=\infty$); Curves $B$ and $C$, the calculated curve for the model of hindered rotation with $V_0=14$ and 6 kcal./mol., respectively. (The structure parameters used: C−C=1.54A, C−Cl=1.77Å, and ∠ClCCl=108° 45′.)

the model of hindered rotation with $V_0=10$ kcal./mol. $\times(V_0/kT=17)$. The intensity curve between the 5th and 6th maxima is very sensitive to the barrier height. The diffraction pattern shows that the 6th maximum is very weak compared with the 5th and 7th maxima. But in the intensity curve for the rigid staggered model, both the 5th and 6th maxima are weak compared with the 7th maximum. When the effect of hindering rotation is taken into consideration, with decreasing the value of $V_0/kT$, the 5th maximum increases, while the 6th maximum decreases and disappears for $V_0/kT$ smaller than 12. The features of the intensity curve between the 5th and 7th maxima agree well with the observed pattern at the value of $V_0/kT=17$–25. From this result the barrier height of hexachloroethane is estimated to be 10–15 kcal./mol.

The structure parameters which were determined by considering the effect of hindering rotation are as follows: C−Cl=1.77±0.02A, C−C=1.54±0.07A and ∠ClCCl =108° 45′±1° 30′.

I. Miyagawa[3] in our laboratory computed the interatomic potential between chlorine atoms,

$$V=-1.515\times10^{-10}/r^6+1.620\times10^{-7}/r^{12}\ \text{erg/molecule}$$
($r$ in A unit),

from the second virial coefficients of the gas. By assuming that this function can also be applied to intramolecular potential, the hindering potential barrier of hexachloroethane is calculated to be 12 kcal./mol., which agrees with the observed value stated above.

For the determination of potential barrier it is desirable to study the temperature variation of the diffraction pattern of hexachloroethane, and we are now undertaking the experiment.

[1] J. Karle, J. Chem. Phys. **15**, 202 (1947).
[2] Y. Morino, S. Yamaguchi, and S. Mizushima, Sci. Pap. Inst. Phys. Chem. Research (Tokyo) **42**, 5 (1944); Y. Morino and M. Kimura, J. Chem. Soc. (Japan) **68**, 78 (1947).
[3] Y. Morino and I. Miyagawa, J. Chem. Soc. (Japan) **68**, 62 (1947).

## Intrinsic Viscosity of Linear Polymers

J. N. WILSON
*Shell Development Company, Emeryville, California*
December 28, 1948

RECENT theoretical developments have led to the proposal of several new expressions relating the intrinsic viscosity of a linear polymer to its molecular weight and structure.[1-4] The following simple interpolation formula, which gives results similar to these, was independently proposed by the author at these laboratories in May, 1947:

$$[\eta]=K_1Z/(1+K_2Z^{\frac{1}{2}}), \tag{1}$$

where $Z$ is the number of links in the polymer chain and in the terminology of Kirkwood and Riseman[3]

$$K_1=(\zeta/\eta_0)(N/3600\text{Mo})b^2, \tag{2}$$

$$K_2=(\zeta/\eta_0)/15\pi\alpha^3b. \tag{3}$$

This expression was chosen because it is the simplest one which at low values of $Z$ approximates the Staudinger equation in accordance with theory[5-8] and experiment,[9,10] and at high values of $Z$ approximates the proportionality to $Z^{\frac{1}{2}}$ first suggested by Kuhn.[11] The value of $K_1$ was taken in accordance with the theory of the Staudinger equation, and the value of $K_2$ was determined from the consideration that at high values of $Z$ the solution of convoluted polymer molecules with solvent trapped within their coils should approximate a suspension of Einstein spheres with effective diameter $D$ equal to $\alpha R$, where $R$, the root mean square distance between the ends of the chain, is equal to $bZ^{\frac{1}{2}}$.

Equation (1) is a remarkably good approximation to the theoretical formula of Kirkwood and Riseman, in which the term $(1+K_2Z^{\frac{1}{2}})^{-1}$ is replaced by

$$\frac{6}{\pi^2}\sum_{k=1}^{\infty}k^{-2}[1+\lambda_0(Z/k)^{\frac{1}{2}}]^{-1}. \tag{4}$$

The latter expression for values of $Z$ up to the order of $10^5$ is approximately equal to $(1+0.76\lambda_0Z^{\frac{1}{2}})^{-1}$. The factor 0.76 is correct for $\lambda_0Z^{\frac{1}{2}}=1.5$ and is in error by about 6 percent at the extremes of the range given. It is doubtful whether the precision with which the molecular weight distributions of polymer fractions can be measured is sufficient to provide a distinction between the expression (4) and its approximation. Substituting for $\lambda_0$ (3) we obtain

$$K_2=(\zeta/\eta_0)0.76/(6\pi^3)^{\frac{1}{2}}b. \tag{5}$$

By comparison with Eq. (3) we obtain 0.72 for the theoretical value of $\alpha$, the factor relating the diameter of the equivalent Einstein sphere to the root mean square distance between the chain ends.

Experimental data may readily be fitted to Eq. (1) by plotting $M/[\eta]$ *vs.* $M^{\frac{1}{2}}$ where $M$ is the molecular weight of the polymer. Osmotic data obtained by the author for acetone solutions of seven fractions of polymethacrylonitrile covering the range 90,000 to 950,000 in Mn are in accordance with Eq. (1) with $K_1=(2.66\pm0.21)\times10^{-4}$ $(\text{g}/100\text{ ml})^{-1}$; $K_2=(9.4\pm1.5)\times10^{-3}$. From the ratio of these constants and the value 33.5 for Mo, the mean molecular weight per chain-element, we obtain $\alpha b=5.0\pm0.3$A. The value 7.7A for $b$ was obtained from measurements of the asymmetry of light-scattering by the solutions. Thus the experimental value for $\alpha$ is $0.65\pm0.04$, in approximate agreement with the Kirkwood-Riseman theory. The value of $\zeta/\eta_0$ is 0.9A; thus the effective Stokes' law radius of a chain-element is computed to be 0.05A, comparable to the abnormally low values reported for polystyrene.[3,4]

Weight-average molecular weights computed from light-scattering data were in reasonable agreement with the osmotic molecular weights in the range 90,000 to 400,000; above this range $M_w$ was larger than $M_n$ by a factor which increased rapidly as $M_n$ increased and was of the order of 2 at $M_n=10^6$. In this range and above, the plot of $M_w/[\eta]$ *vs.* $M_w^{\frac{1}{2}}$ deviates rapidly from the similar plot involving $M_n$, in the direction of higher values of $M_w/[\eta]$. These effects suggest that in the higher molecular-weight range a portion of the solute molecules aggregates into large clusters; the effect of clustering on the value of $[\eta]$ will be small if the volume of the equivalent Einstein sphere of a cluster is not too greatly different from the sum of the volumes of the equivalent spheres of its constituent solute molecules.

[1] P. Debye, Phys. Rev. **71**, 486 (1946).
[2] H. C. Brinkman, Physica **13**, 447 (1947).
[3] J. G. Kirkwood and J. Riseman, J. Chem. Phys. **16**, 565 (1948).
[4] P. Debye and A. M. Bueche, J. Chem. Phys. **16**, 573 (1948).
[5] W. Kuhn, Zeits. f. physik. Chemie **A161**, 1 (1932).
[6] M. L. Huggins, J. Phys. Chem. **43**, 439 (1939).
[7] H. A. Kramers, J. Chem. Phys. **14**, 415 (1946).
[8] P. Debye, J. Chem. Phys. **14**, 636 (1946).
[9] H. Staudinger, *Die Hochmolekularen Organischen Verbindungen* (Verlag Julius Springer, Berlin, 1932).
[10] M. Lauffer, Chem. Rev. **31**, 561-86 (1942).
[11] W. Kuhn, Kolloid Zeits. **68**, 2 (1934).

## The Vibrational Spectra of Some Metal Borohydrides*

W. C. PRICE,** H. C. LONGUET-HIGGINS, B. RICE, AND T. F. YOUNG***
*Departments of Physics and Chemistry, University of Chicago, Chicago, Illinois*
December 27, 1948

THE infra-red spectra of aluminum, lithium, and sodium borohydrides have been studied by W. C. Price, that of beryllium borohydride by H. C. Longuet-Higgins, and the Raman spectrum of aluminum borohydride by T. F. Young and B. Rice. Details will be published shortly in separate papers, but we here give the main results so far obtained.

TABLE I. Vibrational frequencies in borohydrides.

| | $B_2H_6$ | | $Al(BH_4)_3$ | | $Be(BH_4)_2$ | $LiBH_4$ | $NaBH_4$ | |
|---|---|---|---|---|---|---|---|---|
| | I.R.[a] | R.[b] | I.R. | R. | I.R. | I.R. | I.R. | |
| (a) | 974 | | 978 | 977 | 940 | | | |
| | | 1008 | 1114 | 1122 | to | 1096 | 1080 | (a) |
| | 1175 | 1180 | | 1156 | 1090 | | | |
| | 1283 | | | | | | | |
| | | | 1450 | | | | | |
| | 1604 | | to | 1502 | 1530 | | | |
| | | | 1550 | | | | | |
| (b) | 1850(?) | | | | | | | |
| | 1984 | | 2031 | 2082 | 1985 | | | |
| | | 2102 | 2154 | | 2060 | | | |
| | | | | | 2165 | 2245 | 2150 | |
| | | | | | | to | to | |
| | | 2489 | 2493 | 2480 | | | | |
| (c) | 2522 | 2523 | 2559 | 2553 | 2515 | 2404 | 2380 | (c) |
| | 2614 | | | | 2630 | | | |

[a] See reference 1.
[b] See reference 2.

The frequencies of the principal bands occurring in the range 900–2700 $cm^{-1}$ are shown in Table I, which includes the most recent data on $B_2H_6$ for comparison.[1,2] The frequencies in class (a) are attributed to B-H deformations, and those in class (c) to ordinary B-H stretching modes. The presence of strong absorption around 1500 and 2000 $cm^{-1}$ in the Be and Al compounds is very strong evidence that these molecules have bridged structures, as suggested already by one of us.[3] In these two molecules there are two groups of frequencies in the range (b); by analogy with diborane, these are probably associated with motion of the bridge hydrogen atoms parallel and perpendicular to the bridge axis, respectively. However, when we pass to the more ionic lithium and sodium borohydrides, these frequencies respectively degenerate into bending and stretching frequencies of the $BH_4^-$ ion.

The B-H stretching frequencies in class (c) are probably associated with terminal $BH_2$ groups in the Al and Be compounds, but until detailed assignments can be made it would probably be wiser not to draw conclusions as to the relative force constants in these molecules.

Our warmest thanks are due Professor R. S. Mulliken for constant encouragement and help in many ways.

* The infra-red work was done under Contract N6ori-20, Task Order IX, NR 019 101, with the Office of Naval Research.
** Now at King's College, Strand, London, England.
*** W. C. Price and H. C. Longuet-Higgins, Physics Department. B. Rice and T. F. Young, Chemistry Department.
[1] W. C. Price, J. Chem. Phys. **16**, 894 (1948).
[2] T. F. Anderson and A. B. Burg, J. Chem. Phys. **6**, 586 (1938).
[3] H. C. Longuet-Higgins, J. Chem. Soc., 139 (1946).

## The Infra-Red Spectra of Borine Carbonyl and Tetramethyldiborane*

R. D. Cowan**
*Ryerson Physical Laboratory, The University of Chicago, Chicago, Illinois*
December 27, 1948

THE infra-red spectra of borine carbonyl and of tetramethyldiborane have been obtained in the interval 2 to 25 microns with a Perkin-Elmer spectrometer.

In the spectrum of borine carbonyl ($H_3BCO$) the coarse structures of two bands (a strong one at 2440 and a weak one at 810 $cm^{-1}$) have been resolved. In each case the structure is typical of perpendicular-type bands of a symmetric-top molecule, and successive maxima show a distinct intensity alternation of the type strong, weak, weak, strong, . . . which is to be expected in the case of a threefold symmetry axis. These results thus indicate a molecular structure with symmetry $C_{3v}$, in agreement with Bauer's electron-diffraction results[1] and with the conclusions of Gordy, Ring, and Burg[2] from microwave rotation spectra. The spacing between adjacent $Q$-maxima of the perpendicular bands is 6.7 $cm^{-1}$ in the case of the 2440-$cm^{-1}$ band and 3.1 $cm^{-1}$ for the 810-$cm^{-1}$ band. Because of the large but uncertain amount of Coriolis coupling which is present, it is difficult to compare these values with the value 8.2 $cm^{-1}$ to be expected from Bauer's data in the absence of such coupling. The band at 2440 $cm^{-1}$ can be ascribed to the degenerate B—H stretching vibration, and a very strong parallel band at 2164 $cm^{-1}$ is due probably to the corresponding symmetrical vibration.

The spectrum of tetramethyldiborane provides further evidence in support of the bridge structure for diborane ($B_2H_6$). The complete absence of other than weak bands at frequencies greater than 1700 $cm^{-1}$ indicates there are no B—H bonds of the type which gives rise to the very strong bands at 2522 and 2614 $cm^{-1}$ in diborane;[3] trimethyldiborane, which was also investigated, has, on the other hand, a single strong band at 2509 $cm^{-1}$. The strongest band in the tetramethyldiborane spectrum lies at 1602 $cm^{-1}$ and is almost certainly the analog of the bridge-hydrogen band of diborane at 1604 $cm^{-1}$.[3] A weak band at 1968 $cm^{-1}$ may similarly correspond to the bridge-hydrogen band of $B_2H_6$ at 1984 $cm^{-1}$. The analog of the third bridge-hydrogen vibration (probably 1283 $cm^{-1}$ in diborane), if present, is probably obscured by numerous strong methyl bands in the interval 900 to 1400 $cm^{-1}$.

Detailed reports on these spectra and on those of boric acid and dimethyl boric acid will be published later.

* This work was supported by Office of Naval Research Contract N6ori-20, Task Order IX.
** Present address: Friends University, Wichita, Kansas.
[1] S. H. Bauer, J. Am. Chem. Soc. **59**, 1804 (1937).
[2] W. Gordy, H. Ring, and A. B. Burg, Phys. Rev. **74**, 1191 (1948).
[3] W. C. Price, J. Chem. Phys. **16**, 894 (1948).

## Infra-Red Absorption Spectra of Organic Compounds

Earle K. Plyler
*National Bureau of Standards, Washington, D. C.*
December 27, 1948

THE infra-red absorption spectra of some derivatives of methane, ethane, and benzene have been measured in the region from 22 to 39$\mu$. The method of measurement in this spectral region has been previously described.[1] All the compounds were measured in the liquid state and the cells were from 0.2 to 1.6 mm in thickness. The observed bands, all of medium or of low intensity, are listed in Table I. The wave numbers listed for the regions of maximum absorption are accurate to about $\pm 2$ $cm^{-1}$. The accuracy is sufficient for survey work. One source of error arises from changes in the temperature of the prism. The temperature coefficient of the index of refraction for the TlBr-I prism is $-0.00016$ as measured in the visible region. Changes in refractive index of these crystals over a period of time have also been observed. Hyde[2] has reported changes in the index of refraction of 0.0048 over a period of a few months. For work of high accuracy the instrument should be calibrated before and after each substance is measured. Methods of annealing recently developed by the Engineer Research and Development Laboratories give promise of producing more stable prisms than those which have been available.

Most of the compounds listed in Table I have been measured in the NaCl and KBr regions. Many bands appear in the region of wave-lengths from 2 to 22$\mu$. Carbon tetrachloride in cell thicknesses of 1.0 mm has been investigated with a KBr prism. Bands have been found at 17.59, 18.82, 20.73, and 22.43$\mu$. These have all been interpreted in

TABLE I. List of observed bands.

| Substance | Wave-length ($\mu$) | Wave number ($cm^{-1}$) |
|---|---|---|
| Chlorodibromomethane | 26.2 | 381 |
| | 35.8 | 279 |
| Dichlorobromomethane | 22.9 | 437 |
| | 26.2 | 381 |
| | 30.3 | 330 |
| Dichlorodibromomethane | 22.6 | 442 |
| | 25.2 | 397 |
| | 26.7 | 375 |
| | 28.4 | 351 |
| Trichlorobromomethane | 23.8 | 420 |
| | 28.4 | 351 |
| | 34.0 | 294 |
| Ethylene chloride | 24.3 | 412 |
| | 36.7 | 272 |
| Ethylene bromide | 24.9 | 402 |
| | 28.1 | 355 |
| *s*-Tetrachloroethane | 28.4 | 352 |
| | 30.7 | 326 |
| | 34.5 | 290 |
| Ethylcyclopentane | 23.6 | 424 |
| | 25.4 | 393 |
| *cis*-1,3-Dimethylcyclopentane | 23.5 | 426 |
| Methylcyclohexane | 22.6 | 442 |
| | 24.7 | 405 |
| 1-Methyl-2-ethylbenzene | 22.1 | 452 |
| | 22.9 | 437 |
| | 31.1 | 322 |
| 1-Methyl-3-ethylbenzene | 22.9 | 437 |
| 1-Methyl-4-ethylbenzene | 27.3 | 366 |
| | 32.5 | 308 |
| 2-Methyl-2-phenylpropane | 25.3 | 395 |
| | 32.5 | 308 |
| Chlorobenzene | 23.9 | 418 |
| | 33.8 | 296 |
| Bromobenzene | 31.9 | 313 |
| Iodobenzene | 22.3 | 448 |
| *o*-Dichlorobenzene | 22.9 | 437 |
| | 29.8 | 335 |
| 1,2,4-Trichlorobenzene | 22.8 | 438 |
| | 25.2 | 397 |
| | 32.6 | 307 |
| *p*-Chlorobenzotrifluoride | 24.4 | 409 |
| | 26.0 | 385 |
| | 31.9 | 313 |
| | 33.1 | 302 |
| | 36.5 | 274 |
| *o*-Bromoanisole | 22.9 | 437 |
| | 30.3 | 330 |
| | 35.7 | 280 |
| *p*-Bromoanisole | 30.7 | 326 |
| | 37.9 | 264 |
| $\alpha$-Bromonaphthalene | 24.9 | 402 |
| | 33.5 | 298 |
| Diethyl ether | 22.7 | 440 |
| | 26.7 | 374 |

accordance with the known energy level scheme for $CCl_4$, and include the difference bands at 20.73 and 22.43$\mu$, predicted by Herzberg as of sufficient intensity for observation. A detailed report is in preparation.

[1] Earle K. Plyler, J. Research Nat. Bur. of Stand. **41**, 125 (1948).
[2] W. L. Hyde, J. Chem. Phys. **16**, 744 (1948).

## Structure—Optical Studies. II. Aqueous Dispersion of Polyvinyl Borate—Iodine and Its Heat of Formation

C. D. WEST
*Polaroid Corporation, Cambridge, Massachusetts*
December 27, 1948

AQUEOUS dispersions of polyvinyl borate (PVB), formed by mixing dilute polyvinyl alcohol (PVA) with boric acid solution, react to iodine in the same way as do amylose solutions by giving a blue color due to a strong absorption band in the near red. If the boric acid is omitted from the reaction mixture, no blue color results because of complete dissociation of the blue PVA-iodine compound at the dilutions in question. The wave-length of maximum absorption for PVB-iodine solution is 670 mmu, while that of soluble starch-iodine is only 590 mmu under parallel conditions; that reported[1] for amylose-iodine is 628 mmu. The absorption bands of these compounds are symmetrical and are similar to each other in height and half-width. The triple color reaction of boric acid, PVA, and iodine, by reason of its marked specificity, has analytical possibilities for the detection or determination of any one of its three components, more especially the latter two. Colloidal polyvinyl phenylborate, made in the same way and having similar properties, does not give a color reaction with iodine under similar conditions. When bromine is added to rather concentrated soluble starch or PVB solutions, we observe a distinct color change from yellow to orange or red but have failed to measure an intense absorption band here; the spectrophotometric data suggest extensive dissociation of such compounds in solution.

(With E. Emerson.) We find unexpectedly large heats are evolved when one mole of halogen (iodine or bromine) is added to an excess of organic polymer in aqueous dispersion under conditions to give as complete formation of addition compound as possible. Our results, which we did not reproduce to better than 10 percent, are summarized as the starred figures in Table I, together with data from the literature.[2] All values here are in kcal. per mole of halogen and refer to the halogens in their standard (condensed) states. While the complexity of the colloidal systems (lines 2 and 3 of Table I) prevents a detailed interpretation of these figures taken by themselves, they suggest that the energy of formation of these compounds from halogen molecules is an appreciable fraction of the energy of formation of the molecules from neutral atoms, and is considerably greater than the heat of formation of simple crystalline trihalides from the crystalline halides (last line of Table I). It would be of considerable interest to know the heat of formation of the present dry addition compounds from the dry reactants, which is in principle determinable.

These findings are of interest in connection with the x-ray diffraction results reported in Paper I of this series.[3] With the polymers there listed as showing the characteristic interferences of linear polyiodine we should have included the poorly crystalline polyvinyl silicate, made by esterifying PVA; we have since added the crystalline polymer known commercially as Terylene. Solid, oriented iodine-bearing polyvinyl silicates and borates have been described

TABLE I. Thermochemistry of halogens.

| | Iodine | Bromine |
|---|---|---|
| Heat of formation from atoms | 51 | 54 |
| Heat of addition to PVB | 20* | 12.5* |
| Heat of addition to potato starch | 10* | 7* |
| Heat of solution in various solvents | −6 to 6*† | −1 to 3 |
| Heat of addition to ionic halides to give trihalides | 0.8(K, Cs) | 5($NH_4$) |

* New results.
† From measured heat of solution of 6.35 g (0.025 mole) $I_2$ in 180 cc EtOH containing 3.6 g (0.025 mole) $NH_4I$.

in patents[4] as offering dichroic polarizer films of usefully enhanced stability over solid PVA-iodine films. Our present results show an analogous enhanced resistance of water-dispersed PVB-iodine to dissociation over PVA-iodine under the same conditions.

Concerning the recent papers of Rundle and Stein[5a, b] we have no evidence to question the quite special pictures drawn by these writers for the structure of starch and of starch-iodine. Our position is that the PVB-iodine structure in the solid and dispersed states must include the starch-iodine structure as a special case. It is difficult for us, in view of the recent work of Bunn and Peiser[6] on the PVA structure, to conceive in PVA or PVB an array of >C—O—X groups "held in such a way that each contributes a reinforcing component of dipole moment along the fiber axis;" it seems more probable to us that in these systems such components would effectively cancel out each other over both shorter and longer ranges.

It is of interest that our heat of addition of iodine to PVB (20 kcal.) is close to the comparable figure of Dube for the addition of iodine to starch (19.6 kcal. derived from electrochemical measurements, reference 5b).

[1] R. Baldwin, R. Bear, and R. Rundle, J. Am. Chem. Soc. **66**, 111 (1944).
[2] F. Bichowsky and F. Rossini, *Thermochemistry of Chemical Substances* (Reinhold Publishing Corporation, New York, 1936).
[3] C. West, J. Chem. Phys. **15**, 689 (1947).
[4] A. Marks *et al.*, U. S. 2,432,113; F. Signaigo, U. S. 2,444,712; M. Hyman, Jr. *et al.*, U. S. 2,445,579; E. Land, U. S. 2,445,581.
[5] (a) R. Rundle, J. Chem. Phys. **15**, 880 (1947); (b) R. Stein and R. Rundle, J. Chem. Phys. **16**, 195 (1948).
[6] C. Bunn, Nature **159**, 161 (1947); **161**, 929 (1948).

## Photographic Infra-Red Emission Bands of $O_2$ from the $CO-O_2$ Flame*

R. C. Herman, H. S. Hopfield, G. A. Hornbeck, and S. Silverman
*Applied Physics Laboratory, The Johns Hopkins University, Silver Spring, Maryland*
December 27, 1948

ONE of the authors recently reported some spectroscopic studies of the $CO+O_2$ reaction carried out by explosion in a spherical vessel.[1] It was noted that the Runge bands of the neutral $O_2$ molecule appeared in emission in the violet and near ultraviolet.[2]

Further investigations have been carried out in the spectral range 7200–8800A in the first order of a 2-meter grating spectrograph (Eagle mounting, Baird Associates), the grating having 15,000 lines per inch. A mixture of CO and $O_2$ was ignited in a gold-plated spherical bomb of 7-liter capacity, provided with fused quartz windows 1 inch in diameter. The commercial CO employed was freed from iron carbonyl but contained about 1.5 percent of $H_2$ impurity. The CO and $O_2$ were admitted to the bomb in the ratio of 1 to 2, to a total pressure of 1.5 atmospheres. This fuel/oxygen ratio produced spectra of optimum contrast. The mixture was ignited at the center of the bomb by means of an ordinary spark coil across tungsten electrodes with $\frac{1}{4}''$ separation.

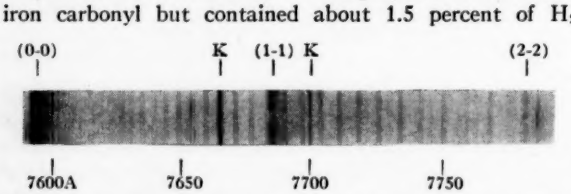


FIG. 1. A portion of the emission spectrum of $O_2$ obtained from the $CO-O_2$ reaction is shown in the spectral region 7590 to 7790A. The heads of the (0−0), (1−1), and (2−2) transitions of $^1\Sigma_g^+ \rightarrow {}^3\Sigma_g^-$, as well as the two potassium resonance lines at 7664.9 and 7699.0A, respectively, are indicated.

A portion of the spectrum obtained is reproduced in Fig. 1. An Eastman X-thin I-N plate was employed, hypersensitized by the usual ammonia-ethyl alcohol method. A Corning filter No. 2424 was used to absorb higher orders of the spectrum. The exposure consisted of forty explosions, corresponding to a total exposure time of about 10 seconds. The plate reproduced shows some of the red bands of neutral $O_2$, heretofore obtained in absorption by the earth's atmosphere. The two most intense of these bands, the *A* band[3] at $\lambda=7593.7$A, identified as the (0−0) band,[4] and the (1−1) band[5] at $\lambda=7683.8$A have been analyzed previously as absorption bands and assigned[6] to the $^1\Sigma_g^+ - {}^3\Sigma_g^-$ transition of neutral $O_2$. In addition to these two bands, Fig. 1 shows also the (2−2) band of the same system with head at $\lambda=7779.0$A. The original plate further shows the (3−3) band at $\lambda=7879.2$A and faint traces of heads of still higher bands of the same sequence,

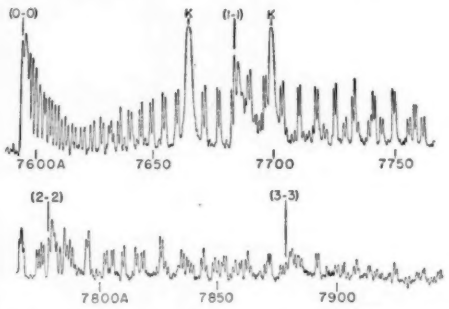


FIG. 2. Densitometer tracing of a portion of the emission spectrum of $O_2$ obtained from the $CO-O_2$ reaction, in the region 7590 to 7945A. The heads of the (0−0), (1−1), (2−2), and (3−3) transitions of $^1\Sigma_g^+ \rightarrow {}^3\Sigma_g^-$, as well as the potassium resonance lines, are indicated.

as well as heads of three bands of another sequence not previously observed: the (0−1), (1−2), and (2−3) bands. These band heads are at $\lambda=8597.8$, 8697.8, and approximately 8803A, respectively. The densitometer tracing of a portion of the same plate, reproduced in Fig. 2, shows the (0−0), (1−1), (2−2), and (3−3) bands.

Because of the inadequate dispersion and the extensive overlapping of bands, it is not feasible to analyze the bands completely from the plates which have been obtained. However, it has been possible to sort out many of the lines. The observed emission lines of the (0−0) band differ on the average from the corresponding absorption lines of Dieke and Babcock by about −0.1A. However, there is no doubt about the identity of this band, since the intervals between successive lines in emission agree extremely well with those between corresponding successive lines in absorption.

The distribution of intensity as obtained in emission is markedly different from that previously obtained in absorption because of the higher temperatures involved. The peak intensity is shifted away from the origin of the band in

both $R$ and $P$ branches, the intensity maximum in the $R$ branch being quite near the head of the band. Many additional lines are therefore observed in both branches of the previously known bands. The head of the (1−1) band is observed in emission at $\lambda = 7683.8$A, while in absorption no lines of this band were observed below 7685.7A, probably because of their low intensity.

We have found no evidence of any radiation from the $CO_2$ molecule, although careful search was made in the interval 7500–8800A, where some of the $CO_2$ bands are expected to lie.[7]

In conclusion, the writers wish to call attention to the note of K. J. Laidler which appears in this issue. From theoretical considerations alone, he concludes that the combustion process of CO and $O_2$ may produce oxygen molecules in either the $^3\Sigma_u^+$ or $^1\Sigma_g^+$ states. Transitions from $^3\Sigma_u^+$ to the ground state $^3\Sigma_g^-$ produce the Schumann-Runge bands and transitions from $^1\Sigma_g^+$ to the ground state yield the currently observed bands.

* The work described in this paper was supported by the Bureau of Ordnance, U. S. Navy, under Contract NOrd-7386.

[1] George A. Hornbeck, J. Chem. Phys. **16**, 845 (1948).
[2] George A. Hornbeck, J. Chem. Phys. **16**, 1005 (1948).
[3] G. H. Dieke and H. D. Babcock, Proc. Nat. Acad. Sci. **13**, 670 (1927).
[4] W. Ossenbrüggen, Zeits. f. Physik **49**, 167 (1928).
[5] R. Mecke and W. Baumann, Zeits. f. Physik **73**, 139 (1932).
[6] R. S. Mulliken, Phys. Rev. **32**, 880 (1928).
[7] D. M. Dennison, Rev. Mod. Phys. **12**, 175 (1940).

## The Formation of Electronically Excited Oxygen in the Carbon Monoxide Flame

K. J. LAIDLER
*Department of Chemistry, The Catholic University of America, Washington, D. C.*
December 22, 1948

THE possibility of the formation of electronically excited oxygen in the carbon monoxide flame, by various processes that may be represented by

$$CO_2^* + O_2 = CO_2 + O_2^*, \quad (1)$$

has been considered in a paper[1] presented at the Third Symposium on Combustion, Flame, and Explosion Phenomena in September, 1948. At the time there was no experimental evidence for such excitation of oxygen, but bands corresponding to two transitions from excited states have now been discovered, and were described in the previous letter.[2] It seems worth while, therefore, to present a more detailed discussion of this type of excitation.

The carbon monoxide flame is known to contain oxygen atoms, which were detected by Gaydon[3] using his nitric oxide method. The luminescence of the flame was previously thought[4] to be due to the formation of electronically excited carbon dioxide by the process

$$O + CO_2 + M = CO_2^* + M \quad (2)$$

where M represents a third body; that excitation occurs in this process is necessary for conservation of spin angular momentum. The more recent discovery[2] that the luminescence is due largely, if not entirely, to radiation by excited oxygen, calls for an explanation of the formation of these molecules. The possibility of their formation by oxygen atom combination, analogous to the radical-radical reactions postulated[5] to explain the formation[6] of excited formaldehyde in hydrocarbon flames, is here excluded by the high quantum yield[4] which indicates that one excited oxygen molecule is formed for about every hundred product molecules. This hypothesis is also eliminated by its failure to explain the disappearance of excited carbon dioxide molecules, which we know from direct evidence[7] to be formed by reaction (2).

These facts seem to point directly to reaction (1) as responsible for the electronic excitation of oxygen. Excited carbon dioxide is in a triplet (probably a $^3\Pi$) state, and its interaction with a $^3\Sigma_g^-$ oxygen molecule will give $^1\Sigma$-, $^1\Pi$-, $^3\Sigma$-, $^3\Pi$-, $^5\Sigma$-, and $^5\Pi$-states of the collision complex. Of these the triplet states will correlate with $CO_2(^1\Sigma) + O_2(^3\Sigma)$, which, therefore, can be formed without a violation of the spin-conservation rule; the process could be represented as

$$CO_2(^3\Pi) + O_2(^3\Sigma_g^-) \rightarrow CO_2O_2(^3\Sigma, {}^3\Sigma) \rightarrow CO_2(^1\Sigma) + O_2(^3\Sigma); \quad (3)$$

however, consideration of the form of the potential-energy surfaces suggests that ionic surfaces are also involved, *viz.*

$$CO_2(^3\Pi) + O_2(^3\Sigma_g^-) \rightarrow CO_2O_2(^3\Sigma, {}^3\Pi) \rightarrow CO_2 + O^-O(^3\Sigma, {}^3\Pi) \rightarrow CO_2(^1\Sigma) + O_2(^3\Sigma). \quad (4)$$

This scheme would account for the production of several triplet states of oxygen. However, formation of the lowest ($^3\Sigma_g^-$) state seems unlikely, since the ionic surfaces do not fall low enough; this would correspond to physical quenching, the energy passing into vibrational, rotational, and translational energy.

The production of oxygen in the $^3\Sigma_u^-$-state, which accounts for the Schumann-Runge bands which are formed by the transition $^3\Sigma_u^- \rightarrow {}^3\Sigma_g^-$, seems much more probable from the standpoint of the smoothness with which the reaction can occur. The process may be represented as

$$CO_2(^3\Pi) + O_2(^3\Sigma_g^-) \rightarrow CO_2O_2(^3\Sigma, {}^3\Pi) \rightarrow CO_2 + O^-O(^3\Sigma, {}^3\Pi) \rightarrow CO_2(^1\Sigma) + O_2(^3\Sigma_u^-), \quad (5)$$

assuming the ionic complex to be formed. However, an important question raised by the observation of these bands is an energetic one, since the reaction must certainly be endothermic. Reaction (2) is exothermic by (126.7-$E$) kcal. where $E$ is the energy of excitation of the carbon dioxide in its $^3\Pi$-state; the energy of activation for the process[7] is about 2 kcal., so that $E$ cannot be greater than about 129 kcal. However, the energy of excitation of $O_2(^3\Sigma_u^-)$ is about 140 kcal., so that reaction (5) must be endothermic by at least 11 kcal., and therefore have an activation energy of at least this amount. If the flame temperature is about 3000°K, as seems to be the case, an activation energy of 15 kcal. would correspond to reaction occurring in one in about every 12 collisions, assuming no steric restrictions to reaction. Since the transition $CO_2(^3\Pi) \rightarrow CO_2(^1\Sigma) + h\nu$ is "forbidden," the radiative life of $CO_2(^3\Pi)$ may well be long enough for a large fraction of the $CO_2(^3\Pi)$ molecules to effect the required number of collisions with $O_2$ and hence transfer their electronic energy. Thus the production of the Schumann-Runge bands, which

at first sight seemed surprising, appears on further discussion to involve no theoretical difficulties; the detailed treatment of the mechanisms of such reactions involving a transfer of electronic energy still needs to be carried out, however.

In addition to the formation of $O_2(^3\Sigma_u^-)$ and $O_2(^3\Sigma_g^-)$ (lowest state), the production of $O_2(^3\Sigma_u^+)$ is possible. Reaction to give oxygen in a singlet state, e.g., $^1\Sigma_g^+$, can, as previously pointed out, proceed on singlet surfaces:

$$CO_2(^3\Pi)+O_2(^3\Sigma_g^-)\rightarrow CO_2O_2(^1\Sigma, {}^1\Pi)\rightarrow CO_2+O^-O(^1\Sigma, {}^1\Pi)\rightarrow CO_2(^1\Sigma)+O_2(^1\Sigma_g^+). \quad (6)$$

The production[2] of this state is probably to be explained by this reaction.

It may be noted in conclusion that the fact that most of the energy goes into the upper $^3\Sigma_u^-$-state, in spite of the endothermicity of the reaction, is a further indication[8] that in processes of this kind transitions are strongly favored which involve the transfer of a minimum amount of energy into non-electronic forms. This may be partly because of the large amount of resonance energy, but in this case perhaps more owing to the fact that the ionic states for the intermediate complex do not lie low enough to permit the formation of oxygen in lower electronic states.

[1] V. F. Griffing and K. J. Laidler, *Third Symposium on Combustion, Flame and Explosion Phenomena* (Madison 1948) (Williams and Wilkins, Baltimore, to be published).
[2] R. C. Herman, H. S. Hopfield, G. A. Hornbeck, and S. Silverman, J. Chem. Phys. **17**, 220 (1949).
[3] A. G. Gaydon, Proc. Roy. Soc. **A183**, 111 (1944); Trans. Faraday Soc. **42**, 292 (1946).
[4] Cf. V. Kontratjew, Zeits. f. Physik **63**, 322 (1930); A. Fowler and A. G. Gaydon, Proc. Roy. Soc. **A142**, 362 (1933); A. G. Gaydon, *Spectroscopy and Combustion Theory* (Chapman and Hall, Ltd., London, 1942), Chapter VI.
[5] A. D. Walsh, Trans. Faraday Soc. **43**, 297 (1947).
[6] Day and R. N. Pease, J. Am. Chem. Soc. **62**, 2234 (1940); Topps and D. T. A. Townend, Trans. Faraday Soc. **42**, 345 (1946).
[7] W. F. Jackson, J. Am. Soc. **56**, 2631 (1934); W. Groth, Zeits. f. physik. Chemie **B37**, 307 (1937).
[8] Cf. K. J. Laidler, J. Chem. Phys. **15**, 712 (1947).